Université de Montréal

Événements de signalisation impliqués dans la production des gamètes, la pollinisation et l'embryogenèse chez *Solanum chacoense* Bitt.

Par

Martin O'Brien

Programmes de Biologie Moléculaire

Faculté des Études Supérieures

Thèse présentée à la Faculté des Études Supérieures

en vue de l'obtention du grade de Philosophiæ doctor

en biologie moléculaire

Décembre 2005

Page d'identification du jury

Université de Montréal

Faculté des Études Supérieures

Cette thèse intitulée :

Événements de signalisation impliqués dans la production des gamètes, la pollinisation et l'embryogenèse chez *Solanum chacoense* Bitt.

Présentée par

Martin O'Brien

a été évaluée par un jury composé des personnes suivantes

Dr David Morse, *président-rapporteur*

et représentant du doyen

Dr Jean Rivoal, *membre du jury*

Dr Brian Ellis, *examinateur externe*

Dr Daniel P. Matton, *directeur de recherche*

Résumé

Notre laboratoire de recherche s'intéresse aux événements de signalisation impliqués dans les diverses facettes de la biologie de la reproduction, plus précisément à ce qui touche à la formation des gamètes femelles, la pollinisation, la fécondation et le développement précoce de l'embryon. La présente thèse décrit le rôle de trois gènes différents qui s'inscrivent dans ce contexte. Le premier d'entre eux code pour une petite protéine nommée HT-B qui joue un rôle dans les mécanismes de reconnaissance du pollen génétiquement semblable lors de la pollinisation. Cette protéine est sécrétée à l'extérieur des cellules du style. Des lignées abolissant l'expression du gène permettent aux tubes polliniques incompatibles de contourner les barrières de l'auto-incompatibilité, et ce, en retardant la sénescence. Les protéines de type HT possèdent plusieurs caractéristiques de petits ligands protéiques. Le récepteur et la voie de signalisation qui en découlent sont inconnus pour l'instant. Par la suite, nous avons caractérisé le gène CYP51G1-Sc qui code pour une 14α-déméthylase qui est impliquée dans la voie de biosynthèse des brassinostéroïdes, une hormone végétale. Une mutation homozygote du gène cause des anormalités de formation dans les jeunes embryons qui ne peuvent alors atteindre le stade adulte. Ce phénotype ne peut être complémenté par l'application exogène de brassinostéroïdes, ce qui laisse supposer qu'un intermédiaire de biosynthèse est directement impliqué. Nous avons pu démontrer que le substrat de l'enzyme est capable d'induire l'expression de cette dernière tout en étant véhiculé à

distance. Nous croyons que l'obtusifoliol, le substrat, peut agir comme lipide bioactif et qu'il pourrait avoir une action au niveau de la pollinisation, de l'embryogenèse et du développement des feuilles. De plus, nous avons caractérisé une nouvelle famille de MAP kinases dont l'un des membres est impliqué dans le développement de l'ovule et des gamètes mâles. Les voies de MAP kinases sont des composantes importantes pour le relais de l'information inter- et intra-cellulaire. La sur-expression de la protéine kinase ScFRK2 cause un changement homéotique des ovules vers un destin tissulaire similaire au carpelle. Pour ce qui est des gamètes mâles, tout le pollen est atteint soit par une mortalité qui touche plus de 60% du pollen ou soit par une réduction de la taille de ceux qui n'ont pas dégénéré. La mortalité du pollen est associée à un effet sporophytique de l'anthère impliquant l'implication du tapetum, le tissu nourricier du pollen en développement.

Mots clés

Solanum chacoense, pollinisation, auto-incompatibilité, protéine HT, embryogenèse, obtusifoliol, signalisation, transduction de signaux, formation des gamètes, MAPK

Abstract

Our research program focuses on signal transduction events involved in different reproductive biology aspects including female gametes formation, pollination, fertilization and early embryogenesis events. This Ph. D. thesis describes the molecular characterization of three genes involved in those above-mentioned processes. The first gene code for a small secreted protein named HT-B, who plays a role in the recognition of genetically similar pollen tube during pollination events. This protein has a signal peptide that permits secretion to the extracellular matrix of the style. We have generated transgenic lines that abolish the expression of *HT-B*. In these lines, self incompatibility is lost due to the delayed abscission of the style correlated to lower abundance of S-RNase transcripts. We believe that the small HT proteins act as a ligand but its signalling pathway or potential receptor remains elusive. We have also characterized the *CYP51G1-Sc* gene, which codes for an obtusifoliol 14α-demethylase involved in sterol biosynthesis pathway. Mutation in this gene causes embryogenesis defects leading to growth arrest at early developmental stages. Embryos are not rescued by the direct application of brasssinosteroids, which implies that a byproduct of the pathway is involved in causing this phenotype. Obtusifoliol, which is the substrate for the 14α-demethylase, is able to induces the expression of *CYP51G1-Sc* gene. Moreover, we where able to show that radiolabelled obtusifoliol is able to move from application site. Taking this into account, we believe that obtusifoliol can acts as a

signalling lipid and have a direct implication on pollination, embryogenesis and leaf development. We have also characterized a new family of MAP kinase with one member (the ScFRK2 kinase) being involved in male gametes formation and ovule development. Usually, MAPK cascades are use for information relay in the cell. Overexpression of *ScFRK2* causes homeotic change of ovules to carpeloid structures. Furthermore, all pollen grains are affected to various extent, from a totally shrivelled appearance (2/3 of the pollen grains) and the remaining being significantly reduced in size. Pollen lethality was linked to a sporophytic defects, which might involve the tapetum cell layer.

Key words

Solanum chacoense, pollination, self-incompatibility, HT protein, embryogenesis, obtusifoliol, signalization, signal transduction, gametes formation, MAPK

Table des matières

Liste des tableaux

Liste des figures

Chapitre IV.

Chapitre V.

Liste des sigles et des abréviations

À moins qu'il ne soit mentionné autrement, le gène et son abréviation proviennent de l'espèce *Arabidopsis thaliana*.

°C	degré Celcius
%	pourcentage
#	numéro
18S	gène *ARN ribosomal 18S* de *Solanum chacoense*
^{14}C	carbone 14
3'	extrémité 3' hydroxyl
314	plante IP 458314
5'	extrémité 5' phosphate
582	plante IP 230582
5' RACE	5' rapid amplification of cDNA ends
°C	degré Celsius
A	adénine
A	alanine
AB	Alberta
ABA	abscisic acid
ABI	Applied Biosystems
ACC	1-aminocyclopropane-1-carboxylic acid
ACR4	gène *CRINKLY4*
Ade/ADE	adénine
ADN	acide désoxyribonucléique
AES	3-aminopropyltriethoxy-silane
AG	gène *AGAMOUS*
AGL	famille de gènes *AGAMOUS-LIKE*
$AgNO_3$	nitrate d'argent
AL	Alabama
ANT	gène *AINTEGUMENTA*
AP	arbitrary primer
AP1	gène *APETALA1*
AP2	gène *APETALA2*
AP3	gène *APETALA3*
ARF	famille de gènes AUXIN RES*PONSE FACTOR*
ARF5	gène *MONOPTEROS*
Arg	arginine
ARN	acide ribonucléique

AS	lignée antisens
Asn	asparagine
Asp	acide aspartique
ATCC	American Type Culture Collection
ATHB-8	gène *ARABIDOPSIS THALIANA HOMEOBOX-8*
ATML1	gène *ARABIDOPSIS THALIANA MERISTEM LAYER1*
ATP	adénosine triphosphate
au	arbitrary units
AUX-IAA	famille de gène *AUXINE/INDOLLE ACETIC ACID INDUCIBLE*
AZ	Arizona
BamHI	endonucléase I de *Bacillus amyloliquefaciens* H
BDL	gène *BODENLOS*
BEL1	gène *BELL1*
bHLH	basic-helix-loop-helix
BM	boiled microsome
bp	base pair
BR	brassinosteroïde
BRI1	gène *BRASSINOSTEROID INSENSITIVE1*
BS	bluescript
BSA	bovine serum albumin
C	cytosine
C	cystéine
C	compatible
C	témoin (control)
C2H2	domaine en doigt de zinc contenant cystéines et histidines
C3	conserved domain 3
CA	California
CaMV 35S	cauliflower mosaic virus 35S promoter
CBS	Center for Biological Sequence analysis
cDNA	complementary DNA
CH_2Cl_2	chloroforme
CLV1	gène *CLAVATA1*
CLV3	gène *CLAVATA3*
cm	centimètre
CNRS	Centre National de la Recherche Scientifique
CO_2	dioxyde de carbone
CPH	gène *CEPHALOPOD*
cpm	compte par minute
CR4	gène *CRINGLY4* de *Zea mays*
CRC	gène *CRABS CLAW*
cRNA	complementary RNA
CS	carpelloid structure
CTAB	cétyl - N, N, N, triméthylammonium bromure
C-Terminal	domaine carboxyl terminal d'une protéine
CUC1	gène *CUP-SHAPED COTYLEDONS1*
CUC2	gène *CUP-SHAPED COTYLEDONS2*

CUC3	gène *CUP-SHAPED COTYLEDONS3*
CYP51G1-At	gène *obtusifoliol 14α-demethylase*
CYP51G1-Sc	gène *obtusifoliol 14α-demethylase* de *Solanum chacoense*
D	acide aspartique
DAP	days after pollination
dATP	déoxyadénosine triphosphate
DD-RT-PCR	differential display retrotranscription PCR
DM	déméthylase
DNA	deoxyribonucleic acid
DPA	days post-anthesis
DPP	days post-pollination
DPW	days post-wounding
Dr.	docteur
E	acide glutamique
EcoRI	endonucléase RI d'*Escherichia coli*
EcoRV	endonucléase RV d'*Escherichia coli*
EDTA	acide éthylènediaminotétraacétique sel disodique
EIL3	gène *ETHYLENE-INSENSITIVE3-LIKE3*
EMS1	gène *EXCESS MICROSPOROCYTES*
ER	endoplasmic reticulum
ERG6	gène *ERGOSTEROL-DEFICIENT6* de la levure
ERG11	gène *ERGOSTEROL-DEFICIENT11* de la levure
EST	expressed sequence tag
ETR1	gène *ETHYLENE RECEPTOR1*
EV	empty vector
EXS	gène *EXTRA SPOROGENOUS CELLS1*
F	phénylalanine
F1	population d'un croisement de première génération
F2	population d'un croisement de deuxième génération
FAA	formaldéhyde acide acétique
FAX	facimile
FBP7	gène *floral binding protein7* de *Petunia hybrida*
FBP11	gène *floral binding protein11* de *Petunia hybrida*
FCAR	Le Fonds pour la Formation des Chercheurs et l'Aide à la Recherche
FF-MAS	follicular fluid meiosis activating sterol
Fig.	figure
FK	gène *FACKEL*
FLS2	gène *FLAGELLIN SENSITIVE2*
FQRNT	Le Fonds Québécois de la Recherche sur la Nature et les Technologies
FRK	fertilization-related kinase
g	gramme
G	guanine
G	glycine
G4	plante G4

GAL4	activateur de la transcription GAL4
GC	gas chromatography
GC/MS	GC/mass spectrometry
GLC-MS	gas/liquid chromatography-MS
GE	General Electric
GEF	guanine exchange factor
GL2	gène *GLABRA2*
GK	gène *GURKE*
GN	gène *GNOM*
GSI	gametophytic self-incompatibility
GUS	gène marqueur *GLUCURONIDASE*
h	heure
H	histidine
H	HindIII
HD	homéodomaine
HD-ZIP	HD-leucine zipper protein
HD2	gène *histone deacetylase2* de *Solanum chacoense*
HindIII	endonucléase III d'*Haemophilus influenzar* RD
His/his	histidine
HLL	gène *HUELLENLOS*
HT	gène modificateur de l'auto-incompatibilité chez les *Solanaceae*
HVa	domaine hypervariable a
HVb	domaine hypervariable b
HYD1	gène *HYDRA1*
I	isoleucine
I	incompatible
IAA12	gène *BODENLOS*
i. e.	c'est-à-dire (*id est*)
IRBV	Institut de Recherche en Biologie Végétale
JA	jasmonic acid
K	lysine
Kan	kanamycine
kb	kilo base
kDa	kilo Dalton
KpnI	endonucléase I de *Klebsiella pneumoniae* OK8
kV	kilo Volt
L/l	litre
L	leucine
L1	première couche de cellules du meristème
L2	seconde couche de cellules du meristème
L3	troisième couche de cellules du meristème
LAT52	gène *LATE ANTHER TOMATO52* de *Lycopersicon esculentum*
LB4404	souche d'*Agrobacterium tumefaciens*
LePRK1	gène *PRK1* de *Lycopersicon esculentum*
LePRK2	gène *PRK2* de *Lycopersicon esculentum*
LEU/leu	leucine

locus S	locus d'auto-incompatibilité
LpHT-A1	gène *HT* de *Lycopersicon peruvianum* isoforme A (allèle 1)
LpHT-B1	gène *HT* de *Lycopersicon peruvianum* isoforme B (allèle 1)
LRR	leucine-rich repeat
LTP	lipid transfer protein
LUG	gène *LEUNIG*
lys	lysine
M	molaire
M	méthionine
M+	mass-to-charge ratio
MA	Massachusetts
MAC1	gène *multiple archesporial cells1* de *Zea mays*
MADS	MCM1, AGAMOUS, DEFICIENS et SRF
MAP	mitogen activated protein
MAPK	mitogen activated protein kinase
MAPKK	mitogen activated protein kinase kinase
MAPKKK	mitogen activated protein kinase kinase kinase
MAPKKKK	mitogen activated protein kinase kinase kinase kinase
MAT	mating locus
MD	Maryland
MeJa	methyl jasmonate
MEKK1	gène qui code pour une MAPKKK
MeOH	méthanol
met	méthionine
min	minute
mg	miligramme
mm	milimètre
mM	milimolaire
mJ	milijoule
ml	mililitre
MKK4	gène qui code pour une MAPKK
MKK5	gène qui code pour une MAPKK
MOPS	acide propanesulfonique 3-(N-morpholino)
MP	gène *MONOPTEROS*
MPK3	gène qui code pour une MAPK
MPK6	gène qui code pour une MAPK
Mr.	monsieur (mister)
MR	maximum resolution
Mrs.	madame (madam)
mRNA	messenger RNA
MS	mass spectrometry
MS	Murashige and Skoog
MSP1	gène *MULTIPLE SPOROCYTE1* d'*Oyiza sativa*
MW	molecular weight
m/z	mass spectra
n	nombre d'échantillon

N	asparagine
Na_2PO_4	sodium phosphate
NADPH	nicotinamide adenine dinucleotide phosphate forme réduite
$NaHPO_4$	tampon phosphate
NaHT-B1	gène *HT* de *Nicotiana alata* isoforme B (allèle 1)
NcoI	endonucléase I de *Nocardia corallina*
ND	pas déterminé (not determined)
ng	nanogramme
nm	nanomètre
nmol	nanomole
Nos	nopaline synthase terminator
NPK1	gène *NICOTIANA PROTEIN KINASE1* de *Nicotiana*
NRC	National Research Council of Canada
NSERC	Natural Sciences and Engineering Research Council of Canada
nt	nucléotide
N-terminal	domaine amino-terminal d'une protéine
NZZ	gene *NOZZLE*
Ont/ONT	Ontario
ORC	gène *ORIGIN RECOGNITION COMPLEX*
p	plasmide
P	proline
Pa	Pascal
PAUP	phylogenetic analysis using parsimony
PCR	polymerase chain reaction
PDF2	gène *PROTODERMAL FACTOR2*
Ph	téléphone (phone)
Ph D	docteur (*Philosophiæ doctor)*
PHB	gène *PHABULOSA*
PHV	gène *PHAVOLUTA*
pI	point isoélectrique
PlantP	plant phosphorylation project (Purdue University)
PI	gène *PISTILLATA*
PIN	protéine permettant le transport polaire de l'auxine
PIN1	gène *PINFORMED1*
PIN7	gène *PINFORMED7*
PJ69-4A	souche de levure
PRK1	gène *POLLEN RECEPTOR KINASE* de *Petunia inflata*
PSI pred	position specific iterated prediction
Pwo	polymérase d'ADN de *Pyrococcus woesei*
Q	glutamine
Qc/QC	Québec
R	arginine
RALF	gène *RAPID ALKALINATION FACTOR*
rel. int.	relative intensity
RFLP	restriction fragment length polymorphism
RLK	receptor-like kinase

RNA	ribonucleic acid
RNAi	RNA interference
RNase T2	gène *RIBONUCLEASE T2* d'*Aspergillus oryzae*
RRM	RNA recognition motif
S	sérine
S	lignée sens
S	unité de sédimentation d'une ou d'un ensemble de molécules
S_{11}-*RNase*	gène *S-RNase* de *Solanum chacoense* (allèle 11)
S_{12}-*RNase*	gène *S-RNase* de *Solanum chacoense* (allèle 12)
S_{13}-*RNase*	gène *S-RNase* de *Solanum chacoense* (allèle 13)
S_{14}-*RNase*	gène *S-RNase* de *Solanum chacoense* (allèle 14)
SA	salicylic acid
SAM	shoot apical meristem
SbHT-$B_{1/2}$	gène *HT* de *Solanum bulbocastanum* isoforme B (allèle 1 et 2)
SC	self-compatible
ScFRK1	gène *FERTILIZATION-RELATED KINASE2* de *Solanum chacoense*
ScFRK2	gène *FERTILIZATION-RELATED KINASE2* de *Solanum chacoense*
ScHT-$A_{1/2}$	gène *HT* de *Solanum chacoense* isoforme A (allèle 1 et 2)
ScHT-B_1	gène *HT* de *Solanum chacoense* isoforme B (allèle 1)
SCR	gène *S-LOCUS CYSTEINE-RICH* des *Brassicaceae*
SCR	gène *SCARECROW*
SDS	sodium dodécyl sulphate
SEM	scanning electron microscopy
SEP1	gène *SEPALATA1*
SEP2	gène *SEPALATA2*
SEP3	gène *SEPALATA3*
SERK1	gène *SOMATIC EMBRYOGENESIS RECEPTOR-LIKE KINASE1*
SERK2	gène *SOMATIC EMBRYOGENESIS RECEPTOR-LIKE KINASE2*
SFB	gène *S-HAPLOTYPE-SPECIFIC F-BOX* de *Prunus mume*
SHP1	gène *SHATTERPROOF1*
SHP2	gène *SHATTERPROOF2*
SHR	gène *SHORT ROOT*
SI	self-incompatibility
SiO_2-TLC	TLC-silice
SLF	gène *S-LOCUS F-BOX* d'*Antirrhinum hispanicum*
Sli	S-locus inhibitor de *Solanum chacoense*
SMT1	gène *STEROL METHYL-TRANSFERASE1*
snRK1	gène *SUCROSE NON-FERMENTING-1-RELATED KINASE* de *Hordeum vulgare*
SHT-$B_{1/2}$	gène *HT* de *Solanum pinnatisectum* isoforme B (allèle 1 et 2)
SPL	gène *SPOROCYTELESS*
SPL	gène *SPATULA*

SRK	gène *S-LOCUS RECEPTOR KINASE* des *Brassicaceae*
S-RNase	gène *SELF-INCOMPATIBILITY RIBONUCLEASE* des *Solanaceae*
SSC	saline sodium citrate
SSI	sporophytic self-incompatibility
StHT-A1	gène *HT* de *Solanum tuberosum* isoforme A (allèle 1)
StART	steroidogenic acute regulatory transfer domain
STE11	gène *STERILE11*
STK	gène *SEEDSTICK*
STM	gène *SHOOT MERISTEMLESS*
SUB	gène *STRUBBELIG*
SUP	gène *SUPERMAN*
T	thymine
T	thréonine
T	tlignée ransformée (transformed)
T-DNA	transfer DNA
TE	Tennessee
tel	téléphone
TLC	thin layer chromatography
T-loop	kinase activation loop
T-MAS	testis meiosis activating sterol
TMM	gène *TOO MANY MOUTHS*
TPD1	gène *TAPETUM DETERMINANT1*
TPL	gène *TOPLESS*
TRP	tryptophane
TSL	gène *TOUSLED*
TX	Texas
U	uracile
U	upregulated
UFO	gène *UNUSUAL FLORAL ORGAN*
UPR	Unité Propre de Recherche
ura	uracile
UTP	uridine triphosphate
UTR	untranslated region
UV	ultra violet
V	valine
V22	plante V22
VIGS	virus-induced gene silencing
W	tryptophane
W	blessure (wounding)
WAT11	souche de levure
WI	Wisconsin
WOL	gène *WOODEN LEG*
WOX2	gène *WUSCHEL HOMEOBOX2*
WRKY22	gène qui code pour un facteur de transcription de type WRKY
WRKY29	gène qui code pour un facteur de transcription de type WRKY

WT	témoin (wild type)
WUS	gène *WUSCHEL*
X	acide aminé quelconque
XbaI	endonucléase I de *Xanthomonas badrii*
Y	tyrosine
YDA	gène *YODA*
ZLL	gène *ZWILLE*
α-^{32}P-dATP	dATP radioactif sur le phosphate α
γ-^{32}P-dATP	dATP radioactif sur le phosphate γ
μCi	micro Curie
μg	microgramme
μl	microlitre
μm	micromètre
μM	micromolaire

Dédicace

À toi, ma tante qui a su m'inspirer le goût de l'aventure,

merci Joan, je ne pourrais jamais t'oublier…

Remerciements

Parce qu'une thèse ne se fait pas seul :

J'aimerais remercier tout particulièrement mes partenaires dans le crime : Sier-Ching et Hugo. Je vous souhaite tout le succès que vous méritez. Je ne saurais jamais comment te remercier pour toutes ces années de complicité, pour ce cadeau qui n'a pas de prix, merci Sier-Ching. Et toi Hugo, fidèle compagnon de sports et de sorties en plein air, merci pour ton aide précieuse au laboratoire.

Merci à Étienne pour partager mon humour. Il faut définitivement se retrouver dans le même institut de recherche plus tard, j'ai plein de plans diaboliques en trois étapes…

Merci à Thierry et Christelle, j'espère toujours rester en contact avec vous. Vous rencontrez à l'IRBV à été définitivement un plus.

Merci également à Papa et Maman qui ont toujours été là, J'aimerais tellement être à la hauteur de votre fierté. Vous êtes des parents en or, merci mille fois.

À ma Stéphanie jolie qui a partagé avec moi les durs labeurs de ma fin de doctorat. J'aurais voulu que tu vives tes rêves comme moi je vis les miens. Je t'aime.

Un merci spécial à Daniel, mon directeur de recherche, ou plutôt, LE directeur de recherche. Celui qui nous rassure, qui nous motive, synonyme d'un succès assuré. Pour mon baptême scientifique je ne pourrais jamais assez te remercier. J'ai adoré les moments où nous élaborions des projets secondaires, plein d'idées, de bonnes volontés. Je me rappellerais toujours le samedi matin, Jean Leloup, dans le tapis, mortiers et pilons en action et un garde de sécurité éberlué…

Merci aussi aux organismes subventionnaires : FCAR, CRSNG, FES et le Programme de Biologie Moléculaire qui ont allégé grandement le fardeau de mon doctorat.

Merci également au comité d'évaluation de cette thèse. Je vous dois une partie de mon avenir, merci.

Un clin d'œil tout particulier à l'équipe de recherche du laboratoire Matton, Je quitte tristement ce havre de connaissances, de complicité et de camaraderie. Merci Christelle, Sier-Ching, Hugo, Corinne, Sébastien, Geneviève, Marie, Éric et Faïza.

et finalement, à tous ceux qui ont fait de mon passage au doctorat un moment agréable et inoubliable, merci !

Avant-propos

Le contenu de cette thèse porte sur trois éléments moléculaires de transduction de signaux reliés respectivement à trois facettes de la biologie de la reproduction. J'aurais pu composer ce manuscrit de thèse en incluant seulement un phénomène biologique et y inclure la contribution que j'y ai apportée. Entre autres, le chapitre II sur la pollinisation aurait pu être suivi d'un autre sur des interactants protéiques de la S-RNase (O'Brien *et al.*, 2004). Dans le même ordre d'idée, les chapitres IV et V sur la formation de l'ovule et des gamètes mâles auraient pu être additionnés d'un autre chapitre sur la caractérisation biochimique de la kinase et de la lignée sur-exprimante, cet article est présentement sous forme d'ébauche. J'ai plutôt opté pour une vision d'ensemble décrivant les divers projets sur lesquels j'ai travaillé durant mon passage au doctorat tout en restant dans le thème préféré de notre laboratoire : la transduction de signaux et les interactions pollen/pistil. En science, nous disons souvent « un doc, un gène ». J'ai malheureusement failli à ce dicton, me comportant plus comme un enfant devant un étalage d'une confiserie. Que voulez-vous, il est difficile de faire un choix quand plus de 25 000 gènes s'offrent à vous, dont près de 7000 dans son propre laboratoire...

Merci et pardon Daniel!

Foreword

This thesis emphasizes three different molecular events related to signal transduction, that are linked to three respective fields in plant reproduction biology. I could have written this manuscript differently by treating only one biology theme and what I contributed to it. A chapter could have followed chapter II on pollination, describing in more details S-RNases and their protein partners (O'Brien *et al.* 2004). One the other hand, chapters IV and V on ovule and male gametes development might have been added with another chapter on the biochemical characterization of the ScFRK2 protein kinase, the transcriptional and protein profiling of mutant overexpressing lines, and hence form a whole story. For that matter, an article is still in a rough draft format. But things went otherwise and I have opted for a more widespread view while keeping in mind our preferred lab themes : Signal transduction and pollen/pistil interactions. Some says that « for each PhD student there's a gene ». I have failed miserably to this saying. I've been acting more like a child in front of a candy shop. Life is hard, so many genes, so little time…

For this Daniel, I beg your pardon and thank you!

Chapitre I. Introduction

Le cycle de la vie d'une plante alterne entre une forme diploïde pluricellulaire et une forme haploïde également pluricellulaire que l'on nomme le sporophyte et le gamétophyte respectivement. Le gamétophyte est sexué. L'anthère produit le gamétophyte mâle que l'on nomme pollen, alors que le pistil génère le gamétophyte femelle : le sac embryonnaire contenant la cellule œuf ou oosphère. La transition entre les deux générations s'effectue dans l'ovule où, suite à la production du sac embryonnaire, ce dernier devient réceptif au tube pollinique qui effectuera la double fécondation nécessaire à la production de la graine. La production de l'ovule par la plante et le bon développement de ce dernier sont donc des étapes capitales pour l'accomplissement de son cycle de vie. Dans le même ordre d'idée, la croissance ininterrompue du tube pollinique dans la matrice du tissu transmetteur et le bon développement de l'embryon suite à la double fécondation est également une étape cruciale pour l'établissement de la seconde génération. Plusieurs mécanismes de régulation ainsi que plusieurs contrôles géniques orchestrent le bon développement de l'ovule, les événements de pollinisation et celui de l'embryon. Les dix dernières années ont été très révélatrices sur la compréhension de ces mécanismes et ce, suite à la caractérisation biochimique et moléculaire de mutants impliqués dans ces événements de développement.

1.1 Le développement de l'ovule et des gamètes mâles

Dans cette section, nous décrirons les événements biologiques et moléculaires qui régulent le développement de l'ovule et celui du gamétophyte mâle.

1.1.1 La fleur

Chez les angiospermes, dites plantes à fleurs, la fleur est composée d'un ensemble d'organes reproducteurs spécialisés (Figure 1) qui, au cours du temps, ont évolué de manière différente selon les espèces au sein de l'embranchement. Par contre, la fonction demeure identique, celle de s'assurer de la propagation efficace de leurs gènes. Le nombre et la morphologie des différentes pièces florales varient selon les espèces et par souci de simplicité, nous présenterons le modèle génique de type ABC décrit chez l'organisme modèle *Arabidopsis thaliana*. Il est également à noter que, au cours du présent manuscrit, nous utiliserons plus souvent les connaissances scientifiques acquises chez *A. thaliana* pour décrire les phénomènes biologiques du développement de l'ovule et de l'embryon, mais il serait scientifiquement incorrect de prétendre que ces connaissances s'appliquent à toutes les espèces car plusieurs exceptions publiées confirment de la complexité et de la diversité du monde vivant.

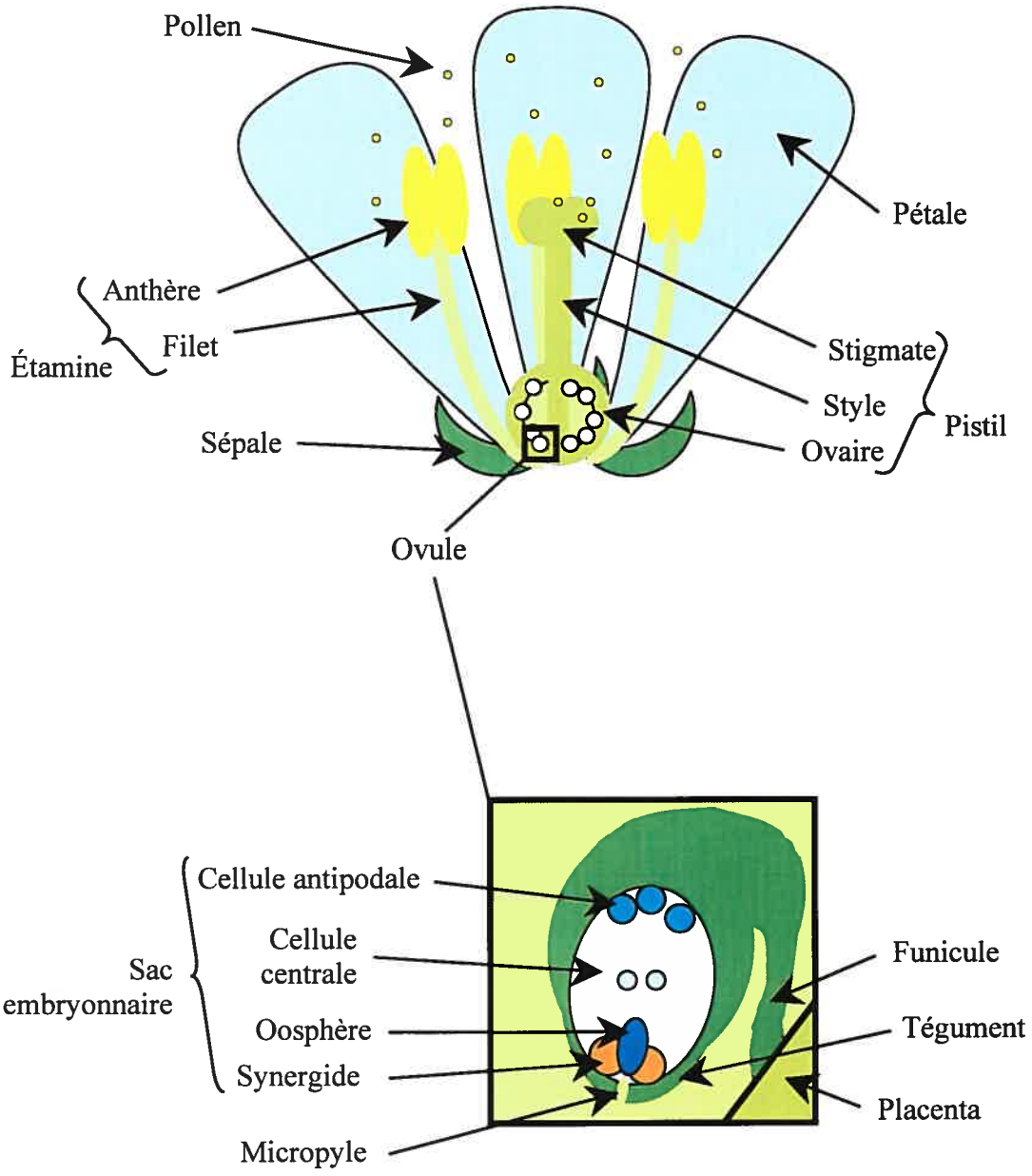

Figure 1

Représentation schématique de la fleur et de l'ovule. Coupe longitudinale d'une fleur et d'un ovule.

Une fleur est formée de plusieurs verticilles où chacun d'entre eux portent un jeu d'organes floraux différents (Figure 1). Le verticille le plus externe est le calice de sépales alors que la corolle de pétales compose le deuxième verticille. Ces pièces sont stériles alors que les étamines et le carpelle sont les structures reproductrices qui génèrent les gamètes mâles et femelles respectivement. Les étamines, composées du filet et de l'anthère, ornent le troisième verticille alors que le verticille central produit les pistils qui, lorsque fusionnés, forme le carpelle. Le pistil est habituellement structuré d'une partie réceptrice pour le pollen, le stigmate, le style et l'ovaire qui contient les ovules. L'identité et le positionnement exacts de ces pièces sur les différents verticilles sont régulés par l'expression précise de facteurs de transcription de classe A, B et C. Les gènes de type A (APETALA1/2 (AP1/2)) sont exprimés uniquement dans les deux verticilles les plus externes, les gènes de type B (AP3 et PISTILLATA (PI)) sont régulés de manière à être exprimés seulement dans le verticille deux et trois alors que les deux verticilles centraux expriment les gènes de type C (AGAMOUS (AG)). Les protéines de type A et C s'excluent mutuellement en réprimant l'expression de l'autre alors que le positionnement précis des gènes B se fait par le biais de protéines de frontières comme UNUSUAL FLORAL ORGAN (UFO), une protéine de type F-box impliquée dans la dégradation des protéines (Levin et Meyerowitz, 1995 et Samach *et al.*, 1999) et SUPERMAN (SUP) un facteur de transcription à doigts de zinc (Bowman *et al.*, 1992 et Sakai *et al.*, 1995). L'expression unique des facteurs de transcription de type A provoque la formation de sépales dans le premier verticille, alors que l'action combinée des protéines de type A et B induit la formation de pétales dans le deuxième verticille. Dans le même ordre d'idée, la combinaison de protéines de type B et C dans le troisième verticille permet la production d'étamines et la présence singulière de protéines de type

C induit la formation de pistils (Coen et Meyerowitz, 1991 et Weigel et Meyerowitz, 1994). Ce modèle classique, qui se voulait être simple lors de son élaboration en 1991, est maintenant beaucoup plus complexe car plusieurs autres gènes sont impliqués lors du développement floral (Theissen, 2001), notamment les gènes de type D et E qui s'ajoutent au modèle ABC.

I.1.2 Le gynécée

Les gènes de type D régulent l'initiation du développement de l'ovule au sein de l'ovaire. Les ovules prennent leur origine à partir des cellules méristématiques du placenta, ce dernier étant une région interne de l'ovaire dont les événements moléculaires de son ontogenèse demeurent encore mal définis. Chez *A. thaliana*, le gynécée est constitué de deux carpelles fusionnés dont les deux locules sont séparés par un septum. Il est à mentionner que l'ovule est une structure évolutive beaucoup plus ancienne que celle du carpelle. Ce dernier aurait évolué à partir de feuilles modifiées qui se seraient enroulées et fusionnées afin de conférer une protection aux ovules alors nus (Cronquist, 1988). Le développement de l'ovule est dissociable et indépendant de celui du carpelle, un fait supporté par la possibilité d'obtenir la formation d'ovules ectopiques hors du contexte du carpelle (Colombo *et al.*, 1995 et Pinyopich *et al.*, 2003). L'ovule est composé du funicule, qui le lie au placenta; du sac embryonnaire, le mégagamétophyte; et de deux téguments qui protègent le sac embryonnaire et permettent une ouverture (le micropyle) vers ce dernier (Figure 1).

9.1.3 Le placenta

On ne connaît pas exactement l'origine du placenta. Par contre, nous savons qu'il est constitué de cellules souches qui donneront naissance aux primordia des ovules. Le placenta tapisse l'intérieur du carpelle et l'expression des facteurs de transcription SHOOT MERISTEMLESS (STM) ainsi que CUP-SHAPED COTYLEDONS1 et 2 (CUC1/2) assurent le maintien des cellules souches du tissu placentaire là où les cellules n'auront pas adopté un patron de différenciation vers l'ovule (Aida *et al.*, 1999). Les expressions de *STM* et de *CUC1/2* bordent donc les sites d'initiations des ovules. Le facteur de transcription AINTEGUMENTA (ANT) et le répresseur transcriptionel LEUNIG (LUG) affectent le développement des structures internes à l'ovaire. Le double mutant *ant lug* est dépourvu de placenta et par le même fait d'ovules (Liu *et al.*, 2000). L'expression conjointe de *ANT* et de *LEU* permet l'établissement du placenta, ce qui établirait une base pour le bon développement de l'ovule.

SPATULA (*SPL*) (Alvarez et Smyth, 1999) et *TOUSLED* (*TSL*) (Roe *et al.*, 1997) sont également des gènes qui influencent la structure du placenta. SPL est un facteur de transcription alors que TSL est une protéine de type sérine/thréonine kinase. Les mutants *spl* et *tsl* affectent la production d'ovules en modifiant le développement de la région du placenta où les ovules doivent prendre origine. C'est aussi le cas pour le mutant *crabs claw* (*crc*) un facteur de transcription de type YABBY qui influencerait l'initiation du placenta et celui des primordia des ovules (Bowman et Smyth, 1999).

1.1.4 Le développement du primordium de l'ovule

Peu de connaissances sont amassées sur le développement des primordia des ovules. Nous savons que le gène *CUC3* est exprimé de manière à encercler le site d'un primordium d'ovule, ce qui laisse penser que ce dernier permettrait de situer exactement la zone d'initiation (Vroemen *et al.*, 2003). Il y a également le mutant *huellenlos* (*hll*) qui génère de petits primordia dont le développement est arrêté très tôt, laissant ainsi une structure dégénérée (Schneitz *et al.*, 1998). HLL code pour une protéine ribosomale de la mitochondrie. Cette protéine est vitale et le phénotype a pu être révélé dans le gynécée car il y a de la redondance due à une famille de gènes exprimée dans les tissus autres que dans celui du gynécée. Son implication directe sur le développement du primordium de l'ovule peut donc être remise en question.

1.1.5 L'identité de l'ovule

Plusieurs gènes affectent l'identité de l'ovule. Tous les gènes impliqués jusqu'à maintenant sont des facteurs de transcription. Le gène *BELL1* (*BEL1*) code pour une protéine à homéodomaine. Dans le mutant *bell*, les téguments de l'ovule cessent de croître et forment un collet autour de ce dernier. Quant à l'ovule, il continue de croître et emprunte un destin développemental différent, ressemblant à celui du carpelle. L'ovule développe des structures qui ressemblent au stigmate, au style et à l'ovaire. Il y a donc

une réitération du carpelle à la place de l'ovule (Modrusan *et al.*, 1994, Ray *et al.*, 1994 et Reiser *et al.*, 1995). Il en est de même pour le triple mutant *shatterproof1/2* (*shp1/2*) et *seedstick* (*stk*) (Pinyopich *et al.*, 2003). Ces trois gènes sont redondants dans l'ovaire et codent pour des protéines à domaine MADS. Dans le même ordre d'idée, les protéines de type MADS SEPALATA1/2/3 (SEP1/2/3) produisent le même phénotype lorsque le triple mutant est généré (Favaro *et al.*, 2003). La famille des facteurs de transcription MADS semble donc être importante pour dicter l'identité de l'ovule. Le mutant *fbp11* de *Petunia hybrida* entraine également une transformation homéotique des ovules vers des structures carpéloïdes (Angenent *et al.*, 1995). *FBP11* code pour un facteur de transcription de type MADS orthologue à *STK*. Sa sur-expression provoque la production d'ovules ectopiques sur les autres pièces florales tout comme la sur-expression de *STK* (Colombo *et al.*, 1995 et Pinyopich *et al.*, 2003), ce qui appuie l'implication de cette famille dans l'instauration de l'identité de l'ovule. Nous avons isolé une protéine kinase de type « mitogen activated protein kinases » (MAPK) que nous avons nommée FERTILIZATION-RELATED KINASE2 (ScFRK2) et dont les lignées sur-exprimantes imitent le phénotype du mutant *fbp11*. Nous présentons l'implication de cette kinase dans le développement de l'ovule au chapitre IV. De plus, nous avons pu constater que la sur-expression de cette dernière causait également des défectuosités au niveau des gamètes mâles. Le rôle de ScFRK2 dans le développement du pollen sera décrit au chapitre V.

I.1.6 Les gamètes

Chez les plantes, les gamétophytes mâles et femelles sont pluricellulaires. Le gamète femelle est représenté par le sac embryonnaire. Ce dernier est protégé par les téguments de l'ovule. Le sac embryonnaire est une structure composée de sept cellules et de huit noyaux. Le sac embryonnaire est polaire disposant de trois cellules antipodales au pôle du chalaze, trois cellules au pôle du micropyle dont deux cellules synergides servant au guidage du tube pollinique ainsi que la cellule œuf et une cellule centrale à deux noyaux (Figure 1).

Les gamètes mâles prennent leur origine à partir des cellules archésporales contenues dans l'anthère. Les différents tissus qui composent l'anthère proviennent des trois couches de cellules du méristème. La couche L1 donne l'épiderme de l'anthère alors que la couche L3 produit le connectif et le tissu vasculaire. La couche de cellules L2 produit les gamètes et le tissu nourricier de ces derniers. La couche L2, composée d'une seule couche de cellules, se divise de manière périclinale et donne naissance à une couche de cellules sporogènes vers l'intérieur et une couche de cellules pariétales vers l'extérieur. La couche de cellules sporogènes se développera et chaque cellule de cette couche donne une cellule précurseure de la tétrade qui, suite à la méiose, produit les quatre microspores. Quant à la couche de cellules pariétales, elle subit à nouveau une division périclinale et forme ainsi les couches pariétales secondaires interne et externe. La couche de cellules pariétales secondaires externe donne l'endothécium, un tissu qui a pour fonction de déshydrater les grains de pollen avant le processus de libération du

pollen. La couche de cellules pariétales secondaires interne se divise encore de manière périclinale afin de former le tapetum ainsi qu'une couche de cellules qui sépare l'endothécium du tapetum (Bowman, 1994). Le tapetum tapisse le locule de l'anthère et sert comme tissu nourricier des microspores. Le tapetum a également pour fonction de sécréter la callase, une enzyme nécessaire à la libération des microspores de la tétrade.

Avant même d'être libérée à l'extérieur de l'anthère par le stomium, la microspore effectue une division mitotique asymétrique qui donne une cellule végétative et une petite cellule germinale. Ces deux cellules forment le grain de pollen qui sera par la suite déshydraté. Lorsque le grain de pollen atterrira sur le stigmate, la cellule végétative produira un tube pollinique qui acheminera la cellule germinale vers l'ovule, où cette dernière, chez les *Solanaceae*, effectuera une dernière division pour produire les deux cellules spermatiques nécessaires à la double fécondation. Par contre, chez *A. thaliana* le grain de pollen a déjà trois noyaux avant même d'entrer en contact avec le stigmate.

1.1.7 Les cascades de MAPK

La plupart des événements moléculaires qui régulent les diverses facettes du développement impliquent des facteurs de transcription. Nous avons pu le constater en ce qui concerne les étapes qui mènent au développement précoce de l'ovule. Nous pourrons également réaffirmer ce fait lorsque nous décrirons le développement

embryonnaire. Jusqu'à maintenant, très peu de protéines kinases ont été caractérisées comme ayant un rôle dans le développement.

Une protéine kinase est une enzyme qui est capable de lier l'adénosine triphosphate (ATP), de reconnaître de façon spécifique un substrat protéique ou non et de transférer le phosphate γ de l'ATP vers des résidus sérine, thréonine, tyrosine ou histidine du substrat protéique. Cet ajout d'un groupement phosphore pourra changer la conformation d'une protéine ce qui permettra de l'activer, de réprimer son activité ou encore de la cibler pour la dégradation. Les modules de signalisation impliquant des MAPKs ont été très bien caractérisés chez la levure et chez les animaux (Piwien-Pilipuk *et al.*, 2002). Les MAPK sont phosphorylées par des MAPK kinases (MAPKK) sur les résidus thréonine et tyrosine dans leur boucle d'activation située entre les sous-domaines VII et VIII. Ces MAPKK ont été préalablement phosphorylées à leur tour par une MAPKK kinase (MAPKKK) et ce, également dans leur boucle d'activation, mais cette fois-ci, sur les résidus sérines ou thréonines. Les MAPKKK peuvent préalablement être phosphorylées par des MAPKKK kinases (MAPKKKK). Ceci est une cascade de phosphorylation typique. La plupart des éléments de cascades de signalisation utilisant des voies de MAPK sont impliqués dans les réponses aux stress et aux pathogènes (Nakagami *et al.*, 2005 et Pedley et Martin, 2005). Chez les plantes, la seule voie de MAPK complète, du récepteur aux facteurs de transcription, est celle qui est impliquée dans la réponse à la flagelline (Asai *et al.*, 2002), une composante des flagelles bactériens. La flagelline est perçue par le récepteur kinase riche en leucines (leucine-rich repeat, LRR) FLS2 qui, suite à son activation, va phosphoryler la MAPKKK MEKK1. La cascade se poursuit et MEKK1 active les MAPKK MKK4 et MKK5 qui à leur tour

vont phosphoryler les MAPK MPK3 et MPK6. Finalement, les facteurs de transcription WRKY22 et WRKY29 sont activés par phosphorylation par MPK3 et MPK6 (Asai *et al.*, 2002). Dans le génome d'*A. thaliana*, il y a environ une vingtaine de protéines MAPK, dix protéines de type MAPKK et entre 50 et 60 protéines de type MAPKKK.

9.1.8 Les kinases et le développement

Comme nous l'avons déjà mentionné auparavant, peu de protéines kinases sont impliquées dans les divers processus de développement. La plupart sont des récepteurs de type kinase comme CLAVATA1 (CLV1) impliqué dans le maintien du méristème apical (Clark *et al.*, 1993); BRASSINOSTEROID INSENSITIVE1 (BRI1) impliqué dans la perception des brassinostéroïdes (Li et Chory, 1997); PRK1 qui est impliqué dans le développement du sac embryonnaire et celui du pollen chez *P. inflata* (Lee *et al.*, 1996 et 1997); CRINKLY4 (ACR4) impliqué dans l'embryogenèse (Tanaka *et al.*, 2002), dans le développement des téguments de l'ovule et celui des sépales (Gifford *et al.*, 2003); SOMATIC EMBRYOGENESIS RECEPTOR-LIKE KINASE (SERK1) impliqué dans l'embryogenèse somatique (Schmidt *et al.*, 1997) et le développement du tapetum (Colcombet *et al.*, 2005 et Albrecht *et al.*, 2005); LePRK2 impliqué dans la croissance du tube pollinique chez la tomate (Johnson et Preuss, 2003); STRUBBELIG qui affecte la formation du tégument externe de l'ovule (Chevalier *et al.*, 2005); TOO MANY MOUTHS (TMM) impliqué dans la distribution des stomates (Nadeau et Sack, 2002); EXCESS MICROSPOROCYTES/EXTRA SPOROGENOUS CELLS1

(EXS/EMS1) impliqué dans le développement du tapetum et celui de l'embryon (Canales *et al.*, 2002 et Zhao *et al.*, 2002) et MULTIPLE SPOROCYTE1 (MSP1) son orthologue chez *Oryza sativa* (Nonomura *et al.*, 2003). Un seul élément d'une voie de MAPK a été caractérisé à ce jour. Il s'agit du gène *YODA* (*YDA*) qui code pour une protéine de type MAPKKK. Dans le mutant *yda*, l'élongation du zygote est perturbée et le suspenseur reste fusionné à l'embryon (Bergmann *et al.*, 2004 et Lukowitz *et al.*, 2004). De plus, YODA serait aussi impliqué dans la distribution et l'initiation des stomates ce qui pourrait le placer dans la voie de signalisation de TMM (Bergmann *et al.*, 2004). Comme nous l'avons mentionné plus haut, nous décrirons aux chapitres IV et V le rôle de ScFRK2 dans le développement de l'ovule et celui des gamètes mâles.

I.2 La pollinisation

Entre la déposition d'un grain de pollen et la fécondation d'un ovule dans l'ovaire, plusieurs phénomènes biologiques interviennent. Ces événements sont considérés comme les diverses facettes de la pollinisation. Parmi ceux-ci, on retrouve en premier lieu la germination du grain de pollen sur le stigmate, la croissance directionnelle de ce dernier dans le style, son guidage vers le sac embryonnaire et plus spécifiquement vers une des cellules synergides pour ainsi terminer avec la double fécondation de la cellule œuf et de la cellule centrale (Sanchez *et al.*, 2004 et Weterings et Russell, 2004). Chez certaines espèces, un phénomène de reconnaissance des tubes polliniques génétiquement semblables est impliqué dans le processus de pollinisation.

Plus de cinquante pour cent des familles contiennent des espèces dont la fleur est incapable de s'auto-féconder par son propre pollen, alors que leur fécondation est possible quand le pollen provient d'un autre individu de la même espèce. Ces systèmes de reconnaissance sont appelés système d'auto-incompatibilité (de Nettancourt, 1977).

1.2.1 L'auto-incompatibilité gamétophytique

Au cours de l'évolution, certaines plantes ont évolué de manière à exclure l'apport de leur propre pollen lors de leur reproduction sexuée. En augmentant le brassage du matériel génétique de sa descendance, ce type de plante aura donc, comme avantage, la possibilité de coloniser des niches écologiques plus vastes et diversifiées, d'augmenter la vigueur de sa progéniture et d'éviter l'accumulation de tares génétiques.

Chez les *Solanaceae*, les *Scrophulariaceae* et les *Rosaceae*, le système d'auto-incompatibilité est de type gamétophytique. Cela signifie que l'identité du pollen est déterminée par l'un ou l'autre des allèles contenus chez le parent pollinisateur et donc par le génotype du pollen même. Le locus multigénique et polymorphique appelé locus S, est composé d'un gène codant pour une protéine stylaire aux propriétés ribonucléasiques (S-RNase) et d'un autre gène exprimé dans le pollen qui code pour une protéine de type F-box (SLF/SFB). Les protéines contenant un F-box sont généralement impliquées dans la dégradation spécifique de protéines. Il y a reconnaissance et arrêt de

la croissance du tube pollinique quand celui-ci porte le même allèle S que l'une ou l'autre des deux copies exprimées au niveau du style (Kao et Tsukamoto, 2004).

Les premières S-RNases ont été clonées en 1986 (Anderson *et al.*, 1986). Ces glycoprotéines sont sécrétées à l'extérieur de la cellule à même la matrice du tissu transmetteur du style. Les S-RNases disposent de cinq sous-domaines qui leur confèrent une activité ribonucléasique similaire à la RNase T2 (McClure *et al.*, 1989) et elles ne semblent pas avoir de substrat spécifique (Singh *et al.*, 1991). Il a été démontré, par gain et perte de fonction, que la S-RNase est suffisante et nécessaire pour médier la réponse de reconnaissance spécifique du pollen génétiquement semblable dans le style (Lee *et al.*, 1994, Murfett *et al.*, 1994 et Matton *et al.*, 1997). De plus, l'activité ribonucléasique de la protéine est également nécessaire à son fonctionnement (Huang *et al.*, 1994). L'activité ribonucléasique de la S-RNase jouerait un rôle cytotoxique une fois intégrée dans le cytoplasme du tube pollinique. Elle y dégraderait tous les ARN présents ce qui empêcherait la synthèse de protéines dans le tube pollinique et donc sa mort subséquente (McClure *et al.*, 1990). La spécificité allélique des S-RNases est dictée par deux domaines hypervariables que l'on nomme HVa et HVb. Il a été démontré qu'il est possible de changer le potentiel de reconnaissance d'une S-RNase pour une autre en permutant les acides aminés qui diffèrent au sein des domaines hypervariables, renforçant l'hypothèse que ces régions sont impliquées dans la reconnaissance spécifique de la contrepartie pollinique (Matton *et al.*, 1997).

En ce qui concerne le produit du gène pollinique reconnu par la S-RNase et qui est responsable de la reconnaissance allélique du pollen, il se présente sous la forme

d'une protéine à domaine F-box nommée SLF/SFB (Lai *et al.*, 2002, Entani *et al.*, 2003 et Ushijima *et al.*, 2003). Les F-box sont impliqués généralement dans la dégradation spécifique de protéines par le protéasome 26S. La protéine SLF/SFB produite par le pollen dispose d'un F-box en N-terminal et, tout comme les S-RNases, de deux domaines hypervariables (Kao et Tsukamoto, 2004). Dans le cas de SLF/SFB, le F-box servirait pour la reconnaissance spécifique d'une forme allélique de S-RNase, plutôt que pour la dégradation de celle-ci (voir plus bas pour le modèle du double inhibiteur).

1.2.2 Le modèle génétique

Quelle que soit la forme allélique des S-RNases, elles sont incorporées dans le tube pollinique lors de sa croissance dans le tissu transmetteur (Luu *et al.*, 2000). De plus, nous savons que le pollen diploïde provenant d'une plante tétraploïde n'est pas reconnu même si celui-ci possède un allèle S en commun au style qui le reçoit (de Nettancourt, 1977 et Chawla *et al.*, 1997). Dans ce cas, seuls les grains de pollen diploïde portant deux locus S différents peuvent former des graines lors d'une auto-pollinisation, alors qu'un pollen homogénique diploïde se comporte comme un grain de pollen haploïde normal (Chawla *et al.*, 1997). Par contre, un style exprimant une S-RNase à double spécificité (qui est capable de reconnaître plus d'un allèle pollinique) est tout de même capable de reconnaître le pollen d'une plante tétraploïde (Luu *et al.*, 2001). Prenant compte de ces informations, le modèle le plus accepté à ce jour de la réponse d'auto-incompatibilité est celui du double inhibiteur. C'est-à-dire que, lorsqu'un

tube pollinique croît dans la matrice du style, les deux allèles de la S-RNase sont incorporés dans le tube. Un inhibiteur général des ribonucléases inhibe l'action de toutes les S-RNases. Si le tube pollinique dispose d'un locus S différent, il y a alors croissance ininterrompue du tube pollinique. Dans le cas où le tube pollinique aurait un locus S identique au parent femelle, l'inhibiteur général inhibe la S-RNase compatible abolissant ainsi son activité. Par contre l'allèle pollinique SLF/SFB reconnaîtra la forme allélique incompatible de l'autre S-RNase, empêchant l'action de l'inhibiteur général. Cette S-RNase sera donc active, dégradera les ARNs et le tube pollinique arrêtera sa croissance (Luu *et al.*, 2001 et Kao et Tsukamoto, 2004). L'hypothèse du double inhibiteur n'implique pas nécessairement deux éléments, il se pourrait fort bien qu'une seule et même protéine porte les deux activités. Dans ce cas, SLF/SFB aurait, en plus de son domaine de reconnaissance allèle-spécifique, un domaine d'inhibition générale des S-RNases.

1.2.3 Les gènes modificateurs

Une expérience de transfert de fragments chromosomiques contenant le locus S de l'espèce auto-incompatible *Lycopersicon hirsutum* vers l'espèce auto-compatible *L. esculentum* s'est soldée par un échec (Bernatzky *et al.*, 1995). Dans certains cas, il semble qu'il soit impossible d'introduire un système d'auto-incompatibilité fonctionnel, le locus S est donc insuffisant pour modifier la réponse de reconnaissance. Il y a par conséquent d'autres gènes, non liés au locus S, qui affectent le fonctionnement de la

réaction d'auto-incompatibilité. Ces gènes sont nommés gènes modificateurs et rendent la plante auto-compatible malgré le fait que la paire S-RNase / SLF/SFB soit intacte. Le produit de certains de ces gènes modificateurs demeure encore inconnu. Un gène modificateur peut affecter l'expression de l'un ou l'autre des composantes du locus S, comme c'est le cas pour le locus Sli (S locus inhibitor) chez *S. chacoense* qui inactive l'allèle pollinique (Hosaka et Hanneman, 1998a et b). Alors que chez *P. axillaris*, il existe un modificateur qui module négativement l'expression spécifique de l'allèle S-RNase S_{13} qui rend auto-compatible l'individu qui le porte (Tsukamoto *et al.*, 1999). Jusqu'à ce jour, le seul gène modificateur caractérisé à l'échelle moléculaire est le gène *HT*, qui code pour une petite protéine riche en asparagine. Le gène *HT* a été isolé chez *Nicotiana alata* et est exprimé dans le style (McClure *et al.*, 1999). La protéine possède en N-terminal un peptide signal de sécrétion qui la localiserait à l'extérieur de la cellule. Chez *Nicotiana*, il a été démontré que lorsque que l'expression du gène *HT* est abolie par sur-expression antisens, les plantes transgéniques deviennent auto-compatibles permettant ainsi aux tubes polliniques de croître au travers du style et ce, malgré le fait que les niveaux de transcrits des S-RNases restent inchangés (McClure *et al.*, 1999). D'autres évidences corrélatives ont été publiées sur l'implication du modificateur HT sur l'auto-incompatibilité de diverses espèces auto-compatibles de tomate (Kondo *et al.*, 2002a et b).

Certains auteurs prétendent que la protéine HT aide au transport des S-RNases de la matrice du style vers l'intérieur du tube pollinique où elles pourraient alors jouer leurs rôles cytotoxiques dans les gamétophytes mâles incompatibles (Cruz-Garcia *et al.*, 2003 et Kao et Tsukamoto, 2004). Nous croyons que ce n'est pas tout à fait le cas. Nous

présentons au chapitre II la caractérisation fonctionnelle de la famille des protéines HT chez *S. chacoense*. Nous y proposons également un mode d'action basé sur le prolongement de la sénescence du style.

1.2.4 Les récepteurs / ligands et l'auto-incompatibilité

Pour relayer l'information intercellulaire, les plantes, comme les animaux, utilisent des systèmes de communication impliquant entre autres des récepteurs transmembranaires. Chez *A. thaliana*, il existe plus de 400 récepteurs kinases (Shiu et Bleecker, 2001). Un récepteur kinase est une protéine transmembranaire qui dispose d'un domaine extracellulaire récepteur et un domaine intracellulaire kinase. La perception d'hormones et de petites protéines de signalisation se fait par le domaine récepteur ce qui active par la suite l'activité du domaine kinase qui peut alors moduler une réponse dans la cellule. En ce qui concerne les petites protéines sécrétées qui agissent comme peptides de signalisation, il existe moins de consensus de structure moléculaire. Ces types de peptides sont souvent variés et codés par de larges familles de gènes (Germain *et al.*, 2005b). Chez les *Brassicaceae*, le système de reconnaissance du pollen génétiquement semblable est de type sporophytique nécessitant deux composantes multi-alléliques. La reconnaissance est établie par une voie de signalisation impliquant un récepteur transmembranaire kinase, nommé SRK, exprimé dans le stigmate (Takasaki *et al.*, 2000) et un ligand pollinique sécrété qui se retrouve à la surface du grain de pollen, nommé SCR (Schopfer *et al.*, 1999 et Takayama *et al.*,

2000). Lorsqu'une des formes alléliques du ligand pollinique est reconnue par le récepteur SRK, une voie de signalisation est activée dans la cellule papillaire du stigmate ce qui empêchera ce pollen de s'hydrater et de germer.

La famille de protéines HT présente plusieurs caractéristiques propres aux peptides de signalisation. Le gène de *HT-B* code pour une petite protéine d'environ 9 kDa ayant un peptide de localisation extracellulaire en N-terminal et un agencement conservé des cystéines qui suggère que ces dernières sont importantes pour la structure de la protéine par l'établissement de ponts disulfures dans le réticulum endoplasmique. De plus, plusieurs peptides de signalisation sont préalablement clivés d'une prépropeptide avant d'être fonctionels. Les phytosulfokines (Yang *et al.*, 1999), la systémine (Pearce et Ryan, 2003) et les « rapid alkalination factors » (RALF) (Franssen et Bisseling, 2001) sont des peptides de signalisation dont la forme mature est produite par le clivage d'un précurseur. Tout comme les prépropeptides RALFs, la présence de deux résidus basiques successifs dans la séquence peptidique de HT laisse présager que ce dernier pourrait être clivé en un peptide actif plus petit d'environ 5,5 kDa. Pour le préproRALF, le clivage pourrait se faire par une sérine protéase de la famille des kexines (Franssen et Bisseling, 2001). Pour ces raisons, nous croyons que les protéines HT pourraient agir comme peptides de signalisation. Aucune évidence n'indique que la protéine HT est reconnue par un récepteur de type kinase, mais c'est le cas pour plusieurs autres peptides de signalisation dont seules les fonctions sont connues mais dont le mode de signalisation en aval demeure encore mystérieux (Germain *et al.*, 2005b).

1.3 L'embryogenèse

Sans mauvais jeux de mots, les premiers concepts d'embryogenèse prennent naissance suite à la double fécondation de la cellule œuf et de la cellule centrale. La cellule centrale donnera un tissu nourricier triploïde, l'albumen, qui assurera un support nutritif durant le développement de l'embryon alors que la cellule œuf, une fois fécondée, devient le zygote. Peu après la fécondation, la cellule du zygote s'allonge et se divise de manière asymétrique pour générer un embryon polaire formé de deux cellules de taille et de densité cytosolique différentes. La cellule apicale et ses cellules descendantes subiront deux divisions longitudinales successives suivies d'une division transversale donnant naissance à l'embryon proprement dit. Chez les *Solanaceae*, il n'y a pas de division transversale, mais bien trois divisions longitudinales. Quant à la cellule basale et ses cellules descendantes, elles se diviseront de manière transversale uniquement ce qui donnera origine à une pile de cellules dont la cellule la plus apicale formera l'hypophyse et les autres formeront le suspenseur. À ce point, quatre régions distinctes de cet embryon donneront naissance à différentes couches de cellules avec des destins cellulaires qui leur sont propres (Figure 2). Premièrement, les quatre cellules apicales de l'embryon vont donner naissance au méristème apical et à la majeure partie des cotylédons. Ensuite, les quatre autres cellules de cet embryon à huit cellules seront les précurseurs de l'hypocotyle, la racine et une partie de son méristème ainsi qu'une contribution minimale au développement des cotylédons. La cellule hypophysale contribue à générer le reste du méristème de la racine, le centre quiescent et, bien sûr, les cellules souches produisant la coiffe de la racine. Les cellules du suspenseur sont, quant

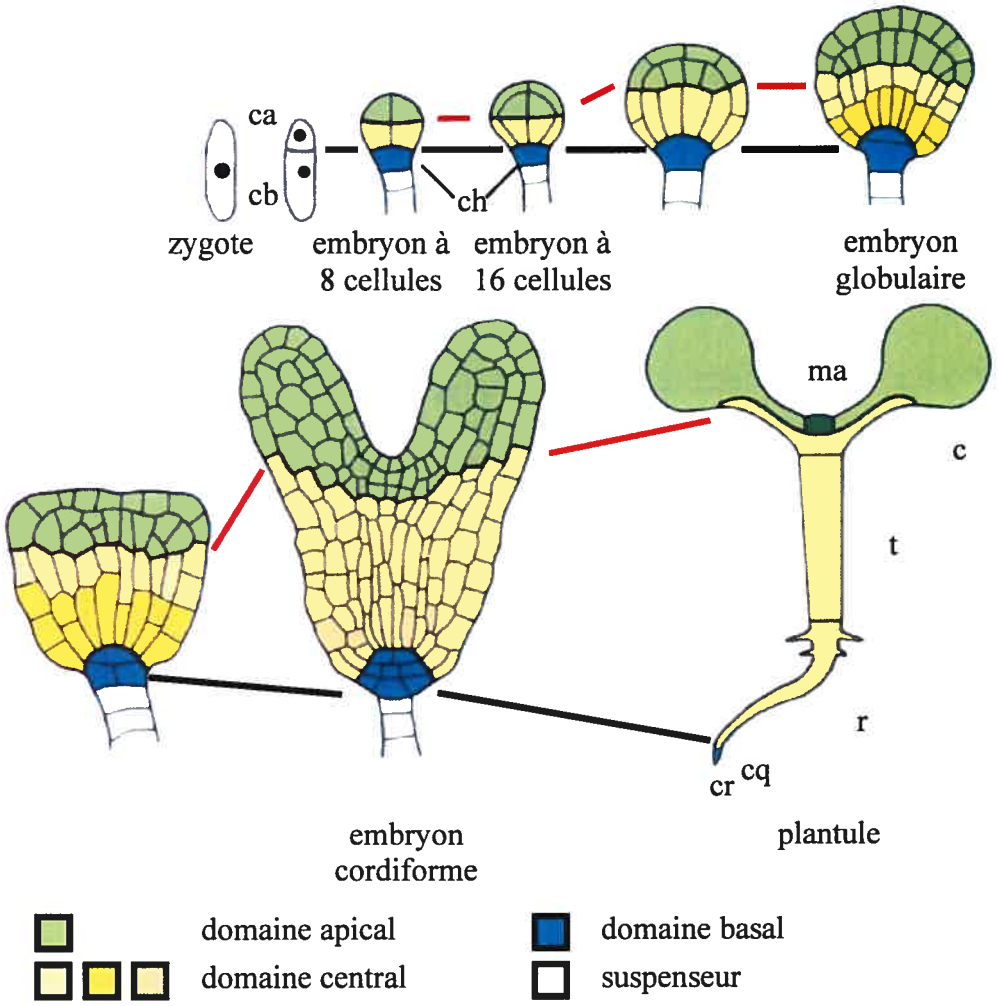

Figure 2

Représentation schématique de l'embryogenèse. Coupes longitudinales d'embryons à différents stades de développement. Les cellules au dessous des traits noirs prennent leur origine de la cellule basale (cb) et, celles au dessus des traits noirs, de la cellule apicale (ca). Les traits rouges délimitent le domaine apical de l'embryon du domaine central. Cellule hypophysale (ch), centre quiescent (cq), coiffe de la racine (cr), méristème apical (ma), racine (r) et tige (t). Tiré et modifié de Laux *et al.* (2004, page S191) avec la permission de ©2004 American Society of Plant Biologist.

à elles, sollicitées pour relier l'embryon aux tissus maternels. Après plusieurs divisions orchestrées, cet embryon changera de forme afin d'atteindre un stade mature. Dans l'ordre, l'embryon à huit cellules passera à seize cellules et par la suite à un stade globulaire. Au stade cordiforme, les premières ébauches des cotylédons sont visibles alors qu'au stade torpille, les méristèmes apical et racinaire sont établis ainsi que l'ensemble de cellules qui donneront naissance au tissu vasculaire. À partir de ce stade, les patrons de développement sont bien entamés et l'organisation tissulaire est déjà garante de la structure mature. Le processus d'embryogenèse se termine par l'obtention d'une entité végétale pourvue de deux cotylédons, d'un méristème apical, d'un hypocotyle, d'un système vasculaire et d'un méristème racinaire (Figure 2).

1.3.1 Le développement moléculaire de l'embryon

L'information positionnelle d'une cellule dicte son cheminement de différenciation au sein de l'embryon (Poethig *et al.*,1986 et Malamy et Benfey, 1997). Ce type de mécanisme de différenciation nécessite une communication entre cellules. Dès la première division du zygote, plusieurs mécanismes moléculaires sont enclenchés. Plusieurs facteurs de transcription et modules de signalisation orchestrent ainsi les différents patrons de formation et les divers destins cellulaires. Nous décrirons brièvement les éléments moléculaires impliqués dans les divers patrons de formation afin de nous attarder sur le rôle des lipides de la voie de biosynthèse des

brassinostéroïdes dans le développement du domaine central de l'embryon. L'orientation développementale de l'embryon s'organise selon un axe apical/basal et un axe radial (Bowman, 1994). Nous verrons que, selon l'axe ou la région de l'embryon, plusieurs événements moléculaires différents sont solicités afin d'établir le bon patron développemental nécessaire à l'embryon.

1.3.2 La première division du zygote

Nous avons déjà mentionné que, dès la première division de la cellule zygotique, l'embryon montrait une polarité distincte entre la cellule basale et la cellule apicale. À ce jeune stade de développement, on observe déjà les premiers événements moléculaires qui généreront cette polarité marquée et des destins cellulaires très différents. Les gènes *PINFORMED7* (*PIN7*) et *WUSCHEL HOMEOBOX2* (*WOX2*) sont tous deux exprimés dans la cellule basale de l'embryon. La protéine PIN7 est un membre de la famille des PINs qui permet le transport polaire de l'auxine. PIN7 est localisée à la membrane apicale de la cellule basale et permet l'efflux d'auxine vers la cellule apicale (Friml *et al.*, 2003). Dans le mutant *pin7*, l'efflux d'auxine est modifié et la cellule apicale se divise alors de manière aberrante. Le mutant *wox2* possède le même phénotype que *pin7* (Haecker *et al.*, 2004). La première division cellulaire de l'embryon chez *A. thaliana* est invariable, et l'expression de PIN7 et WOX2 est capitale pour l'établissement de l'identité cellulaire de la cellule apicale à ce stade très précoce du développement embryonnaire.

De plus, la différence de taille entre les deux premières cellules n'influence pas leur identité. L'analyse du mutant *gnom* (*gn*) nous indique que la position des cellules, l'une par rapport à l'autre, est plus importante pour l'identité cellulaire. En effet, dans le mutant, le zygote se divise de manière aléatoire donnant une cellule apicale et basale de taille variable. La cellule basale formera tout de même le suspenseur et la cellule apicale, l'embryon à huit cellules (Mayer *et al.*, 1993). Ce n'est que plus tard que l'embryon subira des répercussions plus graves, où, dans le pire des cas, l'axe apical/basal est complètement aboli laissant un embryon mature de forme globulaire (Mayer *et al.*, 1993). Le produit du gène GN code pour une protéine qui inhibe l'activité de protéines G par l'échange de guanosine (protéine GEF). GN influence la localisation de la protéine PIN1 au niveau de la membrane plasmique, permettant un efflux d'auxine dans la bonne direction (Geldner *et al.*, 2003).

1.3.3 L'organisation du méristème embryonnaire apical

Le méristème apical est le centre de formation post-embryonnaire des organes. L'ébauche de ce méristème se forme entre le stade cordiforme et le stade torpille, mais les cellules initiatrices sont présentes dès le stade globulaire. La spécification des cellules initiatrices pour la formation du domaine apical est influencée par les gènes *GURKE* (*GK*) et *TOPLESS* (*TPL*). Dans le mutant *gk*, le méristème embryonnaire apical ne se forme pas correctement (Torres-Ruiz *et al.*, 1996) alors que dans le mutant *tpl* le

méristème embryonnaire apical peut opter pour un méristème racinaire donnant ainsi naissance à des racines plutôt que des primordia de feuilles (Long *et al.*, 2002). L'établissement des cellules souches est établi par l'activité du facteur de transcription WUSCHEL (WUS) et du couple récepteur/ligand CLAVATA1/3 (CLV1/3). WUS maintient les cellules dans un état indifférencié alors que le rôle du peptide de signalisation CLV3 est de restreindre l'expression de *WUS* dans les cellules souches. Cette boucle de rétroaction négative régule l'homéostasie du méristème, qui est établie dès le stade cordiforme (Schoof *et al.*, 2000). Le développement du méristème apical est également limité de manière radiale, dans ce cas l'implication de WUS et de CLV3 n'est pas sollicitée et ce sont les protéines CUC1/2/3 qui prennent cette fonction. L'expression des gènes *CUC1/2/3* est périphérique à la zone centrale du méristème (Aida *et al.*, 1999). Dans les doubles mutants et le triple mutant *cuc*, les cellules qui délimitent les marges de croissance des cotylédons se fusionnent créant par le fait même la perte du méristème apical et la fusion des cotylédons (Aida *et al.*, 1999 et Vroemen *et al.*, 2003).

L'endroit exact où doit se développer le méristème apical serait dicté par le gène *ZWILLE* (*ZLL*) qui code pour une protéine de la famille PIWI/ARGONAUTE impliquée dans les mécanismes d'interférence d'ARN. L'expression ectopique de ZLL provoque l'apparition de méristème apical là où il est exprimé (Newman *et al.*, 2002) alors que dans le mutant *zll*, diverses structures différenciées sont formées à la place du méristème apical embryonnaire (Lynn *et al.*, 1999).

1.3.4 L'organisation du méristème embryonnaire de la racine

À l'intérieur du centre quiescent, un groupe de cellules maintient les cellules souches du méristème racinaire dans une forme indifférenciée et ce, par une accumulation d'auxine. Ce sont les cellules différenciées autour du méristème racinaire qui incitent les cellules sœurs des cellules souches à opter pour un destin cellulaire autre que celui d'une cellule indifférenciée. En somme, le contexte environnemental d'une cellule prête à se différencier lui indique quel destin cellulaire adopter. L'activité du méristème racinaire est donc maintenue par une signalisation des cellules du centre quiescent qui inhibe la différenciation alors que les cellules matures en périphérie induisent la différenciation aux cellules qui quittent la zone du méristème (Malamy et Benfey, 1997).

L'établissement des cellules initiatrices du méristème embryonnaire de la racine s'effectue par une sur-accumulation d'auxine dans la région de l'hypophyse. Les mutants *bodenlos* (*bdl*) (Hamann *et al.*, 1999) et *monopteros* (*mp*) (Berleth et Jurgens, 1993) ont un impact sur le développement des cellules basales de l'embryon à huit cellules. Étant donné que ces dernières sont ontologiquement impliquées dans l'établissement d'une partie des cotylédons, de la racine et d'une partie de son méristème, les mutants les plus sévères montrent des phénotypes où les jeunes plantules n'ont plus de racines, de méristème racinaire et même d'hypocotyle. BDL et MP sont

impliqués dans la réponse à l'auxine. Le gène *MP* code pour une protéine ARF (ARF5) qui module négativement l'activité de régulateurs de transcription de type AUX-IAA. En présence d'auxine, les protéines ARF peuvent se libérer des AUX-IAA. Quant au gène *BDL*, il code justement pour un AUX-IAA (IAA12). Ces derniers ont pour effet de réprimer l'activation des gènes qui répondent à l'auxine. Puisque le mutant *mp* est une perte de fonction et le mutant *bdl* un gain de fonction, l'expression des gènes qui répondent à l'auxine est donc réprimée ce qui a pour effet de perturber le développement racinaire et ce, même si *BDL* et *MP* ne sont pas exprimés dans l'hypophyse (Hamann *et al.*, 2002).

1.3.5 L'organisation radiale de l'embryon

La première manifestation de l'organisation radiale s'établit très tôt dans le développement de l'embryon. Dès le stade globulaire, on peut observer dans les plans radial et transversal, la présence d'une couche de cellules épidermales, une couche de cellules corticales et des cellules qui occupent le centre de l'embryon. Ces dernières feront office de cellules vasculaires. Si la formation de l'axe radial est bien connue au niveau histologique, elle l'est beaucoup moins au niveau moléculaire. Plusieurs facteurs de transcription montrent une expression radiale dans l'embryon d'*A. thaliana*: ARABIDOPSIS THALIANA MERISTEM LAYER1 (ATML1) (Abe *et al.*, 2003), PROTODERMAL FACTOR2 (PDF2) (Abe *et al.*, 2003), SHORT ROOT (SHR) (Helariutta *et al.*, 2000), SCARECROW (SCR) (Di Laurenzio *et al.*, 1996) et

GLABRA2 (GL2) (Costa et Dolan, 2003). De plus, dans le mutant *wooden leg* (*wol*), les cellules précurseures du système vasculaire subissent une division périclinale en moins, ce qui a pour effet de réduire le nombre de cellules dans l'hypocotyle et dans le système vasculaire (Mahonen *et al.*, 2000). WOL est un récepteur transmembranaire de type histidine kinase qui pourrait moduler la perception des cytokinines dans la racine.

1.3.6 L'organisation du domaine central

Les quatre cellules basales de l'embryon à huit cellules se divisent horizontalement et donnent naissance ainsi à des cellules filles apicales, qui donneront la base des futurs cotylédons et à des cellules filles basales, qui donneront l'hypocotyle, la racine et les cellules proximales du méristème embryonnaire racinaire (Figure 2). Plusieurs mutants affectent l'organisation du domaine central de l'embryon. Étrangement, les gènes qui sont impliqués dans le développement du domaine central codent pour des enzymes liées à la voie de biosynthèse des brassinostéroïdes : FACKEL (FK) (Jang *et al.*, 2000 et Schrick *et al.*, 2000), HYDRA1 (HYD1) (Topping *et al.*, 1997), STEROL METHYL-TRANSFERASE1 (SMT1) (Diener *et al.*, 2000) et l'obtusifoliol 14α-déméthylase (CYP51G1-At) (O'Brien *et al.*, 2005a). En ce qui concerne les mutants *fk*, *hyd1* et *stm1*, les cellules du domaine central de l'embryon n'arrivent pas à s'allonger et à se diviser de manière asymétrique afin de donner naissance aux cellules précurseures du tissu vasculaire. Ce n'est que plus tard dans le développement de l'embryon, que les mutants *fk* (Jang *et al.*, 2000 et Schrick *et al.*,

2000), *hyd1* (Topping *et al.*, 1997), *smt1* (Diener *et al.*, 2000) et *cyp51g1-at* (O'Brien *et al.*, 2005a) montrent des anormalités dans les domaines apical et basal affectant par la même occasion la viabilité de l'embryon mature. Tous ces mutants ne peuvent être sauvés par l'application exogène de brassinostéroïdes, ce qui laisse présager qu'une sur-accumulation d'un ou plusieurs intermédiaires de synthèse en amont crée une désorganisation du patron de développement de l'embryon ou bien, qu'un intermédiaire en aval autre que le brassinostéroïde est nécessaire au bon développement de l'embryon. La désorganisation du patron développemental de l'embryon ainsi que l'inefficacité de l'application exogène de brassinostéroïdes à rétablir le phénotype normal sont caractéristiques de tous les mutants affectant les enzymes de la voie de biosynthèse en amont du stérol 24-méthylène-iophénol. Trois hypothèses sont avancées. Premièrement, soit l'accumulation de l'intermédiaire en amont est toxique et cause la désorganisation embryonnaire, soit un intermédiaire en aval est maintenant manquant et ne peut effectuer sa fonction de signalisation comme lipide bioactif, ou bien, un ou plusieurs intermédiaires en aval sont nécessaires pour la composition de la membrane plasmique. On pourrait penser, que dans ce dernier cas, l'établissement des radeaux lipidiques serait affecté de manière à désorganiser la localisation de récepteurs transmembranaires, comme les protéines PIN, affectant ainsi la polarité des cellules. Cette hypothèse pourrait expliquer les phénotypes observés chez les mutants *fk*, *hyd1* et *stm1* que nous avons mentionnés précédemment. En effet, dans le mutant *stm1*, la localisation de protéines PIN est affectée (Willemsen *et al.*, 2003). Les radeaux lipidiques sont des sous-domaines lipidiques de la membrane plasmique et qui permettraient le partitionnement de cette dernière comme une mosaïque. Les radeaux lipidiques créent des micro-environnements qui permettent le rassemblement et l'activation de récepteurs

et de canaux (Simons et Toomre, 2000). Chez les plantes, ce type de contextes plasmiques commence tout juste à être étudié (Bhat et Panstruga, 2005).

I.3.7 Les 14α-déméthylases

Le chapitre III traitera de l'implication des stérols dans le développement embryonnaire et la signalisation lipidique par l'obtusifoliol, mais plus spécifiquement sur le rôle de l'enzyme CYP51G1-Sc et CYP51G1-At. Cette enzyme, l'obtusifoliol 14α-déméthylase, fait partie de la famille des cytochromes P450, des enzymes qui utilisent un hème de fer pour l'oxydation de divers produits chimiques. Cette 14α-déméthylase est le seul cytochrome P450 qui se retrouve dans presque tous les règnes du vivant. Le substrat, quant à lui, diffère selon le règne, le lanostérol chez les mammifères, le 24-méthylène-24,25-dihydrolanostérol chez les champignons et l'obtusifoliol chez les plantes. Chez les mammifères et les champignons, l'enzyme est capable de reconnaître les substrats des enzymes des autres règnes alors que l'enzyme chez les plantes à une spécificité stricte pour son substrat, l'obtusifoliol (Lamb *et al.*, 1998). La déméthylation des stérols nécessite trois étapes successives de monooxygénation du groupement méthyl-C14α afin de produire une double liaison du carbone numéro quatorze (Werck-Reichhart et Feyereisen, 2000). La voie de biosynthèse impliquant la 14α-déméthylase mène à la production de cholestérol chez les animaux, d'ergostérol chez les levures et les champignons et de brassinostéroïdes chez les plantes (Schuler et Werck-Reichhart,

2003). Les brassinostéroïdes sont des phytohormones qui agissent en tant que régulateurs de la croissance comme l'élongation cellulaire, l'inhibition de la croissance racinaire, le développement de la feuille, la croissance du tube pollinique et sur la photomorphogenèse (Clouse, 2002a et b).

Acronyme	Nom du gène	Identité biochimique	Fonction biologique
ACR4	*CRINKLY4*	Récepteur kinase de type LRR	Développement des sépales Développement des téguments Embryogenèse
AG	*AGAMOUS*	Facteur de transcription de type MADS	Gène de type C Développement des étamines Développement du pistil Développement de l'ovule
ANT	*AINTEGUMENTA*	Facteur de transcription de type AP2	Développement du placenta
AP1	*APETALA1*	Facteur de transcription de type MADS	Gène de type A Développement des sépales Développement des pétales
AP2	*APETALA2*	Facteur de transcription de type AP2	Gène de type A Développement des sépales Développement des pétales
AP3	*APETALA3*	Facteur de transcription de type MADS	Gène de type B Développement des pétales Développement des étamines
ARF5 (ou *MP*)	*AUXIN RESPONSE FACTOR 5*	Répresseur de la transcription de type ARF	Développement de la racine de l'embryon
ATML1	*ARABIDOPSIS THALIANA MERISTEM LAYER1*	Facteur de transcription de type HD-Zip	Établissement de l'organisation radiale de l'embryon
BDL (ou *IAA12*)	*BODENLOS*	Répresseur de la transcription de type AUX-IAA	Développement de la racine de l'embryon
BEL1	*BELL1*	Facteur de transcription de type HD-Zip	Développement de l'ovule Développement des téguments
BRI1	*BRASSINOSTEROID INSENSITIVE 1*	Récepteur kinase de type LRR	Perception des brassinostéroïdes
CLV1	*CLAVATA1*	Récepteur kinase de type LRR	Développement du méristème
CLV3	*CLAVATA3*	Peptide de signalisation	Développement du méristème
CPH (ou *SMT1*)	*CEPHALOPOD*	Méthyle transférase	Voie de biosynthèse des brassinostéroïdes Développement du domaine central de l'embryon Polarité des PINs

Acronyme	Nom du gène	Identité biochimique	Fonction biologique
CRC	*CRABS CLAW*	Facteur de transcription de type YABBY	Développement du placenta Initiation des ovules
CUC1/2/3	*CUP-SHAPED COTYLEDONS 1/2/3*	Facteur de transcription de type NAC	Délimitent le méristème apical de l'embryon Délimitent le site d'initiation des ovules Développement des cotylédons
EMS1 (ou *EXS*)	*EXCESS MICROSPOROCYTES*	Récepteur kinase de type LRR	Développement du tapetum Développement de l'embryon
EXS (ou *EMS1*)	*EXTRA SPOROGENOUS CELLS1*	Récepteur kinase de type LRR	Voir *EMS1*
GL2	*GLABRA2*	Facteur de transcription de type HD-Zip	Expression radiale dans l'embryon
GK	*GURKE*	Acétyl-CoA Carboxylase	Initiation du méristème apical de l'embryon
GN	*GNOM*	Facteur d'échange de la guanine (GEF)	Influence la première division du zygote Développement de l'embryon Localisation de PIN1
HLL	*HUELLENLOS*	Protéine ribosomale L14	Développemenet du primordium de l'ovule
HYD1	*HYDRA1*	Isomérase	Voie de biosynthèse des brassinostéroïdes Développement du domaine central de l'embryon
IAA12 (ou *BDL*)	*BODENLOS*	Répresseur de la transcription de type AUX-IAA	Voir *BDL*
LUG	*LEUNIG*	Répresseur de la transcription	Développement du placenta
MP (ou *ARF5*)	*MONOPTEROS*	Répresseur de la transcription de type ARF	VOIR *ARF5*
PDF2	*PROTODERMAL FACTOR 2*	Facteur de transcription de type HD-Zip	Expression radiale dans l'embryon

Acronyme	Nom du gène	Identité biochimique	Fonction biologique
PI	*PISTILLATA*	Facteur de transcription de type MADS	Gène de type B Développement des pétales Développement des étamines
PIN1	*PINFORMED 1*	Transport polaire de l'auxine	Développement de l'embryon
PIN7	*PINFORMED 7*	Transport polaire de l'auxine	Polarité de l'embryon à deux cellules Transport de l'auxine vers la cellule apicale
SEP1/2/3	*SEPALATA1/2/3*	Facteur de transcription de type MADS	Identité de l'ovule
SERK1/2	*SOMATIC EMBRYOGENESIS RECEPTOR-LIKE KINASE1/2*	Récepteur kinase de type LRR	Développement de l'embryon somatique Développement du tapetum
SHP1/2	*SHATTERPROOF1/2*	Facteur de transcription de type MADS	Identité de l'ovule Ouverture des siliques
SHR	*SHORT ROOT*	Facteur de transcription de type GRAS	Expression radiale dans l'embryon Développement radial de la racine
SMT1 (ou *CPH*)	*STEROL METHYL-TRANSFERASE 1*	Méthyle transférase	Voir *CPH*
SPL	*SPATULA*	Facteur de transcription de type bHLH	Développement du placenta Développement de la marge des siliques Site d'initiation des primordia d'ovules
STK	*SEEDSTICK*	Facteur de transcription de type MADS	Identité de l'ovule
STM	*SHOOT MERISTEMLESS*	Facteur de transcription de type HD	Maintien des cellules souches du placenta Délimite le site d'initiation des ovules
SUB	*STRUBBELIG*	Récepteur kinase de type LRR	Développement du tégument externe de l'ovule
SUP	*SUPERMAN*	Facteur de transcription de type zinc finger (C2H2)	Répression des gènes de type B dans le dernier verticille Développement du tégument externe de l'ovule

Acronyme	Nom du gène	Identité biochimique	Fonction biologique
TPD1	*TAPETUM DETERMINANT 1*	Peptide de signalisation	Développement du tapetum
TPL	*TOPLESS*	WD40	Identité du méristème apical de l'embryon
TSL	*TOUSLED*	Kinase de type sérine/thréonine	Développement du placenta Site d'initiation des primordia d'ovules
UFO	*UNUSUAL FLORAL ORGAN*	Ligase ubiquitine E3 de type f-box	Positionnement des gènes de type B dans le deuxième et le troisième verticille
WOL	*WOODEN LEG*	Récepteur kinase de type histidine	Perception des cytokinines Développement radial de l'embryon Développement du système vasculaire
WOX2	*WUSCHEL HOMEOBOX 2*	Facteur de transcription de type HD	Polarité de l'embryon à deux cellules
WUS	*WUSCHEL*	Facteur de transcription de type HD	Maintien des cellules souches dans un état indifférencié
YDA	*YODA*	Kinase de type MAPKKK	Développement des stomates Développement de l'embryon
ZLL	*ZWILLE*	Protéine de type PAZ se liant à l'ADN et l'ARN	Site d'initiation du méristème apical de l'embryon

Tableau 1

Description des fonctions biologiques des gènes liés au développement. Liste et descriptif des gènes qui ont été cités dans le chapitre I de cette thèse et qui ont une implication développementale chez *A. thaliana*.

Chapitre II.

Molecular analysis of the stylar-expressed Solanum chacoense small asparagine-rich protein family related to the HT modifier of gametophytic self-incompatibility in Nicotiana

Martin O'Brien, Christelle Kapfer, Geneviève Major, Mélanie Laurin, Charles Bertrand, Katsuhiko Kondo, Yasuo Kowyama, et Daniel P. Matton

Publié dans The Plant Journal (2002) 32, 985-996

II.1 Contribution des coauteurs

Les formes alléliques du gène HT chez *Solanum chacoense* et chez les autres espèces n'ont pas été trouvées par moi (travail de G. Major, M. Laurin stagiaires d'été, C. Bertrand assistant de recherche, K. Kondo un collaborateur étudiant japonais et Y. Kowyama son directeur de recherche). Par contre, j'ai moi-même isolé la version HT-B chez *S. chacoense* par PCR avec des amorces dégénérées. J'ai fait toutes les expérimentations nécessaires à la production de cinq des six figures. La production des plantes transgéniques HT-A par C. Kapfer ont été utilisées pour deux de ces cinq figures, alors que j'ai généré les lignées d'interférence pour HT-B. Presque la totalité des données non montrées de l'article (« data not shown »), n'impliquant pas les analyses de séquences, sont des expériences que j'ai faites (7 expériences sur les 8 non montrées).

II.2 Page titre

Molecular analysis of the stylar-expressed *Solanum chacoense* small asparagine-rich protein family related to the HT modifier of gametophytic self-incompatibility in *Nicotiana*

O'Brien, M.[1], Kapfer, C.[1], Major, G.[1], Laurin, M.[1], Bertrand, C.[1], Kondo, K.[2], Kowyama, Y.[2], and Matton, D. P.[1]*

*Author for correspondance

[1]Institut de recherche en biologie végétale,

Département de Sciences Biologiques, Université de Montréal

4101 Sherbrooke est, Montréal, Québec, Canada H1X 2B2

Tel: 514-872-3967

FAX: 514-872-9406

[redacted]

[2] Faculty of Bioresources, Mie University,

Tsu, 514-8507, Japan

99.3 Keywords

Self-incompatibility, S-RNase, Solanaceae, *HT* modifier gene, RNA interference.

99.4 Genbank accession number

ScHT-A$_1$ (AF442139), *ScHT-A*$_2$ (AF442140), *ScHT-B*$_1$ (AF442141), *StHT-A*$_1$ (AF442142), *SbHT-B*$_1$ (AF442143), *SbHT-B*$_2$ (AF442144), *SpHT-B*$_1$ (AF442145), *SpHT-B*$_2$ (AF442146), *LpHT-A*$_1$ (AB066582) *LpHT-B*$_1$ (AB066583), and *S*$_{14}$*-RNase* (AF232304).

99.5 Abstract

Gametophytic self-incompatibility (GSI) systems involving the expression of stylar ribonucleases have been described and extensively studied in many plant families including the *Solanaceae*, the *Rosaceae*, and the *Scrophulariaceae*. Pollen recognition and rejection is governed in the style by specific ribonucleases called S-RNases, but in many SI systems, modifier loci that can modulate the SI response have been described at the genetic level. Here we present at the molecular level, the isolation and characterization of two *Solanum chacoense* homologues of the *Nicotiana* HT modifier, that had been previously shown to be necessary for the SI reaction to occur in *Nicotiana alata* (McClure *et al.*, 1999). HT homologues from other solanaceous species have also been isolated and a phylogenetic analysis reveals that the *HT* genes fall into two groups. In *S. chacoense*, these small proteins named ScHT-A and ScHT-B are expressed in the style and are developmentally regulated during anthesis identically to the S-RNases, as well as following compatible and incompatible pollinations. To elucidate the precise role of each HT isoform, anti-sense *ScHT-A* and RNAi *ScHT-B* lines were generated. Conversion from SI to self-compatibility was only observed in RNAi *ScHT-B* lines with reduced levels of *ScHT-B* mRNA. These results confirm the role of the HT modifier in Solanaceous SI and indicate that only the HT-B isoform is directly involved in SI.

II.6 Introduction

Self-incompatibility (SI) constitutes an important mechanism for preventing inbreeding through specific pollen recognition and rejection. In the most widespread type of gametophytic SI (GSI), the haploid pollen is rejected when the S-allele it expresses matches either of the two S-alleles expressed in the sporophytic tissue of the pistil. For the *Solanaceae*, the GSI phenotype is specified by a highly multiallelic S-locus (de Nettancourt, 1977, 1997), whose only known product is a secreted ribonuclease (McClure *et al.*, 1989) expressed in the transmitting tissue of the style (Anderson *et al.*, 1986; Matton *et al.*, 1998) and called an S-RNase. Gain-of-function experiments in self-incompatible plants have shown that expression of an *S-RNase* transgene is sufficient to alter the SI phenotype of the pistil but not that of pollen (Lee *et al.*, 1994; Murfett *et al.*, 1994; Matton *et al.*, 1997). Furthermore, transgenic plants made to express high levels of an S-RNase in pollen did not acquire the new phenotype (Dodds *et al.*, 1999), indicating that the *pollen S* gene (unknown to date) is clearly distinct from the *S-RNase* (Kao and McCubbin, 1996). In order to determine if expression of an active S-RNase is the sole determinant of SI in styles, transformation of closely related self-compatible species with *S-RNases* were attempted. Transformation of self-compatible *Nicotiana tabacum* or *Nicotiana plumbaginifolia* with an S-allele from the self-incompatible species *Nicotiana alata,* did not result in the acquisition of the SI phenotype (Murfett *et al.*, 1996), nor did the introgression of a chromosome fragment bearing the S-locus from the SI *Lycopersicon hirsutum* in SC *L. esculentum* (Bernatzky *et al.*, 1995), or the expression of an *S-RNase* from the SI *L. peruvianum* in

the SC *L. esculentum* (Kondo *et al.*, 2002b). Conversely, when an S-allele from the SC *Petunia hybrida* was introduced in SI *P. inflata*, it became functional in rejecting its corresponding self pollen, indicating that factors expressed in the *P. inflata* SI genetic background were needed for the SI reaction to occur (Ai *et al.*, 1991). These results strongly suggest that other factors are necessary for the SI reaction to occur. Some of these factors that affect the SI response have been described in numerous SI systems and often been named S-locus inhibitors or modifiers (de Nettancourt, 1977). In *S. chacoense*, an S-locus inhibitor (Sli) has been mapped to the distal end of chromosome 12, but has not been cloned yet (Hosaka and Hanneman, 1998a, b). To date, the only modifier functionally characterized at the molecular level is the *HT* gene, a stylar-expressed small asparagine-rich protein in *N. alata* (McClure *et al.*, 1999). The *NaHT* (*Nicotiana alata HT*) cDNA was isolated from a differential screen for SI stylar-specific transcripts, and anti-sense *Nicotiana HT* plants became self-compatible, although they still expressed normal levels of stylar *S-RNases*. Recent correlative evidence from mRNA expression studies in *Lycopersicon* species also suggest the involvement of the HT modifier in SI (Kondo *et al.*, 2002a; Kondo *et al.*, 2002b). Here we describe the characterization of *HT* homologues that are coordinately expressed with the *S-RNases* during pistil development in the SI species *S. chacoense*, and show that only the HT-B isoform is involved in SI.

99.7 Results

Isolation of the *Solanum* HT homologues and sequence comparison

The *ScHT-A1*, *ScHT-A2*, and *S14-RNase* cDNAs were isolated from a pollinated pistil cDNA library (see experimental procedures section). The *ScHT-A1* cDNA codes for a small protein of 99 amino acid residues with a highly predicted N-terminal signal peptide as determined from the SignalP algorithm (Nielsen *et al.*, 1997). The predicted cleavage site for ScHT-A_1 is before Arg-25, producing a mature polypeptide of 75 amino acids (8 kDa). The *ScHT-A2* cDNA is incomplete in the 5' region, but would comprise all of the mature protein (77 residues, 8,3 kDa) as predicted from the ScHT-A_1 deduced cleavage site. Both ScHT-A_1 and ScHT-A_2 predicted mature proteins are acidic with pIs of 3.98 and 4.11 respectively. Amino acid sequence comparison of the predicted mature polypeptides indicate that ScHT-A_1 and ScHT-A_2 are 96% identical (93% nucleotide sequence identity) and most probably correspond to allelic variants of the same gene (see linkage analysis below of the *ScHT-A* isoforms). The *ScHT-B1* isoform was obtained by PCR amplification with an upstream primer located in the signal peptide region and a downstream primer located 3' of the predicted stop codon from the *N. alata HT* and *S. chacoense HT-A1* isoforms. The ScHT-B_1 mature protein comprises 79 amino acids for a MW of 8.7 kDa with an acidic pI of 4.67, and is ≈ 51% identical (57% similar) at the amino acid level to the ScHT-A isoforms. No N-glycosylation sites are found on either polypeptide but 6 cysteine residues that could be involved in disulfide bonding are conserved between all HT homologues, except from the *Solanum pinnatisectum* B_1 isoform, that lacks one cysteine, and are found flanking a

striking C-terminal region containing 16 to 20 Asp (D) or Asn (N) residues. In the mature ScHT proteins, asparagine and aspartic acid residues account for roughly 30% of the total amino acids. A sequence alignment of the deduced amino acid sequences corresponding to the mature protein region of the *S. chacoense* HT isoforms as well as HT homologues from other SI solanaceous plants including *Lycopersicon peruvianum*, *Nicotiana alata*, *Solanum pinnatisectum*, *Solanum bulbocastanum* and from the self-compatible species *Solanum tuberosum,* is shown in Figure 1A. All *Solanum* and *Lycopersicon* sequences were obtained by PCR amplification with the same primer pairs as described for the amplification of *ScHT-B1*. Although all the HT sequences share some specific structural features, e.g., a C-terminal Asn/Asp-rich region flanked by conserved cysteine residues, they can be easily classified in two groups when the amino-terminal half of the protein is considered. Based on the Clustal X alignment, a phylogenetic analysis was performed to determine if this preliminary classification would hold true. Figure 1B shows that all the « B » isoforms fell into a highly supported cluster, while more sequence data would be needed to determine if the « A-type » sequences form one or more group. Interspecific amino acid sequence identities between the predicted mature polypeptides ranges from 76 to 86% in the A-isoform group, and 36 to 92% in the B-isoform group. The *ScHT-A1* and *ScHT-A2* (94%), *SbHT-B1* and *SbHT-B2* (98%) and SpHT-B_1 and *SpHT-B2* (97%) are most probably alleles of the same genes in their respective species. When the only non-*Solanum* sequence is removed (NaHT-B), the B-isoform group sequence identity is in the 77 to 92% range. One surprising feature is the very high conservation of the predicted signal peptides between species, as determined from the available complete HT cDNA sequences (ScHT-A_1, NaHT-B, LpHT-A_1, and LpHT-B_1), ranging from 66% to 100% identity

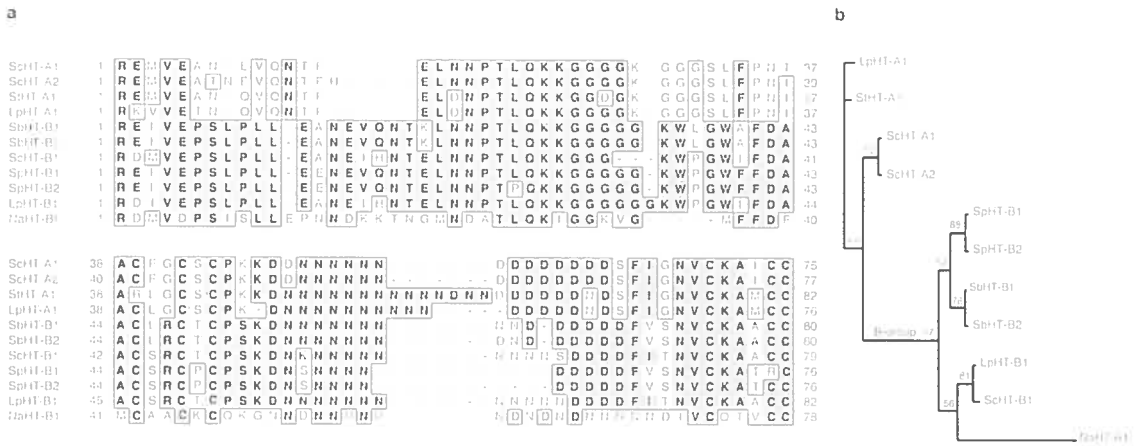

Figure 1

Sequence alignment (A) and phylogenetic analysis (B) of the deduced mature protein sequences of ScHT-A_1, ScHT-A_2 and ScHT-B_1 with related sequences from other solanaceous species. A Clustal X alignment was used to produce a phylogenetic analysis of related HT sequences in six solanaceous species. A jacknife analysis using Paup 4.08b was used to produce the phylogram shown in **B**.

(82% to 100% similarity), when compared to the mature protein sequences (data not shown). This intriguing situation is also observed with the sporophytic self-incompatibility (SSI) pollen S gene where the signal peptides are also far more similar to each other (mean of 77% identity and 89% similarity) than the mature protein sequences (29% identity and 38% similarity on average) when the sequences of five different SSI pollen S gene are compared (Schopfer *et al.*, 1999; Takayama *et al.*, 2000).

Tissue-specific and developmental regulation of the ScHT modifiers

Tissue-specific expression of *ScHT-A* and *ScHT-B* isoforms was determined using RNA extracted from different tissues of *S. chacoense*. Since the *ScHT-A*$_1$ and *ScHT-A*$_2$ cDNAs are 93% identical at the DNA level, the RNA gel blot analyses most probably reflect the expression of both genes although the probe used at all times was *ScHT-A*$_1$. Overall DNA sequence identity between the *ScHT-A* and *Sc-HT-B* isoforms is around 73%, and long stretches of identity might also produce cross-hybridization. In order to avoid this, an oligonucleotide specific to the B isoform and corresponding to the N-terminal sequence PSLPLLEA was synthesized. Both *ScHT-A* and *ScHT-B* isoforms are almost exclusively expressed in styles with very weak expression detected in ovary upon prolonged exposures (data not shown). No *ScHT-A* or *B* mRNAs could be detected in leaf, stem, root, petal, anther, pollen or pollen tube tissues (data not shown). This expression pattern is identical to the one observed for the *S-RNases* (Matton *et al.*, 1998). Since the *S-RNase* genes are themselves developmentally regulated during anthesis (Anderson *et al.*, 1986; Cornish *et al.*, 1987), we determined the RNA expression pattern of *ScHT-A* and *ScHT-B*, and compared these with the one obtained

from S_{14}-*RNase* (Fig. 2A and B). Both *ScHT* isoforms and the S_{14}-*RNase* are identically regulated during pistil development and reach a maximum level of expression around anthesis (Fig. 2A and B). Figure 2A and 2B also shows that, in unpollinated flowers, *ScHT-A*, *ScHT-B*, and S_{14}-*RNase* mRNA levels decline from around two days after anthesis, coinciding with a reduced fertilization receptivity.

In S-RNase mediated gametophytic self-incompatibility, rejection of the pollen tubes mostly occurs in the top half of the style. To determine if there could be a correlation with pollen tube arrest and the expression levels of genes involved in SI, mRNA levels of *ScHT-A* and S_{14}-*RNase* were measured in the upper and lower halves of styles around peak expression time (Fig. 2C). Both genes were more strongly expressed in the upper half of the style, consistent with the site of most pollen tube arrest as determined by aniline blue staining in *S. chacoense* styles (Matton *et al.*, 1999).

Effect of compatible and incompatible pollinations on *ScHT* and *S-RNase* gene expression

In many species, pollination is known to induce deterioration and death of the secretory cells in the stigmatic region and in the transmitting tissue of the style (Cheung, 1996). We have previously shown that some genes that respond to pollination, also respond to wounding stress and wound hormone treatments, mainly jasmonates (Lantin *et al.*, 1999a, b). Wounding, as well as wound hormone treatment (JA, ABA, MeJA) and elicitors of defense responses (salicylic acid, arachidonic acid) had no effect on either *ScHT-A* or S_{14}-*RNase* mRNA levels (data not shown, except for wounding in Fig. 2D).

a

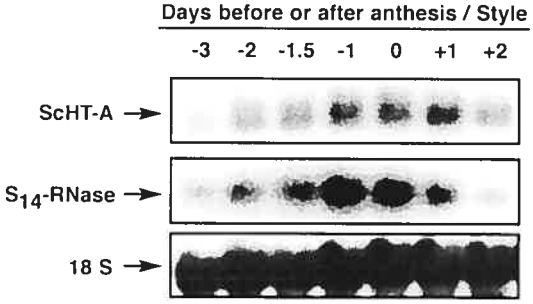
Days before or after anthesis / Style
-3 -2 -1.5 -1 0 +1 +2
ScHT-A
S14-RNase
18 S

b

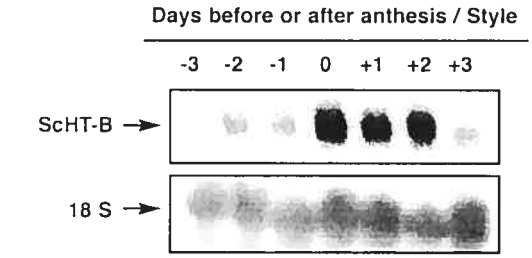
Days before or after anthesis / Style
-3 -2 -1 0 +1 +2 +3
ScHT-B
18 S

c

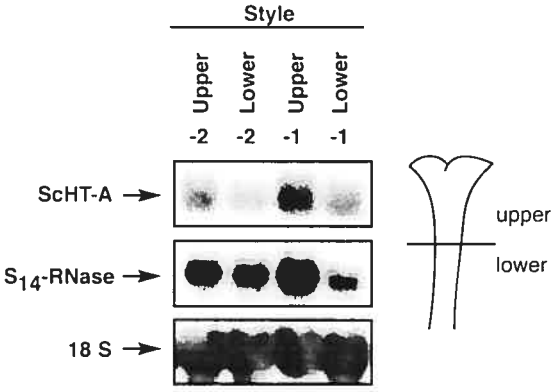
Style
Upper Lower Upper Lower
-2 -2 -1 -1
ScHT-A
S14-RNase
18 S
upper
lower

d

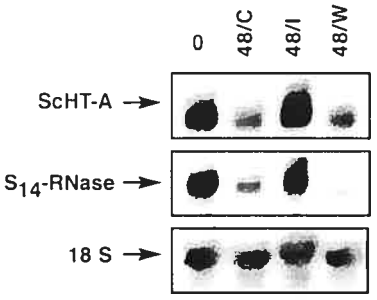
0 48/C 48/I 48/W
ScHT-A
S14-RNase
18 S

Figure 2

RNA expression analysis of *ScHT* transcript levels in styles. A. Developmental expression pattern of *ScHT-A* and S_{14}*-RNase* mRNA levels in unpollinated pistil tissues. *ScHT-A* and S_{14}*-RNase* transcript levels were determined by RNA gel blot analysis of unpollinated pistil tissues from three day before anthesis (-3) to two days (+2) after anthesis. Ten μg of total style RNA from each developmental stage was probed with the *ScHT-A*$_1$ cDNA insert, stripped and reprobed with the S_{14}*-RNase* cDNA insert. **B.** Developmental expression pattern of *ScHT-B* mRNA levels in unpollinated pistil tissues. Same conditions as in **A**, except that an identical RNA gel blot was probed with the *ScHT-B*$_1$ specific oligonucleotide. **C.** Differential expression of *ScHT-A* and S_{14}*-RNase* transcript levels in upper and lower part of the style. *ScHT-A* and S_{14}*-RNase* transcript levels were determined by RNA gel blot analysis in upper and lower halves of styles collected two (-2) and one day (-1) before anthesis. Conditions same as in **A**. **D.** Effect of compatible and incompatible pollinations on *ScHT-A* and S_{14}*-RNase* transcript levels.*ScHT-A* and S_{14}*-RNase* transcript levels were determined by RNA gel blot analysis in unpollinated styles at anthesis day (0), in styles collected 48 h after a fully compatible ($S_{11}S_{12}$ x $S_{13}S_{14}$) pollination (C/48), in styles collected 48 h after a fully incompatible ($S_{13}S_{14}$ x $S_{13}S_{14}$) pollination (48/I), and in styles collected 48 h after wounding (48/W). Conditions same as in **A**. To ascertain equal loading conditions, all RNA gel blots were stripped and reprobed with an *18S* ribosomal cDNA probe from *S. chacoense*.

Expression of these genes thus seemed to be exclusively controlled by developmental cues during pistil maturation, except for a differential response toward the type of pollination. *ScHT-A* and *S-RNases* responded differentially to a compatible or an incompatible pollination. In Figure 2D, flowers were pollinated with either compatible or incompatible pollen and tissues were harvested 48h later. For the wounding treatment, the upper part of the style including the stigma was slightly crushed with tweezers and tissues were also harvested 48h later. Following a compatible pollination, or wounding, both *ScHT-A* and S_{14}-*RNase* mRNA levels declined similarly to the developmentally regulated decrease observed in unpollinated flowers (compare Fig. 2A and D). An incompatible pollination had the opposite effect. The *ScHT-A* and S_{14}-*RNase* mRNA levels stayed as high as found on anthesis day, indicating that the developmentally programmed decrease in *S-RNase* and *ScHT* mRNA levels could be reversed, at least transiently, following an incompatible pollination.

Polymorphism of the HT modifiers and linkage to the *S*-locus

Using the *ScHT-A*$_1$ cDNA insert as a probe, an F1 population from a parental cross ($S_{11}S_{12}$ x $S_{13}S_{14}$) was tested for polymorphism and linkage to the S-locus. A fraction of the F1 progeny tested is shown in Figure 3. The S-RNase genotype of the progeny had been determined previously (Rivard *et al.*, 1994) and was confirmed by PCR analyses with allele-specific primers (data not shown). The *ScHT-A* gene is highly polymorphic as four different RFLPs could be detected in these plants. Although four different *S*-alleles also segregated in this population, the *ScHT-A* alleles were completely unlinked to the *S*-locus, as any combination of *ScHT-A* alleles could be found with all

four *S-RNases* in this population. The same population was reprobed with the *ScHT-B* cDNA. Two new RFLPs specific to the B-form were observed (data not shown). Although cross-hybridization does occur between the ScHT-A and ScHT-B probes (see figure 6), no single RFLPs could be linked with the *S-RNase* gene.

Two-hybrid analysis of ScHT and S-RNase protein interaction

A few putative roles have been proposed for the *N. alata* HT protein (McClure *et al.*, 1999). Recently it was shown that, S-RNases in both compatible or incompatible interactions, are taken up by pollen tubes, but the entry mechanism is still unknown (Luu *et al.*, 2000). One possibility is that other stylar factors involved in SI, such as the HT protein, could accompany or interact directly with the S-RNases as they are being transported into the growing pollen tubes. Since HT proteins from either *S. chacoense* or *N. alata* are fairly acidic proteins with pI around 4, and since S-RNases are basic proteins (S_{14}-RNase mature protein predicted pI is 9.12), ScHT proteins could interact directly with S-RNases, albeit not in a sequence-specific manner, as determined by the linkage analysis (Fig. 3). Another possibility would be that the HT proteins could interact with the pollen tubes and facilitate S-RNases uptake. To test if the HT protein can interact directly with the S-RNase, the *ScHT–A1* and *ScHT–B1* cDNAs were PCR amplified with or without the putative signal peptide, and inserted in frame downstream of the yeast GAL4 DNA binding domain in the pBDGAL4 vector. Since the linkage analysis (Fig. 3) showed that all combinations of *ScHTs* and *S-RNases* could be found in the segregating population, this strongly suggested that no allele-specific interactions would be expected. Thus, a single *S-RNase* gene was used to test putative protein-

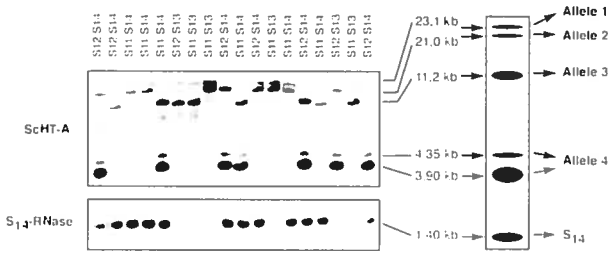

Figure 3

DNA gel blot analysis of *ScHT-A* and linkage analysis with the *S*-locus.

Left panels. Genomic DNA (10 μg) from *S. chacoense* leaves isolated from an F1 population ($S_{11}S_{12}$ x $S_{13}S_{14}$) segregating for four S-alleles was digested with *Hind* III and probed with the *ScHT-A1* cDNA insert (upper panel). Identitical DNA gel blots had been previously probed with the corresponding *S-RNase* cDNAs to determine the genotype of the plants (labeled on top of each lane) and tested by crossing. One S-allele hybridization is shown for the *S_{14}-RNase* (lower panel). Molecular sizes of the fragments appear on the right. Right panel. Schematic drawing of the banding pattern of the four *ScHT-A* alleles.

protein interactions between the ScHT and S-RNase protein products. A modified S_{11}-RNase that was previously produced by site directed mutagenesis was fused to the yeast GAL4 activating domain in the pADGAL4 vector. Because of their intrinsic ribonuclease activity, the S_{11}-RNase used in the two-hybrid analysis was mutagenized to remove one histidine residue involved in the active site of the enzyme (C3 domain) and replaced with a leucine, thus abolishing the ribonuclease activity that could have prevented proper growth in yeast cells. No direct interaction could be detected between the ScHT-A protein, with or without the predicted signal peptide, or the ScHT-B protein without the predicted signal peptide and the modified S_{11}-RNase, as no yeast growth could be observed on histidine-depleted media (data not shown).

Molecular characterization of the anti-sense *Solanum HT-A* plants

To determine if the function of the *ScHT* genes is conserved in solanaceous species other than *N. alata*, anti-sense *HT-A* plants were produced. The *ScHT-A1* cDNA was inserted in the anti-sense orientation downstream of the CaMV 35S promoter with doubled enhancer in the pBIN19 vector and flanked by the nopaline synthase terminator. *S. chacoense* plants of $S_{12}S_{14}$ genotype were transformed with the *Agrobacterium tumefaciens* LBA4404 strain containing the *ScHT-A1* anti-sense construct. Twenty-seven primary transformants were selected. Because *ScHT-A* and *ScHT-B* share 73% nucleotide sequence identity, and since stretches of perfect identity are found between these two sequences, some anti-sense lines for *ScHT-A* might also be suppressed in *ScHT-B* mRNA accumulation. Figure 4 shows RNA gel blots of these 27 transgenic plants probed with either the *ScHT-A1* complete cDNA or the *Sc-HT-B1* specific

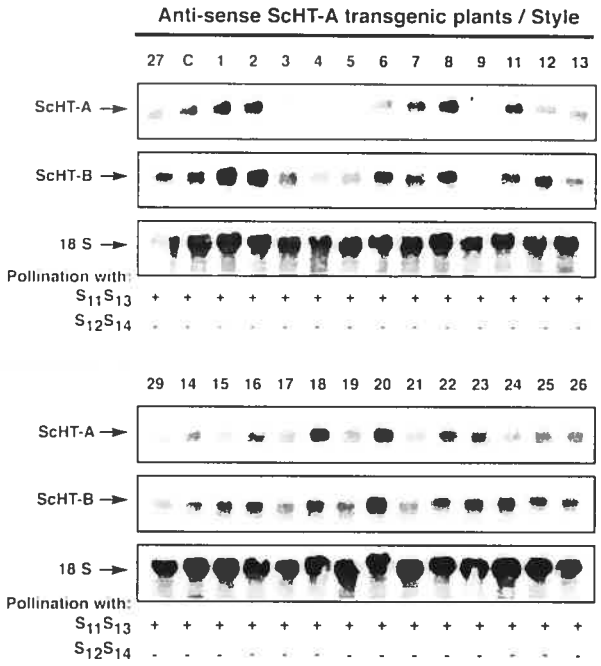

Figure 4

RNA expression analysis of *ScHT* transcript levels in styles of *ScHT-A* antisense transgenic plants and genetic crosses results. *ScHT-A* and *ScHT-B* transcript levels were determined by RNA gel blot analysis of unpollinated styles at anthesis day from 27 antisense *ScHT-A*$_1$ transgenic plants. Control plant (C) is the untransformed host (genotype $S_{12}S_{14}$). All crosses were done on at least 10 flowers with pollen from a fully compatible plant (genotype $S_{11}S_{13}$) or a fully incompatible plant (genotype $S_{12}S_{14}$). Ten μg of total style RNA from each plant was probed with the *ScHT-A*$_1$ cDNA insert and the *ScHT-B*$_1$ specific oligonucleotide. Equal loading conditions were verified with an *18S* ribosomal cDNA probe from *S. chacoense*.

oligonucleotide, and the results of the genetic crosses with either compatible or incompatible pollen are shown below. In some anti-sense lines where *ScHT-A* mRNA accumulation had been suppressed, *ScHT-B* levels were also affected, albeit to a lesser extent (AS plant #4 and 9). Although numerous plants showed strong reduction in *ScHT-A* mRNA levels (plants #3, 4, 5, 9, 29) none set seeds upon self-pollination.

Molecular characterization of the RNAi *Solanum HT-B* plants

Because anti-sense *S. chacoense HT-A* plants did not become SC, even with an almost 15-fold reduction in *ScHT-A* transcripts (*ScHT-A* AS plant #9, as determined by densitometric scans), and since correlative evidence showing weak or complete loss of expression of *HT-B* homologues, but not of *HT-A* homologues in some SC *Lycopersicon* species have been recently obtained (Kondo *et al.*, 2002a; Kondo *et al.*, 2002b), we decided to also target the *ScHT-B* gene through an RNA interference (RNAi) strategy. The *ScHT-B$_1$* cDNA was inserted first in the sense orientation downstream of the CaMV 35S promoter, followed by a 327 bp spacer, and by the *ScHT-B$_1$* cDNA again, but in the anti-sense orientation. This RNAi construct was then inserted in the *Agrobacterium tumefaciens* LBA4404 strain and used to transform *S. chacoense* plants of the $S_{12}S_{14}$ genotype. Sixteen primary transformants were initially selected. All *ScHT-B* RNAi lines were cross-pollinated with pollen from fully compatible ($S_{11}S_{13}$) or fully incompatible ($S_{12}S_{14}$) genotypes. Two plants (#2 and #3) sired seeds upon self-pollination (pollen from genotype $S_{12}S_{14}$), and could be scored as partially or semi-compatible (Fig. 5B). *ScHT-A* and *ScHT*-B mRNA levels were then determined in mature flowers at anthesis. Figure 5A shows an RNA gel blot of all the transgenic plants probed with either the

a

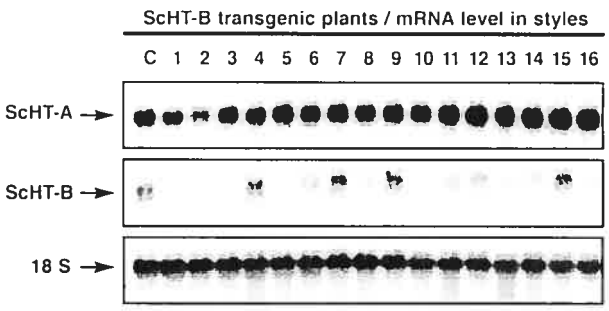

b

ScHT-B transgenic plants / Pollination behavior

	C	1	2	3	4	5	6	7	8	9	10	11	12	13	14	15	16
Single Pollination																	
$S_{11}S_{13}$	+	+	+	+	+	+	+	+	+	+	+	+	+	+	+	+	+
$S_{12}S_{14}$	-	-	8/14	2/7	-	-	-	-	-	-	-	-	-	-	-	-	-

c

ScHT-B transgenic plants / Pollination behavior

	C	1	2	3	4	5	6	7	8	9	10	11	12	13	14	15	16
Multiple Pollination																	
$S_{12}S_{14}$	0/19	0/15	6/18	0/16	0/15	7/14	1/13	0/18	4/16	0/15	9/14	8/14	1/19	3/13	0/16	0/16	7/14

Figure 5

RNA expression analysis of *ScHT* transcript levels in styles of *ScHT-B* RNAi transgenic plants and genetic crosses results. A. *ScHT-A* and *ScHT-B* transcript levels were determined by RNA gel blot analysis of unpollinated styles at anthesis day from 16 RNAi *ScHT-B1* transgenic plants. Control plant (C) is the untransformed host (genotype $S_{12}S_{14}$). Ten µg of total style RNA from each plant was probed with the *ScHT-A1* cDNA insert and the *ScHT-B1* specific oligonucleotide. Equal loading conditions were verified with an *18S* ribosomal cDNA probe from *S. chacoense*. **B.** Genetic crosses results with pollen from SI or SC plants. All crosses were done on at least 10 flowers per plant on anthesis day, with pollen from a fully compatible plant (genotype $S_{11}S_{13}$) or a fully incompatible plant (genotype $S_{12}S_{14}$). The plus (+) sign indicates a fully compatible pollination : crosses were successful, and seed set occurred in more that 90% of the pollinated flowers. The minus (–) sign indicates a fully incompatible pollination : no crosses were successful, and no seed set occurred. For intermediate phenotypes, the number of successful pollination leading to seed set per flower pollinated is indicated. **C.** Genetic crosses results with pollen from a SI plant after repeated pollination (multiple pollination). Same as in **B** except that the flowers were repeatedly pollinated with pollen from a fully SI parent (genotype $S_{12}S_{14}$). Pollinations were done on anthesis day, and then after 24, 48 and 72 hours.

ScHT-A1 complete cDNA or the *Sc-HT-B1* specific oligonucleotide, and the results of the genetic crosses with either compatible or incompatible pollen (Fig. 5B). Unlike the *ScHT-A* anti-sense experiment (Fig. 4), the RNA interference strategy specifically targeted the *ScHT-B* transcript as no significant variation in the *ScHT-A* mRNA levels could be observed (Fig. 5A). Only the transgenic plants with the most reduced *ScHT-B* mRNA level became partially self-compatible (plants #2 and 3), suggesting that a threshold level of *ScHT-B* is necessary to maintain the SI phenotype, and that only the *HT-B* isoform is involved in GSI.

The *ScHT-B* gene affects flower longevity and stylar abscission following an incompatible pollination

One intriguing observation was that, following an incompatible pollination, flowers of *ScHT-B* RNAi plants that had lowered levels of *ScHT-B* transcripts, stayed much longer on the plant than control or transgenic plants not affected in *ScHT-B* mRNA levels (plants #4, 7, 9, and 15). Under normal conditions, abscission of unpollinated flowers in *S. chacoense* occurs ≈ 5 days after anthesis (Fig. 6, unpollinated G4). After a compatible pollination, ovary swelling is clearly detectable 3 days after pollination and stylar abscission occurs ≈ 4 days after pollination (Fig. 6, V22 x G4). Following an incompatible pollination, abscission is delayed by an average of 24 hours when compared to unpollinated flowers (Fig. 6, G4 x G4). In *ScHT-B* suppressed lines, flower abscission was further delayed and only occurred after an 8 to 9 day period following initial pollination (data not shown). This extended flower longevity phenotype caused by a lower than normal *ScHT-B* mRNA level, prompted us to reexamine

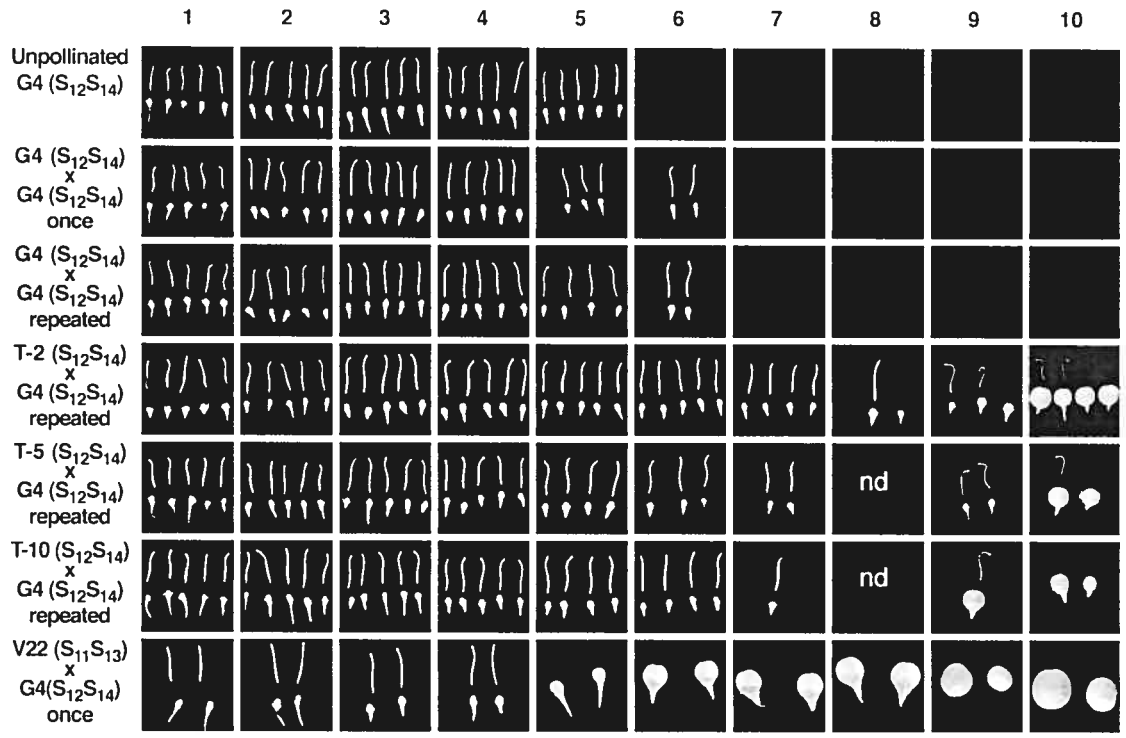

Figure 6

Pistil morphology of *ScHT-B* transgenic plants and control plants after SI and SC pollinations. Floral and stylar abscission was monitored from one day after anthesis or from one day after pollination for control plants, and for three transgenic plants (T-2, T-5, and T-10) until day 10. In all cases, pollination was performed with pollen from the G4 line (genotype $S_{12}S_{14}$). Five flowers per plant and per day (except for the V22 x G4 cross) were hand pollinated on consecutive days and, for the remaining flowers, dissected at the end of the time course. Only the floral parts remaining at the end of the time-course are displayed. ND, not determined. Once, single pollination. Repeated, consecutive pollinations on day 0, 1, 2 and if possible on day 3, depending on the corolla closure.

pollination behavior with SI pollen under a multiple pollinations scheme. In this experiment, *ScHT-B* transgenic plants and untransformed control plants were pollinated on anthesis day, and then on the following three days with similar pollen load. Fruit formation was then monitored from day 6 to day 12 after pollination. As a control, the transformation host genotype was also repeatedly pollinated. Even after multiple pollinations, the untransformed plant (control) and the transgenic plants not affected in *ScHT-B* levels (plants #4, 7, 9, and 15) never sired seeds, indicating that multiple pollinations alone, even over a 72 hours period, was not sufficient to bypass the SI recognition and rejection system (Figure 5C). For the remaining twelve transgenic plants with altered levels of *ScHT-B* mRNA, a total of nine plants were scored as semi-compatible (plants #2, 5, 6, 8, 10, 11, 12, 13, and 16) upon repeated pollination with fully incompatible pollen (genotype $S_{12}S_{14}$). Floral and stylar abscission were also monitored from one day after anthesis or from one day after pollination for control plants, and for three transgenic plants (T-2, T-5, and T-10) that showed a SC behavior following self-pollinations. Five flowers per plant and per day were hand pollinated on consecutive days in order to collect all samples on the same day (except for the unpollinated control plant and the fully compatible cross V22 x G4). As such, with the remaining flowers at the end of the 10 day period, the whole time-course was displayed. Pistil morphology for these plants is shown in Figure 6. Transgenic plants T-2, T-5 and T-10, clearly showed an increased stylar longevity, with turgid styles that appeared receptive to pollination until day 7 or 8 after pollination. Furthermore, stylar abscission from the developing fruit was also delayed, with some styles still attached even after withering (Fig. 6, plants T-2 and T-5 on day 9 and 10; plant T-10 on day 9). When

compared to a fully compatible cross (V22 x G4), fruit formation was also delayed in selfed T-2, T-5 and T-10 transgenic plants. These results confirm the involvement of the *ScHT-B* gene in SI, and suggest that it might act through an increased flower receptivity period.

99.8 Discussion

Mechanisms underlying the breakdown of gametophytic self-incompatibility have been recently reviewed and grouped in three broad categories (Stone, 2002). Firstly, loss of SI occurs following the duplication of the S-locus and the presence of heterozygous pollen (heteroallelic for the S-locus) (Golz *et al.*, 2000). Secondly, mutations affecting either the expression of the S-RNase or its activity also lead to a SC phenotype (Royo *et al.*, 1994). Thirdly, mutations not affecting the enzymatic activity of the S-RNase have also been described at the genetic level and include many so-called modifier loci. Numerous experiments have demonstrated that, although the S-RNase is responsible for pollen recognition and rejection in the style (Lee *et al.*, 1994; Murfett *et al.*, 1994; Matton *et al.*, 1997; Matton *et al.*, 1999), other stylar factors are also necessary for the proper expression of the self-incompatibility phenotype (Ai *et al.*, 1991; Bernatzky *et al.*, 1995; Murfett *et al.*, 1996; Kondo *et al.*, 2002b). Such factors, often considered as modifier loci, are present in the genetic background of SI plants, are unlinked to the S-locus, and have often been lost in SC relatives of SI species. Complementation phenomena of the genetic background have been described in *L. hirsutum* where the F_1 population from two independent SC accessions were all SC, while SI offsprings could be recovered in the F_2 generation from these F_1 plants, consistent with the multigenic nature of the gametophytic self-incompatibility (Ricks and Chetelat, 1991). One such candidate for a modifier gene is the *N. alata* HT gene (McClure *et al.*, 1999). The *NaHT* gene was cloned based on a differential screen between stylar expressed mRNAs from SC *N. plumbaginifolia* and a SC accession of *N.*

alata that is defective in *S-RNase* expression but that is competent to express SI (Murfett *et al.*, 1996). Anti-sense *NaHT* plants with reduced level of the HT protein but with normal levels of S-RNases were either fully of partially self-compatible (McClure *et al.*, 1999). This strongly suggests that the *NaHT* gene is a good candidate for such a modifier factor necessary for the SI reaction to occur. In the present study we have characterized *NaHT* homologues from four different *Solanum* species, and have focussed our attention on the putative function of the *S. chacoense HT* homologues (*ScHT-A* and *ScHT-B*) in gametophytic self-incompatibility.

Phylogenetic analyses of the isolated *NaHT* homologues clearly demonstrated that two different *HT* isoforms exist, and that isoform B is probably the most closely related to the *NaHT* gene. All the HT proteins shared some common features. Firstly, a highly conserved N-terminal region that is strongly predicted to be a signal peptide. The sequence conservation was high enough to originally derive PCR primer pairs from only the *NaHT* and *ScHT-A1* sequences, and amplify both *HT* isoforms from numerous *Solanum* (this study) and *Lycopersicon* species (Kondo *et al.*, 2002a; Kondo *et al.*, 2002b). Secondly, all HT homologues possess a C-terminal region composed of consecutive stretches of asparagine and aspartic acid residues, flanked by conserved cysteines that could be involved in disulfide bridges. Although sequence identity is quite variable, ranging from 36 to 92% in the B-isoform group (77 to 92% when only *Solanum* sequences are considered), the overall structure conservation combined with identical expression pattern, would suggest that the ScHT-B isoform and the NaHT protein are probably true orthologues. *ScHT-A*, *ScHT-B* and *NaHT* are each almost exclusively stylar-expressed, as for the *S-RNases*, and all are developmentally regulated

during pistil maturation (this study and McClure *et al.*, 1999). Interestingly, we found higher expression levels of both *ScHT* and *S-RNase* genes in the upper style region (Fig. 2C), consistent with the pattern of pollen tube arrest that occurs in the top half of the style in *S. chacoense* (Matton *et al.*, 1999). The developmental regulation of *S-RNase* transcript accumulation enables the production of selfed progeny in some GSI species when using very young flowers buds (bud-pollination), but this is very difficult to achieve in *S. chacoense*. One reason could be the elevated level of both S-RNase and HT transcripts, even 2 days before anthesis, and detectable three days before anthesis, combined with a preferential upper style accumulation. One intriguing observation was the differential expression pattern of both *S-RNase* and *HT* transcripts following an incompatible pollination compared to an unpollinated or a compatibly pollinated flower (Fig. 2D). As the flower ages, *S-RNase* and *HT* transcript levels decrease markedly, but low expression levels coincide with reduced fertilization receptivity, and eventually, flower abscission. Surprisingly, *S-RNase* and *ScHT-A* transcript levels do not decrease following an incompatible pollination (for at least 2 days after pollination, Fig. 2D), and this cannot only be the result of stigmatic and transmitting tissue deterioration and death, since this is also induced by a compatible pollination. Furthermore, mechanical wounding or wound hormone treatments had no effect on *S-RNase* and *ScHT-A* transcript levels. This strongly suggests that the presence of dead pollen tubes or molecules liberated from the arrested pollen tubes, either increase the transcription of these genes or reduce their mRNA turnovers, ensuring that the S-RNases and HT proteins are still present in sufficient amount to reject newly incoming pollen from incompatible genotypes. The maintenance of high steady-state levels of *S-RNases* and *ScHT* mRNAs following an initial incompatible pollination, would also lead to a

prolonged reproductive barrier, an important issue since flower senescence is retarded following an incompatible pollination (Fig. 6, G4 x G4).

In order to determine the role of the ScHT genes in SI, functional analysis of ScHT-A and ScHT-B protein-protein interactions with an S-RNase were tested in the yeast two-hybrid system, and transgenic plants with strongly suppressed levels of both isoforms were generated. Although ScHT-A and ScHT-B deduced mature proteins have acidic pIs and the S-RNase is basic (predicted pI=9.25 for S_{11}-RNase mature protein), no direct interactions based either on specific or electrostatic attractions could be detected in the two-hybrid system, as no yeast growth could be observed, with or without the predicted signal peptide. Such direct interaction had also not been detected with the purified HT protein from *N. alata*, although in that case, the NaHT protein appeared to be unstable in stylar extracts (McClure *et al.*, 1999). Both results suggest that HT proteins and S-RNases do not interact directly.

Recently, correlative evidence for the involvement of the NaHT homologues in *Lycopersicon* species has been obtained (Kondo *et al.*, 2002a; Kondo *et al.*, 2002b). In the three *Lycopersicon* SI species tested, all expressed functional *S-RNases* as well as *HT-A* and *HT-B* mRNAs. In the seven *Lycopersicon* SC species tested, no or low stylar ribonuclease activity was observed. This alone would most probably be sufficient to explain their SC phenotype, since a threshold level of S-RNase expression is necessary to confer an SI phenotype (Lee *et al.*, 1994; Matton *et al.*, 1997). Intriguingly, in the seven *Lycopersicon* SC species tested, transcription of the *HT-B* isoform was either weakly or not detected at all, and the HT-B isoform produced had internal stop codons,

while the *HT-A* isoform was strongly expressed at the mRNA level, although some SC species also produced defective (frame-shifted) *HT-A* transcripts. Apart from the *N. alata* transgenic anti-sense lines, no other functional analysis had been made prior to the one presented here. In *N. alata*, plants with reduced levels of the NaHT protein were either fully or partially SC, suggesting that the amount of NaHT protein is important (McClure *et al.*, 1999). In the present study, anti-sense *ScHT-A* and RNAi *ScHT-B* plants were generated. Figure 4 showed that, even with a 15-fold decrease in *ScHT-A* mRNA levels, *ScHT-A* AS plant #9 remained SI. *ScHT-B* mRNA levels in that transgenic line was also affected, although to a lesser extent. This could suggest that, a threshold level of ScHT-B is sufficient to maintain a SI phenotype. In a second series of experiments, *ScHT-B* suppression was achieved through an RNAi strategy. Unlike the anti-sense plants, the *ScHT-B* RNAi plants were only affected in *ScHT-B* mRNA expression (Fig. 5). Plants with severely reduced *ScHT-B* transcripts became SC and produced seeds upon pollination with pollen from an incompatible genotype. RNAi plant #2 had the most severely reduced *ScHT-B* mRNA levels and consistently set seeds upon self pollination. RNAi plant #3 had a less stable phenotype, and only set seeds occasionally. Although at first only two plants became partially SC upon selfing, all the transgenic plants with reduced *ScHT-B* mRNA levels also showed an extended, albeit slightly variable, floral longevity upon pollination with incompatible pollen. This observation led to the hypothesis that the *ScHT-B* gene could be involved in modulating the receptivity period of the flower, perhaps through a control over the abscission of the floral organs. This increase in floral longevity, and in particular in stylar turgidity and receptivity might partially explain the SC phenotype since it could increase the chances that pollen tubes would reach the ovary. To test this, repeated pollinations were

performed on 3 to 4 consecutives days, on the 16 RNAi *ScHT-B* transgenic plants, and on control plants. None of the ScHT-B transgenic plants unaffected in *ScHT-B* mRNA expression, or the untransformed control plant, had an extended floral longevity and none were fertilized upon selfing. Of the remaining 12 transgenic plants expressing reduced levels of *ScHT-B* mRNA, 9 were able to sire seeds. Fruits formed on these plants were smaller than the ones obtained from a compatible cross, and after 10 days, were comparable in size with fruits produced from a compatible pollination after 6 days (Fig. 6, compare the fruits from plants T-2, T-5 and T-10 with the ones from the V22 x G4 cross). These results are entirely consistent with our hypothesis, that reduced level of *ScHT-B* mRNA affects the receptivity period of the flower, and that the self-compatibility phenotype observed in ScHT-B transgenic plants does not only result from the developmentally regulated decrease in both *S-RNase* and *ScHT-B* mRNA levels (Fig. 2A and B), since repeated incompatible pollinations could not induce fertilization in control or unaffected ScHT-B transgenic plants. Furthermore, in *N. alata* HT anti-sense plants, pollen tube growth in the style is observed even when the S-RNase level is high, although in that case, fertilization and production of fruits could not be observed because the recipient plant used is a sterile hybrid between *N. alata* and *N. plumbaginifolia* and only pollen tube growth in the style was used to score the SI or SC phenotype.

Our results clearly indicate that, associated with a decrease in *ScHT-B* transcripts, there is an increase in flower longevity and in pollination receptivity. One possibility would be that the HT-B isoform is involved in a pathway regulating floral abscission. Pollination is known to affect the physiological state of the flower. Pollinated flowers (compatible) senesce rapidly compared to unpollinated flowers or those

pollinated by incompatible pollen grains in the case of a SI plant (Gilissen, 1977; Singh *et al.*, 1992). Early studies in *Petunia* ovaries showed an increase in polyribosomes activity 6 to 12h after pollination, well before the arrival of the pollen tubes in the ovary (~50h) (Deurenberg, 1976). Pollination-induced wilting of the corolla can be prevented if the style is removed early after pollination (Gilissen, 1984). These and other results (Stead, 1992), have led to the hypothesis that a pollination-induced signal is transmitted through the pistil and precedes the growing pollen tube. Ethylene has been shown to have a strong effect on flower abscission in solanaceous species (van Doorn, 2002a, b). Furthermore, pollination itself induces ethylene synthesis (Hall and Forsyth, 1967), and it has been shown that, in *Petunia hybrida*, pollination induces two distinct phases of ethylene production in the flower (Singh *et al.*, 1992). The first phase is common to both self- and cross-pollinated flowers and is dependent on pollen-borne ACC (ethylene precursor). The second phase results from *de novo* synthesis of ethylene from the flower, and occurs 18 hours after a compatible pollination. Following an incompatible pollination, the production of ethylene is delayed to 3 days after pollination (Singh *et al.*, 1992). Since RNAi ScHT-B plants showed delayed floral abscission, we tested these plants for alteration in the expression of ethylene-related genes. No differences could be observed in the expression pattern of two genes involved in ethylene biosynthesis (*ACC synthase* and *ACC oxidase*), or in ethylene perception and signal transduction (ethylene receptor ETR1 and EIL3) in ScHT-B transgenic plants (data not shown). Since the *ACC synthase* and the *ACC oxidase* genes are part of multigene families (at least 8 members for the *ACC synthase* and 4 members for the *ACC oxidase* in *Solanum lycopersicon*) (Llop-Tous *et al.*, 2000), specific probes will need to be designed for individual

members, in order to determine if a given isoform is affected in ScHT-B mutant background.

From our results, we propose that the ScHT-B isoform is involved in at least two phenomena. Firstly, elevated levels of both *S-RNases* and *ScHT-B* would be necessary for the SI reaction to occur, as determined from McClure's work (McClure *et al.*, 1999) and from the phenotype of the *ScHT-B* RNAi plant T-2. When the *ScHT-B* mRNA levels are below a threshold level, pollen tubes would be able to reach the ovary and effect fertilization. The developmentally regulated decrease in both *S-RNase* and *ScHT* mRNA levels (Fig. 2A and B), would normally lead to a SC phenotype in aged flowers, but is accompained by floral abscission. The maintenance of both *S-RNase* and *ScHT* mRNA levels following an incompatible pollination (Fig. 2D) would also ensure the maintenance of a strong reproductive barrier, over a longer period of time. This could be of importance since flowers pollinated with incompatible pollen last an average of 1 day longer on the plant than unpollinated flowers (Fig. 6, G4 x G4), and the receptivity period for a successful pollination is normally limited to the first 2 to 3 days after anthesis. Secondly, the *ScHT*-B RNAi transgenic plants display a novel phenotype that includes a longer floral longevity with delayed stylar abscission and, perhaps, more relevant for the SC phenotype of those plants, the persistence of turgid styles, even 9 days after anthesis (Fig. 6). This phenotype, observed in plants with reduced levels of *ScHT-B* mRNAs, would enable pollen tube growth in older styles with reduced S-RNase level, past their normal flower lifespan and pollination receptivity period. As suggested by McClure (McClure *et al.*, 1999), the HT protein could interact directly with pollen tubes, and facilitate S-RNase uptake. Our yeast two-hybrid results would support a

model in which ScHT-B does not interact directly with the S-RNase. Furthermore, if the HT-B protein is involved in S-RNase uptake, a reduced level of HT-B protein would increase the number of pollen tubes not affected by the presence of the S-RNase, enabling fertilization to take place. This is entirely consistent with our results, since repeated pollinations in *ScHT-B* RNAi plants, increased the percentage of fertilized ovules. Although its mode of action still remains unclear, our data demonstrate a role for the *HT-B* isoform in expression of SI, and points toward a specific role in the control of flower senescence and abscission.

II.9 Experimental procedures

Plant material and transformation

The diploid (2n=2x=24) *Solanum chacoense* Bitt. self-incompatible genotypes used include line 314 ($S_{11}S_{12}$), line 582 ($S_{13}S_{14}$), line G4 ($S_{12}S_{14}$), and V22 ($S_{11}S_{13}$). Plants were grown in greenhouses with 14-16h of light per day. Transformation was done as described previously and the transformation host plant was line G4 (Matton *et al.*, 1997). The *ScHT-A1* cDNA was cloned in anti-sense orientation downstream of a CaMV 35S promoter with doubled enhancers (Skuzeski *et al.*, 1990), and flanked by the nos terminator in the pBIN19 vector (Bevan, 1984). For RNA interference experiments, a new vector was constructed. This new vector called pDARTH (O'Brien and Matton, unpublished), includes a CaMV 35S promoter with doubled enhancers (Skuzeski *et al.*, 1990), an extended multiple cloning site, and a 327 bp intron from a *histone deacetylase 2* (*HD2*) gene from *S. chacoense* (our unpublished results). The ScHT-B_1 cDNA sequence (324 bp) was cloned in sense and anti-sense orientation separated by the *HD2* intron.

Isolation of the *ScHT* cDNAs and PCR amplification of other solanaceous *HT* genes

The *ScHT-A1*, *ScHT-A2*, and *S14-RNase* cDNAs were initially isolated from a pollinated pistil cDNA library using virtual subtraction (Li and Thomas, 1998). In this procedure, genes corresponding to lowly expressed mRNA species are preferentially

isolated. Because the initial screen was for rare mRNA species expressed in ovary tissues, and since the library also contained cDNAs expressed in styles, genes that were highly expressed in styles but only weakly expressed in ovaries were also recovered. A second screening round with a probed derived from stylar mRNAs uncovered all of the stylar expressed genes, including the *ScHT-A1*, *ScHT-A2*, and *S14-RNase* cDNAs. For the isolation of the *ScHT-B1* cDNA, and of related sequences in other solanaceous species, three degenerate primers were designed based on the most conserved amino acid sequence of ScHT-A_1 from *S. chacoense* and HT from *N. alata* (McClure *et al.*, 1999). The sequence of the upstream primers (HT-NS1 : 5'-TTT CTT TGG TTC TT(a/t) TGA T(a/t)A TAT CAT CA-3' ; HT-NS2 : 5'-ATA TCA TCA GA(a/g) GTT ATT GC(a/t) AGG GA(a/t) ATG-3') are derived from the predicted signal peptide sequence, and the sequences of the downstream primers (HT-C1 : 5'-TCC TTT ATT CAA CCA AT(c/t) TCA TAT TA-3' ; HT-C2B : 5'-CAA AAA TAT TAC ATA ATA TTT TGT AGT CG-3') are derived from the C-terminus of the HT protein. The *S. chacoense HT-B1* isoform was obtained by PCR amplification of cDNAs from a pollinated pistil library while *HT* isoforms from *S. pinnatisectum*, *S. bulbocastanum* and *S. tuberosum* were obtained by PCR amplification of genomic DNA.

Isolation and gel blot analysis of RNA and DNA

Total RNA was isolated as described previously (Jones *et al.*, 1985). RNA concentration was determined by measuring its absorbance at 260 nm and verified by agarose gel electrophoresis following ethidium bromide staining. To confirm equal loading of total RNA on RNA gel blots, a 1 kb fragment of the *S. chacoense 18S RNA*

was PCR amplified and used as a probe (Lantin *et al.*, 1999a). Genomic DNA isolation was performed via a modified CTAB extraction method (Reiter *et al.*, 1992) or with the Plant DNeasy kit from Qiagen. DNA gel blot analysis, including restriction, electrophoresis, and capillary transfer to a positively charged nylon membrane, (Hybond N+, Amersham Pharmacia Biotech, Baie D'Urfé, Qc) were performed as described previously (Sambrook *et al.*, 1989). Hybridization of the membrane was performed under high stringency conditions at 65°C as described previously (Church and Gilbert, 1984) for 16 to 24 h and following hybridization, the membrane was washed at room temperature, twice with 2X SSC / 0.1% SDS for 30 min., twice with 1X SSC / 0.1% SDS at 50°C for 30 min. and twice with 0.1X SSC / 0.1% SDS at 55 °C for 10 min. (1X SSC is 0.15 M NaCl, 0.015 M sodium citrate, pH 7.0). RNA gel blot analyses were performed as described in Sambrook *et al.* (1989), following the formaldehyde denaturing protocol. RNAs were capillary transfered to Hybond N+ nylon membranes and cross-linked (120 mJ/cm^2) with a Hoefer UVC 500 UV Crosslinker. Hybridization of the membranes was performed under high stringency conditions at 45°C in 50 % deionized formamide, 5X Denhardt solution, 0.5% SDS, 200 µg/ml denatured salmon sperm DNA and 6X SSC for 16 to 24 h. Following hybridization, the membranes were washed at room temperature twice with 2X SSC / 0.1% SDS for 30 min., twice with 1X SSC / 0.1% SDS at 50°C for 30 min and twice with 0.1X SSC / 0.1% SDS at 55°C for 10 min. Probes for DNA gel blot analysis were synthesized from random-labeled isolated DNA inserts (Roche Diagnostic, Laval, Qc) with α-^{32}P dCTP (ICN Biochemicals, Irvine, CA). For RNA gel blot analyses, cDNA probes were made with α-^{32}P dATP with the Strip-EZ DNA labeling kit (Ambion, Austin, Texas) and

oligonucleotide probes were labeled with γ-^{32}P dATP (Sambrook *et al.*, 1989). The membranes were autoradiographed at –85°C with one intensifying screen on Kodak Biomax MR film (Interscience, Markham, Ont).

Site directed mutagenesis of the S_{11}-RNase and yeast two-hybrid analysis

A mutated *S_{11}-RNase* gene where the conserved His-114 residue (CAT), located in the C3 active site domain, was converted to a leucine residue (CTT) by site-directed mutagenesis using the following oligonucleotide (mutated nucleotide is underlined): 5'-CTAAAGCTTGGATCCTGCTGT-3' (Altered sites II *in vitro* mutagenesis system, Promega, WI). The original construct contained both the *S_{11}* intron and 3' end of the gene, and was expressed in transgenic *S. chacoense* plants (Matton *et al.*, 1997; Matton *et al.*, 1999) under the control of the style specific chitinase promoter (Harikrishna *et al.*, 1996). The spliced His$^-$ *S_{11}-RNase* cDNA was recovered from reversed transcribed style mRNAs, and the coding region corresponding to the mature protein was PCR amplified (Pwo DNA polymerase, Roche Diagnostics, Laval, Qc) and fused in frame with the DNA binding domain of the GAL4 protein in the pBDGAL4 yeast vector (TRP1 selection marker) (Stratagene, LaJolla, CA). The *ScHT-A_1* coding region was PCR amplified with or without the predicted signal peptide and inserted in frame with the GAL4 activation domain in the pADGAL4 vector (LEU2 selection marker). For the *ScHT-B* construct, only the coding region without the predicted signal peptide was inserted in frame with the GAL4 activation domain in the pADGAL4 vector. Integrity of the DNA constructs was verified by sequencing. The constructs were transformed sequentially in the yeast strain PJ69-4A (James *et al.*, 1996) and selected through their

ability to grow on Trp^- and Leu^- media. Protein-protein interaction assays were performed on media lacking Trp, Leu and His and on media lacking Trp, Leu, and Ade.

II.10 Acknowledgements

We thank Dr. Qin Chen (Agriculture and Agri-Food Canada, Lethbridge Research Centre, AB) for the gift of *S. pinnatisectum* and *S. bulbocastanum* plants ; Dr. Mario Cappadocia for the segregating population DNA (Université de Montréal, Montréal, QC) ; Dr. Philip James (University of Wisconsin, Madison, WI) for the gift of the PJ69-4A yeast strain ; Mrs. Annie Archambault for her help with the phylogenetic analysis, and Mr. Gabriel Téodorescu for plant care and maintenance. This work was supported by the Natural Sciences and Engineering Research Council of Canada and by Le Fonds pour la Formation des Chercheurs et l'Aide à la Recherce (FCAR, Québec).

II.11 References

Ai, Y., Kron, E., and Kao, T.-H. (1991). S-alleles are retained and expressed in a self-compatible cultivar of *Petunia hybrida*. Mol. Gen. Genet. 230, 353-358.

Anderson, M.A., Cornish, E.C., Mau, S.-L., Williams, E.G., Hoggart, R., Atkinson, A., Bonig, I., Grego, B., Simpson, R., Roche, P.J., Haley, J.D., Penschow, J.D., Niall, H.D., Tregar, G.W., Coghlan, J.P., Crawford, R.J., and Clarke, A.E. (1986). Cloning of cDNA for a stylar glycoprotein associated with expression of self-incompatibility in *Nicotiana alata*. Nature 321, 38-44.

Bernatzky, R., Glaven, R.H., and Rivers, B.A. (1995). S-related protein can be recombined with self-compatibility in interspecific derivatives of *Lycopersicon*. Biochem. Genet. 33, 215-215-225.

Bevan, M. (1984). Binary *Agrobacterium* vectors for plant transformation. Nucl. Acids Res. 12, 8711-8721.

Cheung, A.Y. (1996). The pollen tube growth pathway: its molecular and biochemical contributions and responses to pollination. Sex. Plant Reprod. 9, 330-336.

Church, G.M., and Gilbert, W. (1984). Genomic sequencing. Proc. Natl. Acad. Sci. USA 81, 1991-1995.

Cornish, E.C., Pettitt, J.M., Bonig, I., and Clarke, A.E. (1987). Developmentally controlled expression of a gene associated with self-incompatibility in *Nicotiana alata.* Nature 326, 99-102.

de Nettancourt, D. (1977). Incompatibility in angiosperms. (New York: Springler-Verlag).

de Nettancourt, D. (1997). Incompatibility in angiosperms. Sex. Plant Reprod. 10, 185-199.

Deurenberg, J.J.M. (1976). In vitro protein synthesis with polysomes from unpollinated, cross- and self-pollinated *Petunia* ovaries. Planta 128, 29-33.

Dodds, P.N., Fergurson, C., Clarke, A.E., and Newbigin, E. (1999). Pollen- expressed S-RNases are not involved in self-incompatibility in *Lycopersicon peruvianum.* Sex. Plan. Reprod. 12, 76-87.

Gilissen, L.J.W. (1977). Style-controlled wilting of the flower. Planta 133, 275-280.

Gilissen, L.J.W. (1984). Pollination-induced corolla wilting in Petunia hybrida. Rapid transfer through the style of a wilting-inducing substance. Plant Physiol 75, 496-498.

Golz, J.F., Clarke, A.E., and Newbigin, E. (2000). Mutational Approaches to the Study of Self-incompatibility: Revisisiting the Pollen-part Mutants. Annals of Botany 85, 95-103.

Hall, I.V., and Forsyth, F.R. (1967). Production of ethylene by flowers following pollination and treatment with water and auxin. Can J Bot 45, 1163-1166.

Harikrishna, K., Jampates-Beale, R., Milligan, S., and Gasser, C. (1996). An endochitinase gene expressed at high levels in the stylar transmitting tissue of tomatoes. Plant Mol. Biol. 30, 899-911.

Hosaka, K., and Hanneman, R.E. (1998a). Genetics of self-compatibility in a self-incompatible wild diploid potato species *Solanum chacoense*. 2. Localization of an S slocus inhibitor (Sli) gene on the potato genome using DNA markers. Euphytica 103, 265-271.

Hosaka, K., and Hanneman, R.E. (1998b). Genetics of self-compatibility in a self-incompatible wild diploid potato species *Solanum chacoense*. 1. Detection of an S slocus inhibitor (Sli) gene. Euphytica 99, 191-197.

James, P., Halladay, J., and Craig, E.A. (1996). Genomic libraries and a host strain designed for highly efficient two-hybrid selection in yeast. Genetics 144, 1425-1436.

Jones, J.D.G., Dunsmuir, P., and Bedbrook, J. (1985). High level expression of introduced chimeric genes in regenerated transformed plants. EMBO J. 4, 2411-2418.

Kao, T.-H., and McCubbin, A. (1996). How flowering plants discriminate between self and non-self pollen to prevent inbreeding. Proc. Natl. Acad. Sci. USA 93, 12059- 12065.

Kondo, K., Yamamoto, M., Itahashi, R., Sato, T., Egashira, H., Hattori, T., and Kowyama, Y. (2002a). Insights into the evolution of self-compatibility in *Lycopersicon* from a study of stylar factors. Plant J 30, 143-154.

Kondo, K., Yamamoto, M., Matton, D.P., Sato, T., Hirai, M., Norioka, S., Hattori, T., and Kowyama, Y. (2002b). Cultivated tomato has defects in both *S-RNase* and *HT* genes required for stylar function of self-incompatibility. Plant J 29, 627-636.

Lantin, S., O'Brien, M., and Matton, D.P. (1999a). Pollination, wounding and jasmonate treatments induce the expression of a developmentally regulated pistil dioxygenase at a distance, in the ovary, in the wild potato *Solanum chacoense* Bitt. Plant Mol Biol 41, 371-386.

Lantin, S., O'Brien, M., and Matton, D.P. (1999b). Fertilization and wounding of the style induce the expression of a highly conserved plant gene homologous to a *Plasmodium falciparum* surface antigen in the wild potato *Solanum chacoense* Bitt. Plant Mol Biol 41, 115-124.

Lee, H.S., Huang, S., and Kao, T.-H. (1994). S proteins control rejection of incompatible pollen in *Petunia inflata*. Nature 367, 560-563.

Li, Z., and Thomas, T.L. (1998). *PEI1*, an embryo-specific zinc finger protein gene required for heart-stage embryo formation in *Arabidopsis*. Plant Cell 10, 383-398.

Llop-Tous, I., Barry, C.S., and Grierson, D. (2000). Regulation of ethylene biosynthesis in response to pollination in tomato flowers. Plant Physiol 123, 971-978.

Luu, D.T., Qin, X., Morse, D., and Cappadocia, M. (2000). S-RNase uptake by compatible pollen tubes in gametophytic self- incompatibility. Nature 407, 649-651.

Matton, D.P., Bertrand, C., Laublin, G., and Cappadocia, M. (1998). Molecular aspects of self-incompatibility in tuber-bearing *Solanum* species. In Comprehensive Potato Biotechnology, S.M.P. Khurana, R. Chandra, and M.D. Upadhya, eds (New Delhi, India: Malhotra Publishing House), pp. 97-113.

Matton, D.P., Maes, O., Laublin, G., Xike, Q., Bertrand, C., Morse, D., and Cappadocia, M. (1997). Hypervariable domains of self-incompatibility RNases mediate allele-specific pollen recognition. Plant Cell 9, 1757-1766.

Matton, D.P., Luu, D.T., Xike, Q., Laublin, G., O'Brien, M., Maes, O., Morse, D., and Cappadocia, M. (1999). Production of an S RNase with dual specificity suggests a novel hypothesis for the generation of new S alleles. Plant Cell 11, 2087-2097.

McClure, B., Mou, B., Canevascini, S., and Bernatzky, R. (1999). A small asparagine-rich protein required for S-allele-specific pollen rejection in *Nicotiana*. Proc. Natl. Acad. Sci. USA 96, 13548-13553.

McClure, B.A., Haring, V., Ebert, P.R., Anderson, M.A., Simpson, R.J., Sakiyama, F., and Clarke, A.E. (1989). Style self-incompatibility products of *Nicotiana alata* are ribonucleases. Nature 342, 955-957.

Murfett, J., Atherton, T.L., Mou, B., Gasser, C.S., and McClure, B.A. (1994). S-RNase expressed in transgenic *Nicotiana* causes S-allele-specific pollen rejection. Nature 367, 563-566.

Murfett, J., Strabala, T.J., Zurek, D.M., Mou, B., Beecher, B., and McClure, B.A. (1996). S RNase and interspecific pollen rejection in the genus *Nicotiana*: multiple pollen-rejection pathways contribute to unilateral incompatibility between self-incompatible and self-compatible species. Plant Cell 8, 943-958.

Nielsen, H., Engelbrecht, J., Brunak, S., and von Heijne, G. (1997). Identitfication of prokaryotic and eukaryotic signal peptides and prediction of their cleavage sites. Protein Eng. 10, 1-6.

Reiter, R.S., Young, R.M., and Scolnik, P.A. (1992). Genetic linkage of the *Arabidopsis genome*: methods for mapping with recombinant inbreds and Random Amplified Polymorphic DNAs (RAPDs). In Methods in *Arabidopsis* Research, C. Koncz, N.-H. Chua, and J. Schell, eds (Singapore: World Scientific Publishing Co.), pp. 170-190.

Ricks, C.M., and Chetelat, R.T. (1991). The breakdown of self-incompatibility in *Lycopersicon hirsutum*. In *Solanaceae* III: taxonomy, chemistry, evolution, L. Hawkes, Nee and Estrada, ed (London: Royal Botanic Garden Kew and Linnean Society of London), pp. 253-256.

Rivard, S.R., Saba-El-Leil, M.K., Landry, B., and Cappadocia, M. (1994). RFLP analyses and segregation of molecular markers in plants produced by in vitro anther culture, selfing, and reciprocal crosses of two lines of self-incompatible *Solanum chacoense*. Genome 37, 775-783.

Royo, J., Kunz, C., Kowyama, Y., Anderson, M., Clarke, A.E., and Newbigin, E. (1994). Loss of a histidine residue at the active site of S-locus ribonuclease is associated with self-compatibility in *Lycopersicon peruvianum*. Proc. Natl. Acad. Sci. USA 91, 6511-6514.

Sambrook, J., Fritsch, E.F., and Maniatis, T. (1989). Molecular cloning: a laboratory manual. (Cold Spring Harbor, New York: Cold Spring Harbor Laboratory Press).

Schopfer, C.R., Nasrallah, M.E., and Nasrallah, J.B. (1999). The male determinant of self-incompatibility in *Brassica*. Science 286, 1697-1700.

Singh, A., Evensen, K.B., and Kao, T.-H. (1992). Ethylene synthesis and floral senescence following compatible and incompatible pollinations in *Petunia inflata*. Plant Physiol 99, 38-45.

Skuzeski, J.M., Nichols, L.M., and Gesteland, R.F. (1990). Analysis of leaky viral translation termination codons in vivo by transient expression of improved β-glucuronidase vectors. Plant Mol. Biol. 15, 65-69.

Stead, A.D. (1992). Pollination-induced flower senescence: a review. Plant Growth Regulat 11, 13-20.

Stone, J.L. (2002). Molecular mechanisms underlying the breakdown of gametophytic self-incompatibility. Q Rev Biol 77, 17-32.

Takayama, S., Shiba, H., Iwano, M., Shimosato, H., Che, F.-S., Kai, N., Watanabe, M., Suzuki, G., Hinata, K., and Isogai, A. (2000). The pollen determinant of self-incompatibility in *Brassica campestris*. Proc. Natl. Acad. Sci. USA 97, 1920-1925.

van Doorn, W.G. (2002a). Does ethylene treatment mimic the effects of pollination on floral lifespan and attractiveness? Ann Bot (Lond) 89, 375-383.

van Doorn, W.G. (2002b). Effect of ethylene on flower abscission: a survey. Ann Bot (Lond) 89, 689-693.

Chapitre III.

Lipid signaling in plants: Cloning and expression analysis of the obtusifoliol 14α-demethylase from Solanum chacoense Bitt., a pollination- and fertilization-induced gene with both obtusifoliol and lanosterol demethylase activity.

Martin O'Brien, Sier-Ching Chantha, Alain Rahier et Daniel P. Matton

Publié dans Plant Physiology (2005) 139, 734-749

III.1 Contribution des coauteurs

J'ai effectué une étape préliminaire de recherche de gènes dont le clone de ce papier a été tiré, et ce, par une représentation différentielle des ARNm. J'ai fait seul toutes les expérimentations nécessaires à la production de cinq des huit figures. J'ai participé à l'élaboration de deux autres figures en fournissant et préparant le matériel biologique et moléculaire nécessaire à l'obtention des résultats finaux. A. Rahier est un collaborateur français qui a synthétisé les lipides utilisés pour certaines expérimentations. Presque la totalité des données non montrées de l'article (« data not shown »), sont des expériences que j'ai fait (7 expériences sur 9 non montrées). Parmi ces expériences, il y a eu l'analyse bio-informatique ainsi que l'obtention et la caractérisation du mutant d'*Arabidopsis thaliana*. Sier-Ching Chantha a effectuée l'hybridation *in situ* alors qu'Alain Rahier a fait l'analyse biochimique des lipides.

III.2 Page titre

Lipid signaling in plants: Cloning and expression analysis of the obtusifoliol 14α-demethylase from *Solanum chacoense* Bitt., a pollination- and fertilization-induced gene with both obtusifoliol and lanosterol demethylase activity.

Martin O'Brien[1], Sier-Ching Chantha[1], Alain Rahier[2] and Daniel P. Matton[1]*

[1] Institut de Recherche en Biologie Végétale (IRBV), Département de Sciences biologiques, Université de Montréal, 4101 rue Sherbrooke Est, Montréal, Québec, Canada, H1X 2B2

[2] Département Isoprénoïdes, Institut de Biologie Moléculaire des Plantes, CNRS UPR 2357, 28 rue Goethe, 67083 Strasbourg Cédex, France

* Corresponding author

[redacted]

Ph. : 1-514-872-3967

Fax : 1-514-872-9406

III.3 Financial source

This work was supported by the Natural Sciences and Engineering Research Council of Canada (NSERC) and from the Canada Research Chair program.

III.4 Keywords

Fertilization, *Solanum chacoense*, embryogenesis, sterol, obtusifoliol, cytochrome P450, *CYP51*, C14-demethylation.

III.5 Genbank accession number

CYP51G1-Sc; AY552551

III.6 Abbreviations

DPP, days post-pollination; DPW, days post-wounding; BR, brassinosteroids

III.7 Abstract

The sterol 14α-demethylase (*CYP51*) is the most widely distributed cytochrome P450 gene family being found in all biological kingdoms. In sterol biosynthesis, it catalyzes the first step following cyclization and leads to the formation of precursors of steroid hormones including brassinosteroids in plants. Most of the enzymes involved in the plant sterol biosynthesis pathway have been characterized biochemically and the corresponding genes cloned. Genes coding for enzymes responsible for substrate modifications before 24-methylenelophenol lead to embryonic and seed defects when mutated, while mutants downstream of the 24-methylenelophenol intermediate show phenotypes characteristic of brassinosteroid mutants. By a differential display approach, we have isolated a fertilization-induced gene, encoding a sterol 14α-demethylase enzyme and named *CYP51G1-Sc*. Functional characterization of *CYP51G1-Sc* expressed in yeast showed that it could demethylate obtusifoliol, as well as non typical plant sterol biosynthetic intermediates (lanosterol), in contrast with the strong substrate specificity of the previously characterized obtusifoliol 14α-demethylases found in other plant species. *CYP51G1-Sc* transcripts are mostly expressed in meristems and in female reproductive tissues where they are induced following pollination. Treatment of the plant itself with obtusifoliol induced the expression of the *CYP51G1-Sc* mRNA, suggesting a possible role of this transient biosynthetic intermediate as a bioactive signaling lipid molecule. Furthermore, treatments of leaves with ^{14}C-labeled obtusifoliol demonstrated for the first time that this sterol could be transported in distal parts of the plant away from the

sprayed leaves. *Arabidopsis thaliana CYP51* homozygous knockout mutants were also lethal, suggesting important roles for this enzymatic step and its substrate in plant development.

III.8 Introduction

Sterols are ubiquitous components of the plasma membrane where they play an important function in membrane fluidity and permeability (Hartmann and Benveniste, 1987; Hartmann, 1998) and as precursors of the brassinosteroids (BR), a group of plant growth regulators known to affect a wide variety of physiological processes. BR are involved in stem elongation, root growth inhibition, leaf bending and unrolling, pollen tube growth, photomorphogenesis, tracheary element differentiation, promotion of ACC production, and cell elongation mediated either through microtubule reorientation or through alteration of the mechanical properties of the cell wall (Clouse and Sasse, 1998; Clouse, 2002a and b). Sitosterol, campesterol, and stigmasterol are the most abundant sterols in the plant membrane. Over thirty enzymatic steps catalyze the sequential reactions of sterols biosynthesis (Benveniste, 2004) resulting in the wide variety of sterols and biosynthetic intermediates found in plants. More than 60 sterols and derivatives have been identified in maize seedlings (Guo *et al.*, 1995), while animals and fungi contain a less complex sterol mixture, composed mainly of cholesterol and ergosterol respectively (Edwards and Ericsson, 1999).

In vertebrates, cholesterol and steroid derivatives are involved in adequate embryonic development and in keeping homeostasis in adulthood (Farese and Herz, 1998). Intermediates in sterol biosynthesis pathway can also act as signaling molecules (Farese and Herz, 1998; Ponting and Aravind, 1999), while lipid rafts composed of lipids and sterols create a microenvironment in the membrane that activates signal

transduction by promoting clustering of specific membrane-associated proteins such as channels, cytoskeletal-associated proteins, and receptor proteins (Simons and Toomre, 2000). In plants, structural platform such as lipid rafts have recently been identified (Mongrand *et al.*, 2004). In yeast the *ERGOSTEROL-DEFICIENT6* (*ERG6*) gene, the homologue of *Arabidopsis SMT1*, affects protein transport and polar localization at the plasma membrane (Fischer *et al.*, 2004). Furthermore, in the *smt1* mutant, cell polarity and PIN protein positioning are affected (Willemsen *et al.*, 2003). Some homeodomain transcription factors of the HD-ZIP family, such as *ATHB-8* expressed in *Arabidopsis* embryo procambial cells (Baima *et al.*, 1995; Sessa *et al.*, 1998), as well as PHAVOLUTA, PHABULOSA, and REVOLUTA involved in leaf adaxial/abaxial patterning (McConnell *et al.*, 2001) contain, in addition to their DNA binding domain, a steroidogenic acute regulatory transfer domain (or StART domain). In animals, StART domain binds sterols which modulate their regulatory function (Ponting and Aravind, 1999). The functionality of StART domains in plant HD-ZIP proteins remains to be proven.

Interestingly, in the plant sterol biosynthesis pathway, mutations that affect enzymes upstream of 24-methylenelophenol impair embryo patterning and seedling development, while mutations in enzymes located downstream do not (Clouse, 2000, 2002a and b). Overexpression, down-regulation, and mutant analyses of enzymes involved in sterol biosynthesis before the step leading to sitosterol and campesterol synthesis (SMT1, C24-methyltransferase; CYP51, C14-demethylase; FACKEL C14-reductase; HYDRA1, Δ8-Δ7 sterol isomerase) influence the amount of campesterol and the balance between sitosterol and brassinosteroids (Schaller *et al.*, 1998; Jang *et al.*,

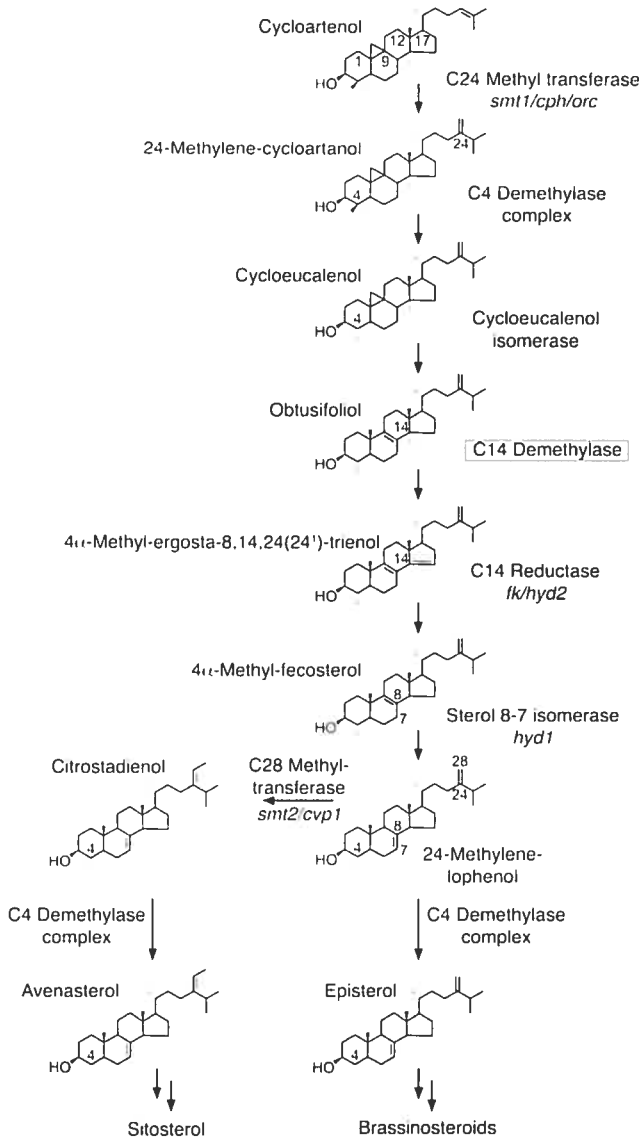

Figure 1.

Schematic representation of the sterol biosynthesis pathway in plants. Only the upper part of the pathway from the first cyclic precursor, cycloartenol, to the first branch point represented by 24-methylene-lophenol is presented. Sterol molecules are labeled with their common names (see sterol nomenclature in the Materials & Methods section). Enzymes involved in the biosynthetic pathway are mentioned and the corresponding genes identified by mutants, when characterized, are shown in italics underneath. The sterol C-14 demethylation step is boxed.

2000; Schrick *et al.*, 2000; Kushiro *et al.*, 2001; Sitbon and Jonsson, 2001; Holmberg *et al.*, 2002; Souter *et al.*, 2002). The *smt1* mutant also shows a defect in vascular patterning (Carland *et al.*, 2002) and *smt1*, *fk*, and *hyd1/2* cannot be rescued by exogenous application of brassinosteroids. While lack of sitosterol and campesterol in these mutants does not seem to explain the embryo defect, abnormal accumulation of biosynthetic intermediates (Jang *et al.*, 2000) or lack of an intermediate sterol as a signal molecule (Schrick *et al.*, 2000) could impair early plant development. The *cvp1/smt2* mutant is slightly different since although it does not exhibit the altered embryogenesis of *fk*, *hyd1* and *smt1*, it also cannot be rescued by BR treatment like the more downstream mutants (Schaeffer *et al.*, 2001; Carland *et al.*, 2002).

The sterol 14α-demethylase is a member of cytochrome P450 gene family which catalyzes the oxidative removal of the 14α-methyl group of lanosterol in mammals and yeast, 24-methylene-24,25-dihydrolanosterol in fungi, and obtusifoliol in plants and some bacteria. In these organisms, this enzymatic oxidative step is considered to be one of the key step of sterol biosynthesis. Sterol 14α-demethylation involves three successive monooxygenation steps of the C14α-methyl group to be removed to produce a C14-double bond and requires NADPH (Werck-Reichhart and Feyereisen, 2000). Genomic analysis revealed more than 280 P450 enzymes in *A. thaliana* which is approximately 5 times more than in any non-plant genome sequenced yet (Schuler and Werck-Reichhart, 2003; Nelson *et al.*, 2004). Out of these P450, CYP51 is the only one that shows conservation between animal, fungi, plant and bacteria phylum (Lepesheva and Waterman, 2004). The enzymatic pathway involving sterol 14α-demethylase

(CYP51) leads to cholesterol formation in mammals, ergosterol in yeast and fungi, and sitosterol and brassinosteroids in plants. Yeast and mammals CYP51 act upstream of the biosynthetic pathway immediately after the production of lanosterol, the first cyclized intermediate, and can oxidize a variety of substrates. In contrast, plants CYP51 are operating several enzymatic steps later and, in relation with their location in the biosynthetic scheme, generally show a strict substrate specificity towards obtusifoliol (Taton and Rahier, 1991; Lamb *et al.*, 1998). Specificity of plant 14α-demethylase has been shown in maize (Taton and Rahier, 1991), wheat (Cabello-Hurtado *et al.*, 1997), sorgho (Bak *et al.*, 1997), and recently in *A. thaliana* (Kushiro *et al.*, 2001). The lack of activity of plants CYP51 toward fungi and mammals substrates has been attributed to a common structural feature common to all these non-plant sterol substrates: the presence of a 4β-methyl group in lanosterol and eburicol, precursors of C14-desmethylsterols, could hinder the binding and (or) demethylation of these sterols (Taton and Rahier, 1991).

Here we report the cloning and characterization of a sterol 14α-demethylase from *Solanum chacoense* (*CYP51G1-Sc*) that can C14-demethylate obtusifoliol, lanosterol, and eburicol, thus being the first plant CYP51 enzyme described with a wider substrate specificity. Expression analyses, translocation of obtusifoliol away from the site of application, and *A. thaliana* knockout insertion mutant phenotype suggest that *CYP51G1-Sc* plays a role in embryogenesis as other members of the sterol pathway located above 24-methylenelophenol, and that obtusifoliol could act as a lipid signaling molecule.

Gene cloning and sequence analysis

We used a differential display approach to isolate genes whose transcription is modulated by pollination and/or fertilization events in pistil tissues. The mRNA profile of pollinated pistils were compared with those of control pistils 24, 36, 48, 72 and 96 hours after pollination. First strand cDNA produced from those RNA were amplified with a combination of seven nucleotides arbitrary primers (H-AP 1 to 16) and a 12 nucleotides anchor primer (H-T11-N), that both included a *Hind* III sequence at their 5' end. One candidate gene, amplified with H-AP-9 (AAGCTTCATTCCG) and H-T11-A (AAGCTTTTTTTTTTTA) (Fig. 2A), showed up-regulation on a differential display gel after pollination, peeking at 72 hours post-pollination. This candidate, named U40 (for up-regulated 40), was excised from the polyacrylamide gel, re-amplified with the H-AP-9 and H-T11-A primer pair, and cloned. Sequence information from this partial cDNA revealed that it belonged to the cytochrome P450 monoxygenase gene family. The initial sequence obtained by DD-RT-PCR covered the 3' untranslated region (UTR) and a small part of the protein C-terminal region. In order to obtain a full-length clone, a cDNA pistil library made from 48 hours post-pollinated pistil tissues was probed with the U40 cDNA fragment and a 1747 bp clone was isolated (Genbank accession number AY552551). The size of this cDNA corresponded to the size estimated on RNA gel blot analysis (1,8 kb), indicating that the cDNA is full-length or near full-length (Fig. 2C). Two in-frame stop codons are found upstream of the longest open reading frame in the 100 nt 5' UTR, indicating that the deduced protein sequence is complete. The gene

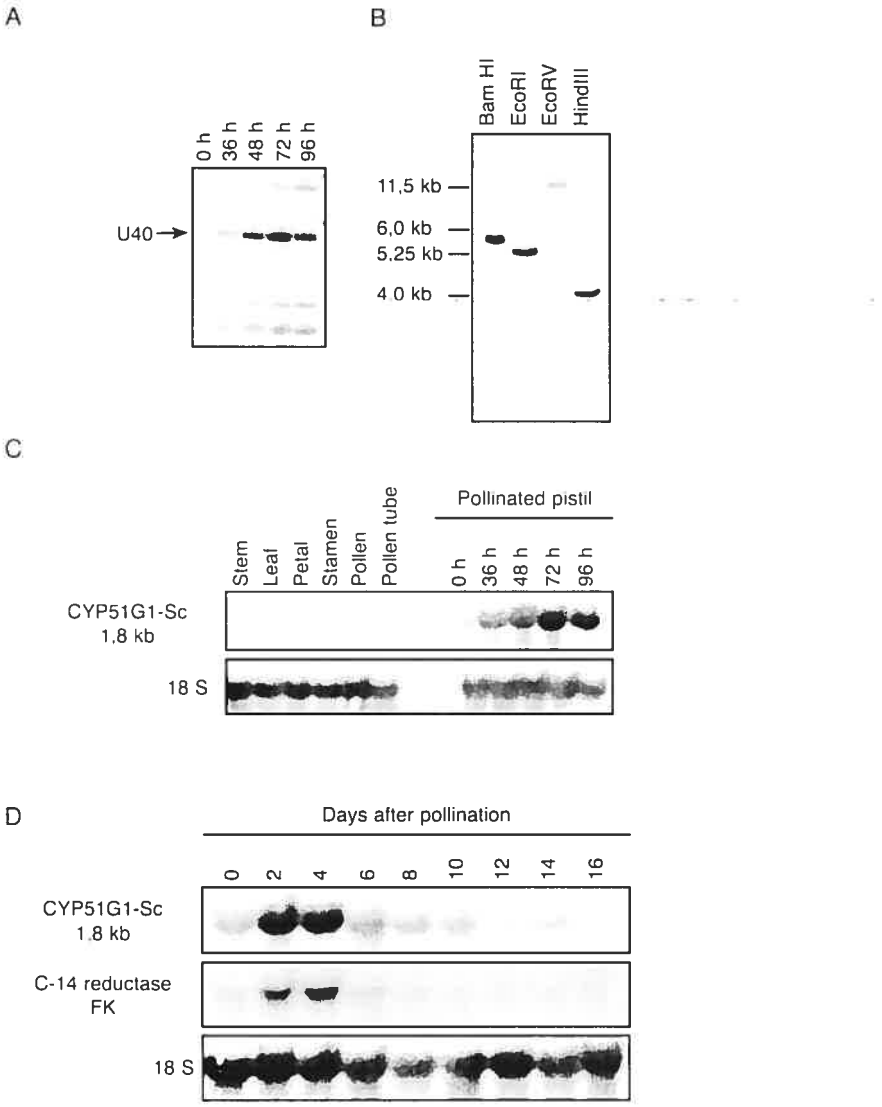
A
0 h
36 h
48 h
72 h
96 h
U40
B
Bam HI
EcoRI
EcoRV
HindIII
11,5 kb
6,0 kb
5,25 kb
4,0 kb
C
Stem
Leaf
Petal
Stamen
Pollen
Pollen tube
Pollinated pistil
0 h
36 h
48 h
72 h
96 h
CYP51G1-Sc
1,8 kb
18 S
D
Days after pollination
0
2
4
6
8
10
12
14
16
CYP51G1-Sc
1,8 kb
C-14 reductase
FK
18 S

Figure 2

Expression analysis and gene copy number of the *S. chacoense CYP51* gene. A. Portion of the differential display gel showing the up-regulated number 40 band (U40). Reverse-transcribed total RNA was extracted from pollinated pistil tissues from 36 to 96 h after pollination, as well as from control unpollinated pistils (0 h), and amplified with the H-AP-9 and the H-T11-A primers. **B**. DNA gel blot analysis of the *CYP51G1-Sc* gene. Genomic DNA (10 μg) isolated from *S. chacoense* leaves was digested with Bam HI, Eco RI, Eco RV or Hind III restriction enzymes, blotted on membrane and probed with the complete 1,7 kb *CYP51G1-Sc* cDNA insert. Molecular weights of the major detected fragments appear on the left. **C**. RNA gel blot analysis of *CYP51G1-Sc* mRNA accumulation in mature tissues and in pistils at different times after pollination. Ten μg of total RNA from the tested tissues was probed with the *CYP51G1-Sc* cDNA insert. **D**. RNA gel blot analysis of *CYP51G1-Sc* mRNA accumulation in isolated ovules (from 6 to 16 DPP) and ovaries without their pericarp (from anthesis to 4 DPP). A *S. chacoense* homologue of the C-14 reductase gene (*FK*) was also used to reprobe the same membrane after stripping.

codes for a 487 amino acids protein with a predicted molecular weight of 55,2 kDa and an isoelectric point of 8,70. The cDNA shared strong sequence identities with sterol 14α-demethylase genes found in yeast, plants and mammals, and was renamed *CYP51G1-Sc* for *S. chacoense* cytochrome P450-sterol 14α-demethylase, following the new nomenclature for the *CYP51* family (Nelson *et al.*, 2004). At the amino acid level (similarity values are shown in parenthesis), CYP51G1-Sc shared 93% sequence identity (97%) with the CYP51 deduced protein from *Nicotiana tabacum*; 82 % (91%) with the *A. thaliana* CYP51A2, recently renamed CYP51G1; 77% (87%) with the CYP51G1 from *Oryza sativa*; 76% (87%) with the CYP51 from *Sorghum bicolor*; 75% (83%) with the CYP51 from *Triticum aestivum*; 37% (55%) with the mouse CYP51; 35% (55%) with the human CYP51; 33% (47%) with the CYP51 from *Mycobacterium tuberculosis*; 32% (53%) with the CYP51 from *Trypanosoma brucei*; 30% (49%) with the CYP51 from the fission yeast (*S. pombe*); and 26% (42%) with the CYP51 from yeast (*S. cerevisiae*).

Gene copy number of the *CYP51G1-Sc* 14α-demethylase

A DNA gel blot of *S. chacoense* genomic DNA was probed with the complete *CYP51G1-Sc* cDNA insert (Fig. 2B). Only one strong hybridizing fragment could be detected for each of the four enzymes used. Since none of these enzymes has a cleavage site in the *CYP51G1-Sc* cDNA, this strongly suggests that *CYP51G1-Sc* is a single copy gene in *S. chacoense*. Although the hybridization and membrane washing conditions were stringent, faint bands could also be observed in some lanes. This could result from

the presence of restriction cleavage sites in introns and/or the presence of a closely related gene in the *S. chacoense* genome. Indeed, a PCR analysis on genomic DNA with primers specific for 5' and 3' ends of the *CYP51G1-Sc* cDNA revealed that it had at least one intron in this region, spanning roughly 700 bp (data not shown). Furthermore, two genes in *A. thaliana* and *N. tabacum* as well as 10 genes in the rice genome have been classified as CYP51 enzymes (Burger *et al.*, 2003; Nelson *et al.*, 2004). This suggests that there might also be related CYP51 isoforms in the *S. chacoense* genome.

CYP51G1-Sc expression profile

A thorough RNA expression profile was conducted in various vegetative tissues as well as in reproductive tissues before and after pollination. The *CYP51G1-Sc* transcript could be detect as a single 1.8 kb band on all tissues tested (Fig. 2, 3 and 5). *CYP51G1-Sc* transcripts were undetectable in stems, petals, stamens, pollen and *in vitro* grown pollen tubes (Fig. 2C). The gene is weakly and similarly expressed in mature leaves and unpollinated pistils on the day of anthesis, as well as in roots (data not shown). Following fertilization, a six fold increase in mRNA levels is detected in pistils, peaking around 72 h post-pollination (Fig. 2C). This increase is transient, as determined by a careful analysis of ovules (from 6 to 16 days post-pollination, DPP) and ovaries without their pericarp (from anthesis to 4 DPP). After peaking between two and four DPP, the *CYP51G1-Sc* mRNA levels steadily decrease thereafter (Fig. 2D). In the sterol biosynthesis pathway (Fig. 1), the next enzymatic step following the 14α-demethylation, is the 14α-reduction, catalyzed by the sterol C14 reductase, encoded by the previously

described *FACKEL* (*FK*) gene (Jang *et al.*, 2000; Schrick *et al.*, 2000). Using sequences selected from tomato ESTs (AI484506, AI485167, AW931153) similar to the *A. thaliana FK* sequence, conserved primers derived from exon nine and thirteen according to the *A. thaliana* sequence, were synthesized and used to obtain a PCR fragment from reverse transcribed ovule mRNAs corresponding to the *S. chacoense FK* gene. A 550 pb DNA fragment was obtained, and sequencing confirmed that the amplified fragment corresponded to the *FK* C14-reductase gene (data not shown). This fragment was used to reprobe the same membrane after complete stripping and the result is shown in Figure 2D. A mRNA expression pattern identical to the one obtained with the *CYP51G1-Sc* probe could also be observed for the *FK* gene in isolated ovules, suggesting similar transcriptional regulation. The *FK* gene has been previously shown to be expressed in the embryo and is involved in cell division and cell expansion (Jang *et al.*, 2000; Schrick *et al.*, 2000).

CYP51G1-Sc expression is regulated both by pollination and fertilization

Since in *S. chacoense* fertilization occurs from 36 h onward after pollination (O'Brien *et al.*, 2002b), we next determined if the strong induction of the *CYP51G1-Sc* mRNA transcripts was triggered by pollination alone, or if fertilization was indeed needed to increase the steady-state levels of the *CYP51G1-Sc* mRNA. To address this issue we both carried a closer time-course analysis and took advantage of the gametophytic self-incompatibility barrier expressed in *S. chacoense* stylar tissues. *S. chacoense* expresses stylar ribonucleases (S-RNases) that can reject pollen having the same genetic constitution at the S-locus, thus preventing inbreeding (Matton *et al.*,

1997). In such an incompatible pollination, pollen tube growth is arrested in the first two-third of the style and pollen tubes never reach the ovules. A pollination time-course was conducted, and RNA gel blot analyses were done on styles and ovaries separately (Fig. 3A and B). Twenty-four hours after either a compatible or an incompatible pollination, *CYP51G1-Sc* mRNA levels were strongly induced in ovaries (Fig. 3B) indicating that the gene was pollination-induced, at a distance, in the ovary. Furthermore, *CYP51G1-Sc* mRNA levels declined in compatibly pollinated styles (see also fig. 5) while they remained constant in styles following an incompatible pollination, albeit *CYP51G1-Sc* mRNA levels are only expressed at a very low level in both cases when compared to the *CYP51G1-Sc* mRNA levels found in the ovary. In a compatible pollination, the *CYP51G1-Sc* mRNA levels remained high in the ovary during the whole time-course period (until 4 days after pollination) while a drastic decrease was observed after three days following an incompatible pollination, leading to nearly undetectable levels of *CYP51G1-Sc* mRNA four days after pollination (Fig. 3B), suggesting that the *CYP51G1-Sc* gene is regulated by both pollination and fertilization. Only during a compatible pollination leading to fertilization and seed set is a sustained accumulation observed (Fig. 2D and 3B), while an incompatible pollination only leads to the first and transient burst of accumulation, corresponding to the pollination-induced phase. This type of response has already been observed for some fertilization-responsive genes and pollination-induced expression had been linked to a wounding effect (Lantin *et al.*, 1999; O'Brien *et al.*, 2002a). Indeed, in many species, pollination is known to induce deterioration and death of cells or tissues, including the secretory cells in the stigma and the transmitting tissue of the style (Cheung, 1996). To determine if cell death caused by wounding could also trigger *CYP51G1-Sc* mRNA accumulation at a distance in the

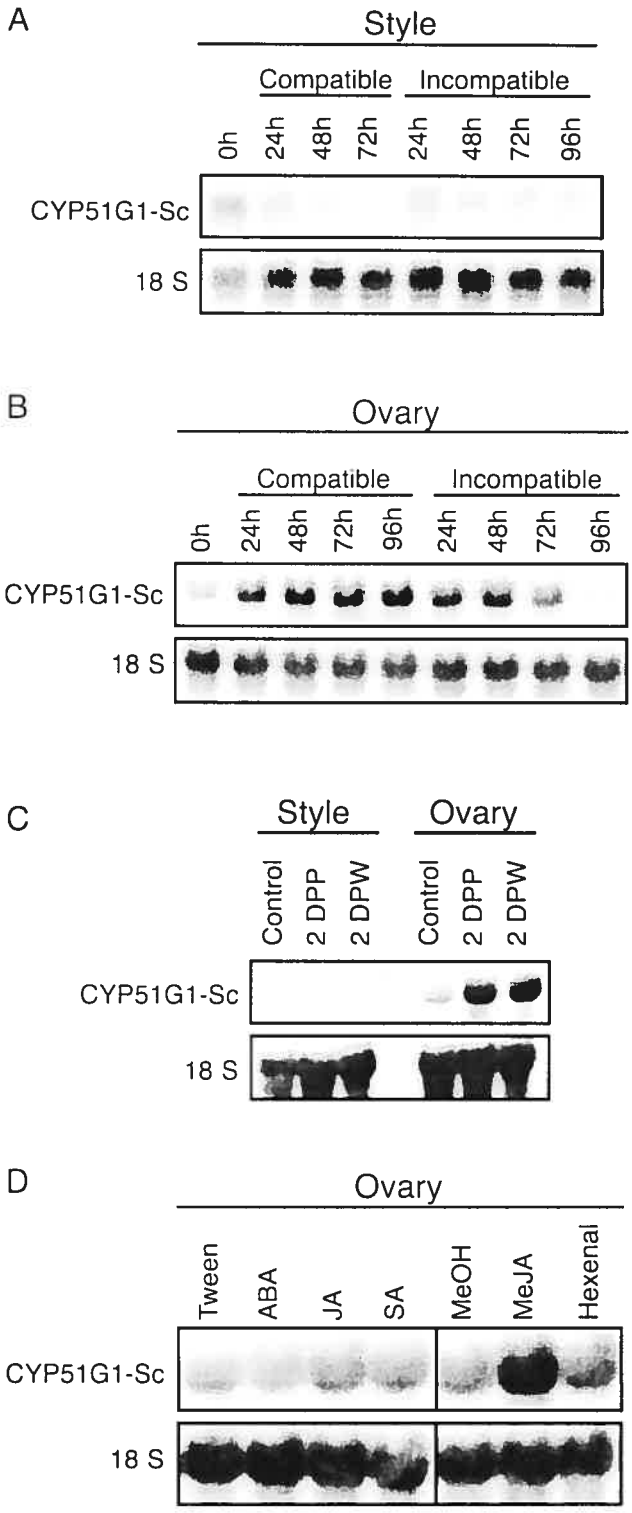
A
Style
Compatible
Incompatible
0h
24h
48h
72h
24h
48h
72h
96h
CYP51G1-Sc
18 S
B
Ovary
Compatible
Incompatible
0h
24h
48h
72h
96h
24h
48h
72h
96h
CYP51G1-Sc
18 S
C
Style
Ovary
Control
2 DPP
2 DPW
Control
2 DPP
2 DPW
CYP51G1-Sc
18 S
D
Ovary
Tween
ABA
JA
SA
MeOH
MeJA
Hexenal
CYP51G1-Sc
18 S

Figure 3

RNA expression analysis of *CYP51G1-Sc* transcript levels in styles and ovaries following pollination and stress treatments. A and B. Effect of compatible and incompatible pollination on *CYP51G1-Sc* transcript levels. *CYP51G1-Sc* transcript levels were determined by RNA-gel blot analysis in unpollinated pistils on anthesis day (0 h), in pistils collected from 24 to 96 h after a fully compatible ($S_{11}S_{13}$ x $S_{12}S_{14}$) pollination or a fully incompatible ($S_{12}S_{14}$ x $S_{12}S_{14}$) pollination. Styles and ovaries mRNAs were extracted and blotted separately. **C**. *CYP51G1-Sc* transcript levels were determined by RNA gel blot analysis of tissues 2 days after pollination (DPP) or 2 days after wounding (DPW). Styles were either compatibly pollinated or slightly crushed with tweezers and collected two days later. Unpollinated and unwounded styles and ovaries served as controls. Ovaries from the same pistils were also collected either 2 DPP or 2 DPW. **D**. *CYP51G1-Sc* transcript levels were determined by RNA gel blot analysis of unpollinated ovary tissues collected 48 h after various hormonal treatments. Spray treatments: ABA and JA as 50 μM solutions in 0.05% Tween; SA as a 5 mM solution in 0.05% Tween. Flowers sprayed with a 0.05% Tween solution served as control. For treatment with volatiles, methyl jasmonate or trans-2-hexenal were first diluted to 0.1 M in ice-cold methanol and 100 μl of the compound (equivalent to 10 μl/l of air space) was added to a piece of Whatman paper suspended over the plant in an airtight container. Treatment with 100 μl of MeOH served as control. For all RNA gel blots, ten μg of total RNA from the various tissues were probed with the *CYP51G1-Sc* cDNA insert. To ascertain equal loading conditions, all RNA-gel blots were stripped and re-probed with an *18S* ribosomal cDNA probe from *S. chacoense*.

ovary, the styles of young flowers were slightly crushed with tweezers and the styles and ovaries were collected separately 48 h later. Figure 3C shows that wounding of the style also induced *CYP51G1-Sc* mRNA accumulation at a distance in the ovary (Fig. 3C, lane 2 DPW), to the same extent as a 48 h compatible pollination (Fig. 3C, lane 2 DPP). Wounding had only a modest effect in the style itself (Fig. 3C), as determined before for pollen tube growth in the style (Fig. 3A). Thus, cellular deterioration and death caused by pollination (either compatible or incompatible) or by wounding, might be the initial trigger that induces *CYP51G1-Sc* mRNA accumulation in the ovary. In order to confirm this, various wound or defense-related hormones were tested. None had a significant effect of *CYP51G1-Sc* mRNA accumulation in styles (data not shown) but in ovaries, methyl jasmonate treatment was able to mimic a wound- or pollination-induced response (Fig. 3D), suggesting that the first and transient *CYP51G1-Sc* mRNA accumulation phase was induced by transmitting tract cell death caused by pollen tube growth.

In situ analysis of *CYP51G1-Sc* mRNA accumulation

In order to determine more precisely the tissular expression pattern of the *CYP51G1-Sc* 14α-demethylase, *in situ* hybridizations were performed on 10 μm sections of fertilized ovaries three days after pollination, where peak accumulation occurs (Fig. 2C and D). The *CYP51G1-Sc* anti-sense probe detected strong expression in the placenta, as well as in the developing pericarp, with much weaker staining in the ovule's integument (Fig. 4A). This expression pattern could explain the RNA gel blot results shown in Figure 2D, where a steep decline was observed in *CYP51G1-Sc* mRNA levels in isolated ovules, from 6 days after pollination. A magnification of the major

accumulation area detected in Figure 4A is shown in Figure 4C. Although *CYP51G1-Sc* mRNAs can be detected everywhere in the placenta and the pericarp, a darker staining band corresponding to thin-walled parenchymatous cells can be observed in the placenta layer immediately underneath the outermost cell layer, that forms the placenta's epidermis. This layer which does not express the *CYP51G1-Sc* mRNAs is continuous with the ovule's integument epidermis, where no *CYP51G1-Sc* mRNAs could be detected, indicating a clear difference and specialization of this layer in both the placenta epidermis and the ovule's integument. As a control, similar sections were hybridized with the *CYP51G1-Sc* sense probe and no significant staining could be observed (Fig. 4B and D). Although *CYP51G1-Sc* mRNA levels were quite low in mature tissues, the fertilization-induced expression could suggest that *CYP51G1-Sc* mRNAs accumulate preferentially in rapidly growing tissues and meristematic cells, as observed for the *FK* gene (Jang *et al.*, 2000; Schrick *et al.*, 2000). *In situ* hybridizations were thus conducted on shoot apex containing shoot apical meristems. Figure 4 (E and F) shows that *CYP51G1-Sc* mRNAs strongly accumulated in the shoot apical meristem (SAM), in young primordia, as well as in the young leaflets that surround the apex. Furthermore, preferential accumulation can distinctly be observed on the adaxial side of the developing leaves. A control hybridization with a *CYP51G1-Sc* sense probe, showing the specificity of the staining pattern, is shown in Figure 4F. Although *CYP51G1-Sc* mRNA accumulation was shown to be very low in mature styles (Fig. 3A and C), the strong accumulation observed in young developing tissues prompted us to determine if other actively growing tissues apart from the meristems and shoot apex, would also accumulate substantial amounts of *CYP51G1-Sc* mRNAs. We had previously shown that a pistil-expressed aquaporin was strongly expressed in young developing styles and that

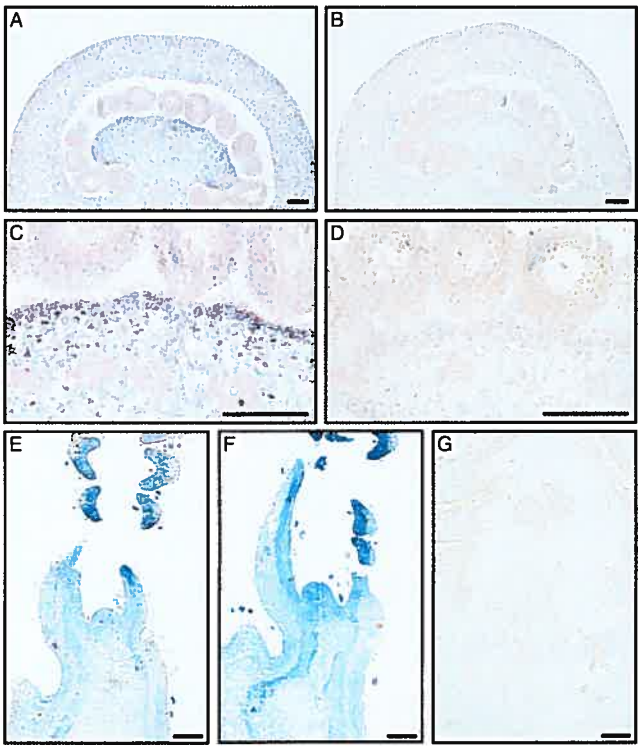

Figure 4

***In situ* localization of *CYP51G1-Sc* transcripts. A and B.** Ovary section 72h after pollination (~36h post-fertilization). **C and D.** Magnification of the dark staining placenta layer shown in A and B. **E, F, and G.** Shoot apex showing both shoot apical meristem and sections of young leaflets covering the shoot apex. **A, C, E,** and **F,** anti-sense probe. **B, D,** and **G,** control sense probe. Digoxigenin labeling is visible as a blueish staining. All hybridizations used 10 μm thick sections and an equal amount of either *CYP51G1-Sc* sense or antisense probe. Scale bars represent 100 μm.

peak accumulation coincided with the zones of fastest growth (O'Brien *et al.*, 2002a). Other reports had also linked aquaporin expression with zones of cell division, cell elongation, and cell expansion in various tissues (Ludevid *et al.*, 1992; Chaumont *et al.*, 1998; Balk and de Boer, 1999). We thus used developing styles to determine the *CYP51G1-Sc* mRNA accumulation profile in a fast growing tissue. Figure 5A shows that *CYP51G1-Sc* mRNA levels are highest in immature developing styles, and that *CYP51G1-Sc* mRNAs are barely detectable in mature tissues after anthesis. Furthermore, an asymmetrical distribution can be observed with a preferential accumulation in the lower style region prior to anthesis (Fig. 5B).

***erg11* yeast complementation**

To further address the functionality of the CYP51G1-Sc enzyme we assessed its potential to rescue the yeast *erg11* mutant strain, that is deficient in the CYP51 lanosterol demethylase enzyme. Under aerobic condition, the homozygote *erg11* mutant is deficient for lanosterol demethylation and is unable to grow without ergosterol supplementation (Kalb *et al.*, 1987). Diploid ERG11/*erg11* yeast strains transformed with the pYeDP60 vector only (control) and ERG11/*erg11* yeasts transformed with *CYP51G1-Sc* coding region in the pYeDP60 vector were grown on a sporulating liquid media to induce the production of haploid spores, hence revealing the mutant phenotype of the *erg11* allele. Recombinant spores that harbored the pYeDP60 vector were selected through an adenine selection (Pompon *et al.*, 1996). Spores were spread on a media supplemented with ergosterol as to obtain non-confluent colony growth. Colonies were replicated and allowed to grow in a selective aerobic media without ergosterol.

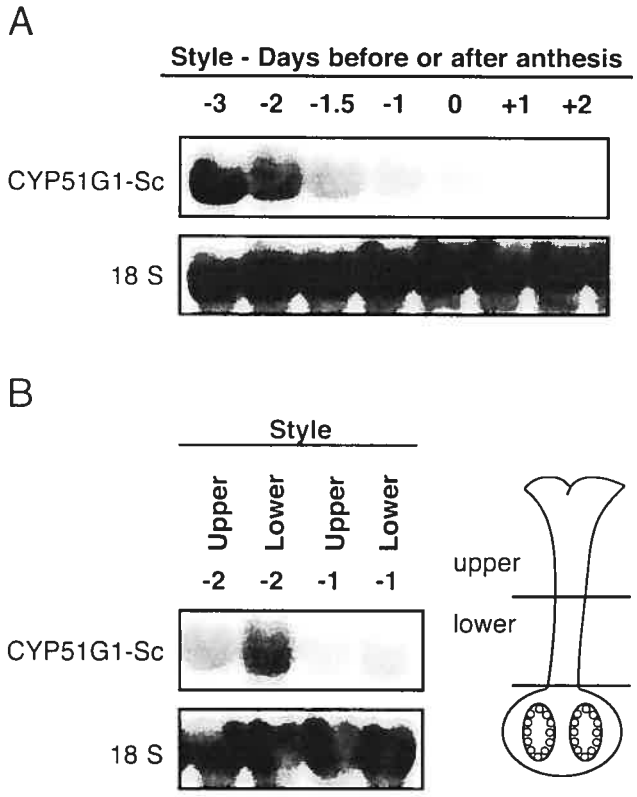

Figure 5

Developmental expression pattern of *CYP51G1-Sc* mRNA levels in unpollinated pistil tissues. **A.** *CYP51G1-Sc* mRNA levels in styles of unpollinated pistil tissues were analyzed by RNA gel blot analysis. Ten μg of total RNA from styles three days before anthesis to two days after anthsesis were probed with the *CYP51G1-Sc* cDNA insert. **B.** RNA gel blot analysis of *CYP51G1-Sc* mRNA levels in the upper and lower halves of styles from flowers two (-2) and one (-1) day before anthesis.

Percentage of viability was inferred by comparison of colony growth between the duplicated pair. The analysis was performed on five independently transformed series of yeast cells for which 36 randomly picked haploid colonies per series were analyzed. Mutant cells transformed with the empty vector only showed 48% viability (17.4 ± 2.3), which is near the expected value for sporulated heterozygous mutant cells (50%). A partial rescue of the mutant cells in the presence of the *CYP51G1-Sc* expressing plasmid was observed with a significant increase in cell viability to 81% (29.0 ± 1.2), indicating that the *S. chacoense* CYP51G1 enzyme could substitute for the yeast endogenous enzyme.

Demethylase activity profile of CYP51G1-Sc expressed protein

To confirm that the *CYP51G1-Sc* clone indeed coded for a C14-demethylase enzyme, the complete open reading frame was cloned in the pYeDP60 yeast expression vector, expressed in the WAT11 yeast strain, and tested for C14-demethylation activity on various substrates. Boiled membrane preparations (Fig. 6A, BM) were used as a control for the presence of endogenous demethylation products. Transformation of the WAT11 yeast strain with the empty pYeDP60 vector (EV) was used to monitor substrate transformation by endogenous CYP51 present in the yeast preparation. After transformation with this empty vector, in addition to the expected C14-demethylation of lanosterol (peak 3) into 4,4-dimethylzymosterol (peak 4) (Fig. 6A, EV) (1.44 nmol mg-1 h-1) by the yeast endogenous ERG11p, a poorer but significant demethylation of obtusifoliol (peak 1) into 4α-methyl-ergosta-8,24(24^1)-dien-3-β-ol (peak 2) (Fig. 6A,

EV) could be detected (0.96 nmol mg-1 h-1), in accordance with previous data showing that this 4α-methylsterol is a possible substrate of ERG11p (Aoyama and Yoshida, 1992). Expression of the *CYP51G1-Sc* construct in the WAT11 yeast strain led to a four fold increase of the demethylation rate of obtusifoliol into 4α-methyl-ergosta-8,24(24^1)-dien-3-β-ol (peak 2) (Fig. 6A, CYP51) (3.54 nmol mg-1 h-1), indicating that CYP51G1-Sc indeed coded for an obtusifoliol 14α-methyl demethylase. Remarkably, when lanosterol was used as a substrate, its demethylation rate into 4,4-dimethyl-zymosterol (peak 4) (Fig. 6A, CYP51) was also increased two fold following expression of the *CYP51G1-Sc* construct. This showed that the CYP51G1-Sc enzyme did not have a strict substrate specificity for the typical plant 4α-methylsterol physiological substrate (Taton and Rahier, 1991), being also able to C14 demethylate a 4,4-dimethylsterol (Fig. 6C). Similarly, we could also observe a significant increase for the C14-demethylation of another 4,4-dimethylsterol, eburicol, in the presence of the CYP51G1-Sc protein when compared to the WAT11 yeast strain transformed with the empty vector (data not shown). However, the observed higher relative increment of activity obtained with obtusifoliol strongly suggests a preference of CYP51G1-Sc for this substrate (Fig. 6B).

Obtusifoliol can act as a signaling molecule and moves through the phloem

The results obtained with the *fk* mutant (sterol C14-reductase) prompted the authors to suggest that the synthesis of sterol signals in addition to brassinosteroids would be important in mediating cell growth and organization during embryo development (Jang *et al.*, 2000; Schrick *et al.*, 2000). This implies that sterols other than

A

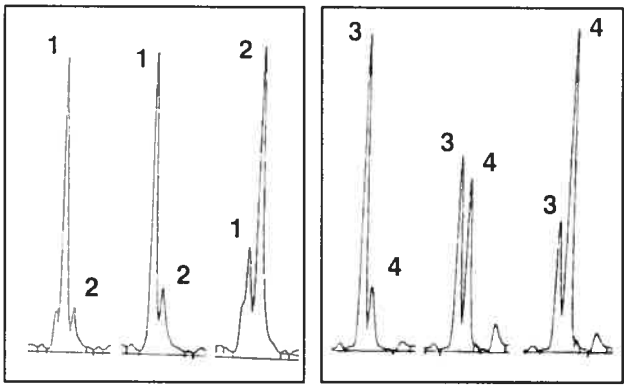

B

Plasmid	Obtusifoliol nmole.mg^{-1}.h^{-1}	Lanosterol nmole.mg^{-1}.h^{-1}
Empty vector	0.96 ± 0.49 (n=3)	1.44 ± 0.56 (n=3)
CYP51G1-Sc	3.54 ± 0.36 (n=3)	3.21 ± 0.46 (n=3)
CYP51G1-Sc/ empty vector	3.7	2.2

C

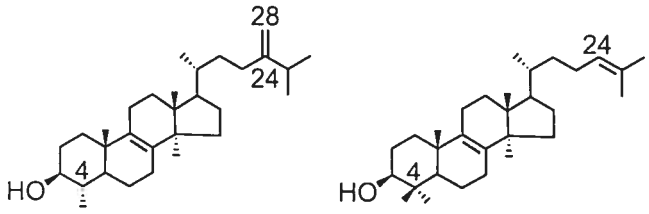

Obtusifoliol Lanosterol

Figure 6

CYP51G1-Sc enzymatic activity assay. A. The CYP51G1-Sc protein was expressed in the WAT 11 yeast strain. After incubation of substrate (50 μM) in the corresponding microsomal preparation and extraction procedure, a GC/MS analysis of the assay was performed. Substrates used: (1), obtusifoliol; (3), lanosterol. Products: (2), 4α-methyl-ergosta-8,24(24^{1})-dien-3-β-ol; (4), 4,4-dimethyl-zymosterol. BM; boiled microsome membrane; EV, pYeDP60 empty vector; CYP51, *CYP51G1-Sc* in pYeDP60 vector. **B**. 14α-demethylation specific activity results from three independent experiments using distinct microsomal preparations. **C**. Chemical structures of obtusifoliol and lanosterol.

brassinosteroids would be active on their own as signaling molecules (Lindsey *et al.*, 2003). In order to test if obtusifoliol could act as a signaling molecule we tested if it could act locally and at a distance in systemic non-inoculated leaves. Figure 7 shows an RNA gel blot analysis probed with the *CYP51G1-Sc* cDNA insert. An isolated compound leaf was protected with a Whatman paper cone and gently sprayed with a solution of either lanosterol, obtusifoliol, or tween as a control, on different plants of the same age and kept in identical conditions in the greenhouse. Two days later, the sprayed leaf as well as an upper leaf were harvested and tested for *CYP51G1-Sc* mRNA levels. When compared to the control leaf, tween and lanosterol had no effect, both locally and systemically. A significant and reproducible two-fold increase could be observed with leaves treated with obtusifoliol, both locally and systemically, suggesting that the obtusifoliol sterol could itself act as a signaling molecule, or alternatively, that the effect could be mediated through another diffusible signal induced by the application of obtusifoliol. Consistent with previous results showing higher *CYP51G1-Sc* mRNA levels in actively growing tissues (Fig. 4 and 5), the basal level of *CYP51G1-Sc* mRNAs were higher in the younger systemic leaf, although an increase in steady state level of *CYP51G1-Sc* mRNAs following obtusifoliol treatment was reproducibly observed both locally and at a distance in systemic leaf. To test if obtusifoliol could itself be a mobile signaling molecule, C14-radiolabeled obtusifoliol was produced and sprayed on a compound leaf again protected with a Whatman paper cone. After two days, detached leaves from the main stem were pressed and dried. Figure 8A shows the arrangement of the pressed leaves as they appear on the main stem. Compound leaf #5 was sprayed and exposed separately. Figure 8B shows an autoradiogram of the dried leaves. Leaves are numbered from the base and the location of the sprayed leaf is indicated with the

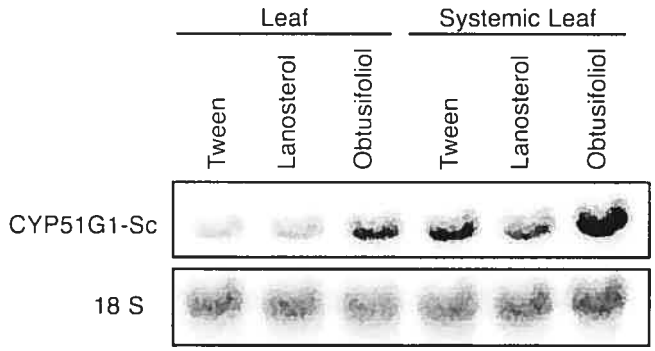

Figure 7

RNA expression analysis of *CYP51G1-Sc* transcript levels in treated and untreated systemic leaves. Lanosterol and obtusifoliol were emulsified with Tween 80 in water and sprayed (250 µl of a 0,5 mM solution) over a whole compound leaf. Tween application served as a control. After 48 h, the treated leaf as well as a younger (upper) systemic leaf were harvested. Ten µg of total RNA from the tissues was probed with the *CYP51G1-Sc* cDNA insert. To ascertain equal loading conditions, all RNA-gel blots were stripped and re-probed with an *18S* ribosomal cDNA probe from *S. chacoense*.

duplication of its internode base (tagged and numbered 5; see also dotted line on Fig. 8A). Apart from residual C14-labeled obtusifoliol on the sprayed leaf, a high amount of labeling was also found in leaf #4, immediately below the sprayed leaf (leaf #5). By overlapping the two pictures, the labeling was detected in the stem as well as in portions of some leaflets in leaf #4. Lower but significant amount of labeling could also be observed in the stems of all leaves (from leaf #1 to 6), both positioned immediately above or below the sprayed leaf #5. This suggested that obtusifoliol or a metabolite of this sterol was transported through the phloem and could act as a mobile signaling molecule. In order to determine the structure of the radiolabeled compound(s) found in leaves distal to the sprayed leaf, the total lipid fraction was isolated from both the inoculated leaf #5 and distal leaf #4, where strong radiolabeling was observed. Thin layer chromatography analysis of this fraction in the absence of addition of any carrier compounds indicated that the bulk of the radioactivity was associated in both cases with the 4α-methylsterols fraction (peak 1 in Fig. 9A and B) and the steryl-esters fraction (peak 2 in Fig. 9A and B). The 4α-methylsterols fraction was acetylated and further analyzed on $AgNO_3$ impregnated SiO_2-TLC. This led in both cases to a single radioactive peak having a RF corresponding to a sterol possessing two double bonds at C8(9) and C24(241) and comigrating with a standard of obtusifoliyl acetate (peak 1 in Fig. 9C and D). Analysis of compound(s) present in peak 1 allowed a single compound to be directly and unequivocally identified as obtusifoliyl acetate by coupled capillary GLC-MS analysis (i.e., by coincidental retention time and identical electron impact spectrum as authentic standard). After saponification, the radioactive steryl-esters fraction (peak 2, Fig. 9A and B) was further analysis as above and allowed also a single

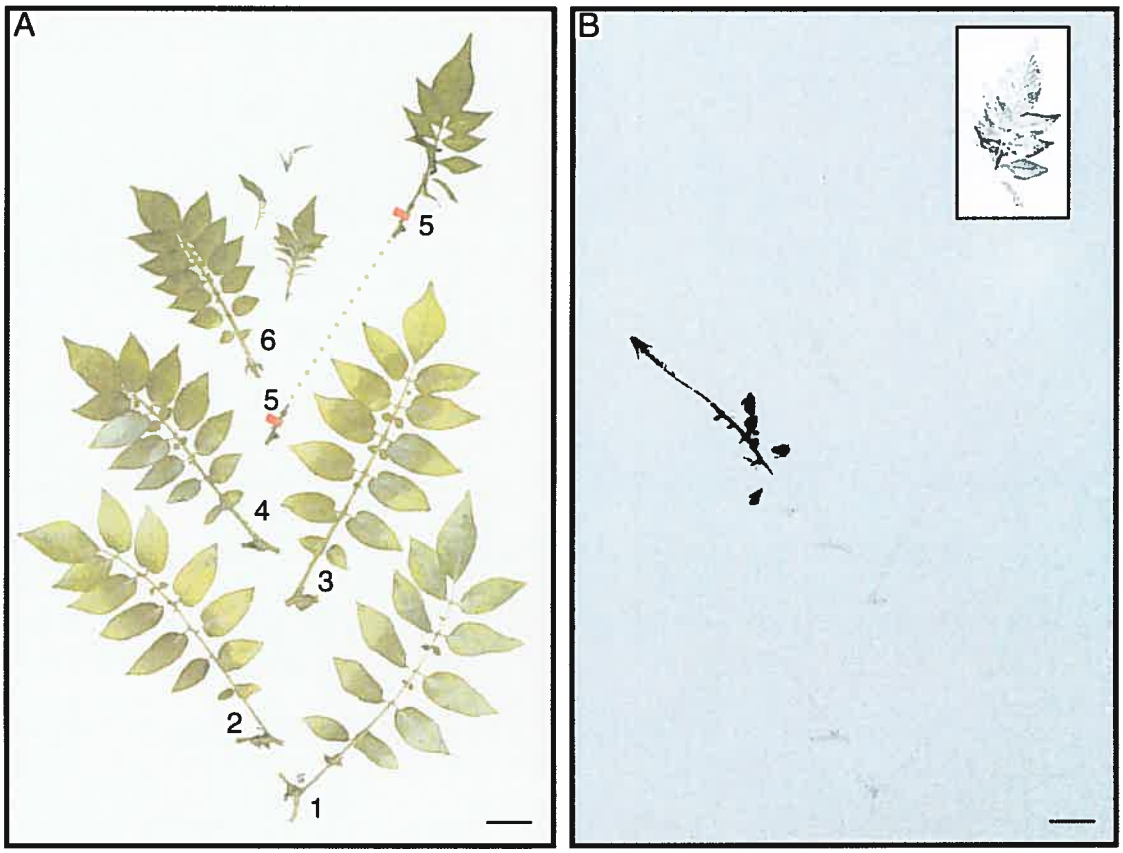

Figure 8

Treatment of *S. chacoense* intact leaves with [^{14}C]-radiolabeled obtusifoliol. A. Compound leaf #5 was sprayed with a radiolabeled obtusifoliol solution (250 µL of a 2,7 mg/mL solution (5,66 mM), with a specific activity of 1 250 000 cpm mg^{-1}) and left for 48 h on an intact plant in the greenhouse. Detached leaves were pressed and dried, and arranged as they appear on the main stem. Location of the sprayed leaf is indicated with the duplication of its internode base (see dotted line). **B.** Autoradiogram of the radioactive pressed specimen in **A** after one week exposure. The sprayed leaf (leaf #5) was exposed separately for 2 days. Bar correspond to 2 cm.

compound, obtusifoliol, to be identified in the fraction.

Physiological relevance of the observed effect of obtusifoliol was determined by the analysis of the recovered C14-labeled obtusifoliol fraction from the treated and distal leaves or stems. The C14-labeled obtusifoliol synthesized had a specific activity of 1.25 x 10^6 cpm mg^{-1}. For the sprayed leaf #5, 1 390 cpm of sterol per mg of dry weight tissue were recovered, which corresponds to 1 112 μg of obtusifoliol per gram of dry weight tissue. For leaf #4, where most of the radioactivity was translocated, 233 cpm of sterol per mg of dry weight tissue were recovered, which corresponds to 186 μg of obtusifoliol per gram of dry weight tissue. For the upper systemic leaf #6, which corresponds to the position of the leaf assayed in fig. 7, 3 cpm of sterol per mg of dry weight tissue were recovered from the petiole, which corresponds to 2.4 μg of obtusifoliol per gram of dry weight tissue. Considering that, in plants, obtusifoliol represents from 0.1 to 1% of the total sterol fraction, and that total sterols sum up to ≈ 2 500 - 4 000 μg per gram of dry weight tissue (Schmitt and Benveniste, 1979; Schaeffer *et al.*, 2001; Holmberg *et al.*, 2002; Schrick *et al.*, 2004), this indicates that a normal physiological concentration of obtusifoliol would be ≈ 2.5 – 40 μg per gram of dry weight tissue, suggesting that the observed levels of C14-labeled obtusifoliol detected in leaf #4 and #6 would be in the physiological range of obtusifoliol concentrations.

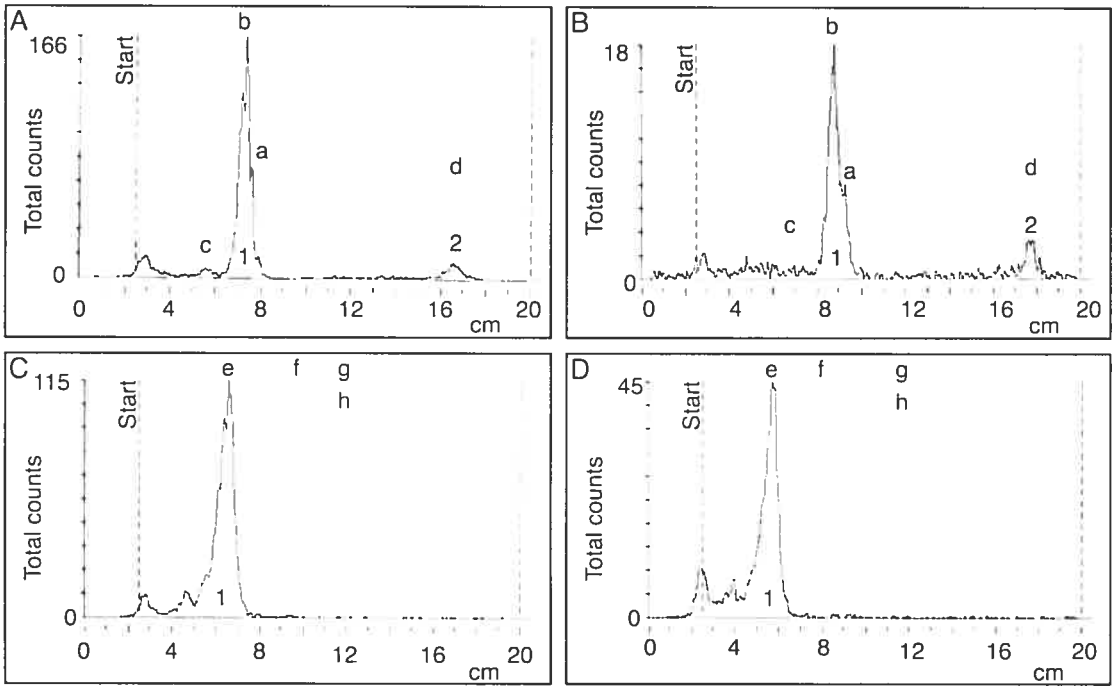
A
166
Start
b
a
d
c
1
2
Total counts
0
0 4 8 12 16 20
cm
B
18
Start
b
a
d
c
1
2
Total counts
0
0 4 8 12 16 20
cm
C
115
Start
e
f
g
h
1
Total counts
0
0 4 8 12 16 20
cm
D
45
Start
e
f
g
h
1
Total counts
0
0 4 8 12 16 20
cm

Figure 9

A and B. Radiochromatogram scans of TLC plates showing accumulation of radioactivity in the 4α-methylsterols (1) and steryl-esters (2) fractions from the unsaponifiable extract from both the initially inoculated compound leaf (panel **A**) and the distal compound leaf (panel **B**) corresponding respectively to leaf #5 and leaf #6 in Fig. 8. In the absence of added cold carrier obtusifoliol, the minor radioactivity peak on the starting line corresponds to degradation products of obtusifoliol during the feeding experiment and analytical procedure. Unlabeled standards: a, lanosterol; b, obtusifoliol; c, cholesterol; d, cholesteryl-stearate. **C and D**. Radiochromatogram scans of $AgNO_3$–impregnated SiO_2–TLC plates from the chromatography of acetylated 4α-methylsterols fractions showing accumulation of radioactivity in fraction (1) migrating as a standard of obtusifoliyl acetate in both the initially inoculated compound leaf (panel **C**) and the distal compound leaf (panel **D**), and corresponding respectively to leaf #5 and leaf #6 in Fig. 8. Radioactivity on and near the starting line corresponds to degradation products due to the absence of addition of cold carrier obtusifoliol. GC-MS analysis of compounds present in peak 1 indicated the presence of a single compound, obtusifoliol acetate, in this fraction, in both samples. Unlabeled standards: Panel **A** and **B**: a, lanosterol; b, obtusifoliol; c, cholesterol; d, cholesteryl-stearate. Panel **C** and **D**: e, obtusifoliyl acetate; f, 4α,14α-dimethyl-stigmasta-8,24-dienyl acetate; g, 4α,14α-dimethyl-cholest-8-enyl acetate; h, 4α,14α-dimethyl-9β,19-cyclo-ergostanyl acetate.

CYP51G1-At homozygous mutant is lethal

The *A. thaliana* genome contains two *CYP51*-related gene, *CYP51G1-At* (formerly *AtCYP51A2*) and *CYP51G2-At* (formerly *AtCYP51A1*). The *CYP51G1-Sc* gene is most closely related to *CYP51G1-At*, sharing 82% sequence identity (91% similarity) with *CYP51G1-At*, compared to 67% sequence identity (79% similarity) with *CYP51G2-At*. In order to determine the role of the CYP51 14α-sterol demethylase in plants, a heterozygous T-DNA insertion line for the *CYP51G1-At* was obtained from the SALK collection. This line (SALK_067630) has a T-DNA insertion in the *CYP51G1-At* open reading frame (ORF), interrupting the ORF around amino acid position 45. DNA primers derived from the *CYP51G1-At* gene confirmed that a T-DNA element was inserted at the reported position in this line (data not shown). After selfing, seeds from this mutant line were collected and germinated on agar plates. Out of 36 seeds, 5 did not germinate, 3 died at the cotyledon stage, and 28 showed a wild type phenotype. A PCR analysis was carried out on genomic DNA extracted from cotyledons or leaves with primers bordering the insertion showed that the three seedlings that died at the cotyledon stage where homozygous for the T-DNA, while out of the 28 normal looking plants, 16 where heterozygous for the T-DNA and the remaining 12 where wild type homozygous plants. As a control, 36 *A. thaliana* WT plant seeds were also plated onto agar media. All germinated and gave normal looking seedlings. The ratio obtained (8:16:12) in the selfed SALK_067630 line is quite close to the expected mendelian ratio if the 5 seeds that did not germinate are counted as putative homozygous mutant. No PCR analysis was carried out on these non-germinated seeds because of the presence of tissues originating from the heterozygous parents. This indicates that, the *CYP51G1-At* homozygous mutant is lethal. As for the *FK* mutant (Jang *et al.*, 2000; Schrick *et al.*,

2000), exogenous application of brassinolide at a concentration of 1 μM could not rescue the seedling lethal phenotype observed in the *CYP51G1-At* homozygous mutant line (data not shown). Furthermore, this result also shows that the *CYP51G2-At* is not redundant with the *CYP51G1-At* gene, and must have evolved a new substrate specificity. Alternatively, it could have retained CYP51 activity but its expression pattern might be completely different than that of *CYP51G1-At*, precluding complementation of the lethality phenotype observed. A SALK T-DNA insertion line for the *CYP51G2-At* (*AtCYP51A1*) gene was also available, and was tested for its phenotype. This line (SALK_070949) has a T-DNA insertion in the 3'UTR of the transcript. After selfing, 36 seeds were germinated on agar media. Thirthy-five reached maturity and only one did not germinate. Six plants where homozygous for the T-DNA, twenty one where heterozygous and eight where wild type. No phenotype could be observed on plant homozygous for the T-DNA insertion, suggesting that, under the conditions used, the gene is dispensable, or alternatively, the T-DNA insertion has no effect on the transcript production or translation.

III.10 Discussion

The recent identification of sterol mutants affecting pattern formation, cell polarity, embryogenesis, vascular patterning and hormone signaling is shedding new light on the role of sterols in plant development (Clouse, 2002a and b; Lindsey *et al.*, 2003; Fischer *et al.*, 2004). Apart from the well described dwarf mutants resulting from reduced brassinosteroid accumulation (Altmann, 1999), other mutants that cannot be rescued by brassinosteroids addition show distinctive defects associated with the body organization of the embryo (Jang *et al.*, 2000; Schrick *et al.*, 2000; Schrick *et al.*, 2004). This suggests that sterols other than the brassinosteroids could also be active signaling molecules in plant development. Using a differential-display approach to identify genes regulated by fertilization we have isolated a cytochrome P450 gene of the *CYP51* family and thereafter named *CYP51G1-Sc*. The sterol C14-demethylase (*CYP51*) is the most widely distributed cytochrome P450 gene family being found in all biological kingdoms and it is considered the most ancient member of the cytochrome P450 superfamily. In the sterol biosynthesis pathway, the obtusifoliol 14α-demethylase step is located immediately upstream of the C14-reductase, characterized through the *fk/hyd2* mutants (Jang *et al.*, 2000; Schrick *et al.*, 2000); two steps upstream of the C-8,7 isomerase, characterized through the *hyd1* mutant (Topping *et al.*, 1997; Souter *et al.*, 2002); and two steps downstream of the C24-methyltransferase characterized through the *smt1/cph/orc* mutants (Diener *et al.*, 2000; Schrick *et al.*, 2002). Loss of function mutations in all these genes lead to embryonic and seed defects that cannot be rescued by exogenous application of brassinosteroids, unlike loss of function mutations

downstream of the 24-methylenelophenol intermediate. Analysis of *A. thaliana* insertional mutant plants for the orthologue of the *S. chacoense CYP51G1-Sc*, the *CYP51G1-At* (82% amino acid sequence identity, 91% similarity) showed that homozygous insertional mutants were lethal and that seedlings, when they were obtained, died very early at the cotyledon stage (data not shown). Furthermore, the mutant could not be rescued by exogenous application of brassinosteroids, as determined for the above mentioned mutants. The analysis of this mutant line (SALK_067630) harboring an insertion at the N-terminus of the coding region thus confirms previous results describing that the embryo defective EMB 1738 mutant from an independent Syngenta line (Tzafrir et al., 2004). In this mutant line, the terminal phenotype was described as the cotyledon stage while most embryos (64%) were arrested at the early transition to heart stage, and a high proportion of aberrant embryos were also detected (for details about this mutant, see http://www.seedgenes.org). This also clearly shows that the second gene classified as a *CYP51* family member in the *Arabidopsis* genome cannot complement the mutant *CYP51G1-At* gene and that this second CYP51 enzyme has most probably evolved a distinct substrate specificity. A structural analysis of the various CYP51 isoforms also strengthens this view. Using various topology prediction tools for transmembrane spanning regions, two transmembrane helices for CYP51G1-Sc and CYP51G1-At were predicted. For both enzymes, a small stretch of amino acids resided in the cytoplasm between both transmembrane helices, which spanned 15 to 23 residues depending of the prediction tool used. The main core of these proteins remained in the ER environment where sterol metabolism occurs (Benveniste, 1986). As for *A. thaliana* CYP51G2-At, all prediction tools revealed only one transmembrane spanning region (data not shown). Furthermore, plants homozygous for a T-DNA insertion in the

3'UTR of this second *CYP51* gene showed no phenotype, suggesting that, under the conditions used, the gene is dispensable. Alternatively, the location of the T-DNA insertion might have no effect on transcript production or translation. Modulation of the C14-demethylase activity has also been attempted through antisense expression constructs in *Arabidopsis* (Kushiro *et al.*, 2001) or a VIGS approach in *Nicotiana benthamiana* (Burger *et al.*, 2003). In both cases, down-regulation of the obtusifoliol 14α-demethylase transcript level was incomplete and the plants could survive, although the altered balance of sterols produced had an effect on the plant's growth and development. In both experiments the plants had a severely reduced stature, and a high obtusifoliol content. The antisense *Arabidopsis* plant also displayed a longer life span. Finally, studies performed in plants with a series of specific obtusifoliol-14DM inhibitors indicated a good correlation between their inhibition constants *in vitro* and their herbicidal activities *in vivo* (Rahier and Taton, 1997). All these results suggest that an altered sterol profile in plants affected at the C14-demethylation step is incompatible with normal growth requirements.

Until this study, no expression data was available for plant C14-demethylases. Here we have shown through RNA expression analyses that the *CYP51G1-Sc* gene is weakly expressed or undetectable in mature tissues, including vegetative and reproductive tissues (Fig. 2). RNA levels markedly increase in young developing tissues like maturing styles (Fig. 5A) where an asymmetrical distribution could be observed with a preferential accumulation in the lower style region prior to anthesis (Fig. 5B). A kinematic analysis of gynoecial growth had previously showed that the basal style region was the predominant site of growth (Crone and Lord, 1991), confirming earlier

results showing that cell divisions were only observed at the base of the style, in early maturing petunia styles (Linskens, 1974). The *CYP51G1-Sc* gene is also expressed at significant levels in meristematic tissues as determined by *in situ* RNA analyses (Fig. 4E) where mRNAs strongly accumulate in the shoot apical meristems, in young primordias, as well as in the young leaflets that surround the apex. Although basal levels of *CYP51G1-Sc* mRNAs are generally quite low, a transient six fold increase in *CYP51G1-Sc* mRNA levels can be observed in ovaries immediately following fertilization (Fig. 2C, D). A similar coordinate increase was also observed for the *FACKEL* gene (*FK*), corresponding to the enzymatic step immediately downstream of the CYP51G1-Sc enzyme (Fig. 2D). *FK* has been previously shown to be expressed in embryos and in actively growing cells (Jang *et al.*, 2000; Schrick *et al.*, 2000). In ovary, this fertilization-induced mRNA accumulation can be seen by *in situ* hybridization to be diffusely localized in both the pericrap and placenta tissues (Fig. 4A), and more intensely in a single thin-walled parenchymatous cell layer immediately beneath the outermost cell layer, that forms the placenta's epidermis. This layer which does not express the *CYP51G1-Sc* mRNAs is continuous with the integument's epidermis, where no *CYP51G1-Sc* mRNAs could be detected, indicating a clear difference and specialization of this layer in both the placenta epidermis and in the ovule's integument. Since the obtusifoliol 14α-demethylase mutant is embryo defective, this suggests that sterols produced in specific cell layers might be translocated to the ovule and embryo during early fertilization steps. The increase in *CYP51G1-Sc* mRNA levels in the ovary can be best described as biphasic since pollination alone also induced a transient increase in *CYP51G1-Sc* mRNA levels. This increase preceded the arrival of the pollen tube in the ovary, and is both observed following compatible and incompatible

pollinations, where pollen tubes are arrested in the first two-third of the style (Fig. 3B). This suggests that a long-distance signal, produced by the pollen tube itself, or in the transmitting tract tissue of the style during pollen-pistil interaction, is perceived at a distance in the ovary. Among the treatments performed, only wounding of the style and methyl-jasmonate application could fully mimic the effect of pollen tube growth on the accumulation of *CYP51G1-Sc* mRNAs at a distance in the ovary (Fig. 3C, D). This suggests that cellular deterioration and death caused by pollination (either compatible or incompatible) or by wounding, is the initial trigger that induces *CYP51G1-Sc* mRNA accumulation in the ovary, and that this response is probably mediated by jasmonates, as for long-distance wound responses (Stratmann, 2003). Sustained levels of *CYP51G1-Sc* mRNAs for a longer period can then only be achieved if fertilization takes place (Figures 2D and 3B).

A totally novel aspect of plant CYP51 substrate specificity was revealed by our biochemical characterization of the enzyme expressed in yeast (Fig. 6). All the previously characterized plant CYP51 enzymes from maize (Taton and Rahier, 1991), wheat (Cabello-Hurtado *et al.*, 1997; Cabello-Hurtado *et al.*, 1999), sorgho (Kahn *et al.*, 1996; Bak *et al.*, 1997; Lamb *et al.*, 1998), and *Arabidopsis* (Kushiro *et al.*, 2001) were shown to have strict substrate specificity towards obtusifoliol. For the three monocot plants, this was determined enzymatically. In *Arabidopsis*, this was shown by the absence of complementation of the yeast *erg11* mutant with the complete *CYP51G1-At* clone, while a chimera between the N-terminus of the CYP51 yeast enzyme and the plant enzyme could rescue the *erg11* mutant. Complementation of the yeast *erg11* mutant with the complete *CYP51G1*-Sc clone leads to a significant increase in cell

viability on a media not supplemented with ergosterol, indicating that the *S. chacoense* CYP51G1 enzyme could substitute for the yeast endogenous enzyme, and use lanosterol as a substrate. Biochemical characterization of the *S. chacoense* CYP51G1-Sc protein expressed in yeast confirmed that the enzyme could indeed use lanosterol as a substrate (as well as eburicol), albeit with lower efficiency than the plant endogenous substrate, obtusifoliol (Fig. 6). The lack of activity of plants CYP51 enzymes toward fungi and mammal substrates had been attributed to a common structural feature common to all these non-plant sterol substrates: the presence of a 4β-methyl group in lanosterol and eburicol, precursors of C14-desmethylsterols (Taton and Rahier, 1991). Since only few plant CYP51 enzymes have been characterized at the biochemical level, sequence comparison and enzymatic characterization of other plant CYP51 combined with the expression of domain swap chimeras and site directed mutagenesis should reveal the protein region(s) involved in substrate specificity (Lepesheva and Waterman, 2004).

Although a brassinosteroid-independent role for sterols in plant development has only been suggested a few years ago, mounting evidences involving numerous mutants affected in early steps of sterol biosynthesis and showing severe defects in embryogenesis and cell patterning are now clearly highlighting new specific roles for sterols in plant development (Lindsey *et al.*, 2003). Modification of the sterol balance as demonstrated for several mutants through chemical analysis of the sterol fraction, could explain some of the observed phenotype. Alternatively, presence of biosynthetic intermediates that could be either toxic or that could act as signaling molecule is also considered. Exogenous treatments with natural plant sterols like sitosterol and stigmasterol or atypical sterols that accumulated in the *fk* mutant have been shown to be

able to modulate the expression of genes involved in cell expansion or cell division (He *et al.*, 2003). To address this issue we have used purified obtusifoliol to determine its ability to modulate gene expression and to act as a signaling molecule. Since the *CYP51G1-Sc* gene was itself found to be highly active in developing tissues like maturing styles, shoot apices and meristems (Figures 4 and 5) we tested the ability of purified obtusifoliol to modulate the expression of its demethylating enzyme in a mature tissue were only a normally weak expression was detected. Application of an obtusifoliol emulsion on mature leaves lead to a local two-fold increase of *CYP51G1-Sc* mRNA levels (Fig. 7). This response was specific and could not be mimicked by application of lanosterol, a structurally highly similar sterol. Thus, similarly to mammals, where genes involved in cholesterol homeostasis (including CYP51) are regulated by cholesterol or its metabolites (Stromstedt *et al.*, 1996), the plant *CYP51G1-Sc* gene was also found to be regulated by sterols. The two-fold increase observed following obtusifoliol application was not only highly reproducible but was also detected in non-treated systemic leaves, suggesting the long-distance transport or production of a signaling molecule triggering the expression of the *CYP51G1-Sc* mRNA. To further test if obtusifoliol could itself be a mobile signaling molecule, we used ^{14}C-labeled obtusifoliol and monitored its distribution throughout the plant after a compound leaf was sprayed (Fig. 8). Not only was labeling detected in the petiole as well as in portions of some leaflets both positioned immediately above or below the sprayed leaf, but a chemical analysis (Fig. 9) revealed that the radioactive compound detected at a distance from the sprayed leaf was almost exclusively composed of obtusifoliol without any other radioactive sterol. Furthermore, the concentrations of radiolabeled obtusifoliol found in the petiole of systemic leaf #6, where a two-fold

increase in *CYP51G1-Sc* mRNA levels was observed, was consistent with the physiological levels found in plants, strongly suggesting that obtusifoliol can act as a mobile signaling molecule, involved in various aspects of plant growth and development, including pollination and fertilization.

The adaxial/abaxial polarity of leaves is establish through the spatially restricted (adaxial) expression of the *PHABULOSA* (*PHB*)/*PHAVOLUTA* (*PHV*) genes in the leaf primordium (Bowman *et al.*, 2002). *PHB* and *PHV* encode type III HD-ZIP transcription factors that contain a StART domain, which in animals binds sterols and modulate the activity of the DNA binding domain. Proper adaxial/abaxial development of the primordium is also known to depend on signal(s) emanating from the meristem to the leaf. The presence of a StART domain in the PHB and PHV proteins has prompted the authors to suggest that a lipid/sterol molecule would be involved in the acquisition of adaxial identity through interaction with these HD-ZIP transcription factors (McConnell *et al.*, 2001). Interestingly, our *in situ* analysis has revealed that the *CYP51G1-Sc* gene is also preferentially expressed on the adaxial side of developing leaves (Fig. 4E, F). This, combined with the ability of obtusifoliol to move away from its site of application (Fig. 8), and to induce the transcription of the C14-demethylase (Fig. 7), creating a localized positive feedback loop, suggest that this sterol intermediate could be involved in such processes.

Interestingly, mammalian sterols homologous to the sterols produced by the plant C14-demethylase and C14-reductase (FK) enzymes have been shown to have important roles in reproduction. In mammals, meiosis of follicule oocytes is maintained

in the prophase of the first meiotic division and oocytes do not resume meiosis spontaneously during oocyte growth and follicule development (Byskov *et al.*, 2002; Tsafriri et al., 2005). *In vitro*, this can be overcome by the addition of meiosis activating sterols, and these were found to be 4,4-dimethyl-5α-cholesta-8,14,24-trien-3β-ol, also named FF-MAS for follicular fluid meiosis activating sterol, and 4,4-dimethyl-5α-cholesta-8,24-dien-3β-ol, also named T-MAS for testis meiosis activating sterol (Byskov *et al.*, 1995). These sterols correspond respectively to the transformation product of lanosterol by the CYP51 C14-demethylase enzyme (FF-MAS) and by the subsequent enzymatic step, the C14-reductase (T-MAS), suggesting that these sterol molecules might have been retained by plants and animals as signaling molecules. Furthermore, lanosterol has also been found to be a candidate endogenous ligand for the farnesoid X receptor β, a new mammalian nuclear receptor (Otte *et al.*, 2003), strengthening the role of these sterols in signal transduction. Because lipids are hydrophobic, lipids involved in long-distance signaling have to be transported by soluble macromolecules like lipid-binding proteins or lipid-transfer proteins. Since these are quite numerous in the plant genome and have been shown to be involved in defense-response signaling and somatic embryogenesis (Blein *et al.*, 2002), it is quite conceivable that sterols intermediates, like obtusifoliol, could also act as a long-distance signaling molecule in plants.

III.11 Materials and methods

Plant material and treatments

The diploid and self-incompatible wild potato *Solanum chacoense* Bitt. (2n=2x=24) was grown in greenhouse with 14-16 hours of light per day. The genotype used were V22 (S allele S_{11} and S_{13}) as pollen donor and G4 (S allele S_{12} and S_{14}) as female progenitor. Phytohormone treatments were done as previously described (Lantin *et al.*, 1999; O'Brien *et al.*, 2002a) and wounding of the style was done by gentle tweezing of the stigma and upper style with forceps. Each hormone application was boosted 24 hours after the initial treatment, and flower tissues were harvested 48 hours after the initial treatment. For obtusifoliol treatment, an emulsion of the compound was performed in Tween 80. The desiccated obtusifoliol (see below for obtusifoliol production) was dissolved in chloroform (1-5 mg/ml final concentration) and mixed with a stock solution (50 mg/ml) of Tween 80 in absolute ethanol. After vigorous mixing, the mixture was desiccated in a speed vacuum apparatus. For leaf treatment, the mixture was dissolved in sterile water to a final concentration of 1 mg/ml (2.34 mM) and 500 µl was sprayed on one compound leaf. In order to prevent the mist to from falling of other leaves, a large Whatman paper cone was placed over the treated leaf. The obtusifoliol in vivo mobile assay was performed in duplicate with C14-radiolabeled obtusifoliol (see below) and gave identical results. The GLC-MS chemical analysis of the radiolabeled compound that was isolated from the sprayed leaf and from the distant leaves was performed on one of these duplicates that showed the best preservation of the pressed and dried leaves.

Isolation of the U40 fragment by differential display and the *CYP51G1-Sc* cDNA

We followed the differential display procedure described in the RNAimage protocol (GenHunter Corporation, Nashville, TE), with some modifications as described previously (O'Brien *et al.*, 2002a). The PCR fragment obtained was cloned in a home-made T-vector derived from a pBS II plasmid vector cut with Eco RV (Marchuk *et al.*, 1991). To validate the differential display autoradiography, the radiolabeled PCR fragment was used to probed an RNA gel blot made with the same mRNAs used for the DD-RT-PCR procedure. After confirmation, the probe was used to screen a cDNA library derived from 48 hours post-pollinated pistil tissue mRNAs (Lantin *et al.*, 1999) to obtain a full-length cDNA clone. For the *S. chacoense* C14-reductase homologue (*FACKEL*), a PCR fragment was obtained either from reverse transcribed ovule mRNAs or leaf genomic DNA with primer sequences selected from tomato ESTs (AI484506, AI485167, AW931153) similar to the *Arabidopsis thaliana FACKEL* sequence. Forward primer: 5'-GTCTTTATACCGTTCACC-3'; reverse primer: 5'-CTTCTCTGCACATCTAGC-3'.

Measure of C-14α-demethylase activity and GC/MS analysis

For activity assays, the complete *CYP51G1-Sc* open reading frame plus vector flanking sequences from the bacterial pBluescript SK- vector was digested with the EcoR I and BamH I restriction enzymes and cloned downstream of the GAL10-CYC1 promoter into the yeast shuttle vector pYeDP60 (Pompon *et al.*, 1996; Cabello-Hurtado *et al.*, 1999). Expression of the CYP51G1-Sc protein was performed in the yeast strain WAT11 (Pompon *et al.*, 1996) and tested for enzymatic activity (demethylation assay)

on various substrates. Yeast microsomal preparations were prepared as described previously (Darnet and Rahier, 2003). Synthesis of obtusifoliol and measurements of sterol 14α-demethylase activity of obtusifoliol, lanosterol, and eburicol were performed as described previously (Taton and Rahier, 1991).

Yeast complementation

Diploid *Saccharomyces cerevisiae ERG 11/erg11* mutant cells designation YHR007C BY4743, (MATa/MATα his3Δ1/his3Δ1 leu2Δ0/leu2Δ0 lys2Δ0/+ met15Δ0/+ ura3Δ0/ura3Δ0 Δ*ERG11*) were obtained from the *Saccharomyces* Genome Deletion Project through Research Genetics Inc. (Huntsville, AL). The corresponding ATCC number for the strain is 4026604. For liquid cultures, the strain was maintained under selection with 200 mg/L of geneticin. Transformation followed the TRAFO procedure (Gietz and Woods, 2002). Yeast strain recombinant for the pYeDP60 vector were selected with the ADE2 selection on a media lacking adenine (Pompon *et al.*, 1996). Sporulation of yeast cells was induced in a sporulation media (http://www.umanitoba.ca/faculties/medicine/biochem/gietz/Trafo.html) and spores were grown on solid media lacking adenine and supplemented with 20 mg/ml ergosterol (Sigma, E-6510). Colonies were replicated on solid media lacking adenine and scored for viability. Values and standard deviation were derived from five independent experiments, each including the viability assessment of 36 haploid yeast colonies grown a media lacking ergosterol.

DNA and RNA gel blot analysis

Total RNA was isolated as described previously (Jones *et al.*, 1985) or with the Plant RNeasy RNA extraction kit from Qiagen (Mississauga, ONT). RNA concentration was determined by measuring its absorbance at 260 nm. Concentration and RNA quality were verified on agarose gel following ethidium bromide staining. For each tissue tested, ten µg of RNA were separated on a formaldehyde/MOPS gel (Sambrook *et al.*, 1989). RNA were then transferred on Hybond N+ membranes (GE Healthcare, Montréal, QC), and cross-linked (120 mJ/cm^2) with a Hoefer UVC 500 UV cross-linker. To confirm equal loading between RNA samples, a 1 kb fragment of *S. chacoense* 18S RNA was PCR amplified and used as a control probe. Prehybridization was performed at 45°C for three hours in 50% formamide solution (50% deionized formamide, 6X SCC, 5X Denhardt solution, 0,5% SDS and 200 µg of denatured salmon sperm DNA). Hybridization of the membranes was performed overnight at 45°C in 50% formamide solution. Genomic DNA isolation was performed by a modified CTAB extraction method (Reiter *et al.*, 1992) or with the Plant DNeasy kit from Qiagen (Mississauga, ONT). Complete digestion of DNA (ten µg) was made overnight with 5 units/µg of either Bam HI, Eco RI, Eco RV or Hind III as recommended by the supplier (New England Biolabs, Beverly, MA). DNA gel blot analysis was performed as previously described (Sambrook *et al.*, 1989). DNA was capillary transferred to Hybond N+ membranes (GE Healthcare) prior to cross-linking. Prehybridization (3 h) and hybridization (overnight) were performed as described for the RNA gel blot analyses except that the temperature was set at 42°C. Probes for RNA and DNA gel blot analyses were synthesized by random labeling using the Strip-EZ DNA labeling kit (Ambion,

Austin, TX) in presence of α-^{32}P-dATP (ICN Biochemicals, Irvine, CA). Following hybridization, membranes were washed 30 min. at 25°C and 30 min. at 35°C in 2X SSC/ 0.1% SDS, 30 min. at 45°C and 30 min. at 55°C in 1X SSC/ 0.1% SDS and a final stringent wash for 10 min. at 55°C in 0.1X SSC/ 0.1% SDS. Prior to *18S* cRNA probe hybridization, RNA gel blots were striped as recommended by the manufacturer (Ambion) and post-hybridization washes were done twice at 60°C for 30 min. in 0.1X SSC/ 0.1% SDS. Membranes were exposed either at room temperature on an europium screen and scanned on a Typhoon 9200 Phosphoimager (Amersham Biosciences, Baie d'Urfé, QC, Canada) or exposed at -86°C on Kodak Biomax MR film (Interscience, Markham, ONT). For quantitative measurements, densitometric scans were performed and normalized against their individual 18S rRNA hybridization level using the ImageQuant software on a Typhoon 9200 phosporimager (GE Healthcare).

***In situ* hybridization**

Ovaries (cut in halves) were fixed in FAA (60% ethanol, 5% acetic acid, 5% formaldehyde) at 4°C overnight. After dehydration with *tert*-butanol and embedding in paraffin, samples were cut into 10-µm sections and mounted on slides coated with AES (3-aminopropyltriethoxy-silane; Sigma, Oakville, Ont). Tissue sections were treated and hybridized as described previously (Lantin *et al.*, 1999).

Sequence analysis

Sequencing was performed on Applied Biosystems ABI Prism 310 or 3100 automated sequencer. Sequence alignments were performed with the ClustalW module in MacVector 7.2.3 (Accelrys, San Diego, CA). Possible signal peptide or membrane anchoring domain were predicted from the CBS Prediction Servers (http://www.cbs.dtu.dk/services/). Transmembrane spanning regions were predicted from various prediction servers: http://sosui.proteome.bio.tuat.ac.jp/sosui_submit.html, http://www.enzim.hu/hmmtop, http://www.ch.embnet.org/software/TMPRED_form.html, and http://www.cbs.dtu.dk/services/. Accession numbers for the CYP51 sequence analyses are as follows: *Solanum chacoense*, AY552551; *Nicotiana tabacum*, AAL54888; *Oryza sativa*, AK060487; *Sorghum bicolor*, P93846; *Triticum aestivum*, CAA70475; *Mus musculus*, AAF74562; *Homo sapiens*, EAL24154; *Mycobacterium tuberculosis*, CAB02394; *Trypanosoma brucei*, AAK97386; *Schizosaccharomyces pombe*, Q09736; *Saccharomyces cerevisiae*, AAA34546.

Biosynthesis of [^{14}C]-obtusifoliol

The suspension cultures (0.8 L) of bramble cells (*Rubus fruticosus*) used have been described previously (Schmitt *et al.*, 1982). At the beginning of the exponential phase of growth, the cells were incubated in the presence of a 14-demethylase inhibitor, CGA214372 [methyl 1-(2,2-dimethyllindan-1-yl)-imidazole-5 carboxylate], at a 5 mg/L final concentration in the medium, and [2-^{14}C-acetate] (600 μCi, 5.1 Ci/Mol) for seven days. The cells were harvested by filtration and lyophilized. The unsaponifiable matter

was isolated and separated on TLC using CH_2Cl_2 (two runs) allowing the separation of 4αmethylsterols from other sterols. After acetylation, this fraction was analyzed on analytical $AgNO_3$-impregnated SiO_2-TLC, using CH_2Cl_2 as the developing solvent allowing isolation of pure [^{14}C]-obtusifoliyl acetate (1.6 mg); GC purity > 98% (tR= ; DB5), MS, m/z (rel. int.) M+ = 468(35), 453(100), 425(8), 393(40), 341(7), 309(16), 227(22), 215(18). Saponification yielded pure [^{14}C]-obtusifoliol (1.4 mg); specific radioactivity: (0.8 Ci/Mol), GC purity > 98% (tR= 1.128, DB1; tR= 1.168, DB5), MS, m/z (rel. int.) M+ = 426(34), 411(100), 393(14), 342(3), 327(14), 227(11).

Chemical analysis of [^{14}C]-labeled sterols from potato leaves

The dried leaves were extracted with a mixture of CH_2Cl_2/MeOH 2:1 for two hours under reflux. After evaporation of the solvent, the residue was separated by TLC with CH_2Cl_2 as the solvent, allowing the radioactivity present into the total 4,4-dimethysterols, 4α-methylsterols, 4-desmethylsterols and steryl-esters fractions to be measured. In order to be able to further identify by GLC-MS the radioactive components present in the 4α-methylsterols fraction, protecting cold carrier sterols were not added to this fraction. It was acetylated and further analyzed on analytical $AgNO_3$-impregnated SiO_2-TLC, using CH_2Cl_2 as the developing solvent, allowing the radioactivity present in fractions migrating as authentic standards of 4α-methylsterols to be determined. The single radioactive 4α-methylsterol fraction which showed an RF identical to that of a standard of obtusifoliyl-acetate was eluted from silica and the sterol(s) present in this fraction was unequivocally identified by coupled capillary GLC-MS analysis (i.e., by

coincidental retention time and identical electron impact spectrum as authentic standard) (Rahier and Benveniste, 1989). The radioactive steryl-esters fractions were saponified under standard conditions and the obtained free sterols were analyzed as described above.

III.12 Nomenclature

The official nomenclature of the sterols mentioned is as follows. Obtusifoliol: 4α,14α-dimethyl-ergosta-8,24(24^1)-dien-3βol. Lanosterol: 4α,14α-trimethyl-cholesta-8,24-dien-3βol. 4,4-dimethyl-zymosterol : 4,4-dimethyl-cholesta-8,24-dien-3βol. Cycloartenol: 4α,14α-trimethyl-9β,19-cyclo-cholest-24-en-3βol. 24-methylene-cycloartanol: 4α,14α-trimethyl-9β,19-cyclo-ergost-24(24^1)-en-3βol. Eburicol: 4α,14α-trimethyl-ergosta-8,24(24^1)-dien-3βol.

III.13 Acknowledgement

We would like to thanks Danièle Werck-Reichhart for the pYeDP60 yeast shuttle vector. Special thanks to Annie Hoeft for technical assistance and to Gabriel Téodorescu for plant care and maintenance. M. O'Brien, and S.-C. Chantha are the recipient of Ph. D. fellowships from NSERC and from Le Fonds Québécois de la Recherche sur la Nature et les Technologies (FQRNT, Québec). D. P. Matton holds a Canada Research Chair in Functional Genomics and Plant Signal Transduction.

III.14 Literature cited

Altmann, T. (1999) Molecular physiology of brassinosteroids revealed by the analysis of mutants. Planta 208, 1-11

Aoyama, Y., and Yoshida, Y. (1992) The 4 beta-methyl group of substrate does not affect the activity of lanosterol 14 α-demethylase (P-450(14)DM) of yeast: difference between the substrate recognition by yeast and plant sterol 14 α-demethylases. Biochem. Biophys. Res. Commun. 183, 1266-1272

Baima, S., Nobili, F., Sessa, G., Lucchetti, S., Ruberti, I., and Morelli, G. (1995) The expression of the *Athb-8* homeobox gene is restricted to provascular cells in *Arabidopsis thaliana*. Development 121, 4171-4182

Bak, S., Kahn, R. A., Olsen, C. E., and Halkier, B. A. (1997) Cloning and expression in *Escherichia coli* of the obtusifoliol 14 α-demethylase of *Sorghum bicolor* (L.) Moench, a cytochrome P450 orthologous to the sterol 14 α-demethylases (CYP51) from fungi and mammals. Plant J. 11, 191-201

Balk, P. A., and de Boer, AD. (1999) Rapid stalk elongation in tulip (*Tulipa gesneriana* L. cv. Apeldoorn) and the combined action of cold-induced invertase and the water-channel protein γTIP. Planta 209, 346-354

Benveniste, P. (1986) Sterol Biosynthesis. Annual Review of Plant Physiology 37, 275-308

Benveniste, P. (2004) Biosynthesis and accumulation of sterols. Annu. Rev. Plant. Biol. 55, 429-457

Blein, J. P., Coutos-Thevenot, P., Marion, D., and Ponchet, M. (2002) From elicitins to lipid-transfer proteins: a new insight in cell signalling involved in plant defence mechanisms. Trends Plant Sci. 7, 293-296

Bowman, J. L., Eshed, Y., and Baum, S. F. (2002) Establishment of polarity in angiosperm lateral organs. Trends Genet. 18, 134-141

Burger, C., Rondet, S., Benveniste, P., and Schaller, H. (2003) Virus-induced silencing of sterol biosynthetic genes: identification of a *Nicotiana tabacum* L. obtusifoliol-14α-demethylase (*CYP51*) by genetic manipulation of the sterol biosynthetic pathway in *Nicotiana benthamiana* L. J. Exp. Bot. 54, 1675-1683

Byskov, A. G., Andersen, C. Y., and Leonardsen, L. (2002) Role of meiosis activating sterols, MAS, in induced oocyte maturation. Mol. Cell Endocrinol. 187, 189-196

Byskov, A. G., Andersen, C. Y., Nordholm, L., Thogersen, H., Xia, G., Wassmann O., Andersen, J.V., Guddal ,E., and Roed, T. (1995) Chemical structure of sterols that activate oocyte meiosis. Nature 374, 559-562

Cabello-Hurtado, F., Taton, M., Forthoffer, N., Kahn, R., Bak, S., Rahier, A., and Werck-Reichhart, D. (1999) Optimized expression and catalytic properties of a wheat obtusifoliol 14α-demethylase (*CYP51*) expressed in yeast. Complementation of *erg11Δ* yeast mutants by plant *CYP51*. Eur. J. Biochem. 262, 435-446

Cabello-Hurtado, F., Zimmerlin, A., Rahier, A., Taton, M., DeRose, R., Nedelkina, S., Batard, Y., Durst, F., Pallett, K. E., and Werck-Reichhart, D. (1997) Cloning and functional expression in yeast of a cDNA coding for an obtusifoliol 14α-demethylase (*CYP51*) in wheat. Biochem, Biophys, Res, Commun, 230, 381-385

Carland, F. M., Fujioka, S., Takatsuto, S., Yoshida, S., and Nelson, T. (2002) The identification of CVP1 reveals a role for sterols in vascular patterning. Plant Cell 14, 2045-2058

Chaumont, F., Barrieu, F., Herman, E. M., and Chrispeels, M. J. (1998) Characterization of a maize tonoplast aquaporin expressed in zones of cell division and elongation. Plant Physiol. 117, 1143-1152

Cheung, A. Y. (1996) The pollen tube growth pathway: its molecular and biochemical contributions and responses to pollination. Sex. Plant Reprod. 9, 330-336

Clouse, S. D. (2000) Plant development: A role for sterols in embryogenesis. Curr. Biol. 10, R601-604

Clouse, S. D. (2002a) *Arabidopsis* mutants reveal multiple roles for sterols in plant development. Plant Cell 14, 1995-2000

Clouse, S. D. (2002b) Brassinosteroids. The *Arabidopsis* Book, 1-23

Clouse, S. D., and Sasse, J. M. (1998) BRASSINOSTEROIDS: Essential Regulators of Plant Growth and Development. Annual Review of Plant Physiology and Plant Molecular Biology 49, 427-451

Crone, W., and Lord, E. M. (1991) A kinematic analysis of gynoecial growth in *Lilium longiflorum*: surface growth patterns in all floral organs are triphasic. Dev. Biol. 143, 408-417.

Darnet, S., and Rahier, A. (2003) Enzymological properties of sterol-C4-methyl oxidase of yeast sterol biosynthesis. Biochim Biophys Acta 1633, 106-117

Diener, A. C., Li, H., Zhou, W., Whoriskey, W. J., Nes, W. D., and Fink, G. R. (2000) Sterol methyltransferase 1 controls the level of cholesterol in plants. Plant Cell 12, 853-870

Edwards, P. A., and Ericsson, J. (1999) Sterols and isoprenoids: signaling molecules derived from the cholesterol biosynthetic pathway. Annu. Rev. Biochem. 68, 157-185

Farese, R. V., and Jr., Herz, J. (1998) Cholesterol metabolism and embryogenesis. Trends Genet. 14, 115-120

Fischer, U., Men, S., and Grebe, M. (2004) Lipid function in plant cell polarity. Curr Opin Plant Biol. 7, 670-676

Gietz, R. D., and Woods, R. A. (2002) Screening for protein-protein interactions in the yeast two-hybrid system. Methods Mol. Biol. 185, 471-486

Guo, D. A., Venkatramesh, M., and Nes, W. D. (1995) Developmental regulation of sterol biosynthesis in *Zea mays*. Lipids 30, 203-219

Hartmann, M.-A. (1998) Plant sterols and the membrane environment. Trends Plant Sci. 3, 170-175

Hartmann, M.-A., and Benveniste, P. (1987) Plant membrane sterols: isolation, identification and biosynthesis. Methods Enzymol. 148, 632-650

He, J. X., Fujioka, S., Li, T. C., Kang, S. G., Seto, H., Takatsuto, S., Yoshida, S., and Jang, J. C. (2003) Sterols regulate development and gene expression in *Arabidopsis*. Plant Physiol. 131, 1258-1269

Holmberg, N., Harker, M., Gibbard, C. L., Wallace, A. D., Clayton, J. C., Rawlins, S., Hellyer, A., and Safford, R. (2002) Sterol C-24 methyltransferase type 1 controls the flux of carbon into sterol biosynthesis in tobacco seed. Plant Physiol. 130, 303-311

Jang, J. C., Fujioka, S., Tasaka, M., Seto, H., Takatsuto, S., Ishii, A., Aida, M., Yoshida, S., and Sheen, J. (2000) A critical role of sterols in embryonic patterning and meristem programming revealed by the fackel mutants of *Arabidopsis thaliana*. Genes Dev. 14, 1485-1497

Jones, J. D. G, Dunsmuir, P., and Bedbrook, J. (1985) High level expression of introduced chimeric genes in regenerated transformed plants. EMBO J. 4, 2411-2418

Kahn, R. A., Bak, S., Olsen, C. E., Svendsen, I., and Moller, B.L. (1996) Isolation and reconstitution of the heme-thiolate protein obtusifoliol 14α-demethylase from *Sorghum bicolor* (L.) Moench.. J. Biol. Chem. 271, 32944-32950

Kalb, V. F., Woods, C. W., Turi, T. G., Dey, C. R., Sutter, T. R., and Loper, J. C. (1987) Primary structure of the P450 lanosterol demethylase gene from *Saccharomyces cerevisiae*. DNA 6, 529-537

Kushiro, M., Nakano, T., Sato, K., Yamagishi, K., Asami, T., Nakano, A., Takatsuto, S., Fujioka, S., Ebizuka, Y., and Yoshida, S. (2001) Obtusifoliol 14α-demethylase (CYP51) antisense *Arabidopsis* shows slow growth and long life. Biochem. Biophys. Res. Commun. 285, 98-104

Lamb, D. C., Kelly, D. E., and Kelly, S. L. (1998) Molecular diversity of sterol 14α-demethylase substrates in plants, fungi and humans. FEBS Lett. 425, 263-265

Lantin, S., O'Brien, M., and Matton, D. P. (1999) Pollination, wounding and jasmonate treatments induce the expression of a developmentally regulated pistil dioxygenase at a distance, in the ovary, in the wild potato *Solanum chacoense* Bitt. Plant Mol. Biol. 41, 371-386

Lepesheva, G. I., and Waterman, M. R. (2004) CYP51--the omnipotent P450. Mol Cell Endocrinol. 215, 165-170

Lindsey, K., Pullen, M. L., and Topping, J. F. (2003) Importance of plant sterols in pattern formation and hormone signalling. Trends Plant Sci. 8, 521-525

Linskens, H. F. (1974) Some observations on the growth of the style. Incompatibility Newsletter 4, 4-15

Ludevid, D., Höfte, H., Himelblau, E., and Chrispeels, M. J. (1992) The expression pattern of the tonoplast intrinsic protein γ-TIP in *Arabidopsis thaliana* is correlated with cell enlargement. Plant Physiol.. 100, 1633-1639

Marchuk, D, Drumm, M., Saulino, A., and Collins, F. S. (1991) Construction of T-vectors, a rapid and general system for direct cloning of unmodified PCR products. Nucleic Acids Res. 19, 1154

Matton, D. P., Maes, O., Laublin, G., Xike, Q., Bertrand, C., Morse, D., and Cappadocia, M. (1997) Hypervariable domains of self-incompatibility RNases mediate allele-specific pollen recognition. Plant Cell 9, 1757-1766

McConnell, J. R., Emery, J., Eshed, Y., Bao, N., Bowman, J., and Barton, M. K. (2001) Role of PHABULOSA and PHAVOLUTA in determining radial patterning in shoots. Nature 411, 709-713

Mongrand, S., Morel, J., Laroche, J., Claverol, S., Carde, J. P., Hartmann, M. A., Bonneu, M., Simon-Plas, F., Lessire, R., and Bessoule, J. J. (2004) Lipid rafts in higher plant cells: purification and characterization of Triton X-100-insoluble microdomains from tobacco plasma membrane. J. Biol. Chem. 279, 36277-36286

Nelson, D. R., Schuler, M. A., Paquette, S. M., Werck-Reichhart, D., and Bak, S. (2004) Comparative genomics of rice and *Arabidopsis*. Analysis of 727 cytochrome P450 genes and pseudogenes from a monocot and a dicot. Plant Physiol. 135, 756-772

O'Brien, M., Bertrand, C., and Matton, D. P. (2002a) Characterization of a fertilization-induced and developmentally regulated plasma-membrane aquaporin expressed in reproductive tissues, in the wild potato *Solanum chacoense* Bitt. Planta 215, 485-493

O'Brien, M., Kapfer, C., Major, G., Laurin, M., Bertrand, C., Kondo, K., Kowyama, Y., and Matton, D. P. (2002b) Molecular analysis of the stylar-expressed *Solanum chacoense* small asparagine-rich protein family related to the HT modifier of gametophytic self-incompatibility in Nicotiana. Plant J. 32, 985-996

Otte, K., Kranz, H., Kober, I., Thompson, P., Hoefer, M., Haubold, B., Remmel, B., Voss, H,, Kaiser. C., Albers, M., Cheruvallath, Z., Jackson, D., Casari, G., Koegl, M., Paabo, S., Mous, J., Kremoser, C., and Deuschle, U. (2003) Identification of farnesoid X receptor beta as a novel mammalian nuclear receptor sensing lanosterol. Mol. Cell. Biol. 23, 864-872

Pompon, D., Louerat, B., Bronine, A., and Urban, P. (1996) Yeast expression of animal and plant P450s in optimized redox environments. Methods Enzymol. 272, 51-64

Ponting, C. P., and Aravind, L. (1999) START: a lipid-binding domain in StAR, HD-ZIP and signalling proteins. Trends Biochem. Sci. 24, 130-132

Rahier, A., and Benveniste, P. (1989) Mass spectral identification of phytosterols. In WD Nes, E Parish, eds, Analysis of Sterols and Other Biologically Significant Steroids. Academic Press, San Diego, pp 223-250

Rahier, A., and Taton, M. (1997) Fungicides as Tools in Studying Postsqualene Sterol Synthesis in Plants. Pesticide Biochemistry and Physiology 57, 1-27

Reiter, R. S., Young, R. M., and Scolnik, P. A. (1992) Genetic linkage of the *Arabidopsis* genome: methods for mapping with recombinant inbreds and Random Amplified Polymorphic DNAs (RAPDs). In C Koncz, N-H Chua, J Schell, eds, Methods in *Arabidopsis* Research. World Scientific Publishing Co., Singapore,170-190

Sambrook, J., Fritsch, E. F., and Maniatis, T. (1989) Molecular cloning: a laboratory manual. Cold Spring Harbor Laboratory Press, New York

Schaeffer, A., Bronner, R., Benveniste, P., and Schaller, H. (2001) The ratio of campesterol to sitosterol that modulates growth in *Arabidopsis* is controlled by STEROL METHYLTRANSFERASE 2;1. Plant J. 25, 605-615

Schaller, H., Bouvier-Nave, P., and Benveniste, P. (1998) Overexpression of an *Arabidopsis* cDNA encoding a sterol-C24(1)-methyltransferase in tobacco modifies the ratio of 24-methyl cholesterol to sitosterol and is associated with growth reduction. Plant Physiol. 118, 461-469

Schmitt. P,, and Benveniste, P. (1979) Effect of fenarimol on sterol byosynthesis in suspension cultures of bramble cells. Phytochemistry 18, 1659-1665

Schmitt, P., Rahier, A., and Benveniste, P. (1982) Inhibition of sterol biosynthesis in suspension-cultures of bramble cells. Physiol.. Vég.. 20, 559-571

Schrick, K., Fujioka, .S, Takatsuto, S., Stierhof, Y. D., Stransky, H., Yoshida, S., and Jurgens, G. (2004) A link between sterol biosynthesis, the cell wall, and cellulose in *Arabidopsis*. Plant J. 38, 227-243

Schrick, K., Mayer, U., Horrichs, A., Kuhnt, C., Bellini, C., Dangl, J., Schmidt, J., and Jurgens, G. (2000) FACKEL is a sterol C-14 reductase required for organized cell division and expansion in *Arabidopsis* embryogenesis. Genes Dev. 14, 1471-1484

Schrick, K., Mayer, U., Martin, G., Bellini, C., Kuhnt, C., Schmidt, J., and Jurgens, G. (2002) Interactions between sterol biosynthesis genes in embryonic development of *Arabidopsis*. Plant J. 31. 61-73

Schuler, M. A., and Werck-Reichhart, D. (2003) Functional genomics of P450s. Annu. Rev. Plant Biol. 54, 629-667

Sessa, G., Steindler, C., Morell,i G., and Ruberti, I. (1998) The *Arabidopsis Athb-8, -9* and *-14* genes are members of a small gene family coding for highly related HD-ZIP proteins. Plant Mol. Biol. 38, 609-622

Simons, K., and Toomre, D. (2000) Lipid rafts and signal transduction. Nat. Rev. Mol. Cell Biol 1, 31-39

Sitbon, F., and Jonsson, L. (2001) Sterol composition and growth of transgenic tobacco plants expressing type-1 and type-2 sterol methyltransferases. Planta 212, 568-572

Souter, M., Topping, J., Pullen, M., Friml, J., Palme, K., Hackett, R., Grierson, D., and Lindsey, K. (2002) *hydra* Mutants of *Arabidopsis* are defective in sterol profiles and auxin and ethylene signaling. Plant Cell 14, 1017-1031

Stratmann, J. W. (2003) Long distance run in the wound response-jasmonic acid is pulling ahead. Trends Plant Sci, 8, 247-250

Stromstedt, M., Rozman, D., and Waterman, M. R. (1996) The ubiquitously expressed human *CYP51* encodes lanosterol 14 α-demethylase, a cytochrome P450 whose expression is regulated by oxysterols. Arch. Biochem. Biophys. 329, 73-81

Taton, M., and Rahier, A. (1991) Properties and structural requirements for substrate specificity of cytochrome P-450-dependent obtusifoliol 14 α-demethylase from maize (*Zea mays*) seedlings. Biochem J. 277 (Pt 2), 483-492

Topping, J. F., May, V. J., Muskett, P. R., and Lindsey, K. (1997) Mutations in the *HYDRA1* gene of *Arabidopsis* perturb cell shape and disrupt embryonic and seedling morphogenesis. Development 124, 4415-4424

Tsafriri, A., Cao, X., Ashkenazi, H., Motola, S., Popliker, M., and Pomerantz, S. H. (2005) Resumption of oocyte meiosis in mammals: on models, meiosis activating sterols, steroids and EGF-like factors. Mol. Cell Endocrinol. 234, 37-45

Tzafrir, I., Pena-Muralla, R., Dickerman, A., Berg, M., Rogers, R., Hutchens, S., Sweeney, T. C., McElver, J., Aux, G., Patton, D., and Meinke, D. (2004) Identification of genes required for embryo development in *Arabidopsis*. Plant Physiol. 135, 1206-1220

Werck-Reichhart, D., and Feyereisen, R. (2000) Cytochromes P450: a success story. Genome Biol. 1, REVIEWS3003

Willemsen, V., Friml, J., Grebe, M., van den Toorn, A., Palme, K., and Scheres, B. (2003) Cell polarity and PIN protein positioning in *Arabidopsis* require STEROL METHYLTRANSFERASE1 function. Plant Cell 15, 612-625

Chapitre IV.

The Solanum ScFRK2 protein kinase defines a new MAPK family and affects ovule identity

Martin O'Brien, Charles Bertrand, Sébastien Caron et Daniel P. Matton

Soumis dans Journal of Experimental Botany le 18 octobre 2005

IV.1 Contribution des coauteurs

Une des trois séries de transgéniques a été générée par S. Caron. J'ai effectué seul toutes les expériences nécessaires à l'obtention d'un tableau et de quatre des six figures. J'ai contribué partiellement aux expériences nécessaires à une des deux autres figures dont C. Bertrand a effectué la microscopie (SEM et optique). La totalité des données non montrées de l'article (« data not shown »), sont des expériences que j'ai faites.

IV.2 Page titre

The *Solanum* ScFRK2 protein kinase defines a new MAPK family and affects ovule identity

By Martin O'Brien, Charles Bertrand, Sébastien Caron and Daniel P. Matton

Corresponding author:

Dr. Daniel P. Matton

Institut de recherche en biologie végétale, Département de sciences biologiques, Université de Montréal, 4101 rue Sherbrooke est, Montréal, Québec, Canada, H1X 2B2.

Tel: +1 514-872-3967

FAX: +1 514-872-9406

[redacted]

IV.3 Keywords

MAP Kinase, Ovule development, Carpel, Fruit development, Solanaceae.

IV.4 Genbank accession number

ScFRK1, AY427828; *ScFRK2*, AY427829.

IV.5 Abbreviations

FRK, Fertilization-related kinase; MAPK, Mitogen-activated protein kinase; MAPKK, Mitogen-activated protein kinase kinase; MAPKKK, Mitogen-activated protein kinase kinase kinase; DAP, days after pollination; CS, carpelloid structure; RLK, Receptor-like kinase; SEM, scanning electron microscopy.

IV.6 Abstract

The vast majority of plant developmental mutants described have been found to be impaired mainly in the expression of transcription factors. Only few mutants affecting plant development have been described as encoding protein kinases. In order to gain information about protein kinases acting during plant fertilization and embryogenesis, we used a reverse genetic approach to determine the role of protein kinases expressed in reproductive tissues. Out of an EST library normalized for weakly expressed genes in fertilized ovaries, we isolated two cDNA clones named *ScFRK1* and *ScFRK2* (*Solanum chacoense* Fertilization-Related Kinase 1 and 2) that showed significant homology to members of the MAPKKK family. Phylogenic analyses were unable to clearly resolve these kinases between the MAPKKK and the MAPKK families. Two similar kinases were also found in the *Arabidopsis thaliana* genome that also fall into this new category of MAPK, intermediate between the MAPKK and the MAPKKK, suggesting that they could belong to a novel MAPK group. Sense overexpression of *ScFRK2* leads to the production of seedless fruits or with a severely reduced number of seeds. Further analyses on the *ScFRK2* mutant phenotype revealed that this protein kinase was also involved in ovule development, but had no visible effect on the overall aspect of the plant. Analysis of ovaries prior to fertilization showed that the seedless phenotype was caused by a homeotic conversion of ovules into carpel-like structures, ovules being transformed into stylar projections terminated with cells similar to stigmatic papillae.

IV.7 Introduction

The pivotal role played by protein phosphorylation in eukaryotic signal transduction is well illustrated by the wide range of phosphorylation cascades that involve Mitogen-Activated Protein Kinases (MAPK) (Treisman, 1996; Robinson and Cobb, 1997). In vertebrates, MAPK are typically activated in response to various mitotic agents such as hormone and growth factors (Piwien-Pilipuk *et al.*, 2002). They have been shown to play an important role in the regulation of cell division and differentiation. The activation of MAPK occurs by phosphorylation of conserved threonine and tyrosine residues in the activation loop between the catalytic subdomain VII and VIII. This phosphorylation step is produced by dual specificity MAPK Kinases (MAPKK). These MAPK kinases are themselves activated on serine and/or threonine by serine/threonine MAPKK Kinase (MAPKKK) (Nishihama *et al.*, 1995; Madhani and Fink, 1998). In non-plant organisms, the activation of MAPKKK occurs either through phosphorylation by MAPKKK Kinase (MAPKKKK) (Sells *et al.*, 1997; Elion, 2000), by the receiver domain of a two-component histidine kinase module (Posas and Saito, 1997), or commonly by G proteins (Fanger et al., 1997) and G protein-coupled receptors (Sugden and Clerk, 1997). Cell signals are thus transmitted through a chain of phosphorylation events. In plants, direct modulators of MAPKKK are yet unknown and complete cascade modules are only starting to unfold (Asai *et al.*, 2002).

The vast majority of plant developmental mutants described so far have been found to be impaired in the expression of transcription factors, many from the MADS-box family (Jack, 2001). Only few mutants affecting plant development have been described as encoding protein kinases, although it would be reasonable to assume that post-translational modifications through phosphorylation of a protein involved in a key developmental pathway could be an important regulatory step for its intrinsic activity. Disruption of the signaling cascade would thus also lead to developmental defects. Among the protein kinases known to affect key developmental aspects of plant growth and development, many are part of the large receptor kinase (RLK) family (Becraft, 2002). Some have also been shown to affect reproductive development. These include the *Clavata 1* RLK gene involved in the regulation of meristem size and maintenance (Clark *et al.*, 1993); the *BRI1* RLK involved in brassinosteroid perception (Li and Chory, 1997); the *Petunia PRK1* RLK involved in pollen and embryo sac development (Lee *et al.*, 1996; Lee *et al.*, 1997); the extra sporogenous cells (*EXS*) RLK which regulates male germ line cell number, tapetal identity, as well as promoting seed development (Canales *et al.*, 2002); the maize *CRINKLY4* (*CR4*) RLK involved in aleurone cell fate (Becraft and Asuncion-Crabb, 2000) and the *Arabidopsis CRINKLY4* (*ACR4*), required for proper embryogenesis (Tanaka *et al.*, 2002) and involved in cell layer organisation during ovule integument and sepal margin development (Gifford *et al.*, 2003); the somatic embryogenesis receptor-like kinase (*SERK1*) involved in somatic embryogenesis (Schmidt *et al.*, 1997), and expressed in developing ovules and embryo (Hecht *et al.*, 2001); and the *Strubbelig* RLK that affects outer integument formation and organ shape although is does not encode a functional kinase domain (Chevalier *et al.*, 2005). As for the involvement of MAPK transducing modules, none have yet been

characterized in development, and only few MAPK family members have been shown to be involved in developmental processes (Hirt, 2000). Recently, a mutation in the *Arabidopsis thaliana YODA* (*YDA*) gene, which codes for a MAPKKK, has been shown to cause early embryonic defect (Bergmann *et al.*, 2004; Lukowitz *et al.*, 2004). In this mutant, the zygote does not elongate properly and the suspensor cells are fused to the embryo. Mutant *yda* seedlings that can make it through maturity show overproduction and crowding of stomata cells (Bergmann *et al.*, 2004), reminiscent of the receptor kinase *two many mouths* (*tmm*) mutant phenotype (Nadeau and Sack, 2002), This hints at the presence of a MAPK module involved in embryo development and stomata distribution. As for most MAPK cascades described so far, their involvement in limited to stress and disease responses (Hirt, 2000; Romeis, 2001; Zhang and Klessig, 2001; Asai *et al.*, 2002), and hormone perception (Kieber et al., 1993).

In this study we described the isolation and functional characterization of a new family of MAP kinases that shows an atypical sub-family kinase signature. This new family consists of two *Solanum chacoense* weakly expressed kinases and the two most similar kinases from *A. thaliana*. Functional characterization of these two protein kinases, named ScFRK1 and ScFRK2, showed that they are both involved in seed and fruit development. In this paper we show that the ScFRK2 kinase also affects the determination of carpel identity.

IV.8 Material and methods

Plant material

The diploid and self-incompatible wild potato *Solanum chacoense* Bitt. (2n=2x=24) was grown in greenhouse with 14-16 hours of light per day. The genotype used were V22 (S alleles S_{11} and S_{13}) as pollen donor and G4 (S alleles S_{12} and S_{14}) as female progenitor. Plants were hand-pollinated. Transgenic lines were generated in the G4 background.

DNA and RNA gel blot analysis

Total RNA was isolated as described previously (Jones *et al.*, 1985) or with the Plant RNeasy RNA extraction kit from Qiagen (Mississauga, ONT, Canada). RNA concentration was determined by measuring its absorbance at 260 nm. Concentration and RNA quality were verified on agarose gel and ethidium bromide staining and RNA concentration adjustment was done if needed. For each tissue tested, ten μg of total RNA were separated on a formaldehyde/MOPS gel. RNA was then blotted on Hybond N+ membranes (GE Healthcare, Baie d'Urfée, QC, Canada), and were UV cross-linked with a Hoefer UV crosslinker (120 mJ/cm^2). To confirm equal loading between RNA samples, a 1 kb fragment of *S. chacoense 18S* RNA was PCR amplified and used as a control probe. Pre-hybridization was performed at 45°C for three hours in 50% formamide solution (50% deionized formamide, 6X SCC, 5X Denhardt solution, 0.5%

SDS and 200 μg ml^{-1} of denatured salmon DNA). Hybridization of the membranes was performed overnight at 45°C in 50% formamide solution. Genomic DNA isolation was performed with the Plant DNeasy kit from Qiagen. Complete digestion of DNA (10 μg) was made overnight with 10 units of restriction enzymes as recommended by the supplier (New England Biolab, Beverly, MA, USA). DNA gel blot analysis was performed as previously described (Sambrook *et al.*, 1989) and DNA was transfered to Hybond N+ membranes prior to cross-linking. Pre-hybridization was performed for three hours at 65°C in 50% phosphate solution (50% of 0.5 M Na_2 PO_4 pH 8.0, 1% BSA, 7% SDS and 1mM EDTA), while hybridization was made overnight in the same conditions used for pre-hybridization. Probes for the RNA and DNA gel blot analysis were synthesized by random labelling using the Strip-EZ DNA labeling kit (Ambion, Austin, TX, USA) in presence of α-dATP-^{32}P (ICN Biochemicals, Irvine, CA, USA). Following hybridization, membranes were washed 30 minutes at 25°C and 30 minutes at 35°C in 2X SSC/ 0.1% SDS, 30 minutes at 45°C and 30 minutes at 55°C in 1X SSC/ 0.1% SDS, and for 10 minutes at 55°C in 0.1X SSC/ 0.1% SDS. Prior to control hybridization with the *18S* probe, the membranes were striped as recommended by the manufacturer (Ambion, Austin, TX, USA), and post-hybridization washes were done twice at 60°C for 30 minutes in 0.1X SSC/ 0.1% SDS. Autoradiography was performed at -86°C on Kodak Biomax MR film (Interscience, Markham, ONT, Canada).

Sequence analysis and phylogeny

The catalytic kinase domain structure of ScFRK2 was defined following the twelve kinase subdomains assignation described previously (Hanks and Hunter, 1995). Protein secondary structure prediction needed for the ScFRK2 subdomain designation was performed with these four prediction tools: JUFO (http://www.jens-meiler.de/jufo.html), PORTER (http://distill.ucd.ie/porter/), PSIpred (http://bioinf.cs.ucl.ac.uk/psipred/) and SCRATCH (http://www.igb.uci.edu/tools/scratch/). Designations of subdomain boundaries were obtained from a consensus of all prediction tools and conserved amino acids specific to each domains. The phylogenetic analysis was accomplished with the catalytic kinase domain only. Alignment of the protein sequences was performed using Clustal X and used to generate a relationship tree using the neighbour-joining distance method together with a bootstrap analysis to validate node support on 100 replicates in the PAUP4.08b software (Swofford, 1998).

Plant transformation

The *ScFRK2* cDNA was PCR amplified with Pwo polymerase (Roche Diagnostic, Laval, QC, Canada) with Kpn I overhang primers. Primers used were FRK2Kpn1: 5'-GGGGTACCGCGGTCGGCGCAATCTT-3' and FRK2Kpn2: 5'-GGGGTACCACTTCCATCAGGCTTTG-3'. The PCR product was cleaved with Kpn I and inserted in a modified pBin19 transformation vector (Bussière *et al.*, 2003) with a double enhancer CaMV 35S promoter. Sense and antisense constructs were determined by plasmid digestion with Eco RI, which gives an asymmetric fragmentation according

to the orientation of cloned PCR products. Sense and antisense constructs were individually transformed in *Agrabacterium tumefaciens* LBA4404 by electroporation. *S. chacoense* plants were transformed by the leaf disc method as previously described (Matton *et al.*, 1997).

Tissue fixation and SEM observations

Dissected ovaries were fixed in 4% glutaraldehyde for 4 hours at room temperature in 0.1 M phosphate buffer ($NaHPO_4$, pH 7.0). After two rinsing steps in 0.1 M phosphate buffer, the tissues were dehydrated in an increasing ethanol series (from 30% to 100%) and critical-point-dried with CO_2, coated with gold-palladium, and viewed in a JEOL JSM-35 SEM.

Tissue fixation and optical microscopy observations

Pistils were fixed in 70% FAA for 24 hours at 4°C (90 % ethanol 70%, 5% formaldehyde 37% and 5% glacial acetic acid). Samples were then dehydrated in increasing series of tert-butyl alcohol (from 70% to pure tert-butyl alcohol). Pistils were infiltrated with Paraplast Plus (Tyco Healthcare Group LP, Mansfield, MA, USA) at 56°C. Thin sections (10 µm) were prepared from embedded samples and tissue sections were stained in 0.5% Astra Blue and 1% safranine after removal of paraffin. *In situ* hybridizations were performed as described previously (O'Brien *et al.*, 2005). Microscopic observations were taken on a Leica OrthoPlan microscope.

IV.9 Results

Isolation and sequence analysis of the ScFRK1 and ScFRK2 kinases

Key regulatory genes involved in development are generally weakly and transiently expressed as well as being highly tissue-specific (Hu *et al.*, 2003). Using a negative selection screen targeting only weakly expressed genes expressed during fertilization and early embryogenesis, we have isolated 16 different protein kinase clones from the Mitogen-Activated Protein Kinase (MAPK) family in *Solanum chacoense*, a self-incompatible wild potato species close to potato and tomato (Germain *et al.*, 2005). Two of these, named *ScFRK1* and *ScFRK2*, had an atypical kinase domain structure and were further investigated for their possible role in fertilization and embryogenesis. Both clones showed strong sequence similarity with the catalytic domain of various MAPKKK, but both also showed incomplete signatures (Jouannic *et al.*, 1999; Tena *et al.*, 2001), and lacked a regulatory domain characteristic of these MAPKKK (Tu *et al.*, 1997; Wu *et al.*, 1999) (see below).

The *ScFRK1* kinase clone (accession number AY427828) is 1539 bp long (excluding the poly A tail) and is likely to represent the full-length *ScFRK1* mRNA since the size of this cDNA corresponded exactly to the size of the mRNA as determined from RNA gel blot analyses (~1.5 kb, data not shown). It codes for an open reading frame of 320 amino acids with an estimated molecular weight of 36.2 kDa, and acidic isoelectric point of 5.48. A stop codon is found upstream and in frame with the first ATG initiation codon, indicating that the coding region is complete. The *ScFRK1*

mRNA also has an unusually long 3' untranslated region of 560 nt, excluding the poly A tail. The longest *ScFRK2* cDNA isolated (accession number AY427829) consisted of 1115 bp (excluding the poly A tail) and codes for a predicted 304 amino acids long protein with an estimated molecular weight of 34.3 kDa and a basic isoelectric point of 9.4. A stop codon is also found upstream and in frame with the first ATG initiation codon, indicating that the coding region is also complete. Both proteins are composed of a catalytic domain that constitutes the major part of the protein (Fig. 1A). The kinase domain starts after the first 10 (for ScFRK1) and 5 (for ScFRK2) amino acids, and stops 42 (for ScFRK1) and 47 (for ScFRK2) amino acids before the end of the protein, leaving approximately 50 amino acids for putative regulatory domains.

The ScFRK2 deduced protein showed strongest amino acid sequence identity with ScFRK1 (45% identity, 60% overall similarity), and with a predicted protein kinase from *Arabidopsis thaliana* (At5g67080, renamed MAPKKK19 by the PlantsP database, http://plantsp.sdsc.edu/) with 36% identity (51% overall similarity) (Fig. 1A). The At5g67080 gene codes for a 344 amino acids long protein with a predicted molecular weight of 37.9 kDa. The ScFRK1 deduced protein showed greatest sequence identity with the At3g50310 protein sequence (renamed MAPKKK20 by the PlantsP database, http://plantsp.sdsc.edu/), a putative protein kinase from *A. thaliana*. ScFRK1 and At3g50310 shared 39% sequence identity and 50% overall similarity (Fig. 1A). The At3g50310 gene codes for a 342 amino acids long polypeptide with a predicted molecular weight of 37.5 kDa. Since initial Blast comparisons retrieved mostly protein kinases defined as MAPKKK, and since ScFRK1 and ScFRK2 were considerably smaller than those kinases, we performed a phylogenetic analysis with representatives

A

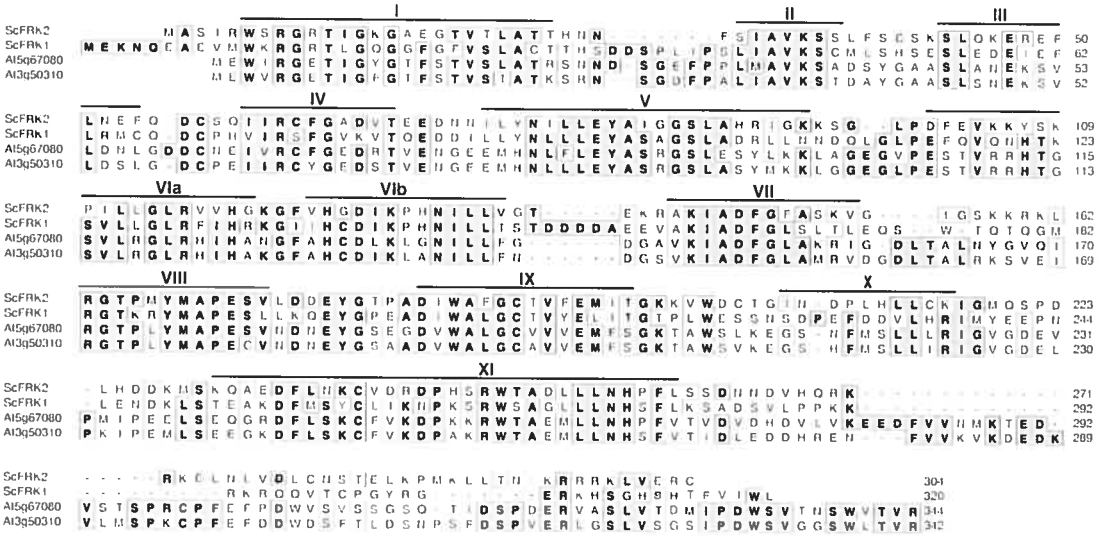
I
II
III
IV
V
VIa
VIb
VII
VIII
IX
X
XI
ScFRK2
ScFRK1
At5g67080
At3g50310

B

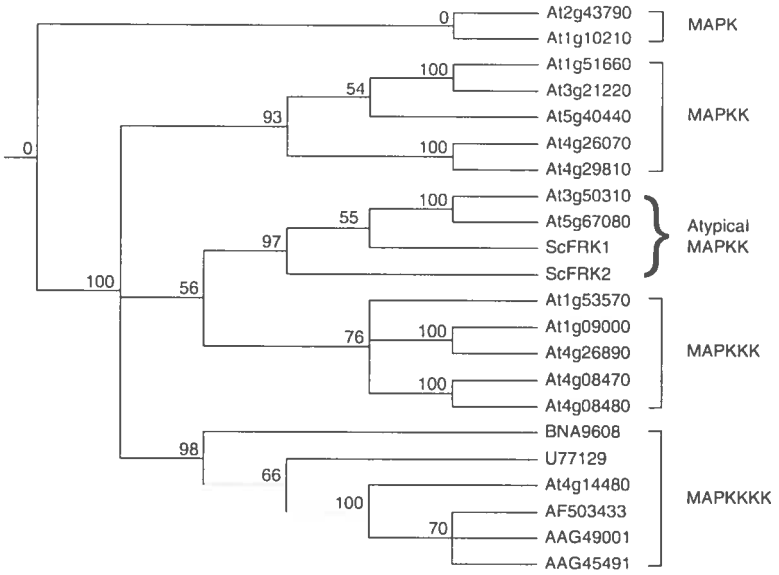
At2g43790
At1g10210
MAPK
At1g51660
At3g21220
At5g40440
At4g26070
At4g29810
MAPKK
At3g50310
At5g67080
ScFRK1
ScFRK2
Atypical MAPKK
At1g53570
At1g09000
At4g26890
At4g08470
At4g08480
MAPKKK
BNA9608
U77129
At4g14480
AF503433
AAG49001
AAG45491
MAPKKKK
0
100
54
93
100
100
55
97
100
56
76
100
100
98
66
100
70

Figure 1

A. Sequence alignment of the deduced protein sequences from *S. chacoense* ScFRK1 and ScFRK2, and with the most similar kinases, At5g67080 and At3g50310, from *A. thaliana*. Kinase subdomains are identified with thick black lines and were defined as described by Hanks and Hunter (1995) where alpha helices and beta sheets were deduced by four different prediction tools. **B** Dendrogram showing the phylogenic link between ScFRK1, ScFRK2, At5g67080 and At3g50310 proteins. The dendrogram was generated using PAUP4.08b (Swofford, 1998), with protein sequences used in **A** and with other defined MAPK, MAPKK, MAPKKK and MAPKKKK available in GenBank. Except for the new phylogenic group of ScFRK1, ScFRK2, At5g67080 and At3g50310, all other kinase entries are described by their accession number. MAPK: MPK1 from *A. thaliana* (GenBank accesion number At1g10210), MPK6 from *A. thaliana* (GenBank accesion number At2g43790), MAPKK: MKK3 from *A. thaliana* (GenBank accesion number At5g40440), MKK4 from *A. thaliana* (GenBank accesion number At1g51660), MKK1 from *A. thaliana* (GenBank accesion number At4g26070), MKK2 from *A. thaliana* (GenBank accesion number At4g29810), MKK5 from *A. thaliana* (GenBank accesion number At3g21220), MAPKKK: NPK1-related kinase 2 from *A. thaliana* (GenBank accesion number At1g09000), MAPKKK3 from *A. thaliana* (GenBank accesion number At1g53570), MAPKKK9 from *A. thaliana* (GenBank accesion number At4g08480), MAPKKK10 from *A. thaliana* (GenBank accesion number At4g08470), MAPKKK16 from *A. thaliana* (GenBank accesion number At4g26890), MAPKKKK : MAP4K10 from *A. thaliana* (GenBank accesion number At4g14480), 3615.3 from *Oryza sativa* (GenBank accesion number AAG45491), putative serine/threonine kinase

from *Hordeum vulgare* (GenBank accesion number AAG49001), MAP4Kα1 from *Brassica napus* (GenBank accesion number BNA9608), KHS1 *Homo sapiens* (GenBank accesion number U77129), putative MAP4K from *Sorghum bicolor* (GenBank accesion number AF503433). The phylogenic analysis was accomplished with the catalytic kinase domain only. Protein sequences were trimmed following sub-domain identity as described by Hanks and Quinn (1991). Numerical values represent the support percentage for each node (Bootstrap method).

from the MAPK (as the outgroup), MAPKK, MAPKKK, and MAPKKKK families, in order to determine to which family of MAPK did ScFRK1 and ScFRK2 belong. The phylogenetic analysis was achieved after aligning trimmed kinase domains based on previous sequence alignments and secondary structures predictions (Hanks and Quinn, 1991). Two members of the MAPK family from *A. thaliana* (MPK1 and MPK6), five members of the MAPKK family from *A. thaliana* (MKK1, MKK2, MKK3, MKK4 and MKK5), five members of the MAPKKK family from *A. thaliana* (MAPKKK3, MAPKKK9, MAPKKK10, MAPKKK16 and NPK1-related kinase 2) and six members of the MAPKKKK family from *A. thaliana* (MAP4K10), *Brassica napus* (MAP4Kα1), *Sorghum bicolor* (putative MAP4K), *Hordeum vulgare* (putative serine/threonine kinase), *Oryza sativa* (3615.3) and *Homo sapiens* (KHS1) were used for the phylogenetic reconstruction (PAUP-mediated classification). All software parameters were kept at default values during sequence alignment. The alignment obtained was used to generate a relationship tree using the neighbour-joining distance method together with a bootstrap analysis to validate node support on 100 replicates. Phylogenic linkage between ScFRK1, ScFRK2, At5g67080, At3g50310 and other members of the different MAPK families, revealed that this group of four proteins, although clearly related to the MAPK superfamily, did not cluster with any individual subfamily, and therefore, could be assigned as a new MAPK subfamily, intermediate between the MAPKK and MAPKKK subfamily (Fig.1B). In order to more precisely characterize this new family, we compared our sequences with the known subdomain signatures from other MAPK subfamilies (Table I). The RAF-subdomain I signature is common to all plant RAF subfamily members (Jouannic *et al.*, 1999). This signature discriminates the RAFs from all other MAPKKK. The PRAF-activation loop sequence embedded in the activation

loop and subdomain VIII is also a determinant for the plant RAF subfamily (Jouannic *et al.*, 1999). Both signatures are too weakly conserved in the FRK1/2 group to assign them to the PRAF family. The best conserved MAPKKK signature is the PMEKK- signature found in the subdomain IX of the MEKK subfamily (Tena *et al.*, 2001). This MEKK signature is the most conserved one found in ScFRK1 and ScFRK2, but is poorly conserved in the two most similar *A. thaliana* sequences. The FRK1/2 group also showed partial sub-domain signature with the MAPKK sub-family. A signature sequence found in subdomain VIII is characteristic of all MAPKK (Hamal *et al.*, 1999). In the FRK1/2 group this sequence differ for two or three conserved amino acid out of ten. Furthermore, the plant MAPKK signature described in subdomain V (Hamal *et al.*, 1999) also differ for the FRK1/2 group. Six conserved amino acids are distinct from the two signature sequences of plant MAPKK.

We then compared the phosphorylation motifs found in the activation (T-loop) located between subdomain VII and VIII. The non-plant phosphorylation motif between subdomain VII and VIII is described as $SX_3[TS]$ (Zheng and Guan, 1994), while the typical MAPKK plant phosphorylation motif has been characterized as $[TS]X_5[TS]$ (Shibata *et al.*, 1995; Morris *et al.*, 1997). ScFRK2 showed one such motif (SX_5S) in the activation loop and another motif (SX_5T) partially embedded in subdomain VIII. ScFRK1 showed two similar phosphorylation motifs (SX_5S and TX_5T) both located in the activation loop and a third motif (TX_5T) overlapping with the subdomain VIII. One SX_3T sequence, typical of non-plant phosphorylation motifs, was also detected in the activation loop. The *A. thaliana* clones showed more peculiar signatures. The At5g67080 kinase showed only one phosphorylable residue in the activation loop, the

threonine-162 and hence, lacked a phosphorylation motif. The At3g50310 kinase showed only one motif (SX_5T), partially embedded in subdomain VIII, similar to one of the possible phosphorylation motifs found in ScFRK1. Serine and threonine residues are also present in the At3g50310 activation loop, but they are spaced by four amino acids, an uncharacterized phosphorylation motif. Clustal X alignment of the FRK1/2 kinase group, also revealed strong similarities between the kinase subdomains and absence of similarity in the activation loop and in the C-terminus end (Fig.1A).

Genomic organization of *ScFRK2*

In *A. thaliana* genome, At5g67080 and At3g50310 are single copy genes without introns. The genomic organization of *ScFRK2* was assayed by PCR amplification on genomic DNA and by restriction enzymedigestion of genomic DNA followed by Southern blotting. PCR amplification was achieved with primers that amplified the complete and full length *ScFRK2* cDNA clone. ScFRK2 cDNA containing and genomic DNA PCR amplification were run side by side on an agarose gel and no differences in the length of the PCR products could be detected (data not shown). This indicates the absence of an intron in the region defined by the primers used. DNA gel blot analyses of genomic DNA restriction fragments revealed a simple multi-banding pattern for *ScFRK2* hybridization (Fig. 2A). The Eco RI and Nco I digestions showed three bands, while the Bam HI and the Xba I digestions showed two bands. Since Eco RI and Bam HI cleave the *ScFRK2* cDNA once, and Nco I and Xba I do not cleave the *ScFRK2* cDNA, these results suggests that, in *S. chacoense*, the *ScFRK2* gene is present possibly in two to three copies if one of the Bam HI fragments contains two copies of *ScFRK2* in tandem.

Signatures	ScFRK1	ScFRK2	At3g50310	At5g67080	Consensus*
RAF-subdomain I	43	57	50	50	57
PRAF-activation loop	22	44	44	33	33
PMEKK-subdomain IX	80	80	50	50	80
MAPKK-subdomain VIII	80	70	70	70	70
PMAPKK-subdomain V	65	65	65	65	71

Table 1

MAPK superfamily protein signatures and percentage of amino acid identity with the new FRK1/2 subfamily.

RAF-subdomain I consensus:

(RK)(IV)GXG(SF)(FY)G(TE)VX(KRH)(GA)X(WF)(HFN)G (Jouannic *et al.*, 1999)

PRAF-activation loop: (LIM)X(SD)X(ST)X(AK)GTP(EQ)W (Jouannic *et al.*, 1999)

PMEKK-subdomain IX: DIWSXGCTXXEXXTXXXP (Tena *et al.*, 2001)

MAPKK-subdomain VIII: (AIVT)(GA)(TC)XX(YF)M(SAG)PER(IL) (Hamal *et al.*, 1999)

PMAPKK-subdomain V:

(SQY)(LIV)(ILAV)LE(YF)M(DN)(GKQR)GSL(AE)(DG)(IFAL)(LHIV)(KIV) (Hamal *et al.*, 1999)

Identity was calculated based on the number of informative residues, excluding positions allowing any amino acids (X). *Percentage of amino acid identity for the consensus of FRK1/2 subfamilly. Because only four sequences are available, identity consensus was set to a minimum of two out of four amino acids (50%).

Expression pattern of *ScFRK2* mRNA

The ScFRK2 expression pattern was determined by RNA gel blot analysis (Fig. 2B) with various vegetative (petals, stems, leaves, roots and tubers) and reproductive tissues (stamens, pollen, pollen tubes, fertilized ovules 2, 3, 4, 5 and 6 days after pollination, and pollinated styles and ovaries 0, 48 and 96 hours post-pollination). Equal loading of mRNA sample in each lane was verified with an *18S* RNA probe (lower panel). *ScFRK2* showed two transcripts with near equimolar amounts although the larger 1.6 kb transcript is slightly less abundant in all tissues tested except stamens, and is not detected in all RNA gel blots (see also Fig. 4A). The larger transcript might therefore correspond to an unspliced *ScFRK2* pre-mRNA or, alternatively, to a cross-hybridizing member of the *ScFRK2* family (Fig. 2A). The lower sized transcript is estimated at 1.1 kb and should correspond to the *ScFRK2* 1.11 kb cDNA. Although the larger 1.6 kb *ScFRK2* transcript could not be detected in all experiments, its nearly equimolar accumulation in most tissues when compared to the 1.1 kb transcript prompted us to attempt its isolation. One million phages from a cDNA library made from 48 hours post-pollination pistils were screened with the full length *ScFRK2* cDNA and only eight clones were retrieved. All corresponded to the 1,1 kb transcript (data not shown). Thus the *ScFRK2* mRNA abundance can be estimated at 0,0008% of total messenger RNAs in pistil tissues. This is reflected in the exposure time of the hybridization membranes, with four days exposure with the *ScFRK2* probe versus five minutes for the control *18S* rRNA probe. 5' RACE PCR was also attempted, but again, no product longer than the original *ScFRK2* cDNA could be isolated. Prior to fertilization, strongest *ScFRK2* mRNA accumulation is observed in stamens and in unpollinated styles, although a basal mRNA level can be detected in all tissues examined (Fig. 2B). Fertilization had a

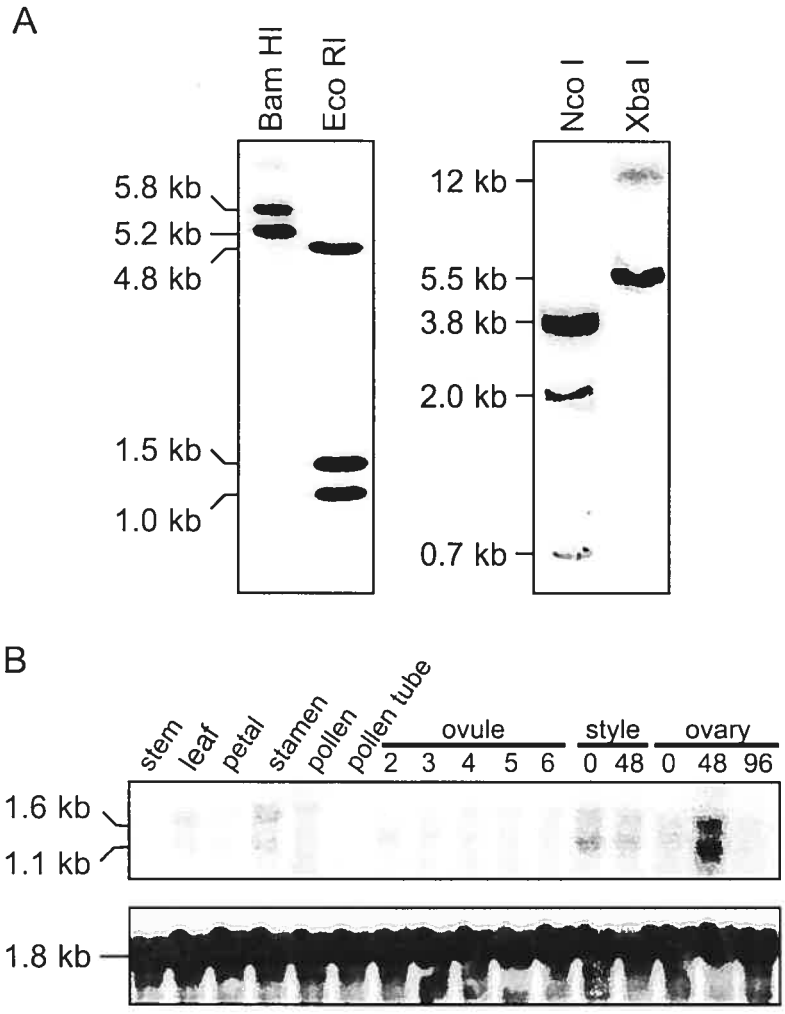
A
Bam HI
Eco RI
Nco I
Xba I
5.8 kb
5.2 kb
4.8 kb
1.5 kb
1.0 kb
12 kb
5.5 kb
3.8 kb
2.0 kb
0.7 kb
B
stem
leaf
petal
stamen
pollen
pollen tube
ovule
style
ovary
2 3 4 5 6
0 48
0 48 96
1.6 kb
1.1 kb
1.8 kb

Figure 2

***ScFRK2* DNA and RNA gel blot analyses. A.** DNA gel blot analysis of the *ScFRK2* gene. Genomic DNA (10 μg) isolated from *S. chacoense* leaves was digested with Bam HI, Eco RI, Nco I or Xba I restriction enzyme, transferred onto membranes and probed with the complete 1.1 kb *ScFRK2* cDNA. Estimated molecular weight of the fragments obtained appear on the left of each DNA blot. **B.** RNA gel blot analysis of *ScFRK2* mRNA accumulation in mature tissues. All tissues were collected from young mature greenhouse grown plants. Pollen tubes are from *in vitro* grown material. Ovules from two to six days after pollination were hand dissected from ovaries. Pistil tissues were analyzed separately as styles and ovaries from 0 to 96 h after pollination. Ten μg of total RNA isolated from *S. chacoense* tissues were blotted and probed with the full-length cDNA insert of *ScFRK2* (upper panel). Membranes were stripped and reprobed with a partial *18S* ribosomal RNA to assure equal loading of each RNA sample (lower panels).

dramatic effect on *ScFRK2* accumulation only in ovaries, as can be seen in 48 h post-pollinated ovaries (Fig. 2B).

Microarray data obtained with the Affymetrix ATH1 *Arabidopsis* Genome Array through the AtGenExpress project and the NASCArrays project, showed that *MAPKKK19*, *A. thaliana ScFRK2* most homologous gene, is expressed predominantly in seeds, anther, mature pollen, ozone treated tissues and *Pseudomonas syringae* infiltrated leaves. All other tissues tested showed either no expression or weak *MAPKKK19* expression. *MAPKKK20* gene, *A. thaliana ScFRK1* most homologous gene, was exclusively expressed in pollen and stamens. *MAPKKK19* (At5g67080) and *MAPKKK20* (At3g50310) microarray data were retrieved from the PlantsP website (http://plantsp.genomics.purdue.edu/).

In Situ Analysis of *ScFRK2* mRNA Accumulation

In order to determine more precisely the tissue expression pattern of the *ScFRK2* gene, *in situ* hybridizations were performed on 10 μm sections of mature but unfertilized ovaries and fertilized ovaries two days after pollination (DAP), where peak accumulation occurs (Fig. 2B). In unfertilized ovaries, detectable *ScFRK2* mRNA accumulation can be observed only in the ovule's integument (Fig. 3A). At peak expression, 2 DAP, *ScFRK2* mRNAs are again strongly detected in the ovule's integument and, more diffusely, in the placenta and pericarp (Fig. 3C and E). Although preservation and observation of the zygote is difficult in these parafilm embedded sections, staining can be occasionally observed in the embryo sac where the zygote

would be located (for example see magnification in Fig. 3E). A comparison of *in situ* analysis between unfertilized and 2 DAP ovules also show the increase in *ScFRK2* mRNA expression as previously observed in RNA gel blot analyses (Fig. 2B). Sense probe hybridizations show the high specificity of the detection pattern obtained (Fig. 3B, D and F).

Plant phenotypes in overexpressing *ScFRK2* sense transgenic lines

We generated transgenic plants expressing the sense and antisense construct of *ScFRK2*. *ScFRK2* sense and antisense cDNA were cloned in a modified pBin19 vector (Bevan, 1984), driven by a doubled enhancer 35S promoter and with the NOS terminator sequence (Bussière *et al.*, 2003). Kanamycin-resistant plants were allowed to grow to maturity in the greenhouse and the *ScFRK2* expression level was monitored by RNA gel blot analysis of stamen, leaf and ovary tissues (Fig. 4A, data not shown for stamen and leaf tissues). All gave identical results, indicating that the CaMV35S promoter used was equally active in ovaries, stamens and leaves. Of the sense overexpressing lines, one showed complete co-suppression for *ScFRK2* (sense construct S20), while 12 others showed various levels of *ScFRK2* mRNA expression. Antisense derived plants showed reduced *ScFRK2* mRNA levels compared to untransformed control (data not shown), but none showed complete mRNA suppression as observed in the co-suppressed line S20 (Fig. 4A). No obvious phenotypes were detected in co-suppressed line S20, as well as from the other antisense lines. Overall plant growth and macroscopic development was unaffected in all *ScFRK2* overexpressing transgenic lines tested and the only phenotypes observed were associated with reproductive tissue defects. In the

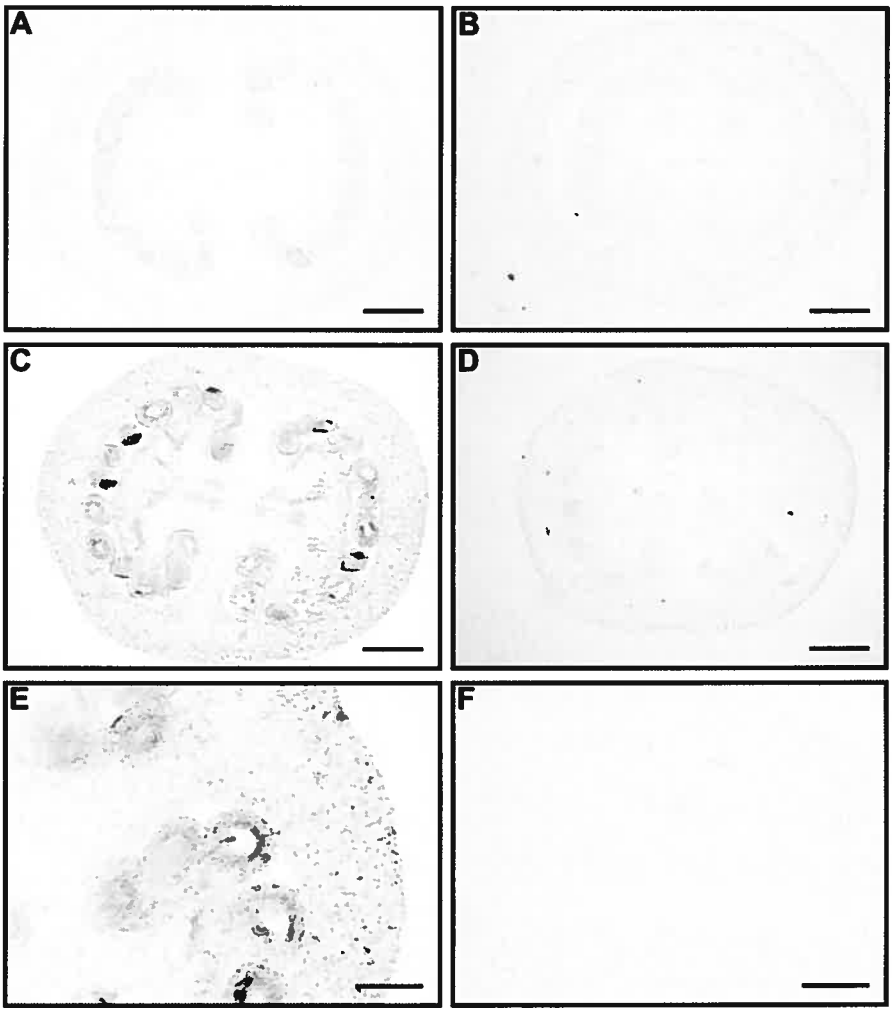

Figure 3

***In situ* localization of *ScFRK2* transcripts.** **A** and **B**, unfertilized mature ovary sections. **C** and **D**, ovary sections 48 h after pollination (approximately 12 h postfertilization). E and F, magnification of ovary sections 48 h after pollination. A, C, and E, antisense probe. B, D, and F, control sense probe. Digoxigenin labeling is visible as a blueish staining. All hybridizations used 10 μm-thick sections and an equal amount of either *ScFRK2* sense or antisense probe. Bars in A to D represent 250 μm. Bars in E and F represent 125 μm.

ScFRK2 overexpression lines, half of them (sense construct transgenic lines S2 and S17, Fig. 4A, and transgenic lines S5, S7, S9 and S11, data not shown) produced smaller than normal fruits and showed a seed-defective phenotype following fertilization (Fig. 4B and C, Table II). Development of the fruit started similarly in WT and transgenic lines, but ten DAP significant differences in fruit size appeared in transgenic lines overexpressing the *ScFRK2* gene (Fig. 4C). In untransformed *S. chacoense* plants, fruits develop to maturity in approximately 21 days after pollination. Thereafter, mature embryos start to desiccate in order to reach seed maturity around 40 days post-pollination. At embryo maturity (21 DAP), fruit diameter from *ScFRK2* transgenic lines reached about 60% of the normal WT fruit diameter, weighed only 36% of normal WT fruits, and had only 6.4 % of the total number of seeds normally produced in wild type fruits. This strongly reduced seed set could explain the small fruit size observed. Furthermore, seeds obtained from overexpressing transgenic lines bore embryos that were retarded in their development, most of them still being at the torpedo stage compared to mature embryos in WT plants (Table II). These embryos would eventually proceed to a mature stage and plants could be regenerated from these when hand dissected and placed on a sterile solid MS media (data not shown).

Further analyses of the *ScFRK2*-S2 and *ScFRK2*-S17 mutants revealed that overexpression of the *ScFRK2* kinase led to the transformation of ovules into carpelloid structures. In hand-dissected ovaries from the *ScFRK2* transgenic lines, the uppermost ovules in the ovary developed as filiform structures (Fig. 5B). A normal ovule in this transgenic background is also visible indicated with a white arrow in Figure 5B, while

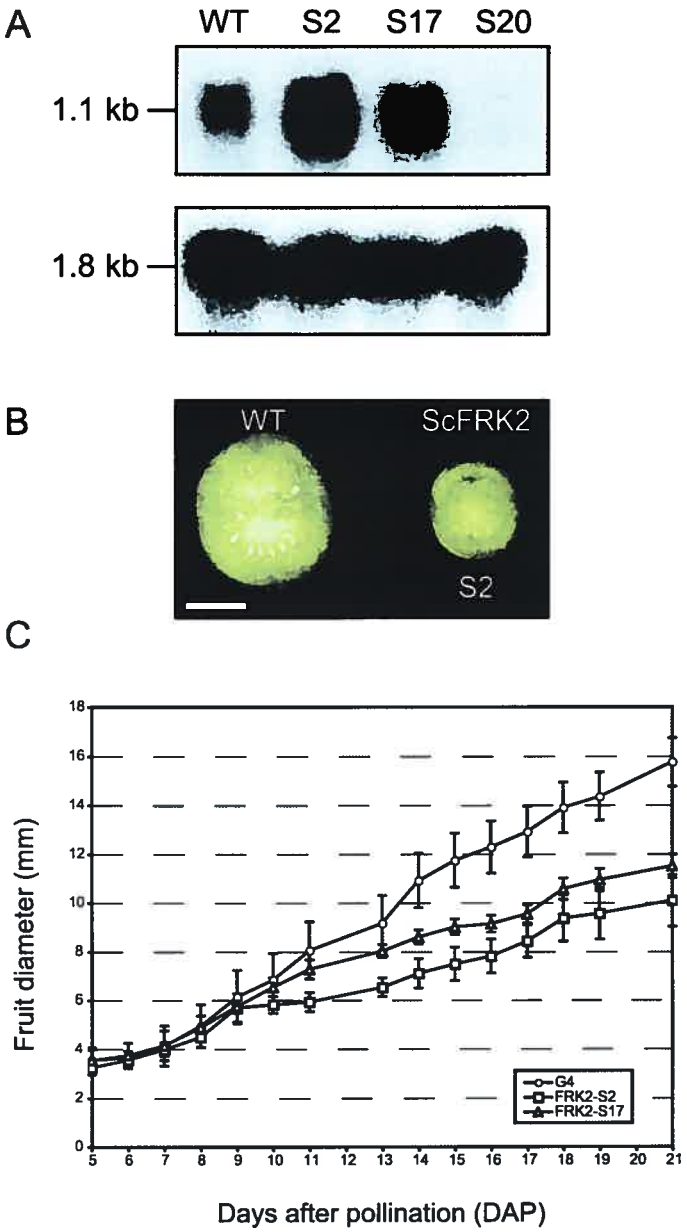
A
WT
S2
S17
S20
1.1 kb
1.8 kb
B
WT
ScFRK2
S2
C
Fruit diameter (mm)
Days after pollination (DAP)
G4
FRK2-S2
FRK2-S17

Figure 4

RNA expression analysis and fruit phenotype in *ScFRK2* transgenic lines. A Upper panel. RNA gel blot analysis of *ScFRK2* mRNA of ovary tissues derived from control line G4 (WT), overexpressing lines S2 and S17, and cosuppressed line S20. Lower panel. Membranes were stripped and reprobed with a partial *18S* ribosomal RNA to assure equal loading of each RNA sample. **B** *S. chacoense* fruit slices from a WT untransformed control plant (left) and from the *ScFRK2* overexpressing S2 plant line (right). Thick white line represents 1 cm. **C.** Graph representing fruit diameter (mm) from 5 to 21 DAP for WT and *ScFRK2* overexpressing lines S2 and S17.

an ovary with removed pericarp from an untransformed control plant is shown in Fig. 5A. Ovaries with a severe phenotype showed small bumps on their surface instead of a perfectly round and smooth surface as seen in control ovaries (data not shown). Inside these ovaries, the filiform structures filled all the locular space, leaving few empty pockets. The transformed ovules took on a twisted spaghetti-like appearance due to the physical constraints of the available growth space in the ovary (Fig. 5B and E). To identify the nature of these transformed ovules, we analyzed their morphology by scanning electron microscopy (SEM). Untransformed control ovaries showed well-distributed ovules in the two locules (Fig. 5C). In contrast, *ScFRK2* overexpressing ovaries showed variable numbers of ovules with abnormal growth. The severity of the phenotype was also influenced by environmental factors, such as daylength or temperature, with more abnormal ovules observed in warmer periods during summer in the greenhouses (data not shown). The length of these modified ovules varied from small outgrowths to long and thin structures (Fig. 5D to G). Fig. 5D shows modified ovules with a mild phenotype, while Fig. 5E shows a more severe phenotype where filiform structures are longer and become twisted (Fig. 5G). These structures developed from the placenta as for normal ovules (Fig. 5F, 6D) and had an intrusive growth that disrupted ovule organization in their surrounding. Cells on filiform ovules were elongated without being wider than normal ovule cells (Fig. 5F). The tip of the modified ovules had cell projections (Fig. 5I) similar to WT stigmatic papillar cells (Fig. 5H). A magnification of the region corresponding to these papillar cells is shown in Fig. 5K. These stigmatic-like papillae resemble normal WT papillar cells (Fig. 5J), except that no mucilage could be observed on their surface. Considering that the carpelloid structures most probably correspond to immature styles, this is not unexpected. We also compared

Plant	Fruit diameter (mm)[1]	Fruit fresh weight (g)[2]	Number of ovule per fruit[3]	21 DAP embryo developmental stage[4]
Wild-type *G4*	15.8 ± 1.0	2.45 ± 0.24	106.2 ± 8.3	Mature
ScFRK2-S2	10.1 ± 1.1	0.89 ± 0.23	6.8 ± 1.9	Torpedo

Table 2

Comparison of fruit size, weight, ovule number and embryo developmental stage between wild type and mutant plants.

[1] Diameter was calculated from 24 fruits for both WT and mutant plants.

[2] Fruit fresh weight was calculated from 24 fruits for both WT and mutant plants.

[3] Number of ovule per fruit was calculated from 24 fruits for both WT and mutant plants.

[4] Developmental stage at which most embryos were found 21 DAP, randomly taken from 24 dissected ovules. For WT plant, out of 24 embryos 19 were mature and 5 were at the torpedo stage. For the *ScFRK2* S2 mutant plant, 3 embryos were at the heart stage; 13 at the torpedo stage; 4 at the walking-stick stage; 4 at the mature embryo stage.

cell morphology between WT stylar and carpelloid ovule cells (Fig. 5L, N and P, and M, O and Q, respectively). Cells from carpelloid structures (Fig. 5M) showed rectangular cells that were more similar to stylar cells (Fig. 5L) than to WT ovule cells. Moreover, transformed ovules shared the same smaller triangular cells found on WT stylar cells (data not shown), but lacked guard cells and stomata that mature WT style shows along their length (Fig. 5L) (O'Brien *et al.*, 2002a). Another feature of *S. chacoense* style is the presence of small papillae-like protrusions that develops as the style matures (O'Brien *et al.*, 2002a). Along their length, style (Fig. 5N) and carpelloid structures (Fig. 5O) shared quite similar protruding papillae-like cells (Fig. 5N, O; black arrows). When magnified, these papillae–like cells showed similar cuticular ornamentations in both transgenic (Fig. 5Q) and WT cells (Fig. 5P).

To analyze the cell types present in the transformed ovule in more detail, we observed thin sections of fixed ovaries from an *ScFRK2* overexpressing plants. The untransformed plants showed an ovary with placenta-attached ovules (Fig. 6A, and C for a close-up view of one locule only). In contrast, *ScFRK2* transgenic plant ovaries showed carpelloid structures (CS) similarly attached to the placenta, but where the locule organization was heavily disrupted due to the formation of the long filiform CS (Fig. 6B, and D for a close-up view of one locule only). These CS ovules showed a clearly different cellular identity than WT ovules. Transverse sections through the CS revealed strands of thin, long and more compacted cells (arrows in figure 6D and F), reminiscent of the transmitting tissue cells found in the style (arrow in figure 6E). An RNA gel blot analysis with molecular markers for mature differentiated style transmitting tissue (*S-RNase*, *HT* gametophytic self-incompatibility modifier)

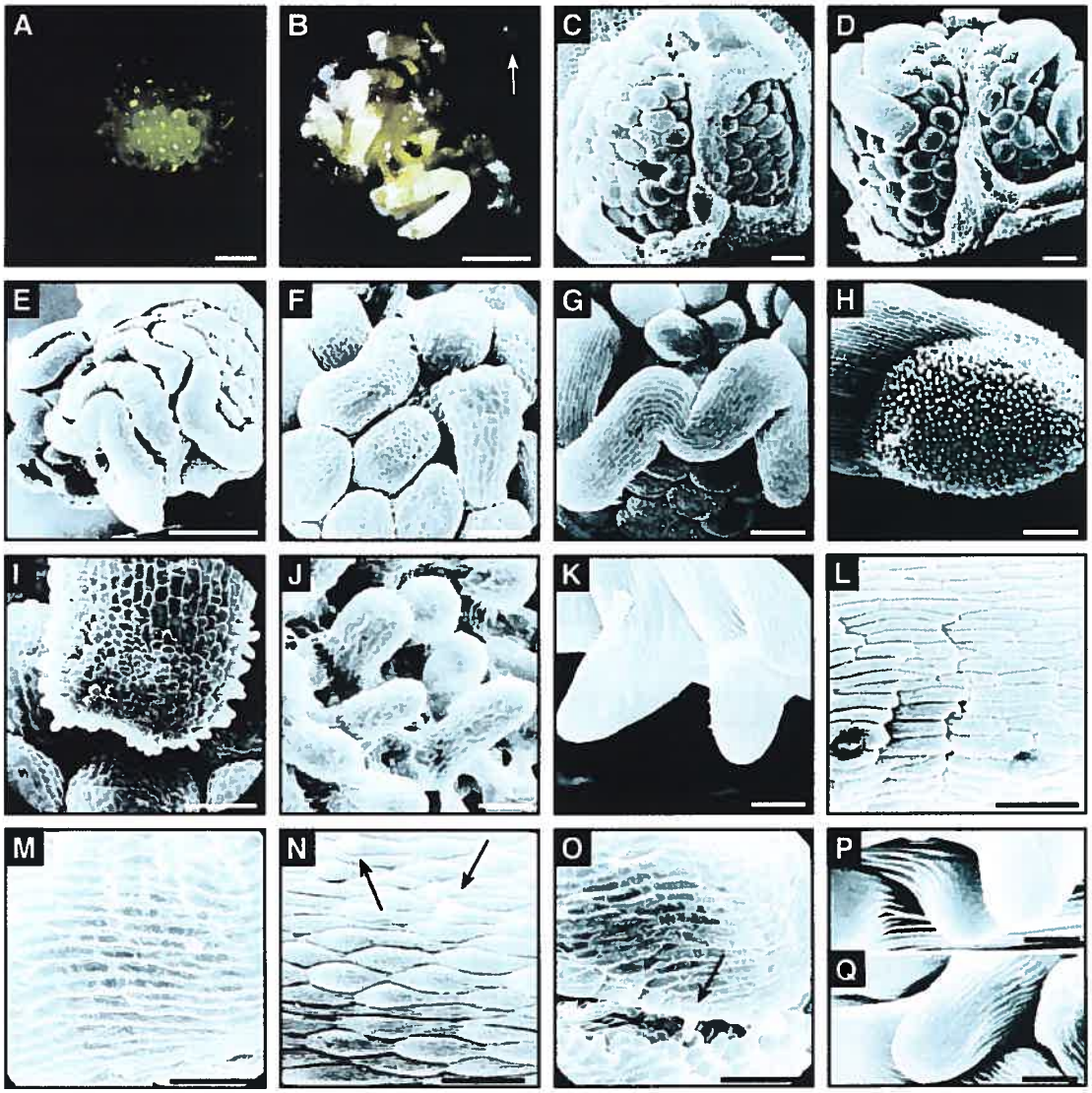
A
B
C
D
E
F
G
H
I
J
K
L
M
N
O
P
Q

Figure 5

Fruit and ovule phenotype of *ScFRK2* overexpressing lines. A. Untransformed control plant ovary without pericarp seen through stereomicroscopy. Bar = 1 mm. **B.** Ovary showing carpelloid structure (CS) of ovules in *ScFRK2* overexpressing plant seen through stereomicroscopy. Pericarp has been removed. The white arrow points to a normal ovule. Bar = 1 mm. **C.** SEM of ovules from untransformed control plant. Bar = 100 μm. **D and E.** SEM of ovules from *ScFRK2* overexpressing plants. Mild carpelloid change is observed in **D** (Bar = 100 μm) and a more severe phenotype in **E** (Bar = 500 μm). **F.** SEM close-up of emerging CS. Bar = 100 μm. **G.** SEM close-up of long carpelloid ovule. Bar = 100 μm. **H.** SEM close-up of stigma-like extremity of a CS. Bar = 100 μm. **I.** SEM close-up of papillae on carpelloid ovule extremity. Bar = 50 μm. **J.** SEM showing stigmatic papillar cells from a control plant. Bar = 10 μm. **K.** SEM showing papillar cells from carpelloid ovule extremity. Bar = 10 μm. **L.** SEM showing cells from the style cortex epidermis of untransformed control plant. Bar = 100 μm. **M.** SEM showing cells from carpelloid ovules of *ScFRK2* overexpressing plant. Bar = 100 μm. **N.** SEM showing small papillae from a WT style three days before anthesis. Bar = 100 μm. **O.** SEM showing small papillae from the stylar section of a carpelloid ovule in *ScFRK2* overexpressing plant. In **N** and **O**, papillae cells are pointed with dark arrows. Bar = 100 μm. **P.** SEM showing close-up on papillae cell ornamentations from style of untransformed control plant. Bar = 10 μm. **Q.** SEM showing close up on papillae cell ornamentations from carpelloid ovule of *ScFRK2* overexpressing plant. Bar = 10 μm.

(O'Brien *et al.*, 2002b) was performed on ovaries from *ScFRK2* overexpressing plants, but no differential signal could be detected when compared to WT ovules (data not shown), suggesting that, in the CS tissue observed, the transmitting tract is mostly immature. Vessels can be observed spanning the transmitting tract of WT plants, and these could also be observed at higher magnification in the filiform ovules (Fig. 6E, F, and data not shown). These were never detected in WT ovules. No embryo sac formation could be observed in any CS.

Abscission of flowers occurs five days after anthesis in unpollinated WT plants. Since fruit formation occurred in *ScFRK2* overexpressing lines, this suggested that fertilization had taken place. We therefore determined the fate of these filiform CS shortly after fertilization, since at fruit maturity, no traces of CS could be observed, as the fruits were filled with placenta and pericarp tissues (Fig. 4B). Fruits were hand dissected at different times after pollination and observed. Seven days after pollination, the filiform CS had already started to wither and turn brown (data not shown).

In *Petunia*, down-regulation of the *FBP11* MADS-box gene causes homeotic change of ovules to carpelloid structures (Angenent *et al.*, 1995), while overexpression of *FBP11* causes development of ectopic ovules on the adaxial side of sepals and abaxial side of petals (Colombo *et al.*, 1995). Our overexpressing *ScFRK2* lines showed a phenotype very similar to the *FBP11* down-regulated lines. If the ScFRK2 kinase acts in the same pathway as the FBP11 MADS box transcription factor, we could have overlooked a phenotype in *ScFRK2* down-regulated plants. However, when we analyzed

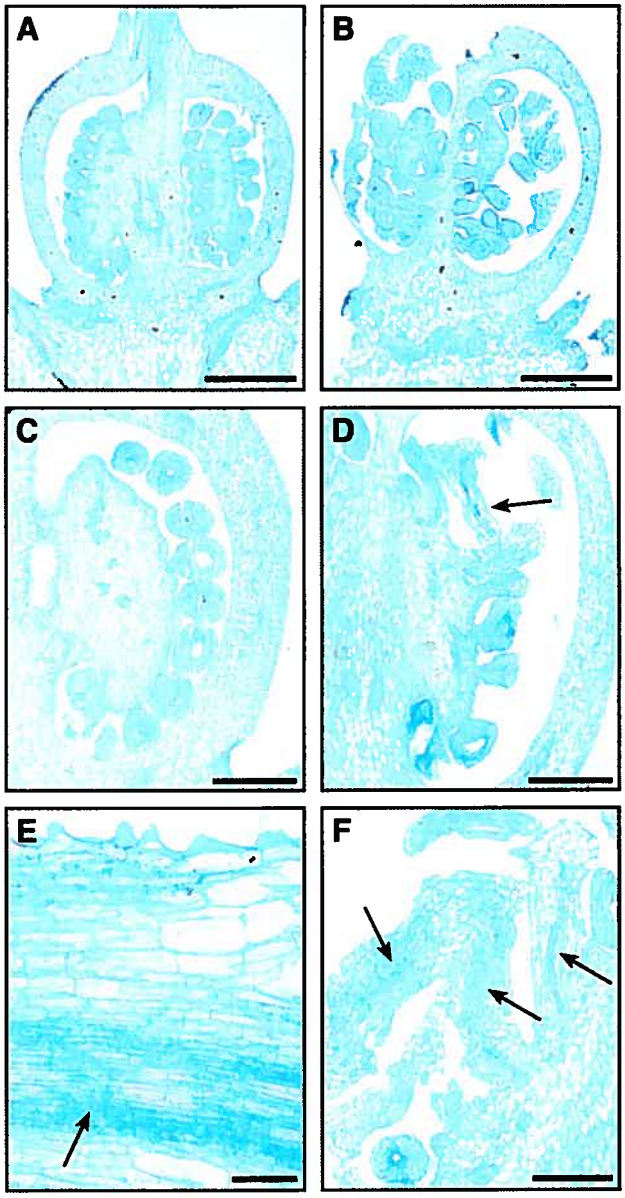
A
B
C
D
E
F

Figure 6

A through F. Optical microscopy of pistil from WT and *ScFRK2* overexpressing line. A. Ovary from an untransformed control plant. Bar = 1 mm. **B.** Ovary from *ScFRK2* overexpressing plant. Bar = 1 mm. **C.** Close up on locule from untransformed control plant. Bar = 250 μm. **D.** Close up on locule from *ScFRK2* overexpressing plant. Bar = 250 μm. **E.** Style from untransformed control plant. Bar = 50 μm. **F.** Cell arrangement of carpelloid ovule. Bar = 100 μm. Black arrows in **D**, **E** and **F** depict dense cells of either transmitting tract (**E**) or carpelloid structures (**D** and **F**).

flower organs of the *ScFRK2* co-suppressed plant (line S20), no development of ectopic ovules could be detected (data not shown).

IV.10 Discussion

We have identified a new group of MAPKs that showed partial similarity to the MAPKK and MAPKKK subfamilies. Both *Solanum chacoense* members of this new protein kinase group showed reproductive tissue defects when either suppressed (*ScFRK1*, in preparation) or overexpressed (*ScFRK2* described here) at the RNA level. In this study we provide evidence for the involvement of the ScFRK2 protein kinase in the determination of ovule identity.

The ScFRK1 and ScFRK2 protein kinases were isolated from a pollinated-pistil library through a negative selection screen for regulatory genes expressed in reproductive tissues. Using the basic local alignment search tool on publicly available databases, both were most similar to the catalytic domain of numerous MAPKKK, as well as to two uncharacterized protein kinases from *Arabidopsis thaliana* (At3g50310 and At5g67080). Structural analysis of the FRK1/2 group for signature sequences found in the MAPK family revealed that they possessed only partially conserved signature sequences from either the MAPKK or the MAPKKK subfamilies (Table I). When compared to the MAPKKK subfamily, they lacked a typical regulatory domain. Furthermore, complementation in a yeast mutant background deficient for the Ste11 MAPKKK could not be achieved with either the ScFRK1 or ScFRK2 kinases (data not shown). The subdomain signature sequences in the FRK1/2 group were overall slightly more similar to the ones found in MAPKK (Table I). The MAPKK plant phosphorylation motif $[ST]X_5[ST]$ was also found in both ScFRK1 and ScFRK2

between subdomains VII and VIII. For the two most similar genes in *A. thaliana*, the At3g50310 kinase showed one SX_5T motif, partially embedded in subdomain VIII, and an unusual SX_4T motif in the activation loop. The At5g67080 kinase completely lacked a recognizable phosphorylation motif. Plant MAPKK also contain a MAPK docking domain of consensus sequence $[KR]_3X_{1-5}[LI]X[LI]$ in the N-terminal region (The MAPK Group, 2002), similar to the one found in animal MAPKK (Bardwell and Thorner, 1996). Such a motif is also found in ScFRK2, but in the C-terminal region between residues 271 and 277. Although the above mentioned criteria suggest that ScFRK1 and ScFRK2 are more closely related to the MAPKK subfamily, a phylogenic analysis could not unambiguously resolve these proteins between the MAPKK and MAPKKK subfamilies. This suggest that these kinases could belong to a new MAPK subfamily, although a higher number of similar sequences would be needed for a thorough phylogenetic analysis. Their peculiar structure is also emphasized by the fact that the two most similar kinases in the *Arabidopsis* genome, At5g67080 and At3g50310, although tentatively assigned as MAPKKK 19 and 20 respectively (see http://plantsp.sdsc.edu/), are also clearly different from the MAPKKK subfamily, based on our phylogenetic analysis.

Overexpression of the *ScFRK2* kinase lead to developmental defects in ovules, and altered seed set as well as fruit development. Although gene overexpression can have pleiotropic effects, the fact that phenotypic abnormalities were only observed in the organ where *ScFRK2* was most strongly expressed suggests that the phenotype observed is specific and quite relevant to the normal biological activity of the endogenous ScFRK2 kinase. The predominant *ScFRK2* expression in pistils prior to fertilization,

taken together with a strong increase in expression observed in ovaries immediately after fertilization, suggest that this protein kinase has both pre- and post-fertilization roles. A post-fertilization role could not be thoroughly assessed in this study since overexpression lead to homeotic conversion of ovules into carpelloid structures that did not give rise to seeds. Antisense or cosuppressed *ScFRK2* lines might have shed some light on this post-fertilization role, but no obvious phenotypes were observed (data not shown). This might result from *ScFRK2* gene redundancy as suggested by the DNA gel blot analyses (Fig. 2A).

Several genes coding for transcription factors have been identified as regulators of ovule development (Schneitz *et al.*, 1997; Gasser *et al.*, 1998), and misexpression of some of these genes leads to either reiteration of carpel development instead of ovules, formation of carpelloid structures, or the production of ectopic ovules (Kunst *et al.*, 1989; Mandel *et al.*, 1992; Modrusan *et al.*, 1994; Ray *et al.*, 1994; Angenent *et al.*, 1995; Colombo *et al.*, 1995; Keck *et al.*, 2003; Pinyopich *et al.*, 2003). The class C gene *AGAMOUS* (*AG*) is necessary for proper stamen and carpel development in whorls 3 and 4 respectively (Bowman *et al.*, 1989). In the *ag* mutant, there is an absence of carpel production, and the third and fourth whorls are homeotically transformed to petals and sepals respectively, due to the unrestricted expression of the class A gene *APETALA2* (*AP2*) in these two inner whorls (Bowman *et al.*, 1989). When overexpressed in the four whorls under the control of the constitutive CaMV 35S promoter, *AG* leads to the formation of CS in whorl 1 (Mandel *et al.*, 1992). Conversely, a mutation in *AP2*, a negative regulator of *AG*, leads to C gene expression in whorls 1 and 2 (Drews *et al.*, 1991), as well as to the formation of CS in whorl 1 (Kunst *et al.*, 1989). In *Antirrhinum*

majus, two class A genes, LIP1 and LIP2, have been identified (Keck *et al.*, 2003). Although the LIP genes are not required for class C repression in the flower's outer whorls, the *lip1/lip2* double mutant causes the homeotic transformation of ovules into style-like outgrowth tipped with cells resembling stigmatic cells. Furthermore, as for *ScFRK2* overexpression, not all ovules are transformed into these carpelloid structures. In the *lip1/lip2* double mutant, it has not been yet confirmed if the effect is class C dependent, although the *LIP* genes could repress C function only in ovules, as suggested by the authors. Transformation of ovules into carpelloid structures is also observed in the *bel1* mutant (Modrusan *et al.*, 1994; Ray *et al.*, 1994; Reiser *et al.*, 1995). Although it is still unclear how BEL1 regulates AG activity (Skinner *et al.*, 2004), in the *bel1* mutant the integument continues to grow and differentiate into structures with carpel-like morphology. Interestingly, the frequency of transformation is decreased with lower temperatures, as well as with a reduced daylength (Modrusan *et al.*, 1994). Furthermore the CS observed eventually degenerate. These two phenotypes were also observed in our *ScFRK2* overexpressing lines.

Ectopic CS have also been observed in different mutant backgrounds without the involvement of AG, indicating that an AG-independent pathway also exists to define the carpel structures. The MADS-box genes *SHATTERPROOF1* (*SHP1*) and 2 (*SHP2*), as well as *SEEDSTICK* (*STK*), are all part of the *AG* clade and have also been shown to participate in carpel development (Pinyopich *et al.*, 2003). In the *ap2 ag* double mutant, CS are formed in whorl 1, including stigmatic papillae, style and ovules. This indicates that other class C genes are involved in the formation of these structures. This function would be filled by the *SHP1* and *SHP*2 genes, which when overexpressed, produce

partial conversion of petals toward carpels. Furthermore, in an *ap2 ag shp1 shp2* quadruple mutant, no CS where produced in whorl 1. Thus, *SHP1* and *SHP2* act redundantly with *AG*. Similarly, overexpression of the *STK* gene alone is sufficient to induce the formation of ectopic ovules (Pinyopich *et al.*, 2003). In the triple mutant *ap2 ag stk*, the ectopic ovules produced by the *ap2 ag* background are redirected toward a carpelloid fate. In the *shp1 shp2 stk* triple, a transformation of ovules into carpel-like or leaf-like structures is observed. Furthermore, the cells on these converted ovules show style-like characteristics, and occasionally, stigmatic tissue is also observed.

In solanaceous plants, CS have also been observed in a tobacco mutant, which produced elongated green outgrowth from placenta tissue (Evans and Malmberg, 1989). These were identified as abnormal stigmas and styles. In *Petunia*, down-regulation of the MADS-box *FBP7* and *FBP11* genes in the carpel changes the fate of the ovule primordia to a carpel primordia. Hence, carpelloid structures develop on the placenta (Angenent *et al.*, 1995). Overexpression of the *FBP11* gene causes the development of ectopic ovules in the first and second whorls (Colombo *et al.*, 1995). This phenotype is highly similar to the one obtained with the *STK* gene (formerly known as *AGL11*), which is the putative orthologue of the *FBP7* and *FBP11* genes.

We have clearly shown that *ScFRK2* overexpressing lines have altered ovule development (Fig. 5 and 6). In the ovary, ovules were transformed into filiform carpelloid structures, with the uppermost ovules being more frequently transformed. An identical situation is also found in the *Petunia* cosuppressed *FBP7* and *11* lines (Angenent *et al.*, 1995). Examination of the CS showed that cells on these newly

produced organs had a similar appearance to WT stylar epidermal cells, being elongated (Fig. 5L and M), as well as having small papillae-like protrusions along their length (Fig. 5N and O), as found on WT stylar cells (O'Brien *et al.*, 2002a). Furthermore, cuticular ornamentations were also similar on these papillae (Fig. 5P and Q). The CS produced in *ScFRK2* overexpressing lines were also terminated with stigma-like cells (Fig. 5I), similar to immature stigma cells found in pistils three days before anthesis (Fig. 5H). Sections through these CS, revealed that they also had long compressed rows of cells (Fig. 6D and F, arrows), similar to WT transmitting tissue cells (Fig. 6E, arrow), although, as for the small papillae discussed earlier, these were most probably quite immature, since molecular markers for mature transmitting tract, like the self-incompatibility RNases (Matton *et al.*, 1999) or the *HT* modifier gene (O'Brien *et al.*, 2002b) were not detected in these CS (data not shown). All of the above-mentioned cell types, were never observed in WT ovule.

We have shown that *ScFRK2* expression level is higher in reproductive organs. Prior to fertilization, *ScFRK2* transcripts are more expressed in stamens and in pistils (Fig. 2B). Following fertilization, a strong increase in expression in the ovaries is detected. In *P. hybrida*, *in situ* hybridization experiments revealed that *FBP11* is expressed in the center of the developing gynoecium, before ovule primordia are visible. At later developmental stages, *FBP11* expression is restricted to the ovules (Angenent *et al.*, 1995). As with *ScFRK2*, the *Petunia FBP11* mRNA level in the ovary is increased 2 DAP (Colombo *et al.*, 1997). These results strongly suggest pre- and post-fertilization roles for both genes. In both species, 2 DAP corresponds to the time when all of the

ovules have been fertilized. In *P. hybrida*, *FBP11* expression in the developing seeds diminishes between 7 and 21 days post-pollination (Colombo *et al.*, 1997). In *S. chacoense*, *ScFRK2* mRNA levels drop to unpollinated ovary levels four DAP (Fig. 2B), which correspond to the pre-globular stage of embryo development (our unpublished data). *FBP11* accumulation following fertilization has been associated with a role in seed development. In cosuppressed *FBP11* transgenic lines, the development of the endosperm is affected (Colombo *et al.*, 1997). Between the time of pollination, and up to 9 DAP, seed development is unaffected. However, later on, the endothelium of the ovule starts to degenerate. By 18 DAP, the endothelium completely degenerates, which leads to disturbance of endosperm development, and delayed embryo development (Colombo *et al.*, 1997). We did not observe macroscopic alteration in endosperm development in overexpressing lines of *ScFRK2*, but embryo development was impaired compared to control lines. Wild type fruits 21 DAP contained a large proportion of mature embryos, the remaining embryos being at the walking-stick stage. *ScFRK2* overexpressing lines, embryo development was slowed down, and at 21 DAP, most embryos are still at the late torpedo stage (data not shown). Although only a few ovules develop to mature seeds (around six per fruit compared to more than 100 seeds in WT plants), this delay has been consistently and repeatedly observed. These embryos would normally correspond to the ones observed 16 to 17 DAP in a WT plant. We also observed a small fruit phenotype (Fig. 4B and C). We believe that low seed sets and hence small fruit size is due to steric encumbrance produce by intricate filiform ovule development in the ovary, resulting in low frequency of pollen tubes reaching the untransformed ovules. Interestingly, siliques also grew to only 60% of the WT length in the *A. thaliana* seedstick (*stk*) mutant

(Pinyopich *et al.*, 2003). As mentioned earlier, *STK* is the *FBP11* homologue, and is also involved in ovule development.

Overexpression of MADS-box genes *FBP11* or *SHP1/2* and *STK*, causes the ectopic development of ovules in outer flower whorls (Colombo *et al.*, 1995; Pinyopich *et al.*, 2003), but we did not observe this phenotype in either sense or antisense *ScFRK2* transgenic constructs. This result suggests that the ScFRK2 substrate(s) producing the homeotic change from ovules to carpel-like structures are only expressed in the fourth whorl, like the WT *FBP11* expression domain. Genes affecting ovule identity have been proposed to be part of a fourth class of genes that complement the initial ABC model. These D class genes are involved in ovule development in the carpel and act directly on ovule primordium fate (Colombo *et al.*, 1995). Our results suggests that the *ScFRK2* kinase could act upstream of these class D genes in ovules only, either directly or through a phosphorylation cascade.

Beside SERK1, a receptor kinase involved in somatic embryogenesis in *Daucus carota* (Schmidt *et al.*, 1997); the *Petunia* Pollen Receptor-kinase 1, involved in pollen and embyo sac development (Lee *et al.*, 1996; Lee *et al.*, 1997); the YODA MAPKKK involved in early embryo elongation and stomata development behavior (Bergmann *et al.*, 2004; Lukowitz *et al.*, 2004); and the SUB receptor-like kinase involved in the formation of the outer integument (Chevalier *et al.*, 2005), no signal transduction modulator has been directly associated with ovule development. Considering the involvement of several transcription factors in this biological process, post-translational modifications are bound to modulate their activity, specificity and stability.

Farnesylation of *APETALA1* has been shown to alter its function (Yalovsky *et al.*, 2000), and phosphorylation of the MADS-box AGL24 by the Meristematic Receptor-Like Kinase (Fujita *et al.*, 2003) are two examples of such post-translational modifications affecting plant transcription factors. Based on the phenotypes observed in transgenic *ScFRK2* overexpressing lines, we suggest that this protein kinase might act in the same pathway as genes previously shown to control ovule identity, like the Petunia FBP11 transcription factor. The overall phenotypic similarities observed between down-regulated *FBP11* lines and overexpressing *ScFRK2* lines suggest that the ScFRK2 kinase might negatively modulatew the activity or stability of a *S. chacoense* transcription factor involved in ovule fate, either directly or through the involvement of a MAPK cascade module.

IV.11 Acknowledgement

We thank Dr. Malcolm Whiteway (Biotechnology Research Institute, NRC, Montréal, Canada) for providing the *ste*11 mutant yeast strain and Gabriel Téodorescu for plant care and maintenance. This work was supported by the Natural Sciences and Engineering Research Council of Canada (NSERC, Canada) and by le Fonds Québécois de la Recherche sur la Nature et les Technologies (FQRNT, Québec). M. O'Brien is the recipient of Ph. D. fellowships from NSERC and from FQRNT. D. P. Matton holds a Canada Research Chair in Functional Genomics and Plant Signal Transduction.

IV.12 References

Angenent GC, Franken J, Busscher M, van Dijken A, van Went JL, Dons HJ, van Tunen AJ (1995) A novel class of MADS box genes is involved in ovule development in petunia. Plant Cell **7:** 1569-1582

Asai T, Tena G, Plotnikova J, Willmann MR, Chiu WL, Gomez-Gomez L, Boller T, Ausubel FM, Sheen J (2002) MAP kinase signalling cascade in *Arabidopsis* innate immunity. Nature **415:** 977-983

Bardwell L, Thorner J (1996) A conserved motif at the amino termini of MEKs might mediate high-affinity interaction with the cognate MAPKs. Trends Biochem Sci **21:** 373-374

Becraft PW (2002) Receptor kinase signaling in plant development. Annu Rev Cell Dev Biol

Becraft PW, Asuncion-Crabb Y (2000) Positional cues specify and maintain aleurone cell fate in maize endosperm development. Development **127:** 4039-4048

Bergmann DC, Lukowitz W, Somerville CR (2004) Stomatal development and pattern controlled by a MAPKK kinase. Science **304:** 1494-1497

Bevan M (1984) Binary *Agrobacterium* vectors for plant transformation. Nucl. Acids Res. **12:** 8711-8721

Bowman JL, Smyth DR, Meyerowitz EM (1989) Genes directing flower development in *Arabidopsis*. Plant Cell **1:** 37-52

Bussière F, Ledû S, Girard M, Héroux M, Perreault J-P, Matton DP (2003) Development of an efficient *cis-trans-cis* ribozyme cassette to inactivate plant genes. Plant Biotechnology Journal **1:** 423-435

Canales C, Bhatt AM, Scott R, Dickinson H (2002) EXS, a putative LRR receptor kinase, regulates male germline cell number and tapetal identity and promotes seed development in *Arabidopsis*. Curr Biol **12:** 1718-1727

Chevalier D, Batoux M, Fulton L, Pfister K, Yadav RK, Schellenberg M, Schneitz K (2005) STRUBBELIG defines a receptor kinase-mediated signaling pathway regulating organ development in *Arabidopsis*. Proc Natl Acad Sci U S A **102:** 9074-9079

Clark SE, Running MP, Meyerowitz EM (1993) CLAVATA1, a regulator of meristem and flower development in *Arabidopsis*. Development **119:** 397-418

Colombo L, Franken J, Koetje E, van Went J, Dons HJ, Angenent GC, van Tunen AJ (1995) The petunia MADS box gene *FBP11* determines ovule identity. Plant Cell **7:** 1859-1868

Colombo L, Franken J, Van der Krol AR, Wittich PE, Dons HJ, Angenent GC (1997) Downregulation of ovule-specific MADS box genes from petunia results in maternally controlled defects in seed development. Plant Cell **9:** 703-715

Drews GN, Bowman JL, Meyerowitz EM (1991) Negative regulation of the *Arabidopsis* homeotic gene *AGAMOUS* by the APETALA2 product. Cell **65:** 991-1002

Elion EA (2000) Pheromone response, mating and cell biology. Curr Opin Microbiol **3:** 573-581

Evans PT, Malmberg RL (1989) Alternative pathways of tobacco placental development: time of commitment and analysis of a mutant. Dev Biol **136:** 273-283

Fanger GR, Gerwins P, Widmann C, Jarpe MB, Johnson GL (1997) MEKKs, GCKs, MLKs, PAKs, TAKs, and tpls: upstream regulators of the c-Jun amino-terminal kinases? Curr Opin Genet Dev **7:** 67-74

Fujita H, Takemura M, Tani E, Nemoto K, Yokota A, Kohchi T (2003) An *Arabidopsis* MADS-box protein, AGL24, is specifically bound to and phosphorylated by meristematic receptor-like kinase (MRLK). Plant Cell Physiol **44:** 735-742

Gasser CS, Broadhvest J, Hauser BA (1998) Genetic analysis of ovule development. Annu. Rev. Plant Physiol. Plant Mol. Biol. **49:** 1–24

Germain H, Rudd S, Zotti C, Caron S, O'Brien M, Chantha S-C, Lagacé M, Major F, Matton DP (2005) A 6374 unigene set corresponding to low abundance transcripts expressed following fertilization in *Solanum chacoense* Bitt., and characterization of 30 receptor-like kinases. Plant Mol Biol **59**: 513-529

Gifford ML, Dean S, Ingram GC (2003) The *Arabidopsis ACR4* gene plays a role in cell layer organisation during ovule integument and sepal margin development. Development **130:** 4249-4258

Hamal A, Jouannic S, Leprince AS, Kreis M, Henry Y (1999) Molecular characterisation and expression of an *Arabidopsis thaliana* L. MAP kinase kinase cDNA, AtMAP2Kα. Plant Science **140:** 49-64

Hanks SK, Hunter T (1995) Protein kinases 6. The eukaryotic protein kinase superfamily: kinase (catalytic) domain structure and classification. Faseb J **9:** 576-596

Hanks SK, Quinn AM (1991) Protein kinase catalytic domain sequence database: identification of conserved features of primary structure and classification of family members. Methods Enzymol **200:** 38-62

Hecht V, Vielle-Calzada JP, Hartog MV, Schmidt ED, Boutilier K, Grossniklaus U, de Vries SC (2001) The *Arabidopsis SOMATIC EMBRYOGENESIS RECEPTOR KINASE 1* gene is expressed in developing ovules and embryos and enhances embryogenic competence in culture. Plant Physiol **127:** 803-816

Hirt H (2000) MAP kinases in plant signal transduction. Results Probl Cell Differ **27:** 1-9

Hu W, Wang Y, Bowers C, Ma H (2003) Isolation, sequence analysis, and expression studies of florally expressed cDNAs in *Arabidopsis*. Plant Mol Biol **53:** 545-563

Jack T (2001) Plant development going MADS. Plant Mol Biol **46:** 515-520

Jones JDG, Dunsmuir P, Bedbrook J (1985) High level expression of introduced chimeric genes in regenerated transformed plants. EMBO J. **4:** 2411-2418

Jouannic S, Hamal A, Leprince AS, Tregear JW, Kreis M, Henry Y (1999) Plant MAP kinase kinase kinases structure, classification and evolution. Gene **233:** 1-11

Keck E, McSteen P, Carpenter R, Coen E (2003) Separation of genetic functions controlling organ identity in flowers. Embo J **22:** 1058-1066

Kieber JJ, Rothenberg M, Roman G, Feldmann KA, Ecker JR (1993) CTR1, a negative regulator of the ethylene response pathway in *Arabidopsis*, encodes a member of the raf family of protein kinases. Cell **72:** 427-441

Kunst L, Klenz JE, Martinez-Zapater J, Haughn GW (1989) *AP2* Gene determines the identity of perianth organs in flowers of *Arabidopsis thaliana*. Plant Cell **1:** 1195-1208

Lee H-S, Chung Y-Y, Das C, Karunanandaa B, van Went JL, Mariani C, Kao T-H (1997) Embryo sac development is affected in *Petunia inflata* plants transformed with an antisense gene encoding the extracellular domain of receptor kinase PRK1. Sex Plant Reprod **10:** 341–350

Lee H-S, Karunanandaa B, McCubbin A, Gilroy S, Kao T-h (1996) PRK1, a receptor-like kinase of *Petunia inflata*, is essential for postmeiotic development of pollen. Plant J **9:** 613-624

Li J, Chory J (1997) A putative leucine-rich repeat receptor kinase involved in brassinosteroid signal transduction. Cell **90:** 929-938

Lukowitz W, Roeder A, Parmenter D, Somerville C (2004) A MAPKK kinase gene regulates extra-embryonic cell fate in *Arabidopsis*. Cell **116:** 109-119

Madhani HD, Fink GR (1998) The riddle of MAP kinase signaling specificity. Trends Genet **14:** 151-155

Mandel MA, Bowman JL, Kempin SA, Ma H, Meyerowitz EM, Yanofsky MF (1992) Manipulation of flower structure in transgenic tobacco. Cell **71:** 133-143

Matton DP, Luu DT, Xike Q, Laublin G, O'Brien M, Maes O, Morse D, Cappadocia M (1999) Production of an S RNase with dual specificity suggests a novel hypothesis for the generation of new S alleles. Plant Cell **11:** 2087-2097

Matton DP, Maes O, Laublin G, Xike Q, Bertrand C, Morse D, Cappadocia M (1997) Hypervariable domains of self-incompatibility RNases mediate allele-specific pollen recognition. Plant Cell **9:** 1757-1766

Modrusan Z, Reiser L, Feldmann KA, Fischer RL, Haughn GW (1994) Homeotic transformation of ovules into carpel-like structures in *Arabidopsis*. Plant Cell **6:** 333-349

Morris PC, Guerrier D, Leung J, Giraudat J (1997) Cloning and characterisation of MEK1, an *Arabidopsis* gene encoding a homologue of MAP kinase kinase. Plant Mol Biol **35:** 1057-1064

Nadeau JA, Sack FD (2002) Control of stomatal distribution on the *Arabidopsis* leaf surface. Science **296:** 1697-1700

Nishihama R, Banno H, Shibata W, Hirano K, Nakashima M, Usami S, Machida Y (1995) Plant homologues of components of MAPK (mitogen-activated protein kinase) signal pathways in yeast and animal cells. Plant Cell Physiol **36:** 749-757

O'Brien M, Bertrand C, Matton DP (2002a) Characterization of a fertilization-induced and developmentally regulated plasma-membrane aquaporin expressed in reproductive tissues, in the wild potato *Solanum chacoense* Bitt. Planta **215:** 485-493

O'Brien M, Kapfer C, Major G, Laurin M, Bertrand C, Kondo K, Kowyama Y, Matton DP (2002b) Molecular analysis of the stylar-expressed *Solanum chacoense* small asparagine-rich protein family related to the HT modifier of gametophytic self-incompatibility in *Nicotiana*. Plant J **32:** 985-996

O'Brien M, Chantha SC, Rahier A, Matton DP (2005) Lipid signaling in plants. Cloning and expression analysis of the obtusifoliol 14α-demethylase from *Solanum chacoense* Bitt., a pollination- and fertilization-induced gene with both obtusifoliol and lanosterol demethylase activity. Plant Physiol **139:** 734-749

Pinyopich A, Ditta GS, Savidge B, Liljegren SJ, Baumann E, Wisman E, Yanofsky MF (2003) Assessing the redundancy of MADS-box genes during carpel and ovule development. Nature **424:** 85-88

Piwien-Pilipuk G, Huo JS, Schwartz J (2002) Growth hormone signal transduction. J Pediatr Endocrinol Metab **15:** 771-786

Posas F, Saito H (1997) Osmotic activation of the HOG MAPK pathway via Ste11p MAPKKK: scaffold role of Pbs2p MAPKK. Science **276:** 1702-1705

Ray A, Robinson-Beers K, Ray S, Baker SC, Lang JD, Preuss D, Milligan SB, Gasser CS (1994) *Arabidopsis* floral homeotic gene *BELL* (*BEL1*) controls ovule development through negative regulation of *AGAMOUS* gene (*AG*). Proc Natl Acad Sci U S A **91:** 5761-5765

Reiser L, Modrusan Z, Margossian L, Samach A, Ohad N, Haughn GW, Fischer RL (1995) The *BELL1* gene encodes a homeodomain protein involved in pattern formation in the *Arabidopsis* ovule primordium. Cell **83:** 735-742

Robinson MJ, Cobb MH (1997) Mitogen-activated protein kinase pathways. Curr Opin Cell Biol **9:** 180-186

Romeis T (2001) Protein kinases in the plant defence response. Curr Opin Plant Biol **4:** 407-414

Sambrook J, Fritsch EF, Maniatis T (1989) Molecular cloning: a laboratory manual. Cold Spring Harbor Laboratory Press, Cold Spring Harbor, New York

Schmidt ED, Guzzo F, Toonen MA, de Vries SC (1997) A leucine-rich repeat-containing receptor-like kinase marks somatic plant cells competent to form embryos. Development **124:** 2049-2062

Schneitz K, Hulskamp M, Kopczak SD, Pruitt RE (1997) Dissection of sexual organ ontogenesis: a genetic analysis of ovule development in *Arabidopsis thaliana*. Development **124:** 1367-1376

Sells MA, Knaus UG, Bagrodia S, Ambrose DM, Bokoch GM, Chernoff J (1997) Human p21-activated kinase (Pak1) regulates actin organization in mammalian cells. Curr Biol **7:** 202-210

Shibata W, Banno H, Ito Y, Hirano K, Irie K, Usami S, Machida C, Machida Y (1995) A tobacco protein kinase, NPK2, has a domain homologous to a domain found in activators of mitogen-activated protein kinases (MAPKKs). Mol Gen Genet **246:** 401-410

Skinner DJ, Hill TA, Gasser CS (2004) Regulation of ovule development. Plant Cell **16 Suppl:** S32-45

Sugden PH, Clerk A (1997) Regulation of the ERK subgroup of MAP kinase cascades through G protein-coupled receptors. Cell Signal **9:** 337-351

Swofford DL (1998) PAUP*: Phylogenetic Analysis Using Parsimony (* and Other Methods). Sinauer, Sunderland, MA

Tanaka H, Watanabe M, Watanabe D, Tanaka T, Machida C, Machida Y (2002) *ACR4*, a putative receptor kinase gene of *Arabidopsis thaliana*, that is expressed in the outer cell layers of embryos and plants, is involved in proper embryogenesis. Plant Cell Physiol **43:** 419-428

Tena G, Asai T, Chiu WL, Sheen J (2001) Plant mitogen-activated protein kinase signaling cascades. Curr Opin Plant Biol **4:** 392-400

The MAPK Group (2002) Mitogen-activated protein kinase cascades in plants: a new nomenclature. Trends Plant Sci **7:** 301-308

Treisman R (1996) Regulation of transcription by MAP kinase cascades. Curr Opin Cell Biol **8:** 205-215

Tu H, Barr M, Dong DL, Wigler M (1997) Multiple regulatory domains on the Byr2 protein kinase. Mol Cell Biol **17:** 5876-5887

Wu C, Leberer E, Thomas DY, Whiteway M (1999) Functional characterization of the interaction of Ste50p with Ste11p MAPKKK in *Saccharomyces cerevisiae*. Mol Biol Cell **10:** 2425-2440

Yalovsky S, Rodriguez-Concepcion M, Bracha K, Toledo-Ortiz G, Gruissem W (2000) Prenylation of the floral transcription factor APETALA1 modulates its function. Plant Cell **12:** 1257-1266

Zhang S, Klessig DF (2001) MAPK cascades in plant defense signaling. Trends Plant Sci **6:** 520-527

Zheng CF, Guan KL (1994) Activation of MEK family kinases requires phosphorylation of two conserved Ser/Thr residues. EMBO J **13:** 1123-1131

Chapitre V.

The ScJRK2 MAP kinase kinase from Solanum chacoense affects pollen development and viability

Martin O'Brien, Christelle Kapfer et Daniel P. Matton

Soumis dans Planta le 15 décembre 2005

V.1 Contribution des coauteurs

L'expérience nécessaire à une des figures a été effectuée par C. Kapfer (hybridation *in situ*). Les trois autres figures ainsi que le tableau sont des expériences effectuées par moi. D. P. Matton a contribué a une des autres figures. Son travail a été choisi plutôt que le mien pour cette figure. La totalité des données non montrées de l'article (« data not shown »), sont des expériences que j'ai faites.

V.2 Page titre

The ScFRK2 MAP kinase kinase from *Solanum chacoense* affects pollen development and viability

Short running title: ScFRK2 MAP2K affects pollen development

Martin O'Brien, Christelle Kapfer and Daniel P. Matton*

Institut de Recherche en Biologie Végétale (IRBV), Département de sciences biologiques, Université de Montréal, 4101 rue Sherbrooke est, Montréal, QC, Canada, H1X 2B2.

*Author for correspondance:

Tel: 1-514-872-3967

Fax: 1-514-872-9406

[redacted]

V.3 Keywords

MAP kinase kinase, Anther, Pollen, *Solanum chacoense*

V.4 Genbank accession number

ScFRK2, AY427829.

V.5 Abstract

We have previously described an atypical MAP kinase kinase family in *Solonanum chacoense* Bitt. that is predominantly expressed in reproductive tissues. Overexpression of the *ScFRK2* gene modifies the cell fate of several ovule initials and induces a homeotic transformation into carpeloid structures. Since the *ScFRK2* gene is also normally expressed in anthers, we extend here our observations to the male reproductive structure in these mutant lines. In wild type plants, *ScFRK2* mRNAs accumulate at a relatively constant level throughout anther development and are detected in epidermal, endothecium, and middle layer cells, while no signal can be observed in the stomium, the connective, and the vasculature tissues. Overexpression of *ScFRK2* transcripts strongly disturbed pollen development. At maturity, almost two-thirds of the pollen produced are severely affected and inviable, while the remaining pollen grains are significantly smaller that WT pollen but are otherwise normal. Crosses with pollen from a *ScFRK2* overexpressing line into a wild type background produced a F1 population with roughly 44% of the progeny having the transgene, suggesting that the observed pollen defect is caused by a sporophytic dysfunction, leading to major structural defects and incomplete pollen development.

V.6 Introduction

Anthers produce the male gametes, the pollen grains, which are a three-celled structures used for long distance fertilization. Pollen grains are generated through spore tetrads enclosed in a thick callose wall, themselves originating from another precursor: the sporogenous cell. The cell lineage that gives rise to the gametes and anther inner cell layers is more complex. At mid-anther development, archesporial initials arise from the L2 layer and divide periclinally to form a primary sporogenous cell facing inward and a pariental cell facing outside the yet unformed locule. The primary sporogenous cell is the precursor of the tetrad, while primary parietal makes another periclinal division to yield an inner and an outer secondary parietal cell. The outer cells develop further to form the endothecium cell layer that will later play a role in pollen dehydration. The inner parietal cells, they divide once more periclinally and form a layer of tapetum cells and a middle cell layer that borders the endothecium and the tapetum (Bowman 1994;Scott *et al.* 2004). The tapetum is the nutritive layer of cells that lines the locule containing the developing microsporocytes. The microspores embedded in each tetrad are freed from one another by the action of callase, an enzyme produced by the tapetum. In later development stages, the tapetum cell layer degenerates, leaving an empty space filled with the enlarging microspores that will in time each divide asymmetrically to give rise to a bicellular pollen grain where each of the two cells has its own developmental fate (Scott *et al.* 2004). Upon shedding, pollen grains are freed from the anther in a dehydrated form. The larger cell of the pollen grain, the vegetative cell, will form the pollen tube when pollen grain hydration occurs on the style's stigma. The smaller cell is

found within the vegetative cell cytoplasm and is called the generative cell. The generative cell will undergo mitosis once more to produce two identical sperm cells (Boavida *et al.* 2005). In most species, including solanaceous plants, this second mitosis occurs during pollen tube growth in the gynoecium. Both sperm cells will be released from the pollen tube upon ovule fertilization. One will fuse with the egg cell to produce the zygote and the other one will fuse with the diploid central cell to generate the triploid endosperm, a process called double fertilization (Esau 1977). Stamen and pollen development has been recently reviewed in Scott *et al.* (2004).

Most of the mutations described that affect anthers or pollen have been shown to disturbs either gamete meiosis, mitosis or chromosome partitioning (recently reviewed in Wilson and Yang 2004). Fewer male defects are known to affect other processes such as anther development or pollen tube germination and growth. Multiple reports link protein kinases to different processes in anther and pollen biology. The EXCESS MICROSPOROCYTES1/ EXTRA SPOROGENOUS CELLS (*EMS1/EXS)* gene codes for a LRR receptor kinase in *Arabidopsis thaliana*, and affects cell lineage fate (Canales *et al.* 2002;Zhao *et al.* 2002). In the *ems1/exs* mutant, more sporogenous cells are produced, which derive from the incorrect cell fate acquisition of the middle cell and tapetum cell layers. The numerous microsporocytes formed do not undergo cytokinesis, which results in complete pollen sterility. This pollen defect could be linked to the absence of the nutritive tapetum cell layer. An orthologous LRR receptor kinase, MULTIPLE SPOROCYTE1 (MSP1) from *Oryza sativa*, also shows the same defect when mutated (Nonomura *et al.* 2003). The *Zea mays multiple archesporial cells1* (*mac1*) mutant also shares some phenotypic features with the above-mentioned kinases,

but the identity of the gene is not yet known (Sheridan *et al.* 1999). The *exs/ems1* and *msp1* mutants also show female gametophyte defects, with altered embryo development (Canales *et al.* 2002;Nonomura *et al.* 2003). Similarly, in the *tapetum determinant 1* (*tpd1*) mutant, the male phenotype appears identical to the phenotype observed in the *exs/ems1/msp1* mutants (Yang *et al.* 2003). The protein encoded by the *TPD1* gene has no known function but it is secreted and has been hypothesized to act as a protein ligand for these receptors (Scott *et al.* 2004). Recently, the double knockout of *serk1/serk2* was shown to affect the cell determinancy of tapetum cells by conversion to sporocyte cells, which will in time lead to pollen abortion and male sterility (Albrecht *et al.* 2005;Colcombet *et al.* 2005). The SERK1/2 LRR receptor kinase affects anther development in a similar way to EMS1/EXS. Furthemore, SERK1 overexpression was earlier shown to enhance the potential of suspension cultured cells to undergo somatic embryogenesis (Hecht *et al.* 2001;Schmidt *et al.* 1997), which marked these receptors as having multiple roles depending on the tissue.

Other receptor kinases such as the *Lycopersicum esculentum* LePRK2 and the *Petunia inflata* PRK1 kinases have been shown to be involved in pollen tube growth and microspore formation respectively. The extracellular domain of LePRK2 interacts with a pollen cysteine-rich secreted protein named LAT52 (Tang *et al.* 2002). LAT52 is known to be expressed in pollen and antisense LAT52 plants show pollen hydration and pollen tube growth defects leading to the inability to effect fertilization (Muschietti *et al.* 1994). LePRK2 and LAT52 binding might play a role in regulating the initiation and maintenance of pollen tube growth in an autocrine-like way (Johnson and Preuss 2003). The *Petunia PRK1* kinase was originally isolated from pollen but was later shown to be

involved both in microspore formation and embryo sac development. Down- regulation of *PRK1* causes microspores to halt their development at the uninucleate stage (Lee *et al.* 1996), while in the embryo sac, the two polar nuclei fail to migrate and fuse to form the central cell (Lee *et al.* 1997). Another anther- and pollen-expressed kinase that causes pollen lethality when down-regulated is the *Hordeum vulgare* SUCROSE NON-FERMENTING-1-RELATED kinase (snRK1) (Zhang *et al.* 2001). In *snRK1* antisense lines, half the pollen grains have their development stopped at the binucleate stage. The *snRK1* transgene is not transmitted through the next generation by the pollen, indicating that the effect is gametophytic (Zhang *et al.* 2001).

We have recently showed that the ScFRK2 MAP kinase kinase is involved in seed and fruit development, and when overexpressed, produces a homeotic conversion of ovules into carpeloid structures. While it is predominantly expressed in ovules, and ts transiently up-reguled following fertilization, the *ScFRK2* kinase is also expressed at low but significant levels in anthers (O'Brien *et al.* 2005). In the present study, we analyze in detail the polen grain and pollen development in transgenic plants overexpressing this protein kinase.

V.7 Materials and methods

Plant material and F1 population generation

The diploid and self-incompatible wild potato *Solanum chacoense* Bitt. (2n=2x=24) was grown in a greenhouse with 14 to 16 hours of light per day. The genotype used for *Agrobacterium tumefaciens* mediated transformation was G4 (self-incompatibility alleles S_{12} and S_{14}). One of the *ScFRK2* overexpressing lines showing a defective pollen phenotype was manually crossed to a fully compatible *S. chacoense* genotype V22 plant (self-incompatibility alleles S_{11} and S_{13}) as female or male progenitor. Twenty days after pollination, fruits were sterilized in a 10% sodium hypochlorite and 0.1% Tween solution for 10 minutes. Fruits were then hand-dissected to isolate fertilized ovules, which were carefully opened under a stereomicroscope in order to obtain undamaged embryos. Nineteen embryos were rescued for both populations. Embryo rescue was performed to accelerate the production of the F1 generations in the reciprocal crosses. Embryos were individually grown in 0.5x MS media until a 10 cm seedling was obtained. Plantlets were then transferred to the greenhouse for further analysis or used as such for DNA extraction.

DNA extraction and PCR analysis

Genomic DNA from leaf tissues of untransformed plants, transgenic plants and from the F1 populations was extracted with the DNeasy Plant Mini Kit (Qiagen, Baie d'Urfé, Québec, Canada). To test the transmittance of the T-DNA, PCR reactions were

conducted on 100 ng genomic DNA with three different primer pairs. Kan-F: 5'-GTCATTTCGAACCCCAGAGTC-3' and Kan-R: 5'-CTGAATGAACTGCAGGACGAG-3'were used to amplify the kanamycin resistance gene; Nos1: 5'-CCCGATCTAGTAACATAGATGACACC-3' and Nos2: 5'-GAGATCTAGATCGTTCAAACATTTGGCAATAAAG-3'were used to amplify the NOS terminator; CaMV35S-Pro: 5'-CTCCACTGACGTAAGGGATG-3' and a ScFRK2 gene specific primer SV2-C7-1: 5'-CTTTCTTCCCAGTAATCATC-3'were used to amplify the exogenous ScFRK2 gene. PCR products were run on a 1% agarose gel and bands were detected with ethidium bromide staining.

RNA isolation and analysis

RNA extraction of anther tissues was conducted as described previously (Jones *et al.* 1985) while ovary RNA from individuals from both population were extracted through columns with RNeasy Plant Mini Kit as described by manufacturer (Qiagen). For each tissue tested, 10 μg RNA was separated in a formaldehyde/MOPS gel, then transferred to Hybond N+ membrane (GE Healthcare), and fixed by UV crosslinking (120mJ/cm^2). To confirm equal loading between RNA samples, a 1 kb fragment of *S. chacoense 18S* RNA was PCR amplified and used as a control probe. Prehybridization was performed at 45°C for 3 h in a when overexpressed 50% formamide solution (50% deionized formamide, 6X SSC, 5X Denhardt's solution, 0.5% SDS and 200 μg/μl denatured salmon DNA). Hybridization of the membrane was performed overnight at 45°C in the same solution. The probe used for the detection of the *ScFRK2* gene

transcripts was synthesized from a full-length cDNA by random labelling using the Strip-EZ DNA labelling kit (Ambion, Austin, Texas) in the presence of α-^{32}P dATP (ICN Biochemical, Irvine, California). Following hybridizations, membranes were washed 30 min at 25°C and 30 min at 35°C in 2X SSC and 0.1% SDS; 30 min at 45°C and 30 min at 55°C in 1X SSC and 0.1% SDS; and finally 10 min at 55°C in 0.1X SSC and 0.1% SDS. Membrane washes for *18S* RNA hybridization were done two times 30 min at 55°C in 0.1X SSC and 0.1% SDS. Prior to the *18S* RNA probe hybridization, blots were stripped following the manufacturer's instructions (Ambion). Signal detection was performed by autoradiography at -86°C on Kodak Biomax MR film (Interscience, Markham, Ontario, Canada) or exposed on a Kodak storage phosphor screen and revealed on a Typhoon 9200 phosphorimager (GE Healthcare).

In situ hybridization

Anther tissues were fixed in FAA (60% ethanol, 5% acetic acid, 5% formalin) at 4°C overnight. After dehydration with *tert*-butanol and embedding in paraffin, samples were cut into 10 µm sections and mounted on slides coated with AES (3-aminopropyltriethoxy-silane, Sigma, Oakville, Canada). Tissue sections were deparaffinized in two sequential xylene baths of 15 min each followed by hydration through decreasing ethanol baths (100%, 95%, 70%, 50%; distilled water twice, 5 min each). Tissue sections were treated and hybridized as described previously (Lantin *et al.*, 1999). Sense and anti-sense labelled riboprobes were synthesized from the *ScFRK2* cDNA clone with digoxigenin-11-UTP (Roche Diagnostics, Laval, Québec, Canada)

using the T7 and T3 RNA polymerases (RNA transcription kit, Stratagene, Palo Alto, CA). Fifty ng of probe was used for each slide's hybridization. Sections were visualized by light microscopy and digitally photographed with a Leica DFC420 Fire Cam.

Pollen viability estimation and callose staining

Fresh pollen grains were powdered on a drop of 1% aceto-carmine and stained for 2 min on a slide. Pollen viability was scored by light microscopy of three to twelve different optical fields and photographed with an Olympus BHT microscope on Kodak Ektachrome 160 T film. Pollen callose deposition was stained for fifteen minutes in 0.1% aniline blue and observed through a Nikon Eclipse TE2000-U inverted microscope with UV light. Images were collected digitally with a CoolSnap fx camera (Photometrics, Tucson, AZ, USA) and visualized in Image-Pro 3DS software (Media Cybernetics, Silver Spring, MD, USA).

Scanning electron microscopy

Pollen grains were harvested manually by shaking and critical-point-dried with CO_2 without prior fixation and dehydration. Pollen grains were coated with gold–palladium, and viewed in a JEOL 840 scanning electron microscope at 10 kV. For pollen viability estimation through outer structure analysis, fresh pollen was observed with a Hitachi S-3000N variable pressure SEM at 30 Pa and 15 kV.

V.7 Results

We have recently described the isolation and functional characterization of a new family of MAP kinases in *Solanum chacoense* that shows an atypical sub-family kinase signature (O'Brien *et al.* 2005). Although phylogenetic analyses could not unambiguously resolve these kinases between the MAPKK and MAPKKK groups, closer examination of the conserved catalytic kinase domains strongly suggested that these kinases are more related to the MAPKK than to the MAPKKK. Most importantly, the typical MAPKK plant phosphorylation motif $[TS]X_5[TS]$ is found in the activation (T-loop) located between subdomain VII and VIII of these two kinases (Morris *et al.* 1997;Shibata *et al.* 1995). Furthermore, although some domains were similar to domains found in MAPKKK, a large regulatory domain typically found in MAPKKK was entirely absent. One of these kinases named *ScFRK2* for *Solanum chacoense* Fertilization-Related Kinase 2, was shown to be involved in seed and fruit development, and when overexpressed, produced a homeotic conversion of ovules into carpeloid structures. Apart from its predominant expression in ovules, and its transient up-regulation following fertilization, *ScFRK2* kinase mRNA is also expressed at low but significant levels in anthers (O'Brien *et al.* 2005). Upon careful phenotypical analyses of the transgenic plants that showed this homeotic transformation, the only other developmental defect that could be found was related to pollen viability, and these results are presented hereafter.

ScFRK2 mRNA expression in anthers

Since *ScFRK2* mRNAs had been previously shown to be expressed in anthers (O'Brien *et al.* 2005), anthers from different developmental stages were collected and RNA levels were determined though RNA gel blot analysis (Fig. 1a). *ScFRK2* mRNA abundance was found to be constant in anthers from widely different developmental stages, from three days prior to anthesis until three days post-anthesis (DPA). However, the *ScFRK2* mRNA levels increased markedly in anthers four and five DPA. Very immature anthers, isolated from 1 mm flower buds, showed the same amount of transcript as that observed in anthers from three days prior to anthesis to three DPA (Fig. 1a, compare lane 1 to lanes 2 through 8). The immature anther at the 1 mm flower bud stage bears spores still enclosed in tetrads (Fig. 2c). Equal RNA loading was verified by reprobing the stripped membrane with an *18S* RNA probe (Fig.1a, lower panel). As observed previously, *ScFRK2* showed two transcripts with near equimolar amounts. The larger transcript might therefore correspond to an unspliced *ScFRK2* pre-mRNA, or to an alternative termination site in the *ScFRK2* gene or to a cross-hybridizing member of the *ScFRK2* family. Attempts to isolate the longer hybridizing fragment were unsuccessful. All cDNAs retrieved from library hybridization corresponded to the 1.1 kb fragment and 5' RACE PCR did not result in the isolation of a longer clone (O'Brien *et al.* 2005).

To better define *ScFRK2* mRNA localization, we conducted *in situ* hybridizations on anthers collected at the time of anthesis (Fig. 1b). Ten μm thick anther sections were hybridized with a digoxigenin-labelled *ScFRK2* anti-sense probe. *ScFRK2*

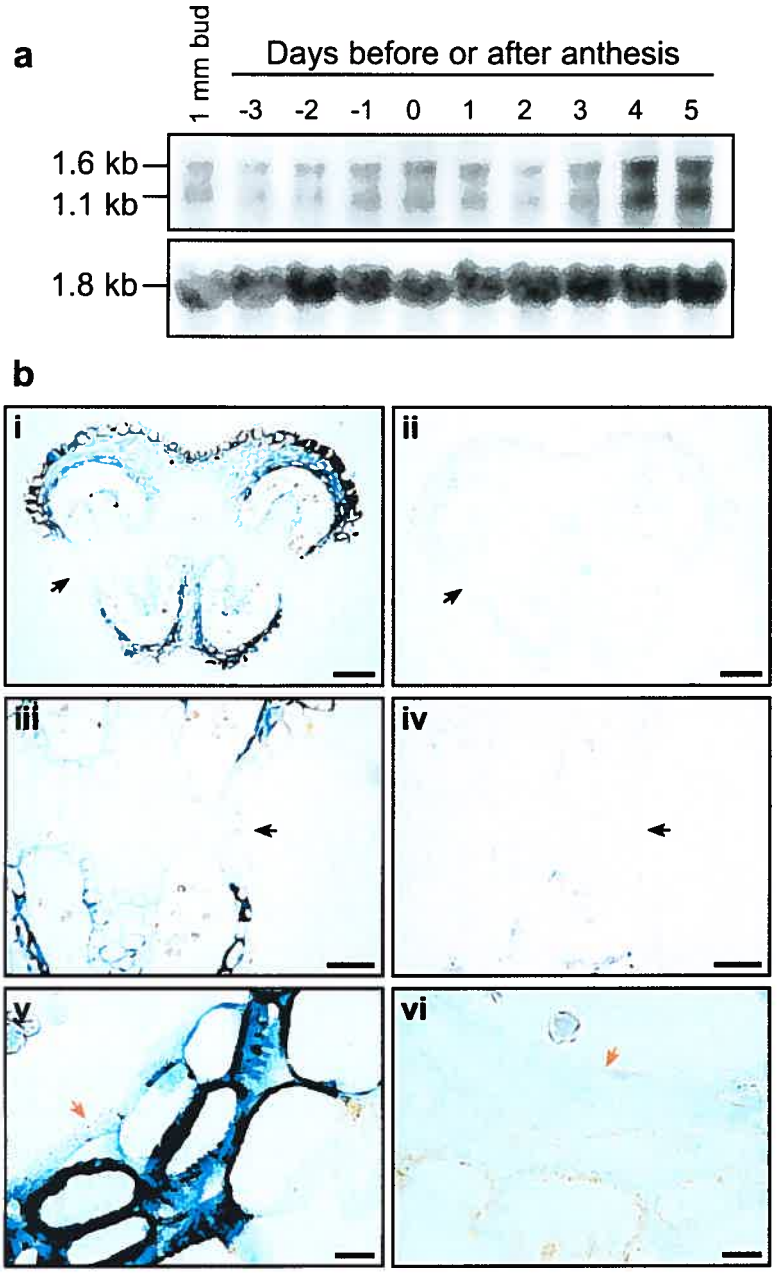
a
1 mm bud
Days before or after anthesis
-3 -2 -1 0 1 2 3 4 5
1.6 kb
1.1 kb
1.8 kb
b
i
ii
iii
iv
v
vi

Figure 1

RNA expression analysis of *ScFRK2* transcript levels in anthers of *S. chacoense*. **a** RNA gel blot analysis of *ScFRK2* mRNA accumulation in anther tissues harvested in 1 mm length flower buds or from three days prior anthesis to five days after anthesis flowers. Ten ug of total RNA from the various tissues was probed with the 1.1 kb complete *ScFRK2* cDNA insert (upper panel). The RNA gel blot was stripped and re-hybridized with a partial *18S* control probe to ensure equal loading of samples (lower panel). **b** *In situ* localization of *ScFRK2* transcripts in WT anthers on anthesis day. **i and ii** Anther cross sections showing the complete anther. Bars = 0.25 mm. **iii and iv** Magnification of the stomium area (black arrow). Bars = 0.1 mm. **v and vi** Magnification of the anther wall cell layers showing the outer tapetum area (red arrow). Bars = 20 μm. Digoxigenin labeling is visible as a blueish staining. All hybridizations used 10 μm-thick sections and equal amounts of either *ScFRK2* antisense (**i**, **iii**, and **v**) or sense probes (**ii**, **iv**, and **vi**).

mRNAs can be observed in epidermal, endothecium, and middle layer cells, while the stomium (black arrows), vasculature, and most of the connective tissue were devoid of transcripts (Fig. 1b, panel i, iii, and vi). No *ScFRK2* transcripts could be observed in the degenerating tapetum layer (Fig. 1b, panel iii and vi, red arrow) or in pollen grains (Fig. 1b, iii), confirming our previous RNA gel blot analysis (O'Brien *et al.* 2005). Sense probe hybridizations (Fig. 1b, panels ii, iv, and vi) confirmed the specificity of the antisense *ScFRK2* probe since no staining could be observed. Light pinkish staining in the pollen and cell wall could be observed in both sense and antisense probe hybridization, and was thus considered as an artifact. Artifactual staining in pollen grains has also been observed with various other types of staining (Mascarenhas and Hamilton 1992).

ScFRK2 transgenic plant analysis

Overexpressing lines of *ScFRK2* show a homeotic conversion of ovules into carpeloid structures while antisense lines showed no obvious phenotypes, possibly because of gene redundancy since the *ScFRK2* gene was estimated to be part of a small gene family with two to three related copies in the *S. chacoense* genome (O'Brien *et al.* 2005). We used these transgenic lines to determine if there were also developmental defects in stamens, since this was the only other organ where significant expression of *ScFRK2* mRNAs could be observed. At the macroscopic level, no phenotype could be observed in either overexpressing or antisense *ScFRK2* lines. Overexpression of *ScFRK2* under the control of the CaMV 35S promoter in regions normally devoided of transcript (Fig. 1b, panel iii) did not cause anther dehiscence defects, as pollen could freely

evacuate the anther through the opened stomium (data not shown). The CaMV 35S promoter had been previously shown to be expressed in all anther cell layers including the stomium (Wilkinson *et al.* 1997), while the GUS staining observed in the pollen of a 35S::GUS transgenic plant was shown to be an artifact due to the diffusion of modified substrate and incorporation by the pollen (Mascarenhas and Hamilton 1992). Since overexpression of *ScFRK2* mRNAs causes structural defects in the ovules, we screened the transgenic lines for more subtle male reproductive defects. At anthesis, pollen from overexpressing lines S1, S2, S8, S16 and S17 showed around 50% pollen viability when stained with 1% aceto-carmine (Table 1 and Fig. 2b) while the WT untransformed host and a *ScFRK2* overexpressing line with no detectable transgene expression showed very low (<0.5%) pollen lethality (Table 1 and Fig. 2a). Viable pollen grains are lightly stained in pink with aceto-carmine, while dead pollen cells are showed as empty and shrivelled shells (Fig. 2a and b). Because the observed mortality ratio was near 50%, this might suggest that *ScFRK2* overexpression in the haploid pollen caused this phenotype, considering that only one transgene insertion was found by DNA gel blot analysis in the genome of each overexpression line tested (data not shown). To test this hypothesis, we stained pollen at the tetrad stage, as well as microspores and pollen grains derived from anthers at different stage of maturity (Fig. 2c to h). *ScFRK2* overexpressing lines showed a steady increase in pollen lethality as the anthers matured (Fig. 2b, f, and h). The first signs of pollen lethality started to be observed around three days prior to anthesis (Fig. 2h; 11.9 ±1.2 and 17.2 ± 1.7% pollen lethality for *ScFRK2* lines S1 and S2, respectively), then increased to 38.8 ± 2.7% and 36.1 ± 3.4 % pollen lethality for *ScFRK2* lines S1 and S2 respectively one day prior to anthesis, and reached nearly 50%

Plant Genotype	Pollen lethality
Wild-type S. chacoense	0.5%
***ScFRK2* overexpression lines**	
ScFRK2-S1 transgenic	55.2%
ScFRK2-S2 transgenic	48.3%
ScFRK2-S8 transgenic	31.5%
ScFRK2-S14 transgenic	42.1%
ScFRK2-S16 transgenic	49.2%
ScFRK2-S17 transgenic	44.6%
***ScFRK2* transgenic non-overexpressing line**	
ScFRK2-S3 transgenic	0.1%

Table 1

Mean lethality percentage of pollen in primary *ScFRK2* overexpression transformants. Pollen lethality was scored in six different optical fields with 1% aceto-carmine.

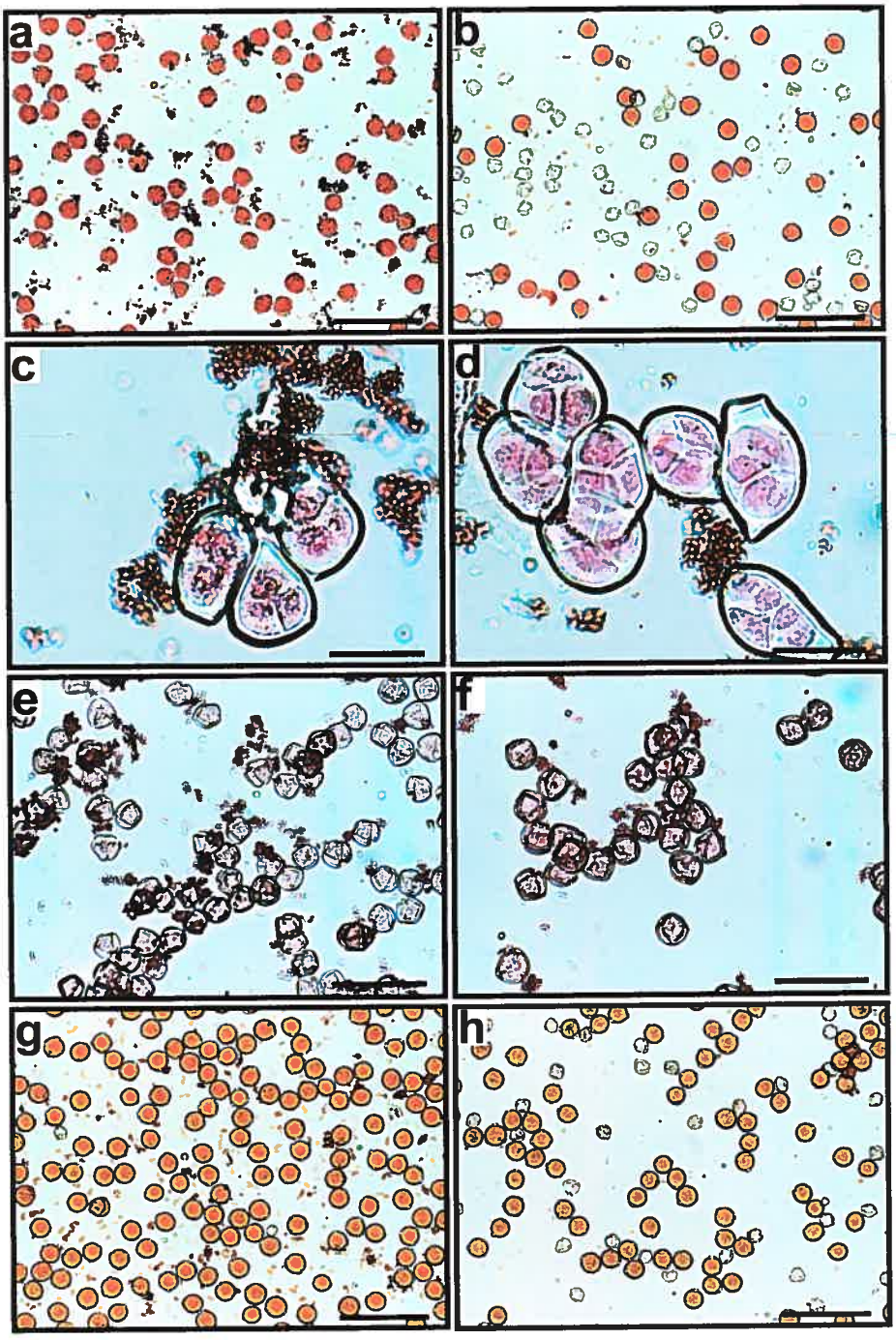
a
b
c
d
e
f
g
h

Figure 2

Pollen viability in WT plants and in *ScFRK2* overexpressing lines. a and b Pollen at anthesis. **c and d** Tedrads of spores from 1 mm long flower buds. **e and f.** Uninucleate microspores from 2 mm long flower buds. **g and h** Pollen three days prior to anthesis. **a**, **c**, **e** and **g** Wild type plant. **b**, **d**, **f** and **h** *ScFRK2* overexpression line S2. **a**, **b**, **g** and **h** Bars = 50 μm ; **c** and **d** Bars = 62.5 μm **; e** and **f** Bars = 25 μm. Pollen was stained with 1% aceto-carmine.

at anthesis (Fig. 2b; 49.3 ± 5.9% and 47.4 ± 0.8 pollen lethality for *ScFRK2* lines S1 and S2 respectively). In both one mm flower buds, with anthers bearing pollen at the tetrad stage (Fig. 2d) and in two to three mm flower buds, with anthers bearing emerging microspores (Fig. 2f), no significant differences could be observed when compared to the untransformed control line (Fig. 2c and e). Wild type pollen presented no significant lethality throughout all the different stages observed (Fig. 2a, c, e and g). These results suggest that either the effect is sporophytic, or that lethality cannot be observed at earlier developmental stages due to a lack of expression of the transgene at these stages. The latter hypothesis seemed unlikely since the 35S promoter does not drive expression of transgene in the pollen (Mascarenhas and Hamilton 1992), and still, pollen lethality increases concomitantly as the pollen matures.

Pollen outer structure analyses

To analyze the pollen defects of the *ScFRK2* overexpressing line in more detail, pollen grains were observed by scanning electron microscopy (SEM). Wild type untransformed plants showed typical tricolpate pollen grains with three equally distributed apertures that run longitudinally to the pollen axis (Fig. 3a). The pollen morphology is different in SEM (Fig. 3a) and in light microscopy (Fig. 2a), as staining with 1% aceto-carmine causes water uptake and hydration of the pollen grain that thus takes on a spherical shape. In the transgenic lines overexpressing the *ScFRK2* gene, more than 50% of the pollen grains appeared shriveled, leaving the impression of an empty collapsed shell (Fig. 3b and data not shown). Close up observations of the pollen wall showed identical sexine patterning (the sculptured outer layer of the exine) for both

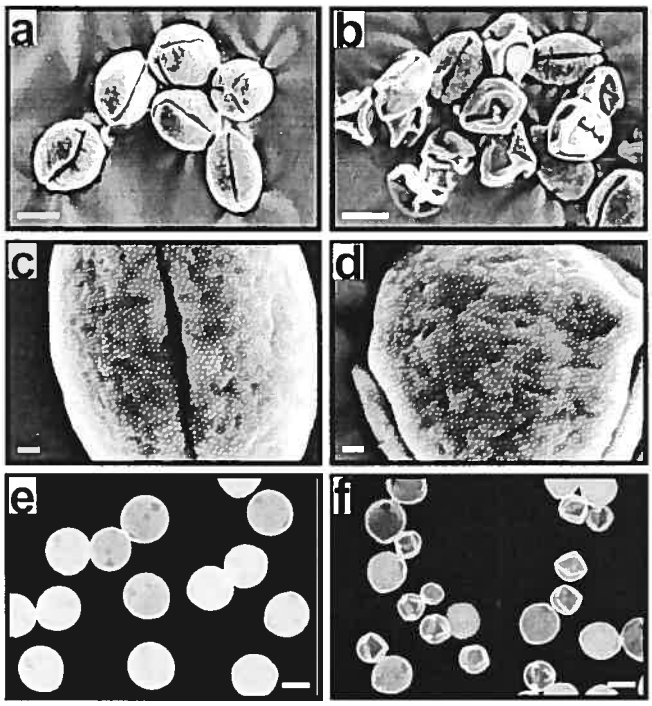

Figure 3

Pollen outer structure analyses. a SEM of wild type pollen at anthesis. Magnification 1300 X. Bar = 10 μm. **b** SEM of *ScFRK2* pollen in overexpressing line S2 at anthesis. Magnification 1400 X Bar = 10 μm. **c** SEM of wild type pollen showing the sexine at 6500 X. Bar = 1 μm. **d** SEM of *ScFRK2*-S2 pollen showing the sexine at 6500 X. Bar = 1 μm. **e** Callose staining with aniline blue of wild type pollen at anthesis. Bar = 10 μm **f** Callose staining with aniline blue of *ScFRK2*-S2 pollen at anthesis. Bar = 10 μm.

untransformed and overexpressing lines (Fig. 3c and d), suggesting that the defect is not related to sporopollenin deposition.

F1 population analysis

Exine formation and patterning occur before microspore shedding (Esau 1977). Since *ScFRK2* overexpression lines showed unperturbed exine patterning (Fig. 3d) and pollen viability in these lines appeared normal at early developmental stages (Fig. 2d and f), this suggested that the defect observed in pollen occured developmentally. Pollen defects thus occurred either because of the presence and expression of the T-DNA in the microspore (gametophytic effect) or because the anther context is altered in a way that pollen does not develop properly (sporophytic effect). To distinguish between those two possibilities, we used an *ScFRK2*-S2 overexpressing line that harboured a single T-DNA insertion (data not shown). Thus, in a primary transformant, only half the pollen grains should carry the transgene. We collected the *ScFRK2*-S2 pollen and crossed it to a *S. chacoense* V22 wild type plant as female progenitor (fully compatible cross). Twenty days after pollination, fruits were harvested and ovules dissected to rescue sixteen embryos which were allowed to grow on MS media. DNA was then extracted from leaflets and used to PCR amplify the kanamycin gene, the NOS terminator and the *ScFRK2* transgene. PCR products were run on an agarose gel, and seven individuals out of sixteen plantlets (44%) scored positive for all three markers (data not shown). Since the T-DNA carrying the 35S::*ScFRK2* construct is genetically transmittable to the F1 population, this indicates that the presence of the T-DNA in the pollen itself is not lethal, and suggests that the defect observed is of sporophytic origin. Thus, the anther tissue

overexpressing *ScFRK2* must be the cause for the observed pollen defect. If this was the case, one would expect that pollen grain lethality should increase as the anthers mature (as observed previously, see Fig. 2) and, remain constant in older stamens if the dysfunction stems from the tapetum. Five DPA, pollen was collected from these anthers and scored for viability with 1% aceto-carmine staining. The proportion of shriveled pollen grains was statistically similar between younger (anthers at anthesis day) and older stamens (anthers 5 DPA, 52.8 ± 6.9% and 47.2 ± 1.2% pollen lethality for *ScFRK2* line S1 and S2 respectively). Why would pollen lethality be halted at 50% while all pollen grains are found in the same locule environment? As aceto-carmine staining is known to overestimate the viability among pollen, thus underestimating the lethality of pollen grains, observation of unfixed pollen with variable pressure SEM was performed to better define the percentage of normal and defective pollen grains. Appearance of pollen grains was scored from seven and nine SEM optical fields for wild type and the *ScFRK2* overexpressing line S2, respectively. The mean percentage lethality (shriveled pollen grains as shown in Fig. 3b) was 4.3 ± 2.8% for wild type pollen and 62.4 ± 1.9% in the *ScFRK2*-S2 overexpressing line. Furthemore, pollen from the *ScFRK2*-S2 overexpressing line was also composed of wild type looking pollen and slightly odd-shaped pollen grains (data not shown). These slight defects could not be observed in aceto-carmine staining as they were still able to hydrate. Thus, the population of deformed pollen grain is in fact higher than expected from the aceto-carmine staining. Since callose is normally observed in mature pollen and since some sporophytic mutants affecting pollen development show an increase in callose accumulation (Canales *et al.* 2002;Zhao *et al.* 2002), we assessed the presence of pollen callose with 0.1% aniline

blue staining under UV light illumination in wild type and *ScFRK2* overexpressing lines. In wild type pollen, callose was mostly observed around the apertures (with short time aniline blue staining) and more diffusely on the pollen cell wall (Fig. 3e). The same staining pattern was also observed in normal looking pollen in the *ScFRK2*-S2 line (Fig. 3f). In the shriveled *ScFRK2*-S2 pollen, callose is observed on all ridges, but overall callose deposition was similar to the level observed in wild type pollen (Fig. 3f). Since the observation of callose staining was performed in a pollen hydration media, it was possible to determine if there was a significant difference in pollen size between normal looking pollen from both WT and mutant plants. Pollen surface area was thus determined for WT and *ScFRK2*-S2 plants. A significant difference was observed between normal looking pollen grains from the WT and *ScFRK2*-S2 plants. Surface area using arbitrary units (au) and determined by pixel filling of entire pollen grain contour was 42.1 ± 2.2 au (n=20) for WT plants, while *ScFRK2*-S2 normal looking pollen had a surface area of 32.2 ± 3.7 au (n=20). Thus, normal looking pollen from the *ScFRK2*-S2 overexpressing transgenic line reached about 76% the surface area (considering the pollen grain as a flat circle) and 65% of the total volume of a WT pollen grain. Obviously, the surface area of shriveled mutant pollen grains was considerably less than WT pollen with a surface area of 17.0 ± 1.3 au (n=20), thus representing roughly 40% that of WT.

Transmittance of the phenotype

To further confirm that the observed pollen phenotype was linked to *ScFRK2* overexpression, we generated a population of nineteen individuals from a cross between a wild type V22 plant as a pollen donor and the *ScFRK2*-S2 overexpressing line as the female progenitor. Wild type V22 pollen was use as donor to ensure that the population generated was not biased by a male parent already showing a pollen defect. Total RNA was extracted from each individual and eleven individuals showing more *ScFRK2* transcript than the untransformed control were kept for further analyses. These selected individuals were grouped in three categories of increasing *ScFRK2* expression levels and tested for the severity of the pollen phenotype. Lethality was estimated by aceto-carmine staining. As shown in Fig. 4, as *ScFRK2* mRNA levels increased, pollen lethality followed accordingly. Although lethality percentage increased markedly as soon as *ScFRK2* is slightly overexpressed (Fig. 4, {+} category), a clear trend is visible, with increased pollen lethality corresponding to an increase in transgene expression (Fig. 4). The homeotic change of ovule shown previously (O'Brien *et al.* 2005) was also transmissable in this population but to a lesser degree than the pollen phenotype (data not shown).

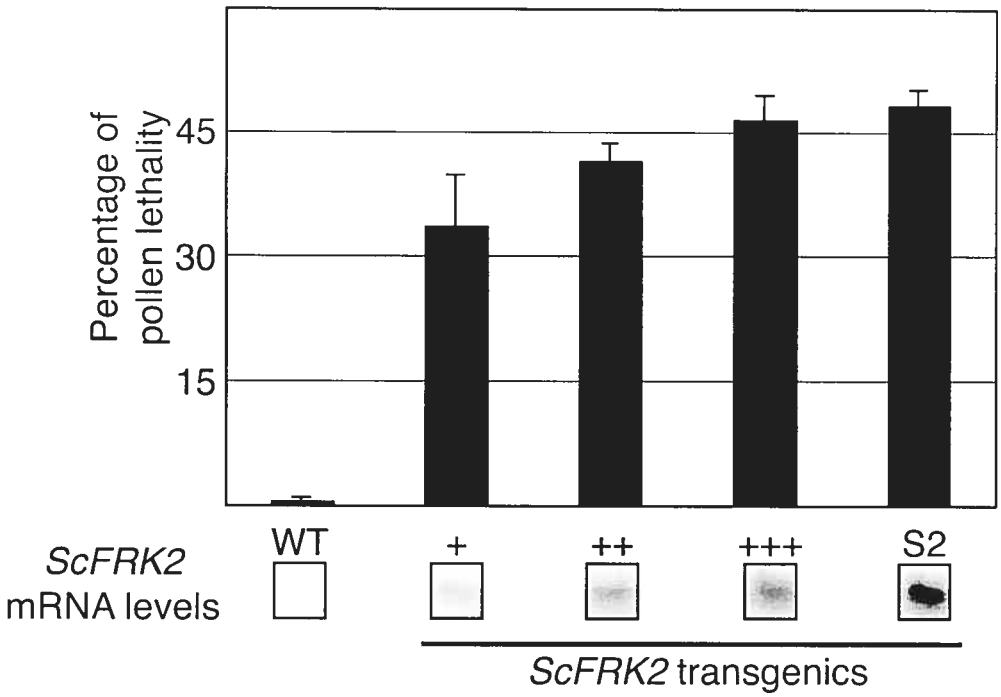

Figure 4

Pollen lethality linked to *ScFRK2* transcript abundance. A population produced from the *ScFRK2*-S2 overexpressing line as the female progenitor (S alleles $S_{12}S_{14}$) and a V22 (S alleles $S_{11}S_{13}$) wild type accession as the pollen donor, was divided in three categories of *ScFRK2* mRNA expression level. Average pollen lethality with standard deviation was scored for each category. For the RNA gel blot analysis, in order to clearly show the differences between the various categories of overexpressing plants, an exposure of one day was used instead of the four days needed to reveal the WT expression of the *ScFRK2* gene (O'Brien *et al.* 2005).

V.9 Discussion

Signal transduction is at the heart of every life process and protein kinases, enzymes capable of modifying other proteins by chemically adding phosphate groups, are key regulators for signaling events. Phosphorylation usually results in a functional change of the target protein or substrate, either by changing its activity, cellular location or association with other proteins. In order to gain information about protein kinases acting during plant fertilization and embryogenesis, we used a reverse genetic approach to determine the role of protein kinases expressed in reproductive tissues (Germain *et al.* 2005). Out of an EST library normalized for weakly expressed genes in fertilized ovaries, we isolated two cDNA clones named *ScFRK1* and *ScFRK2* (*Solanum chacoense* Fertilization-Related Kinase 1 and 2) that showed partial similarity to the MAPKK and MAPKKK subfamilies, but that have a typical MAP kinase kinase phosphorylation motif (O'Brien *et al.* 2005). Both *Solanum chacoense* members of this new protein kinase group showed female reproductive tissue defects when either suppressed (*ScFRK1*, manuscript in preparation) or overexpressed (*ScFRK2*, (O'Brien *et al.* 2005) at the RNA level. In this study we show that the ScFRK2 protein kinase also affects pollen development.

Of all the tissues tested, *ScFRK2* mRNAs are most strongly expressed in anthers, styles and in fertilized ovules (O'Brien *et al.* 2005, and this study), suggesting a particular role in male and female reproductive development for this MAPKK. Although a weak basal expression level can be observed in some vegetative tissues (mainly leaves

and petals), phenotype analyses of *ScFRK2* overexpressing plants only showed female (O'Brien *et al.* 2005) and male (this study) reproductive tissue defects, consistent with the WT *ScFRK2* mRNA expression pattern. *ScFRK2* transcripts were mapped to most anther cells except vascular tissue, pollen, connective tissue cells and stomium cells, as detected by *in situ* hybridizations (Fig.1b). Overexpression of the *ScFRK2* gene caused both severe and mild pollen defects (Table 1 and Fig. 2, 3, and 4). SEM observations showed that almost two-thirds of the pollen grains were heavily shriveled. In all cases of heavily deformed pollen, overall sexine pattern was unaffected (Fig. 3c and d) as was callose deposition on pollen grains when compared to wild type pollen (Fig. 3e and f). Hydration capability or pollen lethality was also linked to *ScFRK2* abundance (Fig. 4). As the endogenous *ScFRK2* transcript is already present in the anther tissues (Fig. 1), the pollen defect caused by *ScFRK2* overexpression might be caused by expression of transcript in the pollen, microsporocyte precursors, or in cell layers where *ScFRK2* is not normally expressed, like the connective tissue (Fig. 1b). Since the pollen in the wild type and the mutant plants are not significantly different up to the tetrad stage, this explanation is probably unlikely. The developmentally regulated increase in pollen lethality from three days prior to anthesis until anthesis day suggests instead that the missexpression or overexpression in the tapetum, or in the middle layer and endothecium cells, might have had a much stronger impact on the pollen phenotype in *ScFRK2* oversexpressing lines. Both layers have respectively an early and late important role on pollen maturation (Bowman 1994), and as shown for other pollen mutants (Albrecht *et al.* 2005;Canales *et al.* 2002;Colcombet *et al.* 2005;Yang *et al.* 2003;Zhao *et al.* 2002). This is further supported by the fact that pollen lethality progression stops with tapetum degeneration, the tapetum having almost completely disappeared by

anthesis day (Fig. 1v). Although phenotypes obtained from overexpressing a transgene in a plant sometimes leads to erroneous interpretations, the observation that the lowest level of *ScFRK2* transcript accumulation over WT levels leads to pollen defect (Fig. 4, {+} category), strongly suggests that the ScFRK2 kinase is a regulator of pollen development, and that its expression needs to be tightly regulated for proper pollen development to occur.

The fact that pollen tetrads were indistinguishable between WT and mutant plants (Fig. 2b and c), combined with the ability of a pollen grain bearing the T-DNA constructs to be passed to the next generation suggest that the pollen defect observed is of sporophytic origin. Even if the T-DNA construct remained silent in pollen, as observed for many genes driven by the CaMV 35S promoter in solanaceous plant species including tobacco, tomato and petunia (Mascarenhas and Hamilton 1992;van der Leede-Plegt *et al.* 1992), or was only weakly expressed, as determined for tobacco in another study (Wilkinson *et al.* 1997), this would not explain why more than 60% of the pollen grains were heavily deformed and why the remaining healthy looking pollen grains were significantly smaller that WT pollen. The fact that all pollen grains in *ScFRK2* overexpressing lines bearing a single T-DNA insertion are affected in some ways indicates that the effect is of sporophytic origin. Thus, in *ScFRK2* overexpressing lines, the anther environment and some specific protein-protein interactions between the ScFRK2 kinase and its substrate(s) are altered in such a way that pollen does not develop properly.

Several genes have been described as having important function in the proper development of both male and female gametes. In the *Petunia* receptor kinase *prk1* mutant, embryo sac formation is abnormal, and the two polar nuclei fail to migrate and fuse together (Lee *et al.* 1997). In addition, pollen development defects are also observed. The microspores are arrested at the unicellular stage and this pollen defect is essentially gametophytic (Lee *et al.* 1996), which is not the case for the *ScFRK2* overexpression. On the other hand, many other mutants show a sporophytic prevalence for male sterility due to disorganization of the tapetum cell layer. In the *A. thaliana sporocyteless/nozzle* (*spl/nzz*) mutant the micro- and macrosprorangia formation is disturbed through disorganization of male and female structures, respectively (Schiefthaler *et al.* 1999;Yang *et al.* 1999). The *SPL/NZZ* gene is a MADS box-related transcription factor that is expressed in both reproductive structures. In the *spl/nzz* mutant, archesporial initiation occurs properly, however, subsequent differentiation of male and female sporocytes does not. Mutant analysis also defined the sporocyte development arrest as a failure of the tapetum cell layer to develop normally in the anther wall (Yang *et al.* 1999), and delayed nucellus development in the ovule (Schiefthaler *et al.* 1999). In the *tpd1* or *exs/ems1* mutant, a putative ligand/receptor pair, cells that should give rise to the tapetum assume an alternative fate and more cells than usual undergo meiosis 1 and 2, which leads to increased tetrad formation and an excess of microsporocytes (Canales *et al.* 2002;Nonomura *et al.* 2003). No cells reach pollen maturity and mutant anthers bear empty pollen shells overloaded with callose (Canales *et al.* 2002;Zhao *et al.* 2002). Moreover, *EXS/EMS1* was shown to be expressed in the inflorescence, floral meristems and developing stamens, as well as the ovules and seeds (Canales *et al.* 2002;Zhao *et al.* 2002), and the *exs/ems1* mutant displays delayed

embryo development (Canales *et al.* 2002). In our previous work, we have shown that *ScFRK2* overexpression also leads to a delayed embryo development rate compared to control untransformed plants, and to the homeotic change of ovules into carpeloid structures (O'Brien *et al.* 2005). As those phenotypes are similar, but not identical, to already described mutants, *ScFRK2* most probably works in a different signaling pathway, which is not surprising considering that ovules and anthers are complex organs.

The accumulated evidence indicates that several key elements regulate the proper establishment of nourishing tissues that give rise to both the male and female sporocytes. Overexpression of the *ScFRK2* gene disturbs pollen and ovule development in a way that is similar to the above-mentioned mutants, but is somehow distinct, since some pollen grains are still viable and can propagate the transgene to the next generation. Our results suggest that *ScFRK2* overexpression disturbs the necessary anther/sporocyte interactions by either tissue missexpression or increased *ScFRK2* transcript accumulation, leading to the shriveled appearance and lethality of more than 60% of the pollen and to overall pollen size reduction. The fact that the slightest modification in *ScFRK2* expression results in pollen lethality suggests that *ScFRK2* is a key regulator of pollen maturation. The sporophytic nature of the observed phenotype, coupled with a lethality progression that stops with the tapetum degeneration, suggest that modified expression of the *ScFRK2* gene most probably affects the cell layers most closely involved in pollen maturation, the tapetum. Proper development and differentiation of the endothecium and tapetum cell fate is of central importance for pollen integrity and viability. Defining the involvement of *ScFRK2* in this process will help us understand

the role of this protein kinase in a new signaling pathway involved in anther and pollen development.

V.10 Acknowledgements

We thank Gabriel Téodorescu for plant care and maintenance, Louise Pelletier and Charles Bertrand for SEM microscopy training. M. O. is the recipient of Ph. D. fellowships from the Natural Sciences and Engineering Research Council of Canada (NSERC) and from Le Fonds Québécois de la Recherche sur la Nature et les Technologies (FQRNT, Québec). D. P. M. holds a Canada Research Chair in Functional Genomics and Plant Signal Transduction.

V.11 References

Albrecht C, Russinova E, Hecht V, Baaijens E, de Vries S (2005) The *Arabidopsis thaliana* SOMATIC EMBRYOGENESIS RECEPTOR-LIKE KINASES1 and 2 control male sporogenesis. Plant Cell 17: 3337-3349.

Boavida LC, Becker JD, Feijo JA (2005) The making of gametes in higher plants. Int J Dev Biol 49: 595-614.

Bowman J (1994) Arabidopsis: An atlas of morphology and development. Springer-Verlag, New York.

Canales C, Bhatt AM, Scott R, **Dickinson H** (2002) EXS, a putative LRR receptor kinase, regulates male germline cell number and tapetal identity and promotes seed development in *Arabidopsis*. Curr Biol 12: 1718-27.

Colcombet J, Boisson-Dernier A, Ros-Palau R, Vera CE, Schroeder JI (2005) *Arabidopsis* SOMATIC EMBRYOGENESIS RECEPTOR KINASES1 and 2 are essential for tapetum development and microspore maturation. Plant Cell 17: 3350-3361.

Esau K (1977) Anatomy of Seed Plants. New York.

Germain H, Rudd S, Zotti C, Caron S, O'Brien M, Chantha SC, Lagace M, Major F, Matton DP (2005) A 6374 unigene set corresponding to low abundance transcripts expressed following fertilization in *Solanum chacoense* Bitt, and characterization of 30 receptor-like kinases. Plant Mol Biol 59: 515-32.

Hecht V, Vielle-Calzada JP, Hartog MV, Schmidt ED, Boutilier K, Grossniklaus U, de Vries SC (2001) The *Arabidopsis* SOMATIC EMBRYOGENESIS RECEPTOR KINASE 1 gene is expressed in developing ovules and embryos and enhances embryogenic competence in culture. Plant Physiol 127: 803-16.

Johnson MA, Preuss D (2003) On your mark, get set, GROW! LePRK2-LAT52 interactions regulate pollen tube growth. Trends Plant Sci 8: 97-9.

Jones JDG, Dunsmuir P, Bedbrook J (1985) High level expression of introduced chimeric genes in regenerated transformed plants. EMBO J 4: 2411-2418.

Lantin S, O'Brien M, Matton DP (1999) Pollination, wounding and jasmonate treatments induce the expression of a developmentally regulated pistil dioxygenase at a distance, in the ovary, in the wild potato *Solanum chacoense* Bitt. Plant Mol Biol 41: 371-386.

Lee H-S, Karunanandaa B, McCubbin A, Gilroy S, Kao T-h (1996) PRK1, a receptor-like kinase of *Petunia inflata*, is essential for postmeiotic development of pollen. Plant J 9: 613-624.

Lee HS, Chung YY, Das C, Karunanandaa B, van Went JL, Mariani C, Kao TH (1997) Embryo sac development is affected in *Petunia inflata* plants transformed with an antisense gene encoding the extracellular domain of receptor kinase PRK1. Sex Plant Reprod 10: 341-350.

Mascarenhas JP, Hamilton DA (1992) Artifacts in the localization of GUS activity in anothers of petunia transformed with a CaMV 35S-GUS construct. Plant J 2: 405-408.

Morris PC, Guerrier D, Leung J, Giraudat J (1997) Cloning and characterisation of MEK1, an *Arabidopsis* gene encoding a homologue of MAP kinase kinase. Plant Mol Biol 35: 1057-64.

Muschietti J, Dircks L, Vancanneyt G, McCormick S (1994) LAT52 protein is essential for tomato pollen development: pollen expressing antisense LAT52 RNA hydrates and germinates abnormally and cannot achieve fertilization. Plant J 6: 321-38.

Nonomura K, Miyoshi K, Eiguchi M, Suzuki T, Miyao A, Hirochika H, Kurata N (2003) The *MSP1* gene is necessary to restrict the number of cells entering into male and female sporogenesis and to initiate anther wall formation in rice. Plant Cell 15: 1728-39.

O'Brien M, Bertrand C, Caron S, Matton DP (2005) The *Solanum* ScFRK2 protein kinase defines a new MAPK family and affects ovule identity. J Exp Bot, submitted.

Schiefthaler U, Balasubramanian S, Sieber P, Chevalier D, Wisman E, Schneitz K (1999) Molecular analysis of *NOZZLE*, a gene involved in pattern formation and early sporogenesis during sex organ development in *Arabidopsis thaliana*. Proc Natl Acad Sci USA 96: 11664-9.

Schmidt ED, Guzzo F, Toonen MA, de Vries SC (1997) A leucine-rich repeat containing receptor-like kinase marks somatic plant cells competent to form embryos. Development 124: 2049-62.

Scott RJ, Spielman M, Dickinson HG (2004) Stamen structure and function. Plant Cell 16 Suppl: S46-60.

Sheridan WF, Golubeva EA, Abrhamova LI, Golubovskaya IN (1999) The mac1 mutation alters the developmental fate of the hypodermal cells and their cellular progeny in the maize anther. Genetics 153: 933-41.

Shibata W, Banno H, Ito Y, Hirano K, Irie K, Usami S, Machida C, Machida Y (1995) A tobacco protein kinase, NPK2, has a domain homologous to a domain found in activators of mitogen-activated protein kinases (MAPKKs). Mol Gen Genet 246: 401-10.

Tang W, Ezcurra I, Muschietti J, McCormick S (2002) A cysteine-rich extracellular protein, LAT52, interacts with the extracellular domain of the pollen receptor kinase LePRK2. Plant Cell 14: 2277-87.

van der Leede-Plegt L, van de Ven B, Bino R, van der Salm T, van Tunen A (1992) Introduction and differential use of various promoters in pollen grains of *Nicotiana glutinosa* and *Lilium longiflorum*. Plant Cell Rep 11: 20-24.

Wilkinson J, Twell D, Lindsey K (1997) Activities of CaMV 35S and nos promoters in pollen: implications for field release of transgenic plants. J Exp Bot 48: 265-275.

Wilson ZA, Yang C (2004) Plant gametogenesis: conservation and contrasts in development. Reproduction 128: 483-92.

Yang SL, Xie LF, Mao HZ, Puah CS, Yang WC, Jiang L, Sundaresan V, Ye D (2003) Tapetum determinant1 is required for cell specialization in the *Arabidopsis* anther. Plant Cell 15: 2792-804.

Yang WC, Ye D, Xu J, Sundaresan V (1999) The *SPOROCYTELESS* gene of *Arabidopsis* is required for initiation of sporogenesis and encodes a novel nuclear protein. Genes Dev 13: 2108-17.

Zhang Y, Shewry PR, Jones H, Barcelo P, Lazzeri PA, Halford NG (2001) Expression of antisense *SnRK1* protein kinase sequence causes abnormal pollen development and male sterility in transgenic barley. Plant J 28: 431-41.

Zhao DZ, Wang GF, Speal B, Ma H (2002) The *EXCESS MICROSPOROCYTES1* gene encodes a putative leucine-rich repeat receptor protein kinase that controls somatic and reproductive cell fates in the *Arabidopsis* anther. Genes Dev 16: 2021-31.

Chapitre VI. Discussion et perspectives

Dans le présent manuscrit, nous avons caractérisé au niveau moléculaire trois gènes impliqués dans divers processus de la biologie de la reproduction chez notre organisme modèle *Solanum chacoense*. Le produit d'un de ces trois gènes, *ScFRK2*, code pour un élément qui est généralement impliqué dans la transduction de signaux par le biais des cascades de type MAP kinase (Chapitre IV et V, O'Brien *et al*, 2005b et c). En ce qui concerne le gène *ScHT-B*, il code pour une protéine qui démontre plusieurs similarités aux ligands peptidiques (Chapitre II, O'Brien *et al.*, 2002b). Alors que *CYP51G1-Sc* code pour une enzyme impliquée dans la voie de biosynthèse des brassinostéroïdes, mais dont l'intermédiaire de biosynthèse est véhiculé à distance et pourrait agir comme lipide de signalisation (Chapitre III, O'Brien *et al.*, 2005a).

VI.1 HT-B et son rôle dans les mécanismes de pollinisation

Les petites protéines riches en asparagine de type HT portent en leur N-terminal un peptide de signal qui les localiserait vers l'extérieur de la cellule. Étant donné leur petite taille, de la richesse en cystéines conservées pouvant participer à la formation de

ponts disulfures et à la présence d'un potentiel site de clivage dibasique similaire à d'autres prépropeptides, il est fort possible qu'elles puissent servir comme peptide de signalisation (Germain *et al.*, 2005b), même si pour l'instant aucune donnée n'indique qu'elles pourraient avoir un partenaire protéique qui ferait office de récepteur. Il a été démontré chez *Nicotiana alata*, que lorsque la protéine HT est absente, le système de reconnaissance du soi lors de la pollinisation est aboli et ce, même si les niveaux de S-RNases demeuraient élevés (McClure *et al.*, 1999). Les mêmes types de corrélations ont pu être observés chez plusieurs espèces de tomates, où le système d'auto-incompatibilité était rendu inefficace par l'absence d'expression du gène *HT* (Kondo *et al.*, 2002a et b). Nous avons obtenu le gène *HT-A* d'une banque normalisée d'EST de pistils pollinisés après 48 heures générée dans notre laboratoire. La version allélique de *HT-B* a été obtenue par PCR en utilisant des amorces dégénérés (O'Brien *et al.*, 2002b). Nous avons pu confirmer les expériences de transgénèse fait chez le tabac en sous-exprimant les transcrits de *HT-B* par une stratégie d'ARN interférence. Nous avons pu également démontrer que seule la forme B a un impact sur l'auto-incompatibilité des plantes transgéniques alors que la forme A n'a aucun effet (Figures II.4 et II.5, O'Brien *et al.*, 2002b). Les plantes transgéniques qui avaient un niveau presque nul de transcrits pour *HT-B* montraient ce phénotype, alors que des plantes transgéniques qui possédaient un niveau sensiblement réduit restaient tout de même auto-incompatibles. Par contre, lorsque les fleurs de ces dernières recevaient des pollinisations subséquentes à la première journée, plusieurs plantes transgéniques pouvaient maintenant produire des fruits suite à une auto-pollinisation (Figure II.5, O'Brien *et al.*, 2002b).

Les gènes *HT-A et HT-B* sont modulés de la même manière que les *S-RNases*, c'est-à-dire qu'ils ont un promoteur fort qui s'exprime de manière développementale ayant un pic d'expression vers l'anthèse mais une absence de transcrits dans les styles immatures ou proches de l'abcision (Figure II.2, O'Brien *et al.*, 2005b). Puisque les S-RNases sont nécessaires pour maintenir un système de reconnaissance du pollen génétiquement semblable (Lee *et al.*, 1994, Murfett *et al.*, 1994 et Matton *et al.*, 1997), nous avons considéré la possibilité que des pollinisations subséquentes pourraient avoir pour effet de permettre aux tubes polliniques de croître vers les ovules de manière ininterrompue et ce, par le fait que les S-RNases sont peu abondantes dans le tissu transmetteur d'un style avant l'abcision (Figure II.2, O'Brien *et al.*, 2002b). Dans ce cas, ce même type de pollinisation subséquente aurait le même effet sur les plantes contrôles ou bien sur les plantes transgéniques sous-exprimant *HT-A*. Nous avons pu montrer que ce n'était pas le cas (Figure II.4, O'Brien *et al.*, 2002b). Suite à une pollinisation incompatible, nous avons pu également démontrer que l'expression des *S-RNases* et de *HT* est maintenue au cours du développement tardif à un taux similaire au pic d'expression de l'anthèse (Figure II.2, O'Brien *et al.*, 2002b), assurant ainsi un niveau de protection adéquat contre les tubes polliniques génétiquement semblables dans ces conditions. Dans le cas d'une vieille fleur, que le niveau de transcrits des *S-RNases* soit élevé ou pas, cela n'a pas d'importance puisque qu'il faut en moyenne 40 heures après une pollinisation pour que la fécondation se produise. Il est alors trop tard car le processus de sénescence de la fleur et du style est déjà entamé.

Puisque les pollinisations subséquentes permettent la production de fruits dans presque tous les transgéniques sous-exprimant *HT-B*, nous avons émis l'hypothèse que

HT-B doit avoir pour fonction d'interférer sur le processus de sénescence du style. Nous avons pu démontrer que, dans les plantes sous-exprimant *HT-B*, le style demeurait attaché plus longuement sur l'ovaire et que parfois, il pouvait rester sur des fruits en développement (Figure II.6, O'Brien *et al.*, 2002b). De plus, ce style demeurait ferme et turgescent, capable de nourrir et guider les tubes polliniques vers l'ovaire. Puisque l'éthylène joue un rôle connu dans les processus de sénescence, nous avons évalué le niveau d'expression d'enzymes impliquées dans la biosynthèse de l'éthylène et le niveau d'expression de deux récepteurs à l'éthylène dans les lignées sous-exprimantes pour *HT-B*. Cette expérience n'a pas été concluante (O'Brien *et al.*, 2002b) et puisqu'il existe plusieurs récepteurs à l'éthylène et que l'ACC synthase et l'ACC oxydase font toutes deux parties d'une famille de gènes, il faudrait tester de manière plus exhaustive ces composantes de la signalisation par l'éthylène. Par contre, l'implication de l'éthylène a pu être confirmée par la production de fruits parthénocarpiques des plantes mutantes pour le gène *HT-B* (O'Brien et Matton, données non-publiées).

Certains auteurs avancent, que les petites protéines de type HT permettraient le transport des S-RNases de la matrice du tissu transmetteur vers l'intérieur du tube pollinique (Cruz-Garcia *et al.*, 2003). Nous avons pu démontrer que les protéines HT ne peuvent interagir directement avec les S-RNases (données non-montrées, O'Brien *et al.*, 2002b). Comme nous avons utilisé un système *in vivo* artificiel, il n'est pas garantie que la structure tridimensionnelle des deux protéines demeure intacte dans la levure. Par contre, il serait possible de vérifier l'incorporation des S-RNases dans nos lignées d'interférence pour HT-B. Mais comme dans ces dernières lignées le style demeure attaché plus longuement à l'ovaire, nous croyons que le système d'auto-incompatibilité

est contourné par un processus de retardement de la sénescence plutôt que par une modification de l'incorporation des S-RNases dans le tube pollinique.

Nous croyons aussi que, par leur structure peptidique, HT-A et B sont des peptides de signalisation. Premièrement, elles disposent d'un peptide signal de sécrétion vers l'extérieur de la cellule. Puis, elles ont six cystéines dont la position est conservée parmi les différentes espèces recensées. Les cystéines permettent la formation de ponts disulphures entres elles et sont donc importantes pour la structure tridimensionnelle d'un peptide. De plus, leurs petites tailles et la présence d'un site potentiel de clivage de type dibasique sont des caractéristiques que l'on retrouve chez plusieurs peptides de signalisation. De plus, HT-A et HT-B ont des fonctions biologiques différentes, encore inconnues pour HT-A, et elles ont également des différences peptidiques notables, cela suggère que des récepteurs différents pourraient moduler leur signalisation. Il n'est pas à exclure la possibilité pour les protéines HT d'agir à la manière des protéines LTP (Lipid Transfer Protein) qui sont de petits peptides sécrétés reconnaissant des lipides de signalisation spécifiques pour les acheminer vers leur site d'action. Évidemment, la molécule reconnue pourrait être autre chose qu'un lipide. Mais que les protéines HT soient reconnues par un récepteur ou qu'elles agissent elles-mêmes comme récepteur pour une petite molécule, plusieurs interrogations restent afin de cerner les voies de signalisation dont elles font parties.

VI.2 Signalisation et embryogenèse, l'implication de CYP51G1-Sc

Les stérols sont des composantes de la membrane plasmique qui ont un rôle très important comme précurseurs des brassinostéroïdes, un groupe de phytohormones qui agissent en tant que régulateur de la croissance comme l'élongation cellulaire, l'inhibition de la croissance racinaire, le développement de la feuille, la croissance du tube pollinique et la photomorphogenèse (Clouse, 2002a et b). Plusieurs enzymes interviennent dans la voie de biosynthèse des brassinostéroïdes. L'une d'elles, la C14 réductase impliquée dans une étape précoce de cette voie de biosynthèse, aurait une implication majeure dans le développement de l'embryon. Chez *A. thaliana*, le mutant qui lui est associé, *fackel/hydra 2*, montre une désorganisation cellulaire du domaine central de l'embryon. Le mutant ne peut se développer correctement et former une graine viable (Jang *et al.*, 2000 et Schrick *et al.*, 2000). Ce mutant ne peut être rétabli par l'application exogène de brassinostéroïdes, ce qui laisse présager qu'une sur-accumulation d'un ou plusieurs intermédiaires de synthèse en amont crée une désorganisation du patron de développement de l'embryon ou bien qu'un intermédiaire en aval autre que le brassinostéroïde soit nécessaire au bon développement de l'embryon. La désorganisation du patron développemental de l'embryon ainsi que l'inefficacité de l'application exogène de brassinostéroïdes à rétablir le phénotype normal sont caractéristiques de tous les mutants affectant les enzymes de la voie de biosynthèse en amont du stérol 24-méthylène-iophénol (Figure III.1, O'Brien *et al.*,

2005a). Nous avons pu montrer que chez *A. thaliana*, l'introduction d'un T-DNA dans le gène *CYP51G1-At* qui code pour l'obtusifoliol 14α-déméthylase, l'enzyme juste en amont de la C14 réductase, est léthale lorsque homozygote (O'Brien *et al.*, 2005a). De plus, le mutant ne peut être sauvé par l'ajout exogène de brassinostéroïdes.

Nous avions préalablement isolé ce gène chez *S. chacoense* lors d'un criblage d'expression d'ARNm exprimés de manière différentielle entre des pistils non pollinisés et des pistils pollinisés de 24 à 96 heures à l'aide de la technique de représentation différentielle des ARNm (O'Brien *et al.*, 2002a). Plusieurs gènes avaient été isolés, dont *CYP51G1-Sc* qui code pour l'obtusifoliol 14α-déméthylase. Cette enzyme fait partie de la famille des cytochromes P450, l'une des plus grosses familles de gènes connues. Cette 14α-déméthylase est le seul cytochrome P450 qui se retrouve dans presque tous les règnes du vivant, le substrat quant à lui diffère selon le règne, le lanostérol chez les mammifères, le 24-méthylène-24,25-dihydrolanostérol chez les champignons et l'obtusifoliol chez les plantes. Chez les mammifères et les champignons, l'enzyme est capable de reconnaître les substrats des enzymes des autres règnes alors que l'enzyme chez les plantes a une spécificité stricte pour son substrat, l'obtusifoliol (Lamb *et al.*, 1998). Nous avons pu démontrer que ce n'était pas le cas pour toutes les plantes. En effet, CYP51G1-Sc est capable d'utiliser le lanostérol et le 24-méthylène-24,25-dihydrolanostérol en plus de complémenter la lignée mutante *erg11* chez *Saccharomyces cerevisiae* déficiente pour la 14α-déméthylase (Figure III.6, O'Brien *et al.*, 2005a).

Nous avons pu montrer l'induction de l'expression de cette enzyme dans les pistils pollinisés et plus précisément dans l'ovaire, l'ovule et de manière plus abondante dans la couche de cellules sous-jacente à l'épiderme du placenta (Figure III.2c et d et III.4a et c, O'Brien *et al.*, 2005a). Nous avons pu également démontrer que l'expression de *CYP51G1-Sc* était modulée à distance dans l'ovaire suite à une pollinisation compatible, une pollinisation incompatible et par la blessure du style par un moyen mécanique (Figure III.3 a à c, O'Brien *et al.*, 2005a). Un traitement de la fleur au méthyle de jasmonate induit également le transcrit de *CYP51G1-Sc* dans l'ovaire alors que d'autres hormones de défense n'ont aucun effet. Nous croyons que les blessures, induites par la croissance du tube pollinique dans la matrice du tissu transmetteur du style, pourraient libérer du méthyle de jasmonate qui informerait à distance l'ovaire et/ou l'ovule de l'arrivée du tube pollinique. Ce signal aurait pour but de préparer les tissus maternels à la fécondation à venir.

Dans le même ordre d'idée, nous avons pu démontrer que l'application de l'obtusifoliol induisait l'expression de l'enzyme dans les feuilles alors que l'application de lanostérol n'avait aucun effet (Figure III.7, O'Brien *et al.*, 2005a). De plus, l'application, sur une feuille, d'obtusifoliol marqué au ^{14}C nous a permis d'observer que ce dernier est véhiculé à distance et qu'il n'est pas métabolisé dans les cellules où il transite (Figure III.8 et III.9, O'Brien *et al.*, 2005a). Pour l'instant, nous ne savons pas si l'obtusifoliol endogène est véhiculé à distance, par contre le transport de l'obtusifoliol appliqué de manière exogène ainsi que son induction sur l'expression de l'enzyme qui le métabolise nous portent à croire que ce composé pourrait agir à la manière d'un lipide bioactif. Chez les plantes, certains intermédiaires de voies de biosynthèse ont déjà été

décrits pour avoir des fonctions de signalisation, c'est entre autre le cas de l'acide jasmonique un intermédiaire de la voie de biosynthèse du méthyle de jasmonate. L'acide jasmonique induit la défense contre les pathogènes, est impliqué dans les mécanismes de réponses à la blessure, la mécanotransduction et les mécanismes de sénescence (Leon *et al.*, 2001 et Schaller, 2001).

Chez les animaux, certains facteurs de transcription portent un domaine de type StART, qui se lie à un stérol et module de cette manière leur activité (Pontig et Aravind, 1999). Ce type de régulation n'a pas encore été démontré dans le règne végétal, par contre, des protéines à homéodomaine de type ZIP (HD-ZIP) ont, en plus de leur domaine de liaison à l'ADN, un domaine de type StART ce qui nous porte à croire que ce type de régulation est également présent chez les plantes. REVOLUTA, PHABULOSA et PHAVOLUTA sont des HD-ZIP qui portent un domaine StART et dont l'expression tissulaire est restreinte à la face adaxiale de la feuille (Bowman *et al.*, 2002). L'analyse des mutants respectifs indique que ces protéines agissent dans l'établissement du patron de formation antéro-postérieur (adaxial/abaxial) de la feuille (McConnel *et al.*, 2001 et Prigge *et al.*, 2005). Nous avons pu démontrer que *CYP51G1-Sc* était lui aussi exprimé sur le côté adaxial des primordia des feuilles (Figure III.4e et f, O'Brien *et al.*, 2005a). Couplé au fait que l'obtusifoliol est diffusible et qu'il induit l'expression de *CYP51G1-Sc*, nous pensons que ce dernier pourrait également jouer un rôle dans le développement de la feuille en parallèle à des facteurs de transcription HD-ZIP à domaine StART.

Nous disposons présentement du cDNA d'*A. thaliana* pour le HD-ZIP à domaine StART *PHABULOSA*. Nous pourrons tester si la protéine est capable de lier l'obtusifoliol et de comprendre si ce dernier module directement l'expression de gènes. Le mutant *cyp51g1-at* est malheureusement léthal, mais la construction d'une lignée interférence inductible nous permettrait d'observer les autres rôles de cette enzyme au-delà de l'embryogenèse. Ce type d'outil nous aiderait aussi à comprendre son implication dans le développement de la feuille. La compréhension du transport de l'obtusifoliol dans la plante serait également un avantage à l'étude de son mode d'action comme lipide bioactif. Comme nous l'avons déjà mentionné, les LTP sont de petites protéines qui assurent le transport de lipides. Quinze LTP ont été répertoriées chez *A. thaliana* (Avarell *et al.*, 2000), il serait intéressant d'observer l'effet sur le développement de la feuille dans chacun de ces mutants. Dans le même ordre d'idée, nous voudrions également comprendre le mécanisme d'induction de l'expression de cette enzyme à distance suite à un événement de pollinisation. De plus, la double spécificité de l'enzyme chez *S. chacoense* est intrigante. Nous pourrions tester l'activité d'enzymes d'un plus grand nombre d'espèces et essayer de localiser les acides aminés importants qui permettent un plus large spectre de reconnaissance de substrats.

VI.3 ScFRK2 et son rôle dans le développement des gamètes

Il y a très peu de protéines de type MAP kinase impliquées dans les divers processus de développement chez les plantes. La plupart des éléments de cascades de signalisation impliquant des voies de MAPK sont impliqués dans les réponses aux stress et aux pathogènes (Nakagami *et al.*, 2005 et Pedley et Martin, 2005). Par contre plusieurs facteurs de transcription et récepteurs de type kinase sont impliqués dans le développement des gamètes mâle et femelle ainsi que le développement de l'embryon. En ce qui concerne les MAPK, la seule répertoriée à ce jour est la protéine YODA, une MAPKKK jouant un rôle dans le développement de l'embryon et dans la distribution spatiale des stomates (Bergmann *et al.*, 2004 et Lukowitz *et al.*, 2004). Nous disposons au laboratoire d'une large banque d'EST de gènes faiblement exprimés dans les étapes précoces et tardives du développement embryonnaire (Germain *et al.*, 2005a). Nous y avons isolé deux membres d'une nouvelle famille de MAPK qui, phylogénétiquement, ne peuvent être associés entièrement ni à la sous-famille des MAPKK, ni à celle des MAPKKK (Figure IV.1 et Tableau IV.1, O'Brien *et al.*, 2005b). *ScFRK1* et *ScFRK2* montrent une expression dans les tissus reproducteurs femelles et femelles et mâles respectivement. Tous deux ont également une implication dans la formation des gamètes. Nous avons fait une caractérisation moléculaire du gène *ScFRK2* ainsi qu'une caractérisation de lignées sur-exprimantes.

ScFRK2 est exprimé légèrement dans tous les tissus, mais montre une plus grande abondance dans les anthères, les ovaires non-fécondés et fécondés (Figures IV.2b, O'Brien *et al.*, 2005b). Par hybridation *in situ*, nous avons pu définir cette expression dans le péricarpe de l'ovaire et les téguments de l'ovule (Figures IV.3, O'Brien *et al.*, 2005b). Pour comprendre la fonction du gène chez la plante, nous avons produit des plantes transgéniques sous- et sur-exprimant l'expression du gène *ScFRK2*. Aucun phénotype visible n'a pu être associé à l'absence de *ScFRK2*, possiblement causé par la redondance due à une famille de gènes qui pourrait jouer un rôle similaire à *ScFRK2*. Entre autres, l'hybridation de type Southern sur de l'ADN génomique et la présence de deux bandes équimolaires sur le Northern (Figure IV. 2a et b, O'Brien *et al.*, 2005b) appuient cette possibilité. En ce qui concerne les plantes sur-exprimantes, nous avons pu remarquer que la taille des fruits était inférieure à la lignée contrôle et que le nombre de graines était dix fois moins abondant. Ces dernières portent des embryons dont le développement est retardé à des stades embryonnaires précoces alors que la lignée témoin montre des embryons matures (Tableau IV.2 et Figure IV.4b et c, O'Brien *et al.*, 2005b). Ces phénotypes et le ralentissement du développement embryonnaire ont pu être associés à l'apparence anormale de plusieurs ovules dans la lignée sur-exprimante (Figure IV.5a à g, O'Brien *et al.*, 2005b). Nous avons pu démontrer que les structures filiformes, qui faisaient office d'ovules, ont une apparence stylaire. Plus précisément, nous avons pu identifier que les cellules qui couvrent les ovules mutants ressemblent plus à des cellules du style qu'à celles d'un ovule témoin (Figure IV.5k et l, O'Brien *et al.*, 2005b). De plus, les structures filiformes contiennent des cellules qui ressemblent aux papilles stylaires (Figure IV.5h à j et m à q, O'Brien *et al.*, 2005b), alors que l'intérieur de la structure montre une couche de cellules denses en son centre,

similaires aux cellules du tissu transmetteur (Figure IV.6, O'Brien *et al.*, 2005b). Nous croyons que la sur-expression de *ScFRK2* cause un changement homéotique de l'ovule. Ce phénotype est similaire à celui observé chez le mutant *fbp11* de *Petunia hybrida* (Angenent *et al.*, 1995) et *stk* chez *A. thaliana* (Pyniopich *et al.*, 2003) où l'identité des ovules est modifiée pour celle de structures carpéloïdes. Les gènes *FBP11* et *STK* codent pour des facteurs de transcription de type MADS box. Il serait envisageable que ScFRK2 influence directement ou indirectement le comportement de cet orthologue chez *S. chacoense*. L'orthologue du gène *FBP11* chez *S. chacoense* pourrait être un substrat direct pour la kinase ScFRK2. Ceci est présentement testé par la production de plantes de pétunia sur-exprimant *ScFRK2*, et par des essais d'interaction directe entre FBP11 et ScFRK2. Par contre, j'ai pu démontrer que la forme non-phosphorylée de ScFRK2 n'interagissait pas directement avec l'orthologue de FPB11 dans le système de double-hybride dans la levure (manuscrit en préparation).

À l'anthèse au niveau de l'anthère, nous avons pu observer que l'expression de *ScFRK2* était exclue du tissu connectif, du tissu vasculaire ainsi que de la région du stomium (Figure V.1b, O'Brien *et al.*, 2005c). Tout comme dans l'ovule, aucun phénotype n'a pu être associé aux lignées sous-exprimantes ou co-supprimées. Par contre, la surexpression de *ScFRK2* cause un problème développemental au niveau du développement des gamètes mâles. Nous avons pu démontrer dans les lignées sur-exprimantes qu'à l'anthèse, plus de 60% des grains de pollen montrent une structure vide et décharnée (Figure V.3, O'Brien *et al.*, 2005c), alors que quelques-uns des autres grains de pollen montrent aussi des défectuosités mineures. Puisque l'intégrité des tétrades et des microspores était intacte et que le transgène peut être transmis à la

seconde génération (Figure V.2c à f et O'Brien *et al.*, 2005c), nous avons pu établir que le phénotype était d'origine sporophytique. De plus, les grains de pollen avec une apparence normale montrent un volume 66% plus petit que la lignée témoin. Ceci indique que la défectuosité atteint tous les grains de pollen et ce, même si l'intégrité de la sexine (Figure V.3c et d, O'Brien *et al.*, 2005c) et de la déposition de callose demeuraient inchangées (Figure V.3e et f, O'Brien *et al.*, 2005c). Étant donné que la mortalité du pollen s'accroît entre la libération des microspores (0%) jusqu'à atteindre un plateau vers l'anthèse (63%), nous avons pu clairement démontrer que l'accroissement de la mortalité du pollen était corrélée à la dégénérescence du tapetum (O'Brien *et al.*, 2005c). Cela nous amène à croire que la sur-expression de *ScFRK2* dans l'anthère cause un dérèglement tissulaire qui affecte le bon développement du pollen.

La sur-expression de *ScFRK2* cause des défectuosités tant dans les structures reproductrices mâle que femelle (O'Brien *et al.*, 2005b et c). Plusieurs mutants chez *A. thaliana* montrent le même type d'effets. Mentionnons entre autres *spl/nzz* un mutant qui affecte le développement des gamètes mâles et femelles sans toutefois influencer celui des cellules archésporales (Yang *et al.*, 1999). Le mutant *exs/ems1* affecte aussi le destin cellulaire des cellules précurseures du tapetum. Dans ce mutant, ces cellules se différencient en microspores. Ces dernières seront surnuméraires alors que l'absence de tapetum ne pourra les soutenir vers une structure viable et fertile (Canales *et al.*, 2002 et Zhao *et al.*, 2002). De plus le mutant *exs/ems1* montre un délai dans le développement de l'embryon (Canales *et al.*, 2002). SPL/NZZ et EXS/EMS1 codent pour un facteur de transcription de type MADS box et un récepteur kinase de type LRR respectivement.

Nous poursuivons présentement la caractérisation biochimique de cette nouvelle famille de MAPK. Plusieurs évidences viennent renforcer le caractère unique et soutenir l'appartenance de ScFRK1/2 à une sous-famille distincte. Nous avons déjà mentionné l'incapacité à complémenter une lignée mutante de MAPKKK chez *S. cerevisiae* (Chapitre IV, O'Brien *et al.*, 2005b), toutefois nous avons pu constater que le domaine kinase de la protéine est fonctionnel en condition *in vitro*. De plus, les partenaires double-hybrides dont nous disposons sont inattendus. Des éléments typiques d'une voie de MAP kinases auraient été espérés, alors que pour l'instant nous avons une calmoduline, une protéine à domaine RRM qui se lie à l'ARN ainsi que deux protéines de fonctions inconnues. Nous disposons maintenant d'un anticorps qui nous aidera grandement à bâtir nos connaissances sur le comportement biochimique de ScFRK2. Cet outil nous a d'ailleurs permis d'établir la liaison de la protéine aux membranes cytosoliques. Étant donné les changements homéotiques dans l'ovule et l'effet sporophytique sur la mortalité du pollen, nous planifions d'effectuer une analyse d'expression comparative entre les lignées sur-exprimantes et les lignées non-transformées. Pour ce faire, nous disposons déjà de biopuces d'ADN comportant plus de 6700 unigènes exprimés dans les tissus reproducteurs femelles de *S. chacoense*, ce qui nous permettra ainsi de comprendre les gènes touchés et régulés par la sur-expression de *ScFRK2*.

Chapitre VII. Conclusion

Au chapitre II, nous avons caractérisé une nouvelle famille de petites protéines sécrétées dont l'un des membres (HT-B) influence le système de reconnaissance du pollen génétiquement semblable au sein du style. Nous exposons un mécanisme d'action où l'absence de cette protéine retarderait la sénescence du style, ce qui aurait pour effet de contourner les barrières de l'auto-incompatibilité plutôt que de les abolir. La capacité de briser le système d'auto-incompatibilité sans égard aux S-RNases exprimées, mais en modulant l'expression d'un seul gène modificateur, comme le gène *HT*, est aussi un atout important dans les programmes d'améliorations génétiques des plantes.

Nous avons pu démontrer au chapitre III l'importance du gène *CYP51G1* dans le développement de l'embryon. Nous avons également pu prouver que cette enzyme a une spécificité plus large de substrats, ce qui est pour l'instant, le premier et unique cas décrit pour cette enzyme chez les plantes. De plus, nous avons pu démontrer le transport à distance de l'obtusifoliol et son impact sur la régulation de l'expression de l'enzyme qui le métabolise. Nous offrons également une piste sur la régulation du développement antéro/postérieur de la feuille par les facteurs de transcription de type HD-ZIP à domaine de type StART par le biais de l'obtusifoliol.

Dans les chapitres IV et V, nous avons caractérisé et défini une nouvelle sous-famille de protéines de type MAPK. Même si elle semble démontrer plus d'homologie

avec les MAPKK, nos analyses phylogéniques n'arrivent pas clairement à la classer entre la sous-famille des MAPKK ou celle des MAPKKK. De plus, nous avons pu montrer l'implication de *ScFRK2* dans le développement des gamètes mâle et femelle. Très peu de kinases ont pour l'instant un rôle connu dans les divers processus de développement de la plante, encore moins les kinases de la famille des MAPK. Le changement homéotique des ovules vers des structures carpéloïdes et l'effet sporophytique sur la mortalité du pollen, soulignent l'importance de *ScFRK2* dans le processus de formation des gamètes.

Références

Abe, M., Katsumata, H., Komeda, Y. et Takahashi, T. (2003). Regulation of shoot epidermal cell differentiation by a pair of homeodomain proteins in *Arabidopsis*. Development **130** : 635-643.

Ai, Y., Kron, E. et Kao, T.-H. (1991). S-alleles are retained and expressed in a self-compatible cultivar of *Petunia hybrida*. Mol. Gen. Genet. **230** : 353-358.

Aida, M., Ishida, T. et Tasaka, M. (1999). Shoot apical meristem and cotyledon formation during *Arabidopsis* embryogenesis: interaction among the *CUP-SHAPED COTYLEDON* and *SHOOT MERISTEMLESS* genes. Development **126** : 1563-1570.

Albrecht, C., Russinova, E., Hecht, V., Baaijens, E. et de Vries, S. (2005). The *Arabidopsis thaliana* SOMATIC EMBRYOGENESIS RECEPTOR-LIKE KINASES1 and 2 control male sporogenesis. Plant Cell **17** : 3337-3349.

Altmann, T. (1999). Molecular physiology of brassinosteroids revealed by the analysis of mutants. Planta **208** : 1-11

Alvarez, J. et Smyth, D. R. (1999). *CRABS CLAW* and *SPATULA*, two *Arabidopsis* genes that control carpel development in parallel with *AGAMOUS*. Development **126** : 2377-2386.

Anderson, M. A., Cornish, E. C., Mau, S.-L., Williams, E. G., Hoggart, R., Atkinson, A., Bonig, I., Grego, B., Simpson, R., Roche, P. J., Haley, J. D., Penschow, J. D., Niall, H. D., Tregar, G. W., Coghlan, J. P., Crawford, R. J. et Clarke, A. E. (1986). Cloning of cDNA for a stylar glycoprotein associated with expression of self-incompatibility in *Nicotiana alata*. Nature **321** : 38-44.

Angenent, G. C., Franken, J., Busscher, M., van Dijken, A., van Went, J. L., Dons, H. J. et van Tunen, A. J. (1995). A novel class of MADS box genes is involved in ovule development in petunia. Plant Cell **7** : 1569-1582

Aoyama, Y. et Yoshida, Y. (1992). The 4 β-methyl group of substrate does not affect the activity of lanosterol 14 α-demethylase (P-450(14)DM) of yeast: difference between the substrate recognition by yeast and plant sterol 14 α-demethylases. Biochem. Biophys. Res. Commun. **183** : 1266-1272

Arondel, V. V., Vergnolle, C., Cantrel, C. et Kader, J. (2000). Lipid transfer proteins are encoded by a small multigene family in *Arabidopsis thaliana*. Plant Science **157** : 1-12.

Asai, T., Tena, G., Plotnikova, J., Willmann, M. R., Chiu, W. L., Gomez-Gomez, L., Boller, T., Ausubel, F. M. et Sheen, J. (2002). MAP kinase signalling cascade in *Arabidopsis* innate immunity. Nature **415**: 977-983

Baima, S., Nobili, F., Sessa, G., Lucchetti, S., Ruberti, I. et Morelli, G. (1995). The expression of the *Athb-8* homeobox gene is restricted to provascular cells in *Arabidopsis thaliana*. Development **121** : 4171-4182

Bak, S., Kahn, R. A., Olsen, C. E. et Halkier, B. A. (1997). Cloning and expression in *Escherichia coli* of the obtusifoliol 14 α-demethylase of *Sorghum bicolor* (L.) Moench, a cytochrome P450 orthologous to the sterol 14 α-demethylases (CYP51) from fungi and mammals. Plant J. **11** : 191-201

Balk, P. A. et de Boer, A. D. (1999) Rapid stalk elongation in tulip (Tulipa gesneriana L. cv. Apeldoorn) and the combined action of cold-induced invertase and the water-channel protein gammaTIP. Planta **209** : 346-354.

Bardwell, L. et Thorner, J. (1996). A conserved motif at the amino termini of MEKs might mediate high-affinity interaction with the cognate MAPKs. Trends Biochem. Sci. **21** : 373-374

Becraft, P. W. (2002). Receptor Kinase Signaling in Plant Development. Annu. Rev. Cell. Dev. Biol. **18** : 163-192

Becraft. P. W. et Asuncion-Crabb, Y. (2000). Positional cues specify and maintain aleurone cell fate in maize endosperm development. Development **127** : 4039-4048

Benveniste, P. (1986). Sterol Biosynthesis. Annu. Rev. Plant Physiol. **37** : 275-308

Benveniste, P. (2004). Biosynthesis and accumulation of sterols. Annu. Rev. Plant. Biol. **55** : 429-457

Bergmann, D. C., Lukowitz W. et Somerville, C. R. (2004). Stomatal development and pattern controlled by a MAPKK kinase. Science **304** : 1494-1497

Berleth, T. et Jurgens, G. (1993). The role of the *MONOPTEROS* gene in organising the basal body region of the *Arabidopsis* embryo. Development **118** : 575-587

Bernatzky, R., Glaven, R. H. et Rivers, B. A. (1995). S-related protein can be recombined with self-compatibility in interspecific derivatives of *Lycopersicon*. Biochem. Genet. **33** : 215-225

Bevan, M. (1984). Binary *Agrobacterium* vectors for plant transformation. Nucl. Acids Res. **12** : 8711-8721

Bhat, R. A. et Panstruga, R. (2005). Lipid rafts in plants. Planta **223** : 5-19

Blein, J. P., Coutos-Thevenot, P., Marion, D. et Ponchet, M. (2002). From elicitins to lipid-transfer proteins: a new insight in cell signalling involved in plant defence mechanisms. Trends Plant Sci. **7** : 293-296

Boavida, L. C., Becker, J. D. et Feijo, J. A. (2005). The making of gametes in higher plants. Int. J. Dev. Biol. **49** : 595-614.

Bowman, J. (1994). *Arabidopsis*: An atlas of morphology and development. Springer-Verlag, New York.

Bowman, J. L., Smyth, D. R. et Meyerowitz, E. M. (1989). Genes directing flower development in *Arabidopsis*. Plant Cell **1** : 37-52

Bowman, J. L., Sakai, H., Jack, T., Weigel, D., Mayer, U. et Meyerowitz, E. M. (1992). *SUPERMAN*, a regulator of floral homeotic genes in *Arabidopsis*. Development **114** : 599-615

Bowman, J. L. et Smyth, D. R. (1999). *CRABS CLAW*, a gene that regulates carpel and nectary development in *Arabidopsis*, encodes a novel protein with zinc finger and helix-loop-helix domains. Development **126** : 2387-2396

Bowman, J. L., Eshed, Y. et Baum, S. F. (2002). Establishment of polarity in angiosperm lateral organs. Trends Genet. **18** : 134-141

Burger, C., Rondet, S., Benveniste, P. et Schaller, H. (2003). Virus-induced silencing of sterol biosynthetic genes: identification of a *Nicotiana tabacum* L. obtusifoliol-14α-demethylase (CYP51) by genetic manipulation of the sterol biosynthetic pathway in *Nicotiana benthamiana* L. J. Exp. Bot. **54** : 1675-1683

Bussière, F., Ledû, S., Girard, M., Héroux, M., Perreault, J.-P. et Matto,n D. P. (2003). Development of an efficient *cis-trans-cis* ribozyme cassette to inactivate plant genes. Plant Biotech. J. **1**: 423-435

Byskov, A. G., Andersen, C. Y., Nordholm, L., Thogersen, H., Xia, G., Wassmann O., Andersen, J. V., Guddal ,E. et Roed, T. (1995). Chemical structure of sterols that activate oocyte meiosis. Nature **374** : 559-562

Byskov, A. G., Andersen, C. Y. et Leonardsen, L. (2002). Role of meiosis activating sterols, MAS, in induced oocyte maturation. Mol. Cell Endocrinol. **187** : 189-196

Cabello-Hurtado, F., Zimmerlin, A., Rahier, A., Taton, M., DeRose, R., Nedelkina, S., Batard, Y., Durst, F., Pallett, K. E. et Werck-Reichhart, D. (1997). Cloning and functional expression in yeast of a cDNA coding for an obtusifoliol 14α-demethylase (CYP51) in wheat. Biochem. Biophys. Res. Commun. **230** : 381-385

Cabello-Hurtado, F., Taton, M., Forthoffer, N., Kahn, R., Bak, S., Rahier, A. et Werck-Reichhart, D. (1999). Optimized expression and catalytic properties of a wheat obtusifoliol 14α-demethylase (CYP51) expressed in yeast. Complementation of *erg11*Δ yeast mutants by plant CYP51. Eur. J. Biochem. **262** : 435-446

Canales, C., Bhatt, A. M., Scott, R. et Dickinson, H. (2002). EXS, a putative LRR receptor kinase, regulates male germline cell number and tapetal identity and promotes seed development in *Arabidopsis*. Curr. Biol. **12** : 1718-1727

Carland, F. M., Fujioka, S., Takatsuto, S., Yoshida, S. et Nelson, T. (2002). The identification of CVP1 reveals a role for sterols in vascular patterning. Plant Cell **14** : 2045-2058

Chaumont, F., Barrieu, F., Herman, E. M. et Chrispeels, M. J. (1998). Characterization of a maize tonoplast aquaporin expressed in zones of cell division and elongation. Plant Physiol. **117** : 1143-1152

Chawla, B., Bernatzky, R., Liang, W. et Marcotrigiano, M. (1997). Breakdown of self incompatibility in tetraploid *Lycopersicon peruvianum*: inheritance and expression of S-related proteins. Therot. App. Genet. **95** : 992-996

Cheung, A. Y. (1996). The pollen tube growth pathway: its molecular and biochemical contributions and responses to pollination. Sex. Plant Reprod. **9** : 330-336

Chevalier, D., Batoux, M., Fulton, L., Pfister, K., Yadav, R. K., Schellenberg, M. et Schneitz, K. (2005). STRUBBELIG defines a receptor kinase-mediated signaling pathway regulating organ development in *Arabidopsis*. Proc. Natl. Acad. Sci. USA **102** : 9074-9079

Church, G. M. et Gilbert, W. (1984). Genomic sequencing. Proc. Natl. Acad. Sci. USA **81** : 1991-1995

Clark, S. E., Running, M. P. et Meyerowitz, E. M. (1993). CLAVATA1, a regulator of meristem and flower development in *Arabidopsis*. Development **119** : 397-418

Clouse, S. D. (2000). Plant development: A role for sterols in embryogenesis. Curr. Biol. **10** : R601-604

Clouse, S. D. (2002a). *Arabidopsis* mutants reveal multiple roles for sterols in plant development. Plant Cell **14** : 1995-2000

Clouse, S. D. (2002b). Brassinosteroids. The *Arabidopsis* Book, 1-23

Clouse, S. D., and Sasse, J. M. (1998). BRASSINOSTEROIDS: Essential Regulators of Plant Growth and Development. Annu. Rev. Plant Physiol. Plant Mol. Biol. **49** : 427-451

Coen, E. S. et Meyerowitz, E. M. (1991). The war of the whorls: genetic interactions controlling flower development. Nature **353** : 31-37

Colcombet, J., Boisson-Dernier, A., Ros-Palau, R., Vera, C. E. et Schroeder, J. I. (2005). *Arabidopsis* SOMATIC EMBRYOGENESIS RECEPTOR KINASES1 and 2 are essential for tapetum development and microspore maturation. Plant Cell **17** : 3350-3361.

Colombo, L., Franken, J., Koetje, E., van Went, J., Dons, H. J., Angenent, G. C. et van Tunen, A. J. (1995). The petunia MADS box gene *FBP11* determines ovule identity. Plant Cell **7** : 1859-1868

Colombo, L., Franken, J., Van der Krol, A. R., Wittich, P. E., Dons, H. J. et Angenent, G. C. (1997). Downregulation of ovule-specific MADS box genes from petunia results in maternally controlled defects in seed development. Plant Cell **9** : 703-715

Cornish, E. C., Pettitt, J. M., Bonig, I. et Clarke, A. E. (1987). Developmentally controlled expression of a gene associated with self-incompatibility in *Nicotiana alata.* Nature **326** : 99-102

Costa, S. et Dolan, L. (2003). Epidermal patterning genes are active during embryogenesis in *Arabidopsis*. Development **130** : 2893-2901

Crone, W. et Lord, E. M. (1991). A kinematic analysis of gynoecial growth in *Lilium longiflorum* : surface growth patterns in all floral organs are triphasic. Dev. Biol. **143** : 408-417

Cronquist, A. (1988). The evolution and classification of flowering plants. (Bronx, NY:New York Botanical Garden).

Cruz-Garcia, F., Hancock, C. N. et McClure, B. (2003). S-RNase complexes and pollen rejection. J. Exp. Bot. **54** : 123-130

Darnet, S. et Rahier, A. (2003). Enzymological properties of sterol-C4-methyl oxidase of yeast sterol biosynthesis. Bioch. Biophys. Acta **1633** : 106-117

de Nettancourt, D. (1977). Incompatibility in angiosperms. (New York: Springler-Verlag).

de Nettancourt, D. (1997). Incompatibility in angiosperms. Sex. Plant Reprod. **10** : 185-199

Deurenberg, J. J. M. (1976). In vitro protein synthesis with polysomes from unpollinated, cross- and self-pollinated *Petunia* ovaries. Planta **128** : 29-33

Diener, A. C., Li, H., Zhou, W., Whoriskey, W. J., Nes, W. D. et Fink, G. R. (2000). STEROL METHYLTRANSFERASE 1 controls the level of cholesterol in plants. Plant Cell **12** : 853–870

Di Laurenzio, L., Wysocka-Diller, J., Malamy, J. E., Pysh, L., Helariutta, Y., Freshour, G., Hahn, M. G., Feldmann, K. A. et Benfey, P. N. (1996). The *SCARECROW* gene regulates an asymmetric cell division that is essential for generating the radial organization of the *Arabidopsis* root. Cell **86** : 423-433

Dodds, P. N., Fergurson, C., Clarke, A. E. et Newbigin, E. (1999). Pollen- expressed S-RNases are not involved in self-incompatibility in *Lycopersicon peruvianum*. Sex. Plant Reprod. **12** : 76-87

Drews. G, N., Bowman, J. L. et Meyerowitz, E. M. (1991). Negative regulation of the *Arabidopsis* homeotic gene *AGAMOUS* by the *APETALA2* product. Cell **65** : 991-1002

Edwards, P. A. et Ericsson, J. (1999). Sterols and isoprenoids: signaling molecules derived from the cholesterol biosynthetic pathway. Annu. Rev. Biochem. **68** : 157-185

Elion, E. A. (2000). Pheromone response, mating and cell biology. Curr. Opin. Microbiol. **3** : 573-581

Entani, T., Iwano, M., Shiba, H., Che, F. S., Isogai, A. et Takayama, S. (2003). Comparative analysis of the self-incompatibility (S-) locus region of *Prunus mume* : identification of a pollen-expressed F-box gene with allelic diversity. Genes Cells **8** : 203-213

Esau, K. (1977). Anatomy of Seed Plants. New York.

Evans, P. T. et Malmberg, R. L. (1989). Alternative pathways of tobacco placental development : time of commitment and analysis of a mutant. Dev. Biol. **136** : 273-283

Fanger, G. R., Gerwins, P., Widmann, C., Jarpe, M. B. et Johnson, G. L. (1997). MEKKs, GCKs, MLKs, PAKs, TAKs, and tpls: upstream regulators of the c-Jun amino-terminal kinases? Curr. Opin. Genet. Dev. **7** : 67-74

Farese, R. V. et Jr., Herz, J. (1998). Cholesterol metabolism and embryogenesis. Trends Genet. **14** : 115-120

Favaro, R., Pinyopich, A., Battaglia, R., Kooiker, M., Borghi, L., Ditta, G., Yanofski, M., Kater, M. et Colombo, L. (2003). MADS-Box protein complexes control carpel and ovule development in *Arabidopsis*. Plant Cell **15** : 2603-2611

Fischer, U., Men, S. et Grebe, M. (2004). Lipid function in plant cell polarity. Curr. Opin. Plant Biol. **7** : 670-676

Franssen, H. J. et Bisseling, T. (2001). Peptide signaling in plants. Proc. Natl. Acad. Sci. USA **98** : 12855-12856

Friml, J., Vieten, A., Sauer, M., Weijers, D., Schwarz, H., Hamann, T., Offringa, R. et Jurgens, G. (2003). Efflux-dependent auxin gradients establish the apical-basal axis of *Arabidopsis*. Nature **426** : 147-153

Fujita, H., Takemura, M., Tani, E., Nemoto, K., Yokota, A. et Kohchi, T. (2003). An *Arabidopsis* MADS-box protein, AGL24, is specifically bound to and phosphorylated by meristematic receptor-like kinase (MRLK). Plant Cell Physiol. **44**: 735-742

Gasser, C. S., Broadhvest, J. et Hauser, B. A. (1998). Genetic analysis of ovule development. Annu. Rev. Plant Physiol. Plant Mol. Biol. **49** : 1–24

Geldner, N., Anders, N., Wolters, H., Keicher, J., Kornberger, W., Muller, P., Delbarre, A., Ueda, T., Nakano, A. et Jurgens, G. (2003). The *Arabidopsis* GNOM ARF-GEF mediates endosomal recycling, auxin transport, and auxin-dependent plant growth. Cell **112** : 219-230

Germain, H., Rudd, S., Zotti, C., Caron, S., O'Brien, M., Chantha, S.-C., Lagacé, M., Major, F. et Matton, D. P. (2005a). A 6374 unigene set corresponding to low abundance transcripts expressed following fertilization in *Solanum chacoense* Bitt., and characterization of 30 receptor-like kinases. Plant Mol. Biol. **59**: 513-529

Germain, H., Chevalier, E. et Matton, D. P. (2005b). Plant bioactive peptides: an expanding class of signaling molecules. Can. J. Bot. (in press)

Gietz, R. D. et Woods, R. A. (2002). Screening for protein-protein interactions in the yeast two-hybrid system. Methods Mol. Biol. **185** : 471-486

Gifford, M. L., Dean, S. et Ingram, G. C. (2003). The *Arabidopsis ACR4* gene plays a role in cell layer organisation during ovule integument and sepal margin development. Development **130**: 4249-4258

Gilissen, L. J. W. (1977). Style-controlled wilting of the flower. Planta **133** : 275-280

Gilissen, L. J. W. (1984). Pollination-induced corolla wilting in *Petunia hybrida*. Rapid transfer through the style of a wilting-inducing substance. Plant Physiol. **75** : 496-498

Golz, J. F., Clarke, A. E. et Newbigin, E. (2000). Mutational approaches to the study of self-incompatibility: Revisisiting the pollen-part mutants. Annals Bot. **85** : 95-103

Guo, D. A., Venkatramesh, M. et Nes, W. D. (1995). Developmental regulation of sterol biosynthesis in *Zea mays*. Lipids **30** : 203-219

Haecker, A., Gross-Hardt, R., Geiges, B., Sarkar, A., Breuninger, H., Herrmann, M. et Laux, T. (2004). Expression dynamics of WOX genes mark cell fate decisions during early embryonic patterning in *Arabidopsis thaliana*. Development **131** : 657-668

Hall, I. V. et Forsyth, F. R. (1967). Production of ethylene by flowers following pollination and treatment with water and auxin. Can. J. Bot. **45** : 1163-1166

Hamal, A., Jouannic, S., Leprince, A. S., Kreis, M. et Henry, Y. (1999). Molecular characterisation and expression of an *Arabidopsis thaliana* L. MAP kinase kinase cDNA, AtMAP2Kα. Plant Science **140** : 49-64

Hamann, T., Mayer, U. et Jürgens, G. (1999). The auxin-insensitive *bodenlos* mutation affects primary root formation and apical-basal patterning in the *Arabidopsis* embryo. Development **126** : 1387-1395

Hamann, T., Benkova, E., Baurle, I., Kientz, M. et Jurgens, G. (2002). The Arabidopsis *BODENLOS* gene encodes an auxin response protein inhibiting MONOPTEROS-mediated embryo patterning. Genes Dev. **16** : 1610-1615

Hanks, S. K. et Hunter, T. (1995). Protein kinases 6. The eukaryotic protein kinase superfamily: kinase (catalytic) domain structure and classification. Faseb J. **9** : 576-596

Hanks, S. K. et Quinn, A. M. (1991). Protein kinase catalytic domain sequence database: identification of conserved features of primary structure and classification of family members. Methods Enzymol. **200** : 38-62

Harikrishna, K., Jampates-Beale, R., Milligan, S. et Gasser, C. (1996). An endochitinase gene expressed at high levels in the stylar transmitting tissue of tomatoes. Plant Mol. Biol. **30** : 899-911

Hartmann, M.-A. (1998). Plant sterols and the membrane environment. Trends Plant Sci. **3** : 170-175

Hartmann, M.-A. et Benveniste, P. (1987). Plant membrane sterols: isolation, identification and biosynthesis. Methods Enzymol. **148** : 632-650

He, J. X., Fujioka, S., Li, T. C., Kang, S. G., Seto, H., Takatsuto, S., Yoshida, S. et Jang, J. C. (2003). Sterols regulate development and gene expression in *Arabidopsis*. Plant Physiol. **131** : 1258-1269

Hecht, V., Vielle-Calzada, J. P., Hartog, M. V., Schmidt, E. D., Boutilier, K., Grossniklaus, U. et de Vries, S. C. (2001). The *Arabidopsis SOMATIC EMBRYOGENESIS RECEPTOR KINASE 1* gene is expressed in developing ovules and embryos and enhances embryogenic competence in culture. Plant Physiol. **127** : 803-816

Helariutta, Y., Fukaki, H., Wysocka-Diller, J., Nakajima, K., Jung, J., Sena, G., Hauser, M. T. et Benfey, P. N. (2000). The *SHORT-ROOT* gene controls radial patterning of the *Arabidopsis* root through radial signaling. Cell **101** : 555-567

Hirt, H. (2000). MAP kinases in plant signal transduction. Results Probl. Cell Differ. **27** : 1-9

Holmberg, N., Harker, M., Gibbard, C. L., Wallace, A. D., Clayton, J. C., Rawlins, S., Hellyer, A. et Safford, R. (2002). Sterol C-24 methyltransferase type 1 controls the flux of carbon into sterol biosynthesis in tobacco seed. Plant Physiol. **130** : 303-311

Hosaka, K. et Hanneman, R. E. (1998a). Genetics of self-compatibility in a self-incompatible wild diploid potato species *Solanum chacoense*. 1. Detection of an S slocus inhibitor (Sli) gene. Euphytica **99** : 191-197

Hosaka, K. et Hanneman, R. E. (1998b). Genetics of self-compatibility in a self-incompatible wild diploid potato species *Solanum chacoense*. 2. Localization of an S slocus inhibitor (Sli) gene on the potato genome using DNA markers. Euphytica **103** : 265-271

Hu, W., Wang, Y., Bower, S. C. et Ma, H. (2003). Isolation, sequence analysis, and expression studies of florally expressed cDNAs in *Arabidopsis*. Plant Mol. Biol. **53** : 545-563

Huang, S., Lee, H. S., Karunanandaa, B. et Kao, T.-H. (1994). Ribonuclease activity of *Petunia inflata* S proteins is essential for rejection of self-pollen. Plant Cell **6** : 1021-1028

Jack, T. (2001). Plant development going MADS. Plant Mol. Biol. **46** : 515-520

James, P., Halladay, J. et Craig, E. A. (1996). Genomic libraries and a host strain designed for highly efficient two-hybrid selection in yeast. Genetics **144** : 1425-1436

Jang, J. C., Fujioka, S., Tasaka, M., Seto, H., Takatsuto, S., Ishii, A., Aida, M., Yoshida, S. et Sheen, J. (2000). A critical role of sterols in embryonic patterning and meristem programming revealed by the *fackel* mutants of *Arabidopsis thaliana*. Genes Dev. **14** : 1485-1497

Johnson, M. A. et Preuss, D. (2003) On your mark, get set, GROW! LePRK2-LAT52 interactions regulate pollen tube growth. Trends Plant Sci. **8** : 97-99

Jones, J. D. G, Dunsmuir, P. et Bedbrook, J. (1985). High level expression of introduced chimeric genes in regenerated transformed plants. EMBO J. **4** : 2411-2418

Jouannic, S., Hamal, A., Leprince, A. S., Tregear, J. W., Kreis, M. et Henry, Y. (1999). Plant MAP kinase kinase kinases structure, classification and evolution. Gene **233** : 1-11

Kahn, R. A., Bak, S., Olsen, C. E., Svendsen, I. et Moller, B. L. (1996). Isolation and reconstitution of the heme-thiolate protein obtusifoliol 14α-demethylase from *Sorghum bicolor* (L.) Moench. J. Biol. Chem. **271** : 32944-32950

Kalb, V. F., Woods, C. W., Turi, T. G., Dey, C. R., Sutter, T. R. et Loper, J. C. (1987). Primary structure of the P450 lanosterol demethylase gene from *Saccharomyces cerevisiae*. DNA **6** : 529-537

Kao, T.-H. et McCubbin, A. (1996). How flowering plants discriminate between self and non-self pollen to prevent inbreeding. Proc. Natl. Acad. Sci. USA **93** : 12059- 12065

Kao, T.H. et Tsukamoto, T. (2004). The molecular and genetic bases of S-RNase-based self-incompatibility. Plant Cell **16** Suppl. : S72-83

Keck, E., McSteen, P., Carpenter, R. et Coen, E. (2003). Separation of genetic functions controlling organ identity in flowers. EMBO J. **22** : 1058-1066

Kieber, J. J., Rothenberg, M., Roman, G., Feldmann, K. A. et Ecker, J. R. (1993). *CTR1*, a negative regulator of the ethylene response pathway in *Arabidopsis*, encodes a member of the raf family of protein kinases. Cell **72** : 427-441

Kondo, K., Yamamoto, M., Itahashi, R., Sato, T., Egashira, H., Hattori, T. et Kowyama, Y. (2002a). Insights into the evolution of self-compatibility in *Lycopersicon* from a study of stylar factors. Plant J. **30** : 143-154

Kondo, K., Yamamoto, M., Matton, D. P., Sato, T., Hirai, M., Norioka, S., Hattori, T. et Kowyama, Y. (2002b). Cultivated tomato has defects in both S-RNase and HT genes required for stylar function of self-incompatibility. Plant J. **29** : 627-636

Kunst, L., Klenz, J. E., Martinez-Zapater, J. et Haughn, G. W. (1989). *AP2* Gene determines the identity of perianth organs in flowers of *Arabidopsis thaliana*. Plant Cell **1** : 1195-1208

Kushiro, M., Nakano, T., Sato, K., Yamagishi, K., Asami, T., Nakano, A., Takatsuto, S., Fujioka, S., Ebizuka, Y. et Yoshida, S. (2001). Obtusifoliol 14α-demethylase (CYP51) antisense *Arabidopsis* shows slow growth and long life. Biochem. Biophys. Res. Commun. **285** : 98-104

Lai, Z., Ma, W., Han, B., Liang, L., Zhang, Y., Hong, G. et Xue, Y. (2002). An F-box gene linked to the self-incompatibility (S) locus of *Antirrhinum* is expressed specifically in pollen and tapetum. Plant Mol. Biol. **50** : 29-42

Lamb, D. C., Kelly, D. E. et Kelly, S. L. (1998). Molecular diversity of sterol 14α-demethylase substrates in plants, fungi and humans. FEBS Lett. **425** : 263-265

Lantin, S., O'Brien, M. et Matton, D. P. (1999a). Pollination, wounding and jasmonate treatments induce the expression of a developmentally regulated pistil dioxygenase at a distance, in the ovary, in the wild potato *Solanum chacoense* Bitt. Plant Mol. Biol. **41** : 371-386

Lantin, S., O'Brien, M. et Matton, D. P. (1999b). Fertilization and wounding of the style induce the expression of a highly conserved plant gene homologous to a *Plasmodium falciparum* surface antigen in the wild potato *Solanum chacoense* Bitt. Plant Mol. Biol. **41** : 115-124

Laux, T., Würschum, T. et Breuninger, H. (2004). Genetic regulationof embryonic pattern formation. Plant Cell **16** Suppl. : S190-202

Lee, H. S., Huang, S. et Kao, T.-H. (1994). S proteins control rejection of incompatible pollen in *Petunia inflata*. Nature **367** : 560-563

Lee, H.-S., Karunanandaa, B., McCubbin, A., Gilroy, S. et Kao, T.-H. (1996). PRK1, a receptor-like kinase of *Petunia inflata*, is essential for postmeiotic development of pollen. Plant J. **9** : 613-624

Lee, H.-S., Chung, Y.-Y., Das, C., Karunanandaa, B., van Went, J. L., Mariani, C. et Kao, T.-H. (1997). Embryo sac development is affected in *Petunia inflata* plants transformed with an antisense gene encoding the extracellular domain of receptor kinase PRK1. Sex. Plant Reprod. **10** : 341–350

Leon, J., Rojo, E. et Sanchez-Serrano, J. J. (2001). Wound signaling in plants. J. Exp. Bot. **52** : 1-9

Lepesheva, G. I. and Waterman, M. R. (2004). CYP51 the omnipotent P450. Mol. Cell Endocrinol. **215** : 165-170

Levin, J. Z. et Meyerowitz, E. M. (1995). *UFO* : An *Arabidopsis* gene involved in both floral meristem and floral organ development. Plant Cell **7** : 529-548

Li, J. et Chory, J. (1997). A putative leucine-rich repeat receptor kinase involved in brassinosteroid signal transduction. Cell **90** : 929-938

Li, Z. et Thomas, T. L. (1998). *PEI1*, an embryo-specific zinc finger protein gene required for heart-stage embryo formation in *Arabidopsis*. Plant Cell **10** : 383-398

Li, H., Zhou, W., Whoriskey, W. J., Nes, W. D. et Fink, G. R. (2000). Sterol methyltransferase 1 controls the level of cholesterol in plants. Plant Cell **12** : 853-870

Lindsey, K., Pullen, M. L. et Topping, J. F. (2003). Importance of plant sterols in pattern formation and hormone signalling. Trends Plant Sci. **8** : 521-525

Linskens, H. F. (1974). Some observations on the growth of the style. Incompatibility Newsletter **4** : 4-15

Liu, Z., Franks, R. G. et Klink, V. P. (2000). Regulation of gynoecium marginal tissue formation by LEUNIG and AINTEGUMENTA. Plant Cell **12** : 1879-1892

Llop-Tous, I., Barry, C. S. et Grierson, D. (2000). Regulation of ethylene biosynthesis in response to pollination in tomato flowers. Plant Physiol. **123** : 971-978

Long, J. A., Woody, S., Poethig, S., Meyerowitz, E. M. et Barton, M. K. (2002). Transformation of shoots into roots in Arabidopsis embryos mutant at the TOPLESS locus. Development **129** : 2797-2806

Ludevid, D., Höfte, H., Himelblau, E. et Chrispeels, M. J. (1992) The expression pattern of the tonoplast intrinsic protein g-TIP in *Arabidopsis thaliana* is correlated with cell enlargement. Plant Physiol. **100** : 1633-1639

Lukowitz, W., Roeder, A., Parmenter, D. et Somerville, C. (2004). A MAPKK kinase gene regulates extra-embryonic cell fate in *Arabidopsis*. Cell **116** : 109-119

Luu, D. T., Qin, X., Morse, D. et Cappadocia, M. (2000). S-RNase uptake by compatible pollen tubes in gametophytic self-incompatibility. Nature **407** : 649-651

Luu, D. T., Qin, X., Laublin, G., Yang, Q., Morse, D. et Cappadocia, M. (2001). Rejection of S-heteroallelic pollen by a dual-specific S-RNase in *Solanum chacoense* predicts a multimeric SI pollen component. Genetics **159** : 329-335

Lynn, K., Fernandez, A., Aida, M., Sedbrook, J., Tasaka, M., Masson, P. et Barton, M. K. (1999). The *PINHEAD/ZWILLE* gene acts pleiotropically in *Arabidopsis* development and has overlapping functions with the *ARGONAUTE1* gene. Development **126** : 469-481

Madhani, H. D. et Fink, G. R. (1998). The riddle of MAP kinase signaling specificity. Trends Genet. **14** : 151-155

Mahonen, A. P., Bonke, M., Kauppinen, L., Riikonen, M., Benfey, P. N. et Helariutta, Y. (2000). A novel two-component hybrid molecule regulates vascular morphogenesis of the *Arabidopsis root*. Genes Dev. **14** : 2938-2943

Malamy, J. E. et Benfey, P. N. (1997). Organization and cell differentiation in lateral roots of *Arabidopsis thaliana*. Development **124** : 33-44

Mandel, M. A., Bowman, J. L., Kempin, S. A., Ma, H., Meyerowitz, E. M. et Yanofsky, M. F. (1992). Manipulation of flower structure in transgenic tobacco. Cell **71** : 133-143

Marchuk, D., Drumm, M., Saulino, A. et Collins, F. S. (1991). Construction of T-vectors, a rapid and general system for direct cloning of unmodified PCR products. Nucl. Acids Res. **19** : 1154

Mascarenhas, J. P. et Hamilton, D. A. (1992). Artifacts in the localization of GUS activity in anothers of petunia transformed with a CaMV 35S-GUS construct. Plant J. **2** : 405-408

Matton, D. P., Maes, O., Laublin, G., Xike, Q., Bertrand, C., Morse, D. et Cappadocia, M. (1997). Hypervariable domains of self-incompatibility RNases mediate allele-specific pollen recognition. Plant Cell **9** : 1757-1766

Matton, D. P., Bertrand, C., Laublin, G. et Cappadocia, M. (1998). Molecular aspects of self-incompatibility in tuber-bearing *Solanum* species. In Comprehensive Potato Biotechnology, S.M.P. Khurana, R. Chandra, and M.D. Upadhya, eds (New Delhi, India: Malhotra Publishing House), pp. 97-113

Matton, D. P., Luu, D. T., Xike, Q., Laublin, G., O'Brien, M., Maes, O., Morse, D. et Cappadocia, M. (1999). Production of an S RNase with dual specificity suggests a novel hypothesis for the generation of new S alleles. Plant Cell **11** : 2087-2097

Mayer, U., Buttner, G. et Jurgens, G. (1993). Apical-basal pattern formation in the *Arabidopsis* embryo: studies on the role of the *GNOM* gene. Development **117** : 149-162

McClure, B. A., Haring, V., Ebert, P. R., Anderson, M. A., Simpson, R. J., Sakiyama, F. et Clarke, A. E. (1989). Style self-incompatibility products of *Nicotiana alata* are ribonucleases. Nature **342** : 955-957

McClure, B. A., Gray, J. E., Anderson, M. A. et Clarke, A. E. (1990). Self-incompatibility in *Nicotiana alata* involves degradation of pollen rRNA. Nature **347** : 757-760

McClure, B., Mou, B., Canevascini, S. et Bernatzky, R. (1999). A small asparagine-rich protein required for S-allele-specific pollen rejection in *Nicotiana*. Proc. Natl. Acad. Sci. USA **96** : 13548-13553

McConnell, J. R., Emery, J., Eshed, Y., Bao, N., Bowman, J. et Barton, M. K. (2001). Role of PHABULOSA and PHAVOLUTA in determining radial patterning in shoots. Nature **411** : 709-713

Modrusan, Z., Reiser, L., Feldmann, K. A., Fischer, R. L. et Haughn, G. W. (1994). Homeotic transformation of ovules into carpel-like structures in *Arabidopsis*. Plant Cell **6** : 333-349

Mongrand, S., Morel, J., Laroche, J., Claverol, S., Carde, J. P., Hartmann, M. A., Bonneu, M., Simon-Plas, F., Lessire, R. et Bessoule, J. J. (2004). Lipid rafts in higher plant cells: purification and characterization of Triton X-100-insoluble microdomains from tobacco plasma membrane. J. Biol. Chem. **279** : 36277-36286

Morris, P. C., Guerrier, D., Leung, J. et Giraudat, J. (1997). Cloning and characterisation of *MEK1*, an *Arabidopsis* gene encoding a homologue of MAP kinase kinase. Plant Mol. Biol. **35** : 1057-1064

Murfett, J., Atherton, T. L., Mou, B., Gasser, C. S. et McClure, B. A. (1994). S-RNase expressed in transgenic *Nicotiana* causes S-allele-specific pollen rejection. Nature **367** : 563-566

Murfett, J., Strabala, T. J., Zurek, D. M., Mou, B., Beecher, B. et McClure, B. A. (1996). S-RNase and interspecific pollen rejection in the genus *Nicotiana*: multiple pollen-rejection pathways contribute to unilateral incompatibility between self-incompatible and self-compatible species. Plant Cell **8** : 943-958

Muschietti, J., Dircks, L., Vancanneyt, G. et McCormick, S. (1994). LAT52 protein is essential for tomato pollen development: pollen expressing antisense LAT52 RNA hydrates and germinates abnormally and cannot achieve fertilization. Plant J. **6** : 321-338

Nadeau, J. A. et Sack, F. D. (2002). Control of stomatal distribution on the *Arabidopsis* leaf surface. Science **296** : 1697-1700

Nakagami, H., Pitzschke, A. et Hirt, H. (2005). Emerging MAP kinase pathways in plant stress signalling. Trends Plant Sci. **10** : 339-346

Nelson, D. R., Schuler, M. A., Paquette, S. M., Werck-Reichhart, D. et Bak, S. (2004). Comparative genomics of rice and *Arabidopsis*. Analysis of 727 cytochrome P450 genes and pseudogenes from a monocot and a dicot. Plant Physiol. **135** : 756-772

Newman, K. L., Fernandez, A. G. et Barton, M. K. (2002). Regulation of axis determinacy by the *Arabidopsis PINHEAD* gene. Plant Cell **14** : 3029-3042

Nielsen, H., Engelbrecht, J., Brunak, S. et von Heijne, G. (1997). Identitfication of prokaryotic and eukaryotic signal peptides and prediction of their cleavage sites. Protein Eng. **10** : 1-6

Nishihama, R., Banno, H., Shibata, W., Hirano, K., Nakashima, M,. Usami, S. et Machida, Y. (1995). Plant homologues of components of MAPK (mitogen-activated protein kinase) signal pathways in yeast and animal cells. Plant Cell Physiol. **36** : 749-757

Nonomura, K., Miyoshi, K., Eiguch, M., Suzuki, T., Miyao, A., Hirochika, H. et Kurata, N. (2003). The *MSP1* gene is necessary to restrict the number of cells entering into male and female sporogenesis and to initiate anther wall formation in rice. Plant Cell **15** : 1728-39

O'Brien, M., Bertrand, C. et Matton, D. P. (2002a). Characterization of a fertilization-induced and developmentally regulated plasma-membrane aquaporin expressed in reproductive tissues, in the wild potato *Solanum chacoense* Bitt. Planta **215** : 485-493

O'Brien, M., Kapfer, C., Major, G., Laurin, M., Bertrand, C., Kondo, K., Kowyama, Y. et Matton, D. P. (2002b). Molecular analysis of the stylar-expressed *Solanum chacoense* small asparagine-rich protein family related to the HT modifier of gametophytic self-incompatibility in *Nicotiana*. Plant J. **32** : 985-996

O'Brien, M., Chantha, S.-C., Rahier, A. et Matton, D. P. (2005a). Lipid signaling in plants: Cloning and expression analysis of the obtusifoliol 14α-demethylase from *Solanum chacoense* Bitt., a pollination- and fertilization-induced gene with both obtusifoliol and lanosterol demethylase activity. Plant Physiol. **139** : 734-749

O'Brien, M., Bertrand, C., Caron, S. et Matton, D. P. (2005b). The *Solanum* ScFRK2 protein kinase defines a new MAPK family and affects ovule identity. J. Exp. Bot., submitted.

O'Brien, M., Kapfer, C. et Matton, D. P. (2005c). The ScFRK2 MAP kinase kinase from *Solanum chacoense* affects pollen development and viability. Planta, submitted.

Otte, K., Kranz, H., Kober, I., Thompson, P., Hoefer, M., Haubold, B., Remmel, B., Voss, H,, Kaiser. C., Albers, M., Cheruvallath, Z., Jackson, D., Casari, G., Koegl, M., Paabo, S., Mous, J., Kremoser, C. et Deuschle, U. (2003). Identification of farnesoid X receptor β as a novel mammalian nuclear receptor sensing lanosterol. Mol. Cell. Biol. **23** : 864-872

Pearce, G. et Ryan, C. A. (2003). Systemic signaling in tomato plants for defense against herbivores. Isolation and characterization of three novel defense-signaling glycopeptide hormones coded in a single precursor gene. J. Biol. Chem. **278** : 30044-30050

Pedley, K. F. et Martin, G. B. (2005). Role of mitogen-activated protein kinases in plant immunity. Curr. Opin. Plant Biol. **8** : 541-547

Pinyopich, A., Ditta, G. S., Savidge, B., Liljegren, S. J., Baumann, E., Wisman, E. et Yanofsky, M. F. (2003). Assessing the redundancy of MADS-box genes during carpel and ovule development. Nature **424** : 85-88

Piwien-Pilipuk, G., Huo, J. S. et Schwartz, J. (2002). Growth hormone signal transduction. J. Pediatr. Endocrinol. Metab. **15** : 771-786

Poethig, R. S., Coe, J. E. H. et Johri, M. M. (1986). Cell lineage patterns in maize embryogenesis: A clonal analysis. Devel. Biol. **117** : 392-404

Pompon, D., Louerat, B., Bronine, A. et Urban, P. (1996). Yeast expression of animal and plant P450s in optimized redox environments. Methods Enzymol. **272** : 51-64

Ponting, C. P. et Aravind, L. (1999). START: a lipid-binding domain in StAR, HD-ZIP and signalling proteins. Trends Biochem. Sci. **24** : 130-132

Posas, F. et Saito, H. (1997). Osmotic activation of the HOG MAPK pathway via Ste11p MAPKKK: scaffold role of Pbs2p MAPKK. Science **276** : 1702-1705

Prigge, M. J., Otsuga, D., Alonso, J. M., Ecker, J. R., Drews, G. N. et Clark, S. E. (2005). Class III homeodomain-leucine zipper gene family members have overlapping, antagonistic, and distinct roles in *Arabidopsis* development. Plant Cell **17** : 61-76

Rahier, A. et Benveniste, P. (1989). Mass spectral identification of phytosterols. In WD Nes, E Parish, eds, Analysis of Sterols and Other Biologically Significant Steroids. Academic Press, San Diego, pp 223-250

Rahier, A. et Taton, M. (1997). Fungicides as tools in studying postsqualene sterol synthesis in plants. Pesticide Biochem. Physiol. **57** : 1-27

Ray, A., Robinson-Beers, K., Ray, S., Baker, S. C., Lang, J. D., Preuss, D., Milligan, S. B. et Gasser, C. S. (1994). *Arabidopsis* floral homeotic gene *BELL* (*BEL1*) controls ovule development through negative regulation of *AGAMOUS* gene (*AG*). Proc. Natl. Acad. Sci. USA **91** : 5761-5765

Reiser, L., Modrusan, Z., Margossian, L., Samach, A., Ohad, N., Haughn, G. W. et Fischer, R. L. (1995). The *BELL1* gene encodes a homeodomain protein involved in pattern formation in the *Arabidopsis* ovule primordium. Cell **83** : 735-742

Reiter, R. S., Young, R. M. et Scolnik, P. A. (1992). Genetic linkage of the *Arabidopsis* genome: methods for mapping with recombinant inbreds and Random Amplified Polymorphic DNAs (RAPDs). In C. Koncz, N.-H. Chua, J. Schell, eds, Methods in Arabidopsis Research. World Scientific Publishing Co., Singapore, pp 170-190

Ricks, C. M. et Chetelat, R. T. (1991). The breakdown of self-incompatibility in *Lycopersicon hirsutum*. In *Solanaceae* III: taxonomy, chemistry, evolution, L. Hawkes, Nee and Estrada, ed (London: Royal Botanic Garden Kew and Linnean Society of London), pp. 253-256.

Rivard, S. R., Saba-El-Leil, M. K., Landry, B. et Cappadocia, M. (1994). RFLP analyses and segregation of molecular markers in plants produced by in vitro anther culture, selfing, and reciprocal crosses of two lines of self-incompatible *Solanum chacoense*. Genome **37** : 775-783

Robinson, M. J. et Cobb, M. H. (1997). Mitogen-activated protein kinase pathways. Curr. Opin. Cell Biol. **9** : 180-186

Roe, J. L., Nemhauser, J. L. et Zambryski, P. C. (1997). TOUSLED participates in apical tissue formation during gynoecium development in *Arabidopsis*. Plant Cell **9** : 335-353

Romeis, T. (2001). Protein kinases in the plant defence response. Curr. Opin. Plant Biol. **4** : 407-414

Royo, J., Kunz, C., Kowyama, Y., Anderson, M., Clarke, A. E. et Newbigin, E. (1994). Loss of a histidine residue at the active site of S-locus ribonuclease is associated with self-compatibility in *Lycopersicon peruvianum*. Proc. Natl. Acad. Sci. USA **91** : 6511-6514

Sakai, H., Medrano, L. J. et Meyerowitz, E. M. (1995). Role of *SUPERMAN* in maintaining *Arabidopsis* floral whorl boundaries. Nature **378** : 199–203

Samach, A., Klenz, J. E., Kohalmi, S. E., Risseeuw, E., Haughn, G. W. et Crosby, W.L. (1999). The *UNUSUAL FLORAL ORGANS* gene of *Arabidopsis thaliana* is an F-box protein required for normal patterning and growth in the floral meristem. Plant J. **20** : 433-445

Sambrook, J., Fritsch, E. F. et Maniatis, T. (1989). Molecular cloning: a laboratory manual. Cold Spring Harbor Laboratory Press, New York.

Sanchez, A. M., Bosch, M., Bots, M., Nieuwland, J., Feron, R. et Mariani, C. (2004). Pistil factors controlling pollination. Plant Cell **16** Suppl : S98-106

Schaeffer, A., Bronner, R., Benveniste, P. et Schaller, H. (2001). The ratio of campesterol to sitosterol that modulates growth in *Arabidopsis* is controlled by STEROL METHYLTRANSFERASE 2;1. Plant J. **25** : 605-615

Schaller, F. (2001). Enzyme of the biosynthesis of octadecanoid-derived signaling molecules. J. Exp. Bot. **52** : 11-23

Schaller, H., Bouvier-Nave, P. et Benveniste, P. (1998). Overexpression of an *Arabidopsis* cDNA encoding a sterol-C24(1)-methyltransferase in tobacco modifies the ratio of 24-methyl cholesterol to sitosterol and is associated with growth reduction. Plant Physiol. **118** : 461-469

Schiefthaler, U., Balasubramanian, S., Sieber, P., Chevalier, D., Wisman, E. et Schneitz, K. (1999). Molecular analysis of *NOZZLE*, a gene involved in pattern formation and early sporogenesis during sex organ development in *Arabidopsis thaliana*. Proc. Natl. Acad. Sci. USA **96** : 11664-11669

Schmidt, E. D., Guzzo, F., Toonen, M. A. et de Vries, S. C. (1997). A leucine-rich repeat-containing receptor-like kinase marks somatic plant cells competent to form embryos. Development **124** : 2049-2062

Schmitt, P., Rahier, A. et Benveniste, P. (1982). Inhibition of sterol biosynthesis in suspension-cultures of bramble cells. Physiol. Veg. **20** : 559-571

Schmitt, P. et Benveniste, P. (1979). Effect of fenarimol on sterol byosynthesis in suspension cultures of bramble cells. Phytochemistry **18** : 1659-1665

Schneitz, K., Hulskamp, M., Kopczak, S. D. et Pruitt, R. E. (1997). Dissection of sexual organ ontogenesis: a genetic analysis of ovule development in *Arabidopsis thaliana*. Development **124** : 1367-1376

Schneitz, K., Baker, S. C., Gasser, C. S. et Redweik, A. (1998). Pattern formation and growth during floral organogenesis: HUELLENLOS and AINTEGUMENTA are required for the formation of the proximal region of the ovule primordium in *Arabidopsis thaliana*. Development **125** : 2555-2563

Schoof, H., Lenhard, M., Haecker, A., Mayer, K.F., Jurgens, G. et Laux, T. (2000). The stem cell population of *Arabidopsis* shoot meristems in maintained by a regulatory loop between the *CLAVATA* and *WUSCHEL* genes. Cell **100** : 635-644

Schopfer, C. R., Nasrallah, M. E. et Nasrallah, J. B. (1999). The male determinant of self-incompatibility in *Brassica*. Science **286** : 1697-1700

Schrick, K., Mayer, U., Horrichs, A., Kuhnt, C., Bellini, C., Dangl, J., Schmidt, J. et Jurgens, G. (2000). FACKEL is a sterol C-14 reductase required for organized cell division and expansion in *Arabidopsis* embryogenesis. Genes Dev. **14** : 1471-1484

Schrick, K., Mayer, U., Martin, G., Bellini, C., Kuhnt, C., Schmidt, J. et Jurgens, G. (2002). Interactions between sterol biosynthesis genes in embryonic development of *Arabidopsis*. Plant J. **31** : 61-73

Schrick, K., Fujioka, .S, Takatsuto, S., Stierhof, Y. D., Stransky, H., Yoshida, S. et Jurgens, G. (2004). A link between sterol biosynthesis, the cell wall, and cellulose in *Arabidopsis*. Plant J. **38** : 227-243

Schuler, M. A. et Werck-Reichhart, D. (2003). Functional genomics of P450s. Annu. Rev. Plant Biol. **54** : 629-667

Scott, R. J., Spielman, M. et Dickinson, H. G. (2004). Stamen structure and function. Plant Cell **16** Suppl : S46-60

Sells, M. A., Knaus, U. G., Bagrodia, S., Ambrose, D. M., Bokoch, G. M. et Chernoff, J. (1997). Human p21-activated kinase (Pak1) regulates actin organization in mammalian cells. Curr. Biol. **7** : 202-210

Sessa, G., Steindler, C., Morell,i G. et Ruberti, I. (1998). The *Arabidopsis Athb-8*, *-9* and *-14* genes are members of a small gene family coding for highly related HD-ZIP proteins. Plant Mol. Biol. **38** : 609-622

Sheridan, W. F., Golubeva, E. A., Abrhamova L. I. et Golubovskaya, I. N. (1999). The *mac1* mutation alters the developmental fate of the hypodermal cells and their cellular progeny in the maize anther. Genetics **153** : 933-941.

Shibata, W., Banno, H., Ito, Y., Hirano, K., Irie, K., Usami, S., Machida, C. et Machida, Y. (1995). A tobacco protein kinase, NPK2, has a domain homologous to a domain found in activators of mitogen-activated protein kinases (MAPKKs). Mol. Gen. Genet. **246** : 401-410

Shiu, S. H. et Bleecker, A. B. (2001). Receptor-like kinases from *Arabidopsis* form a monophyletic gene family related to animal receptor kinases. Proc. Natl. Acad. Sci. USA **98** : 10763-10768

Simons, K. et Toomre, D. (2000). Lipid rafts and signal transduction. Nat. Rev. Mol. Cell Biol. **1** : 31-39

Singh, A., Ai, Y. et Kao, T.-H. (1991). Characterization of ribonuclease activity of three S-allele-associated proteins of *Petunia inflata*. Plant Physiol. **96** : 61-68

Singh, A., Evensen, K. B. et Kao, T.-H. (1992). Ethylene synthesis and floral senescence following compatible and incompatible pollinations in *Petunia inflata*. Plant Physiol. **99** : 38-45

Sitbon, F. et Jonsson, L. (2001). Sterol composition and growth of transgenic tobacco plants expressing type-1 and type-2 sterol methyltransferases. Planta **212** : 568-572

Skinner, D. J., Hill, T. A. et Gasser, C. S. (2004). Regulation of ovule development. Plant Cell **16** Suppl : S32-45

Skuzeski, J. M., Nichols, L. M. et Gesteland, R. F. (1990). Analysis of leaky viral translation termination codons in vivo by transient expression of improved β-glucuronidase vectors. Plant Mol. Biol. **15** : 65-69

Souter, M., Topping, J., Pullen, M., Friml, J., Palme, K., Hackett, R., Grierson, D. et Lindsey, K. (2002). *hydra* mutants of *Arabidopsis* are defective in sterol profiles and auxin and ethylene signaling. Plant Cell **14** : 1017-1031

Stead, A. D. (1992). Pollination-induced flower senescence: a review. Plant Growth Regulat. **11** : 13-20

Stone, J. L. (2002). Molecular mechanisms underlying the breakdown of gametophytic self-incompatibility. Q. Rev. Biol. **77** : 17-32

Stratmann, J. W. (2003). Long distance run in the wound response-jasmonic acid is pulling ahead. Trends Plant Sci. **8** : 247-250

Stromstedt, M., Rozman, D. et Waterman, M. R. (1996). The ubiquitously expressed human CYP51 encodes lanosterol 14 α-demethylase, a cytochrome P450 whose expression is regulated by oxysterols. Arch. Biochem. Biophys. **329** : 73-81

Sugden, P. H. et Clerk, A. (1997). Regulation of the ERK subgroup of MAP kinase cascades through G protein-coupled receptors. Cell Signal. **9** : 337-351

Swofford, D. L. (1998). PAUP*: Phylogenetic Analysis Using Parsimony (* and Other Methods). Sinauer, Sunderland, MA.

Takasaki, T., Hatakeyama, K., Suzuki, G., Watanabe, M., Isogai, A. et Hinata, K. (2000). The S receptor kinase determines self-incompatibility in *Brassica* stigma. Nature **403** : 913-916

Takayama, S., Shiba, H., Iwano, M., Shimosato, H., Che, F.-S., Kai, N., Watanabe, M., Suzuki, G., Hinata, K. et Isogai, A. (2000). The pollen determinant of self-incompatibility in *Brassica campestris*. Proc. Natl. Acad. Sci. USA **97** : 1920-1925

Tanaka, H., Watanabe, M., Watanabe, D., Tanaka, T., Machida, C. et Machida, Y. (2002). *ACR4*, a putative receptor kinase gene of *Arabidopsis thaliana*, that is expressed in the outer cell layers of embryos and plants, is involved in proper embryogenesis. Plant Cell Physiol. **43** : 419-428

Tang, W., Ezcurra, I., Muschietti, J. et McCormick, S. (2002). A cysteine-rich extracellular protein, LAT52, interacts with the extracellular domain of the pollen receptor kinase LePRK2. Plant Cell **14** : 2277-2287

Taton, M. et Rahier, A. (1991). Properties and structural requirements for substrate specificity of cytochrome P-450-dependent obtusifoliol 14 α-demethylase from maize (*Zea mays*) seedlings. Biochem. J. **277** (Pt 2) : 483-492

Tena, G., Asai, T., Chiu, W. L. et Sheen, J. (2001). Plant mitogen-activated protein kinase signaling cascades. Curr. Opin. Plant Biol. **4** : 392-400

Theissen, G. (2001). Development of floral organ identity: stories from the MADS house. Curr. Opin. Plant Biol. **4** : 75-85

The MAPK Group (2002). Mitogen-activated protein kinase cascades in plants: a new nomenclature. Trends Plant Sci. **7** : 301-308

Topping, J. F., May, V. J., Muskett, P. R. et Lindsey, K. (1997). Mutations in the *HYDRA1* gene of *Arabidopsis* perturb cell shape and disrupt embryonic and seedling morphogenesis. Development **124** : 4415-4424

Torres-Ruiz, R. A., Lohner, A. et Jurgens, G. (1996). The *GURKE* gene is required for normal organization of the apical region in the *Arabidopsis* embryo. Plant J. **10** : 1005-1016

Treisman, R. (1996). Regulation of transcription by MAP kinase cascades. Curr. Opin. Cell Biol. **8** : 205-215

Tsafriri, A., Cao, X., Ashkenazi, H., Motola, S., Popliker, M. et Pomerantz, S. H. (2005). Resumption of oocyte meiosis in mammals: on models, meiosis activating sterols, steroids and EGF-like factors. Mol. Cell Endocrinol. **234** : 37-45

Tsukamoto, T., Ando, T., Kokubun, H., Watanabe, H., Masada, M., Zhu, X., Marchesi, E. Kao, T.-H. (1999). Breakdown on self-incompatibility in a natural population of *Petunia axillaris* (*Solanaceae*) in Uruguay containing both self-incompatible and self-compatible plants. Sex. Plant Reprod. **12** : 6-13

Tu, H., Barr, M., Dong, D. L. et Wigler, M. (1997). Multiple regulatory domains on the Byr2 protein kinase. Mol. Cell Biol. **17** : 5876-5887

Tzafrir, I., Pena-Muralla, R., Dickerman, A., Berg, M., Rogers, R., Hutchens, S., Sweeney, T. C., McElver, J., Aux, G., Patton, D. et Meinke, D. (2004). Identification of genes required for embryo development in *Arabidopsis*. Plant Physiol. **135** : 1206-1220

Ushijima, K., Sassa, H., Dandekar, A. M., Gradziel, T. M., Tao, R. et Hirano, H. (2003). Structural and transcriptional analysis of the self-incompatibility locus of almond: identification of a pollen-expressed F-box gene with haplotype-specific polymorphism. Plant Cell **15** : 771-781

van der Leede-Plegt, L., van de Ven, B., Bino, R., van der Salm, T. et van Tunen, A. (1992). Introduction and differential use of various promoters in pollen grains of *Nicotiana glutinosa* and *Lilium longiflorum*. Plant Cell Rep. **11** : 20-24

van Doorn, W. G. (2002a). Does ethylene treatment mimic the effects of pollination on floral lifespan and attractiveness? Ann. Bot. (Lond) **89** : 375-383

van Doorn, W. G. (2002b). Effect of ethylene on flower abscission: a survey. Ann. Bot. (Lond) **89** : 689-693

Vroemen, C. W., Mordhorst, A. P., Albrecht, C., Kwaaitaal, M. A. et de Vries, S. C. (2003). The *CUP-SHAPED COTYLEDON3* gene is required for boundary and shoot meristem formation in *Arabidopsis*. Plant Cell **15** : 1563-1577

Weigel, D. et Meyerowitz, E. M. (1994). The ABCs of floral homeotic genes. Cell **78** : 203-209

Werck-Reichhart, D. et Feyereisen, R. (2000). Cytochromes P450: a success story. Genome Biol. **6** : 1-9

Weterings, K. et Russell, S. D. (2004). Experimental analysis of the fertilization process. Plant Cell **16** Suppl : S107-118

Wilkinson, J., Twell, D. et Lindsey, K. (1997). Activities of CaMV 35S and nos promoters in pollen: implications for field release of transgenic plants. J. Exp. Bot. **48** : 265-275

Willemsen, V., Friml, J., Grebe, M., van den Toorn, A., Palme, K. et Scheres, B. (2003). Cell polarity and PIN protein positioning in *Arabidopsis* require STEROL METHYLTRANSFERASE1 function. Plant Cell **15** : 612-625

Wilson, Z. A. et Yang, C. (2004). Plant gametogenesis: conservation and contrasts in development. Reproduction **128** : 483-492

Wu, C., Leberer, E., Thomas, D. Y. et Whiteway, M. (1999). Functional characterization of the interaction of Ste50p with Ste11p MAPKKK in *Saccharomyces cerevisiae*. Mol. Biol. Cell **10** : 2425-2440

Yalovsky, S., Rodriguez-Concepcion, M., Bracha, K., Toledo-Ortiz, G. et Gruissem, W. (2000). Prenylation of the floral transcription factor APETALA1 modulates its function. Plant Cell **12** : 1257-1266

Yang, H., Matsubayashi, Y., Nakamura, K. et Sakagami, Y. (1999). *Oryza sativa PSK* gene encodes a precursor of phytosulfokine-α, a sulfated peptide growth factor found in plants. Proc. Natl. Acad. Sci. USA **96** : 13560-13565

Yang, W. C., Ye, D., Xu, J. et Sundaresan, V. (1999). The *SPOROCYTELESS* gene of *Arabidopsis* is required for initiation of sporogenesis and encodes a novel nuclear protein. Genes Dev. **13** : 2108-2117

Yang, S. L., Xie, L. F., Mao, H. Z., Puah, C. S., Yang, W. C., Jiang, L., Sundaresan, V. et Ye, D. (2003). Tapetum determinant1 is required for cell specialization in the *Arabidopsis* anther. Plant Cell **15** : 2792-2804

Zhang, S. et Klessig, D. F. (2001). MAPK cascades in plant defense signaling. Trends Plant Sci. **6** : 520-527

Zhang, Y., Shewry, P. R., Jones, H., Barcelo, P., Lazzeri, P. A. et Halford, N. G. (2001). Expression of antisense SnRK1 protein kinase sequence causes abnormal pollen development and male sterility in transgenic barley. Plant J. **28** : 431-441

Zhao, D. Z., Wang, G. F., Speal, B. et Ma, H. (2002). The *EXCESS MICROSPOROCYTES1* gene encodes a putative leucine-rich repeat receptor protein kinase that controls somatic and reproductive cell fates in the *Arabidopsis* anther. Genes Dev. **16** : 2021-2031

Zheng, C. F. et Guan, K. L. (1994). Activation of MEK family kinases requires phosphorylation of two conserved Ser/Thr residues. EMBO J. **13** : 1123-1131